



# GLMRIS – Brandon Road

## Appendix E - Hydrology and Hydraulics



August 2017



**US Army Corps  
of Engineers®**  
Rock Island &  
Chicago Districts

(Page Intentionally Left Blank)

## Table of Contents

<b>TABLE OF CONTENTS .....</b>	<b>E-3</b>
<b>Summary .....</b>	<b>E-4</b>
<b>ATTACHMENT 1</b>	
<b>Site Selection of Brandon Road Lock and Dam as the Southernmost Control Point to prevent the Migration of Asian Carp into the Chicago Area Waterway System Via Aquatic Pathways .....</b>	<b>E-5</b>
<b>ATTACHMENT 2</b>	
<b>H&amp;H Information for Brandon Road Lock (GLMRIS-BR) .....</b>	<b>E-18</b>
<b>ATTACHMENT 3</b>	
<b>GLMRIS Lock, Reducing Risk of Aquatic Nuisance Species Transfer through Brandon Road Lock , Analytical and Numerical Model Study .....</b>	<b>E-41</b>
<b>ATTACHMENT 4</b>	
<b>Reverse Flows in Brandon Road Approach Channel .....</b>	<b>E-166</b>

## Summary

This Appendix contains four separate documents that support the plan formulation for the Brandon Road flushing lock. Project measures are described in more detail in the main report.

The first document ‘Site Selection of Brandon Road Lock and Dam as the Southernmost Control Point to prevent the Migration of Asian Carp into the Chicago Area Waterway System Via Aquatic Pathways’ provides background and evaluation of the three locations considered for the downstream control point: Dresden Island, Brandon Road, and Lockport Lock and Dam, in forming a one way upstream control point for the transfer of Mississippi River Basin ANS to the Great Lakes Basin via the Chicago Area Waterway System.

The second document, ‘H&H Information for Brandon Road Lock (GLMRIS-BR)’, contains pertinent data and physical attributes of the lock and gates, flow durations and modeling discharges, and the range of headwater and tailwater elevations. Available water supply is also identified as a potential limitation for lock flushing. The document investigates potential bypass locations around Brandon Road Lock and Dam, and the potential for fish passage through the dam’s headgates.

The third document ‘GLMRIS Lock [flushing lock at Brandon Road Lock and Dam], Reducing Risk of Aquatic Nuisance Species Transfer through Brandon Road Lock, Analytical and Numerical Model Study’ presents a detailed description of the Brandon Road Lock chamber flushing, along with numerical modeling procedure and results for the evaluation of four lock flushing systems. These systems include use of the existing culvert, two alternatives requiring modifications to the lock structure, and finally one that would provide a continuous supply of clean water to the lower lock approach to prevent ANS from reaching the lock chamber.

The fourth document ‘Reverse Flows in Brandon Road Lock Approach Channel’ describes a reverse flow in the approach channel downstream of Brandon Road Lock. This reverse flow has been observed by lock personnel, and measured by the United States Geological Survey (USGS). These reverse flows could make measures less effective by transporting ANS through deterrent measures. This document describes the development and use of a hydraulic model developed to simulate these reverse flows and compares these reverse velocities to those measures by USGS. The model may be used in the future to evaluate potential mitigating measures or operation changes.

**GLMRIS - Brandon Road**  
**Appendix E - Hydrology and Hydraulics**

**Site Selection for Brandon Road Lock and Dam**



## Title: Site Selection of Brandon Road Lock and Dam as the Southernmost Control Point to prevent the Migration of Asian Carp into the Chicago Area Waterway System Via Aquatic Pathways

This white paper reviews three locations along the Des Plaines River for acceptability as a downstream control point to prevent upstream migration of Asian Carp into the Chicago Area Waterway System (CAWS) and ultimately into the Great Lakes. Three locations have been proposed as potential control points for the Mississippi River Basin (MRB) aquatic nuisance species (ANS):

- Lockport Lock and Dam;
- Brandon Road Lock and Dam; and
- Dresden Island Lock and Dam.

Modifications to the lock chambers and to aquatic pathways around the lock chambers are considered at all three locations. For the purposes of this white paper, an aquatic pathway is defined as a surface water connection between the MRB and the Great Lakes Basin (GLB) chambers which allow for the potential transfer of ANS in various life stages. See *Figure 1* for the locations of Lockport, Brandon Road, and Dresden Island Lock and Dams. A pool is the water impounded upstream of a dam and maintained for navigation. See *Figure 2* for a profile of the normal pool elevations for the Illinois Waterway system including the pools created by the Lockport, Brandon Road, and Dresden Island Locks and Dams.

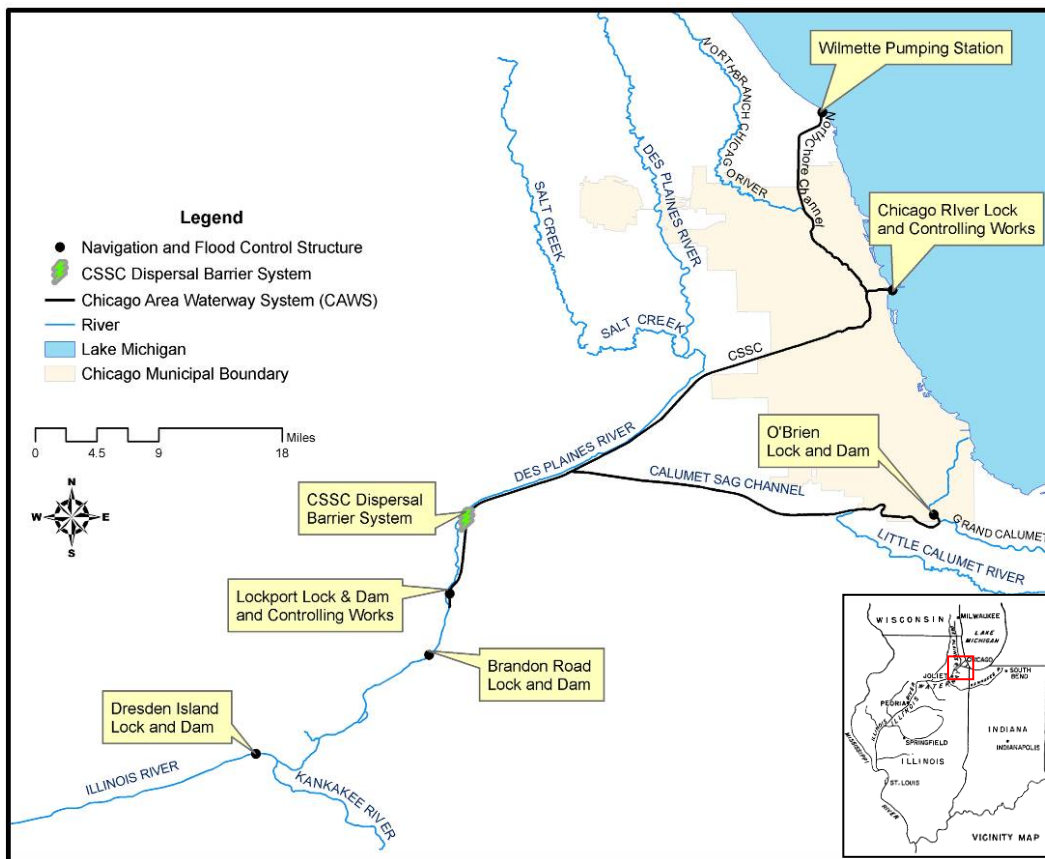


Figure 1: Map of the CAWS Noting the Location of the Lockport Brandon Road, and Dresden Island Locks & Dams

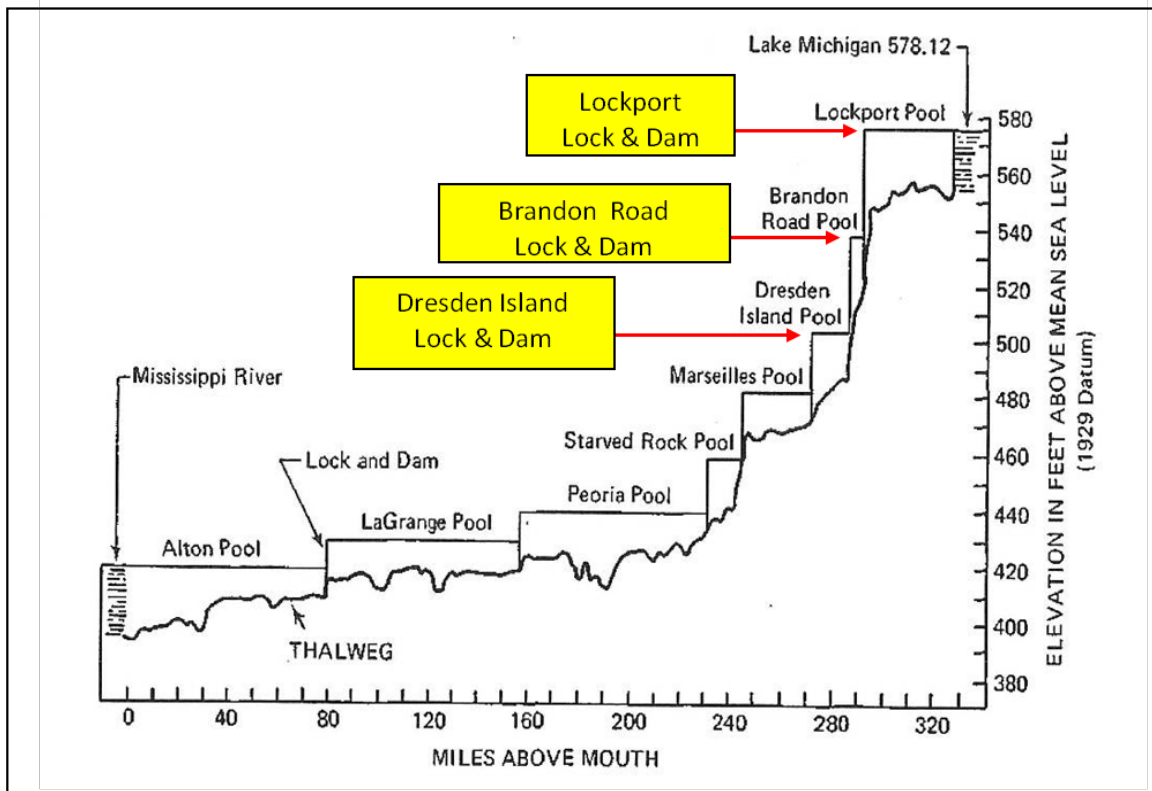


Figure 2: Profile of the Illinois Waterway Noting Pool Elevations Created by the Lockport, Brandon Road, and Dresden Island Lock and Dams.

### Removal of Dresden Island Lock and Dam from Consideration

Prior to completing a full analysis comparing each of the three proposed lock locations based on the above listed criteria, Dresden Island was immediately removed from consideration as an appropriate control point location. Significant Bighead and Silver Asian Carp populations are known to inhabit the Des Plaines and Kankakee Rivers between the Brandon Road and Dresden Island Locks and Dams.

- There is little head difference across Dresden Island Lock and Dam during large flow events and there is no structural barrier to prevent the passage of Asian Carp.
- Asian Carp have been observed on the Des Plaines River 10 miles upstream of Dresden Island Lock and Dam the Rock Run Rookery.
- While the full extent of Asian Carp along the Kankakee River is not known at this time, the USGS has observed Asian carp upstream of the Wilmington dam, located 10.3 miles upstream of the confluence<sup>1</sup>.

Due to the little head difference across Dresden Lock and Dam, and the wide extent of habitation of the Asian Carp, Dresden Island Lock is not considered to be a feasible option.

The Lockport and Brandon Road Lock chambers both are considered to be potential locations to successfully reduce the likelihood of Asian Carp transfer into the Great Lakes Basin because these

<sup>1</sup> US Geological Survey, NAS – Nonindigenous Aquatic Species. Web 6 April 2015. <http://nas2.er.usgs.gov/viewer/omap.aspx?SpeciesID=551>.

chambers are located i) downstream of the current electrical dispersal barrier; and ii) upstream of the confirmed large population of Asian carps.

### Potential Aquatic Pathways- Effectiveness of controlling the upstream transfer of ANS

A companion White Paper to this document, “Potential Modifications to Lockport and/or Brandon Road Lock Chambers to Prevent the Migration of Asian Carps into the Chicago Area Waterway System Via Aquatic Pathways<sup>2</sup>” includes a thorough description of the Lockport and Brandon Road Lock and Dam Facilities including background, photographs, and upstream aquatic pathways associated with each. A summary of each facility is included here with a highlight of potential aquatic pathways which would need to be addressed if either site should be selected as a downstream control point. Based on results presented in that White Paper, the Chicago District had identified fewer and less complex aquatic pathways around the Brandon Road Lock and Dam.

#### LOCKPORT LOCK

As noted in *Figure 3* below, Lockport Lock and Dam consists of one lock chamber, a dam and powerhouse, and an abandoned lock. Upstream of the Lockport Lock and Dam is the Lockport Controlling Works. See *Plate A* for an Illinois Waterway Navigation Chart of the area in the vicinity of the Lockport Lock and Dam.

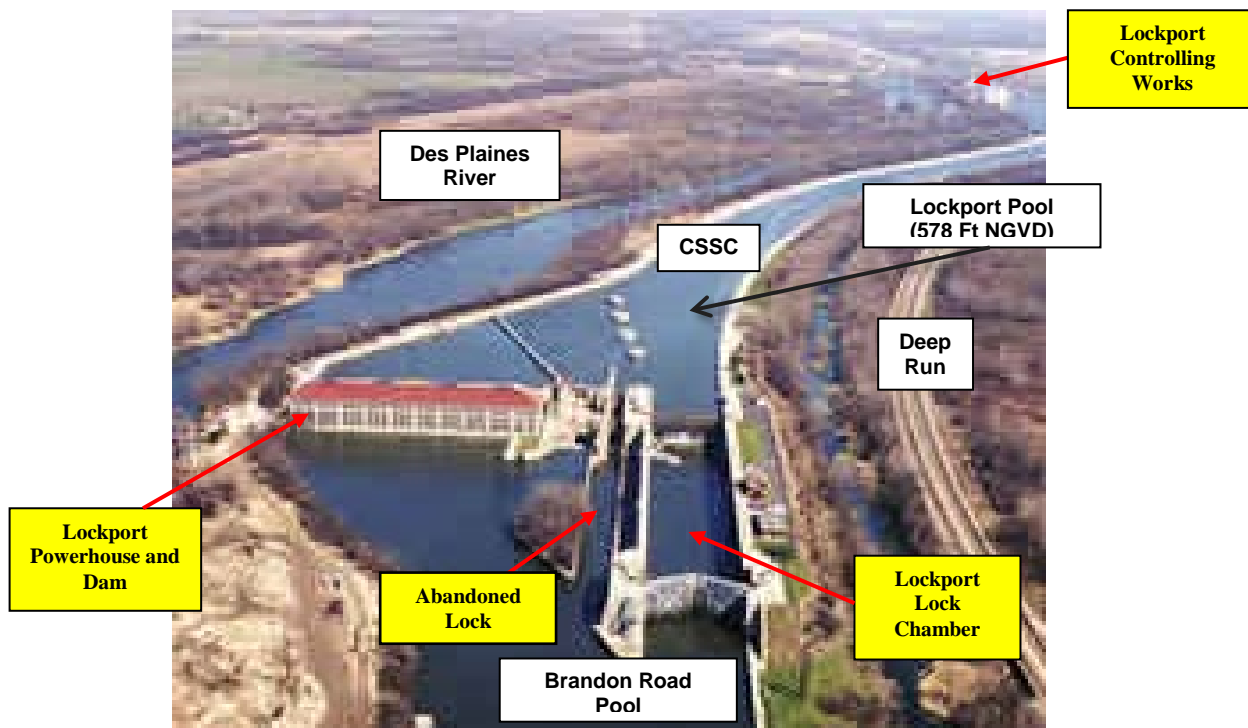


Figure 3: Lockport Lock and Dam (looking upstream)

<sup>2</sup> US Army Corps of Engineers, Potential Modifications to Lockport and/or Brandon Road Lock Chambers to Prevent the Migration of Asian Carps into the Chicago Area Waterway System Via Aquatic Pathways, White Paper. January, 2010.

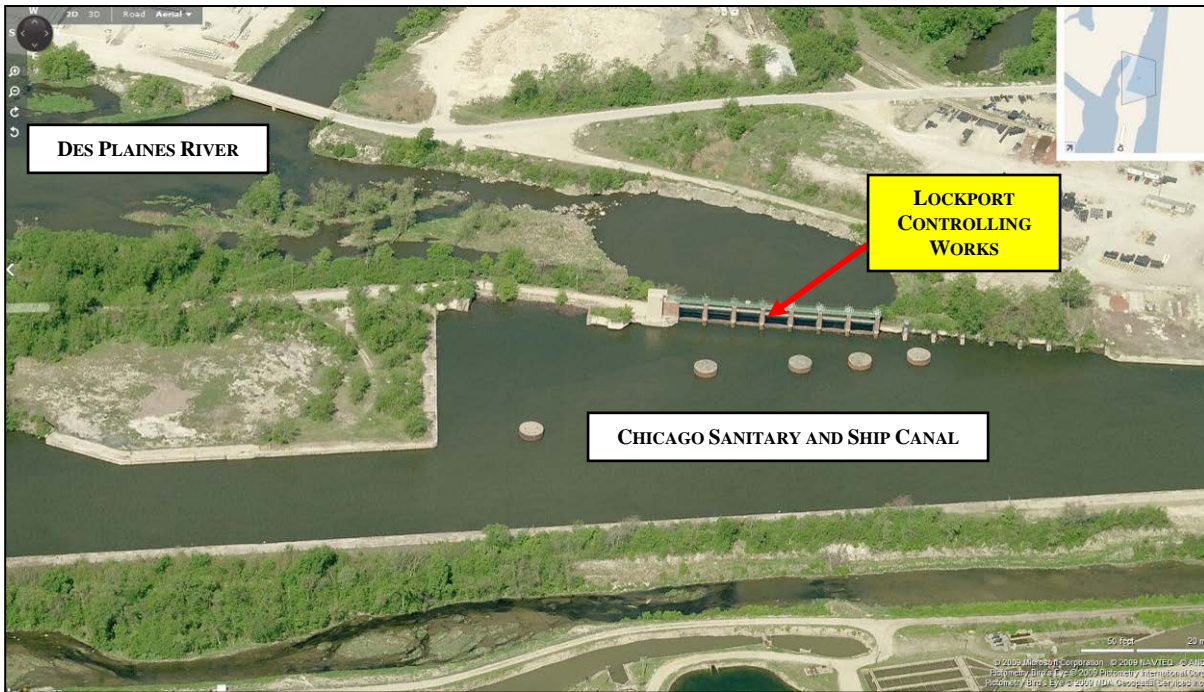


Figure 4: Birds Eye View of Lockport Controlling Works (looking North)

Originally constructed in 1933 and recently rehabilitated in 1989, the Lockport Lock is comprised of a single lock chamber having a width of 110 feet and length of 600 feet. The lock's average filling time is 22.5 minutes, and the average emptying time is 15 minutes.

Six potential aquatic pathways have been identified:

1. Lockport Powerhouse and Dam, which consists of a dam, two (2) turbines, and nine (9) sluice gates. Based on available data, the Chicago District estimates the normal head difference on either side of the powerhouse and dam equals approximately 40 feet.<sup>3</sup> See *Figure 3*. Velocity through the powerhouse gates is estimated to be equal to or greater than 11 feet per second.<sup>4</sup>
2. Lockport Controlling Works, which is located upstream of the Lockport Lock and Dam and connects the CSSC to the Des Plaines River. See *Figure 4* for a photo of this structure. The Lockport Controlling Work's primary purpose is to control flooding by allowing overflow relief for the CSSC into the Des Plaines River, and its secondary purpose is to maintain CSSC's elevations for navigation. Additionally, activities at the controlling works are also coordinated with downstream powerhouse activities to maximize electricity production.<sup>5</sup> The Lockport Controlling Works consists of seven (7) operational vertical lift sluice gates, which are 20 feet

<sup>3</sup> See US Army Corps of Engineer District, Rock Island, Water Control Manual, Brandon Road Lock & Dam, Upper Mississippi River Basin Illinois Waterway – Nine-Foot Channel, Appendix 2, Master Water Control Manual, June 1986, revised April 1996, page 2-1. Lockport pool elevation was estimated by adding the average lift between the Lockport and Brandon Road pools to the nominal Brandon Road pool elevation. See US Army Corps of Engineer District, Rock Island, Lockport Lock and O'Brien Lock & Controlling Works, Illinois Waterway Appendix 1, Master Reservoir Regulation Manual, page vii, June 1986.

<sup>4</sup> Harza Engineering Company, Division of Water Resources, Illinois Department of Transportation, An Evaluation of Flow Measurements & Accounting Methods for Lake Michigan Diversion, Volume III Appendices, Powerhouse Sluice Gates, Rating Curves, Gate C Open, December 1981.

<sup>5</sup> Page 2-10, App. 1 Lockport . . . Master Reservoir Regulation Manual.

high by 30 feet wide. MWRDGC reports the controlling works' gates are opened six (6) to ten (10) times a year and water velocity traveling through these gates can be minimal.<sup>6</sup>

The head difference between the Des Plaines River and CSSC at Lockport Controlling Works reduces while the storm event progresses. Effectively, the water level on the CSSC reduces as a result of canal drawdown, and the water level on the DPR rises as the flood wave passes through it. Gates often remain open until water levels on the Des Plaines River and CSSC equalize and the flow through the gates is nearly stagnant.

3. During 1% annual chance flood events, another potential aquatic pathway is created around the Lockport Lock. This potential pathway occurs in the Lockport Pool between the CSSC and Deep Run. Deep Run is a waterway that i) runs parallel to the CSSC and ii) connects with the Des Plaines River, downstream of the Lockport Lock and Dam. See *Plates B and C* for the Federal Emergency Management Agency's 1% annual chance maps of this area. During flood events, Deep Run could potentially connect to the CSSC and creates an aquatic pathway around the Lockport Lock. A hydraulic study would be required to make this determination.
4. An open aquatic pathway to the Des Plaines River exists downstream of Lockport near the Brandon Road Lock and Dam location. Several overflow locations from the Des Plaines River to the CSSC upstream of the dispersal electric barrier were identified as part of the Chicago District's The Dispersal Barrier Efficacy Study- Interim I. As these locations were upstream of the existing dispersal (electric) barrier system, if the ANS carps were to traverse the Des Plaines River upstream to these overflow areas, and flooding occurs, they could easily gain access to the CSSC and disperse freely to Lake Michigan. A Des Plaines River Barrier was constructed in 2010 to address this overflow concern. The Des Plaines River Barrier consists of jersey barriers and 1/4" mesh fence, which ranges in height from 4' to 8'. The barrier is constructed along the Centennial Trail which begins at 135th Street in Romeoville, IL (Will County) extends through Cook and DuPage County and terminates north of I294 in Cook County. Figure 5 indicates the location of this barrier system. The barrier system was constructed at the 1% annual chance flood elevation with 3 levels of free board. The 1/4" wire mesh of the chain link fence is designed to prevent all fish greater than a 1/4" in girth from bypassing. The current threat of Asian carps dispersal is from large adults. If eggs and larvae were present in the Des Plaines River they will likely be swept downstream to below barrier reaches within hours since they have no swimming capability<sup>7</sup>.

While this open aquatic pathway through the Des Plaines River to the CSSC has been mitigated, a potential for this system to overtop or to fail may be present.

<sup>6</sup> Information obtained from Chicago District phone conversations with MWRDGC's Department of Maintenance and Operations staff and Rock Island District H&H staff.

<sup>7</sup> US Army Corps of Engineers. Dispersal Barrier Efficacy Study: INTERIM I – Dispersal Barrier Bypass Risk Reduction Study & Integrated Environmental Assessment. January 2010.

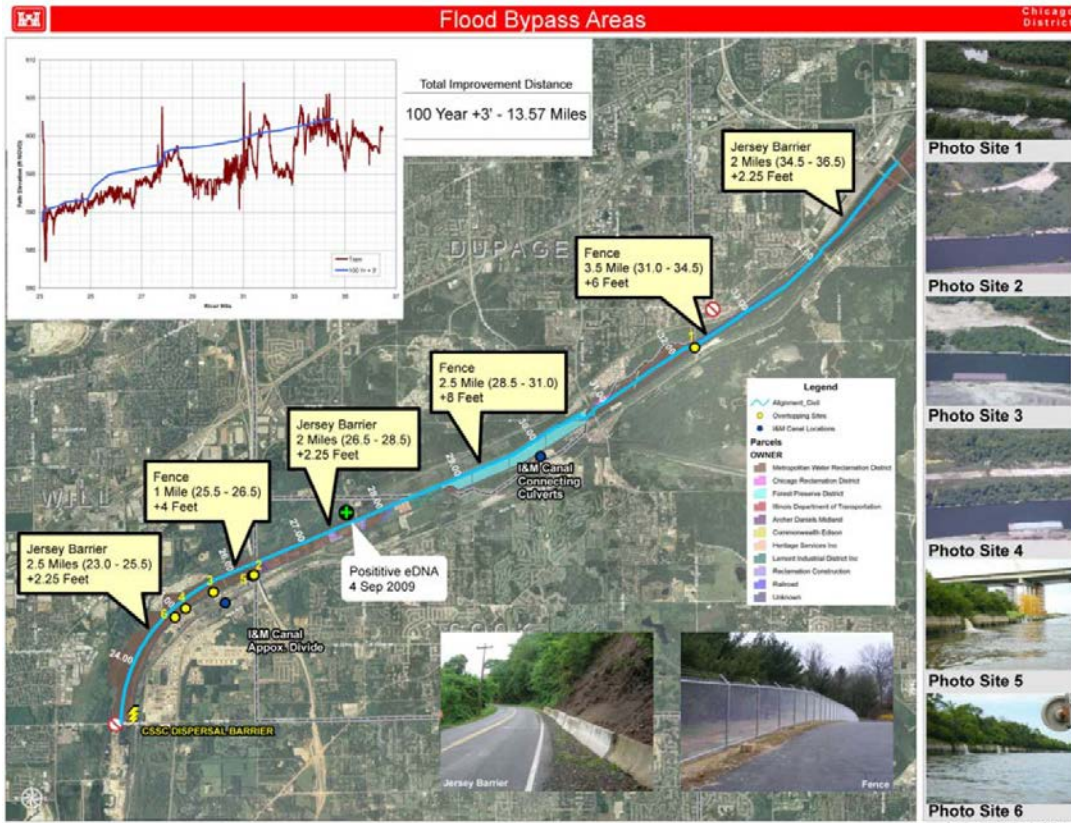


Figure 5: Des Plaines River Barrier Location

5. The Dispersal Barrier Efficacy Study- Interim I also identified that an open aquatic pathway to the I&M Canal existed through a connection to Deep Run, which has a direct connection to the Des Plaines River downstream of Lockport. If ANS were able to traverse upstream in the I&M Canal, culverts between the I&M Canal and the CSSC posed a potential aquatic pathway. A blockage berm was placed within the I&M canal at an identified flow divide location in Lemont, IL to prevent upstream transfer through the Canal's culverts into the CSSC. The berm was constructed at the calculated 1% annual chance flood elevation.
6. Lastly, another potential aquatic pathway around the Lockport Lock and Dam may exist at a small abandoned lock immediately adjacent to the lock and dam.<sup>8</sup> See *Figure 3*. This lock has been bulkheaded.

## II. BRANDON ROAD LOCK

The Brandon Road Lock and Dam is located in Joliet, Illinois on the Des Plaines River at Mile 286. See *Figure 6*. USACE regulates, operates and maintains this lock. Originally constructed in 1933 and rehabilitated from 1984 to 1987, the Brandon Road Lock and Dam contains one lock chamber and a dam. See *Plate D* for an Illinois Waterway Navigational Chart of the area in the vicinity of this lock and dam. The Rock Island District coordinates operations of the Brandon Road pool with MWRDGC. The inflow of this pool is dependent on the outflow from the MWRDGC facility at Lockport, Illinois.<sup>9</sup>

<sup>8</sup> Lockport. . . Master Reservoir Regulation Manual. Abandoned lock noted on the bottom of Plate 2-4

<sup>9</sup> Brandon Rd. . . Master Water Control Manual, page 1-3.

The dimensions of the lock chamber are 600 feet long by 110 feet wide. The lock's average filling time is 19 minutes, and the average emptying time is 15 minutes.

Three potential aquatic pathways have been identified:

1. Brandon Road Dam is an aquatic pathway around the Brandon Road Lock. This dam contains eight (8) operational headgates and 21 tainter gates. Water velocity through the dam's headgates ranges from approximately 28 to 42 feet per second.<sup>10</sup> The nominal lift between the Brandon Road Pool and the Dresden Island Pool equals approximately 34 feet.<sup>11</sup>
2. An inoperable lock is located northwest of the Brandon Road Lock and Dam. See *Figure 7* for the location of the inoperable lock. This inoperable lock connects the Des Plaines River with the Illinois and Michigan Canal (I&M Canal), and it contains a sluice gate. The pathway between the Des Plaines River and the I&M Canal occurs when the sluice gate is occasionally opened to allow water from the river to flow into the canal.
3. A potential bypass has been identified around the Brandon Road Lock and Dam through an open aquatic pathway in the DuPage River basin. The potential pathway follows the DuPage River to the I&M Canal and through the Rock Run Tributary.

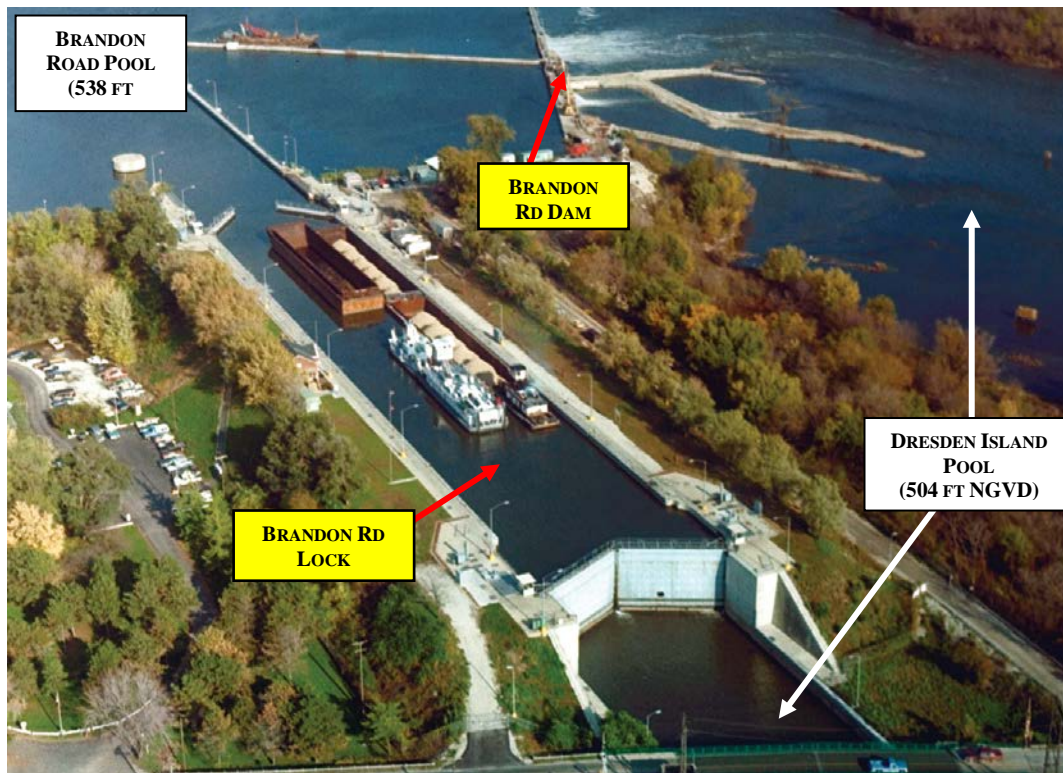


Figure 6: Bird's Eye View of Brandon Road Lock and Dam

<sup>10</sup> US Army Corps of Engineers, Inland Navigation Design Center (INDC), [H&H information for Brandon Road ANS Lock \(GLMRIS\)](#), 28July 2015.

<sup>11</sup> [Brandon Rd. . .Master Water Control Manual](#), page 2-1.

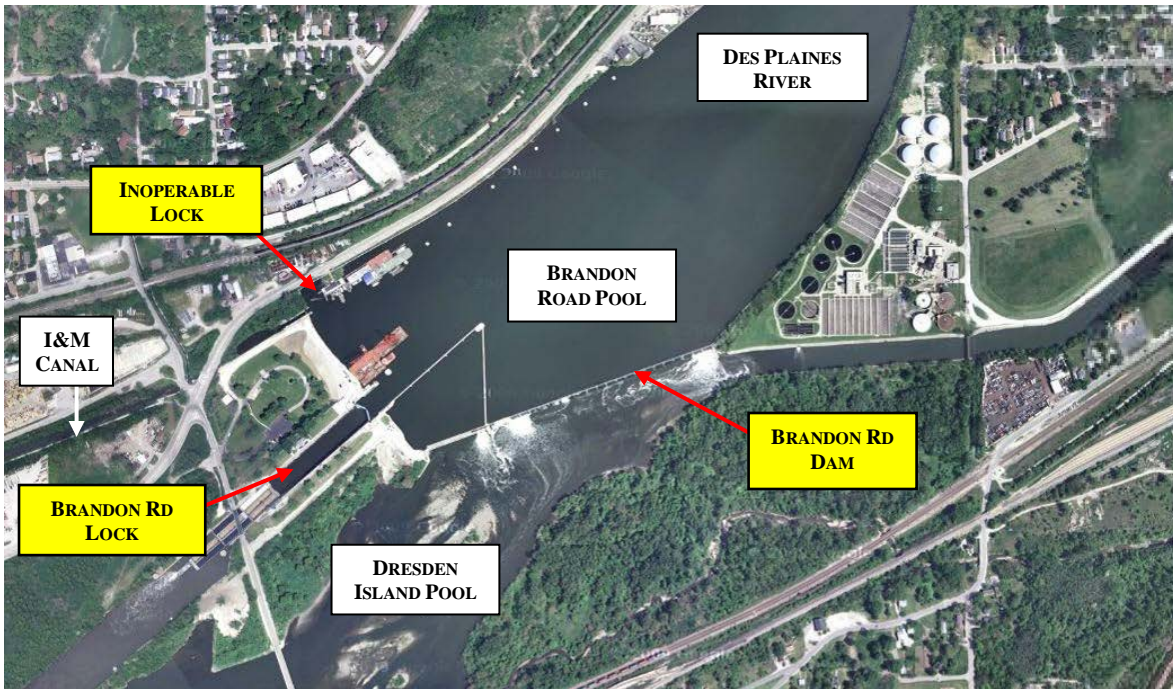


Figure 7: Aerial view of Brandon Road Lock and Dam

### Comparison of Aquatic Pathways at Lockport and Brandon Road:

Potential aquatic pathways at Brandon Road are less complex and less geographically expansive than the pathways at Lockport.

Specifically, modifications to the structure and/ or operations of the Lockport Controlling works would require significant coordination with MWRDGC and modifications to flood control operations may be difficult to adopt due to the direct relationship to flood risk in the Chicagoland area. Additionally, the potential hydrologic bypass (flanking) from the Des Plaines River to the CSSC and from Deep Run to the CSSC that may occur during periods of high flow presents an aquatic pathway for ANS to transfer to the GL basin which may be difficult to fully address.

Due to the complexity of pathways at Lockport Lock and Dam and challenges associated with eliminating those pathways in comparison to the challenges associated with the pathways at the Brandon Road location, *Brandon Road is considered to be preferable to Lockport for this criterion.*

### Review and Recommendation:

Specifically, a review of potential aquatic pathways indicates that selection of Lockport Lock and Dam location as a control point would include numerous challenges related to hydraulic separation at the Controlling Works and at locations where flanking between the CSSC, the Des Plaines River, and Deep Run may occur during high water events occurs. Due particularly to these challenges, in addition to the review of all other considered criteria, the Chicago District recommends that the Brandon Road Lock and Dam facility be selected as the optimal location for the implementation of a downstream control point.

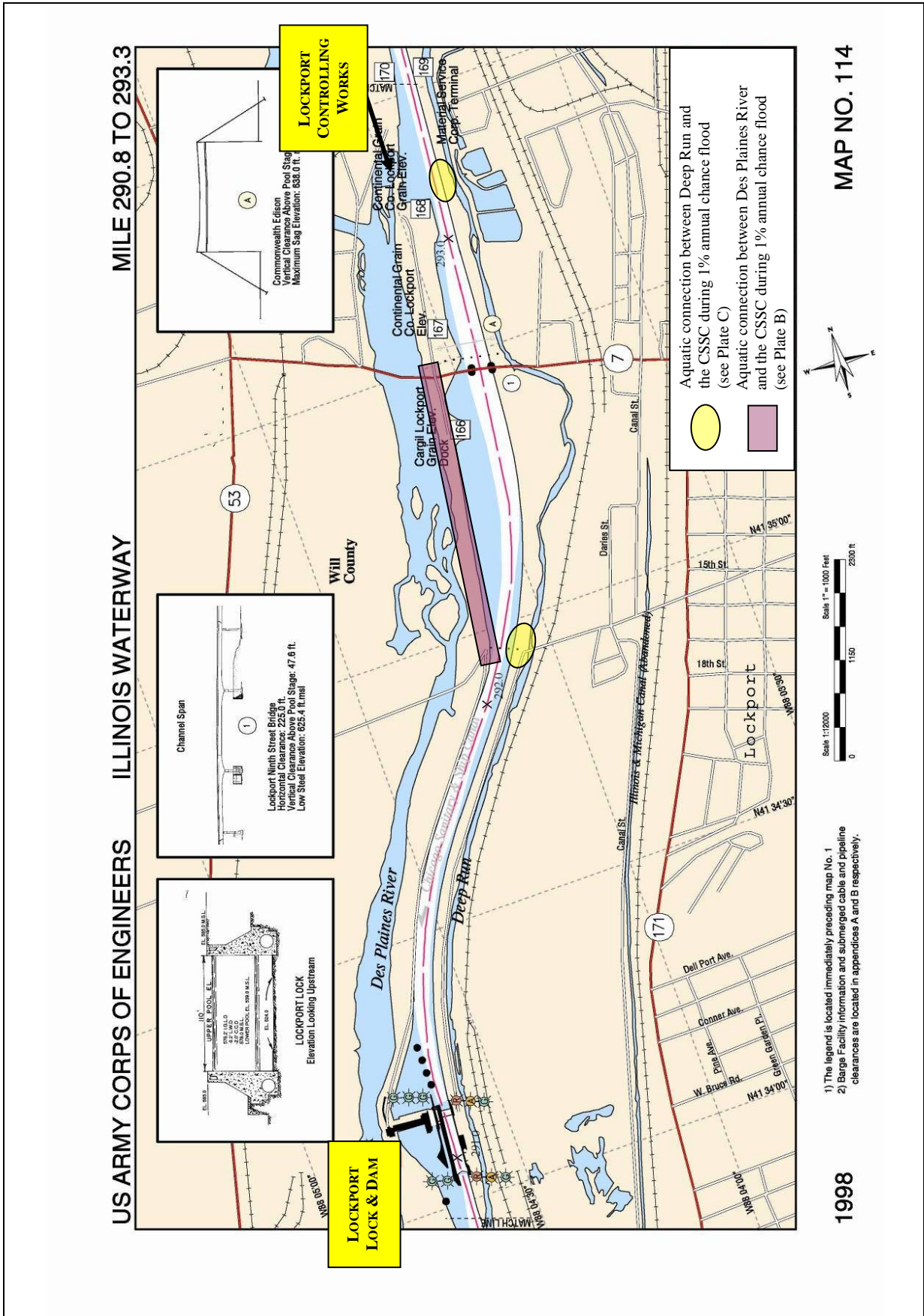


Plate A: Illinois Waterway Navigation Chart in the Vicinity of Lockport Lock and Dam

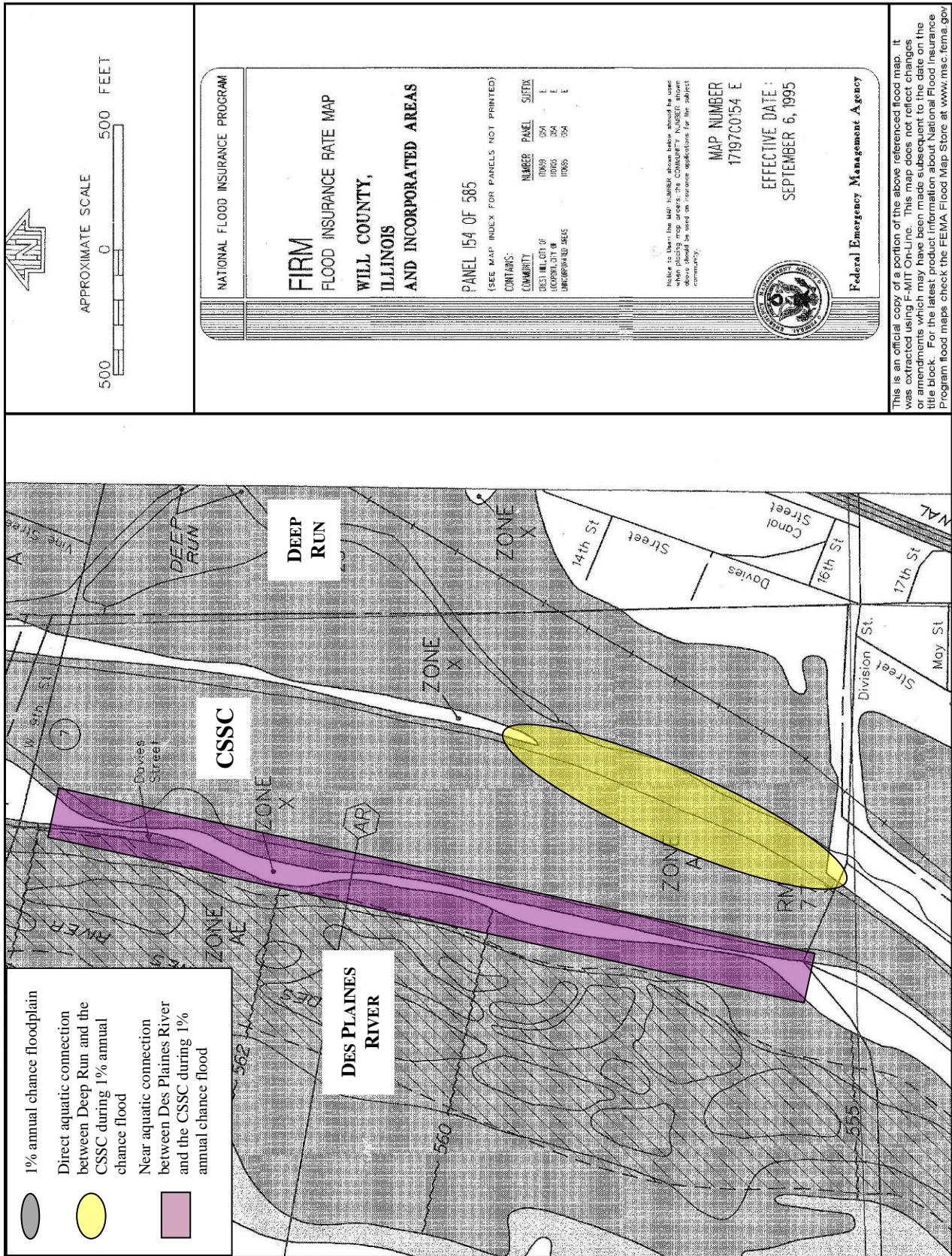
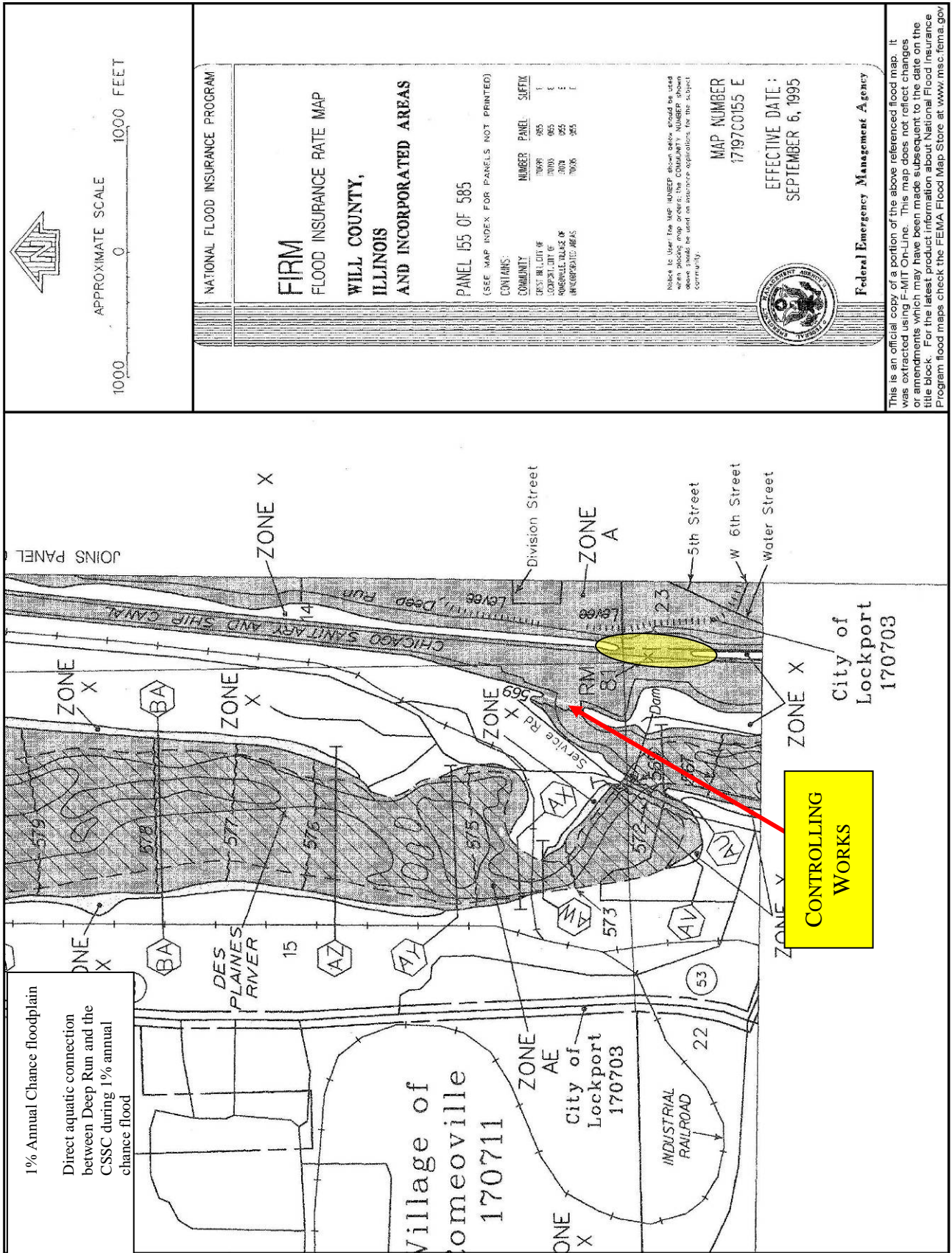


Plate B: 1% Annual Chance Flood Plain Maps - Aquatic Pathway Connecting the CSSC with Deep Run and Possible Aquatic Pathway Connecting the CSSC to the Des Plaines River - Area Located Between Lockport Lock and Dam and Lockport Lockport Controlling Works



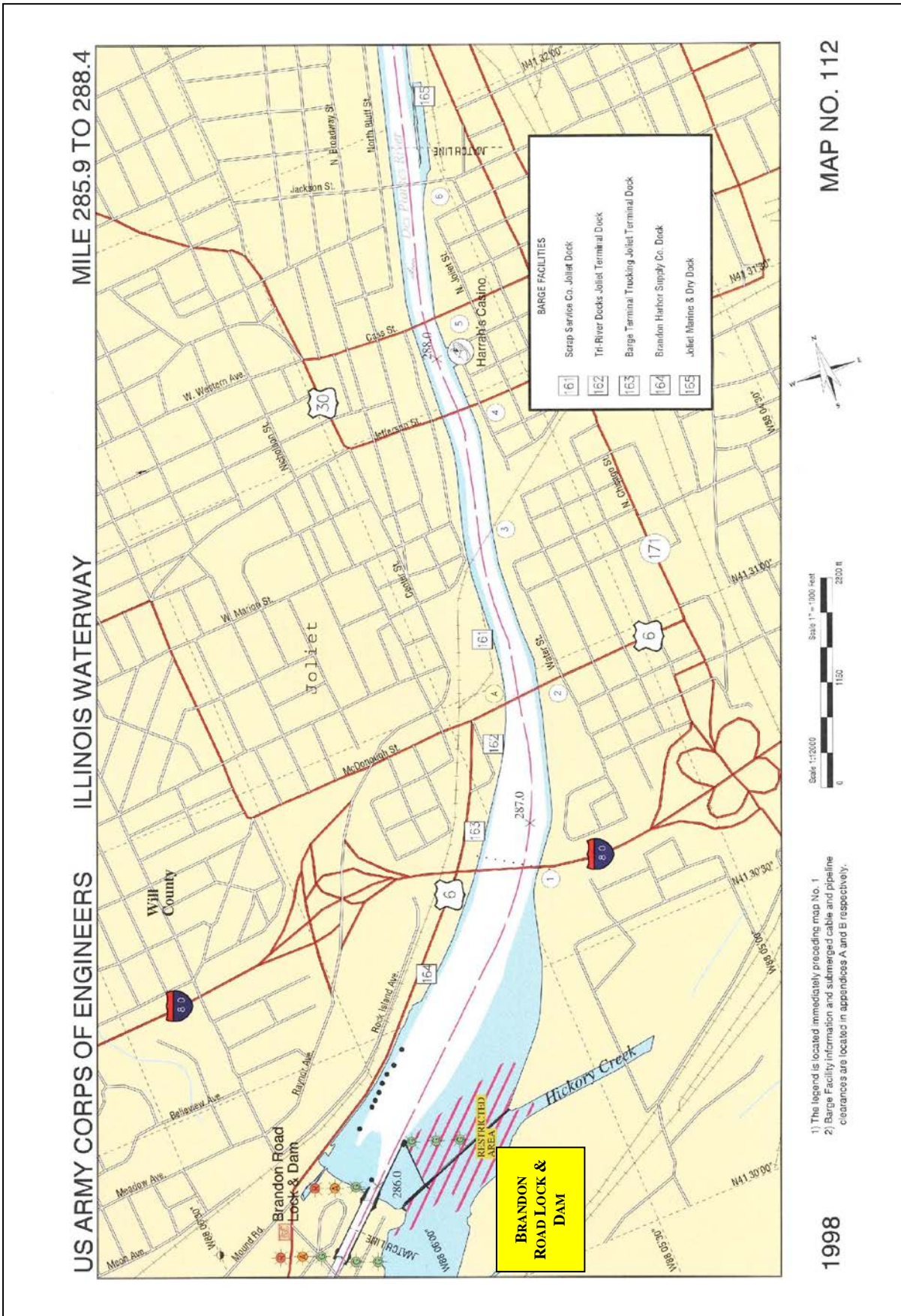


Plate D: Illinois Waterway Navigation Chart in the Vicinity of Brandon Road Lock and Dam

**GLMRIS - Brandon Road**  
**Appendix E - Hydrology and Hydraulics**

**USACE Inland Navigation Design Center (INDC)**  
**H&H Information for Brandon Road Lock**

## CONTENTS

<b>1</b>	<b>GENERAL PURPOSE</b>	<b>E-20</b>
<b>2</b>	<b>PERTINENT DATA FOR BRANDON ROAD LOCK &amp; DAM</b>	<b>E-20</b>
<b>3</b>	<b>MODELING DISCHARGES</b>	<b>E-21</b>
3.1	Flow Duration Flows & Elevations	E-21
3.2	Annual Chance Exceedance (ACE) Flows & Elevations	E-22
<b>4</b>	<b>HEAD GATE VELOCITIES</b>	<b>E-22</b>
4.1	Debris Concern	E-27
4.2	Head Gate Tailwater Submergence	E-27
<b>5</b>	<b>FILLING VALVES</b>	<b>E-28</b>
<b>6</b>	<b>ANS TRANSFER VIA I&amp;M CANAL</b>	<b>E-32</b>
6.1	Brandon Road Pool Fluctuations	E-33
6.2	High Tailwater on the Illinois Waterway	E-34
6.3	I&M Canal Overland Flow	E-35
<b>7</b>	<b>WATER SUPPLY DURING LOW FLOW PERIODS</b>	<b>E-37</b>
7.1	Navigation during Low Flow Periods	E-38
7.2	Required Number of Flushes	E-39
7.3	USGS Lock Chamber Velocity and Discharge Measurements	E-39
7.4	Conclusions on Water Supply	E-40

## 1 GENERAL PURPOSE

The H&H analyses in this summary report were performed through the INDC by Rock Island District. The information in this Appendix was developed to provide background information regarding water resources related topics to the design team throughout the Feasibility Study.

## 2 PERTINENT DATA FOR BRANDON ROAD LOCK & DAM

### Datum Conversions

1929 = 1912 – 0.45 ft

1988 = 1929 – 0.2 ft

1988 = 1912 – 0.65 ft

Original drawings use 1912 datum and many newer texts use 1929 datum. River data is collected in 1929.

### Lock Information

Nominal Length of Chamber 600 ft

Pintle to Pintle Length of Chamber 671 ft

Chamber Width 110 ft

Flat Pool 538.5 ft (1929) (water level data is still being recorded in 1929 datum)

Flat Tail 504.5 ft (1929)

Minimum Tail 504.1 ft (1929)

Operational Pool (High): 538.9 ft

Operational Pool (Low): 538.4 ft

Upper Miter gate leakage 60 cfs (includes valve leakage, valve is shut) USGS measured

Lower Miter gate leakage 185 cfs (also includes valve leakage when valve is shut)

Upper Miter Gate Height 20 ft

Lower Miter Gate Height 50 ft

Sill Elevation (upper) 520.7 ft (1929)

Sill Elevation (lower) 490.75 ft (1929)

Chamber Floor: 489.7 ft (1929)

### Lock Volume Calculations

\*\* Pintle to Pintle distance (671 ft) used for volume computations:

Normal Pool Depth in the Chamber 48.8 ft (538.5 – 489.7)

Minimum Depth in the Chamber 14.8 ft (504.5 – 489.7)

Typical Lift 34.0 ft (48.8 – 14.8)

Lock Volume without vessel displacement: 2,509,540 cubic feet (34.0 \* 110 \* 671)

Lock Volume with 3x3 barges in chamber drafting 9 ft: 1,943,280 cubic feet

Typical Filling Time 19 min  
Typical Emptying Time 15 min  
Average Inflow while Filling 1710 cfs  
Average Discharge while Emptying 2159 cfs  
Peak Discharge while Emptying 7120 cfs (measured by USGS on Dec 8-10, 2014)

Max Flow during a Flushing Operation 1350 cfs (both valves at 1/4 open) (USGS measured)  
Minimum Depth over Lower Sill 13.75 ft (504.5 – 490.75)  
Velocity over Lower Sill while Flushing 0.87 ft/s

Note that during a flushing operation, the discharges are less than instantaneous discharges from a pool to tail chamber discharge. This is because the intake valve (upstream) has a limited range of opening due to pinning forces at full head when used for flushing. As a result, downstream erosion or sedimentation were not specifically addressed or evaluated the potential for downstream erosion.

### **Dam Information**

Tainter crest of skin plate (gate closed) 539.4 ft (1929) overtopping coefficient 3.5  
Bottom Elevation of Open Tainter Gate 539.5 ft (1929)  
Crest of Ogee Spillway under Tainter Gates 536.25 ft (1929) overtopping coefficient 3.3  
Tainter gates are 50 ft wide by 2' 3.5" high, 21 tainter gates  
Each Tainter Gate releases 550 cfs discharge when fully opened; partial openings are not used.  
Head Gate Sill 510.5 ft (1929)  
Head Gates are 15 ft wide by 15.75 ft high, 8 head gates (+8 more that were sealed off)  
Each Head Gate releases approximately 450 cfs per foot of opening, or 6800 cfs fully opened

## **3 MODELING DISCHARGES**

It was concluded that “Low”, “Medium”, and “High” flow rates should be considered as 1260 cfs, 11200 cfs, and 15000 cfs for Brandon Road, respectively. These will be used for design work into the future. Medium and low flow rates were obtained with a duration curve and the high flow came from the navigational restriction of 15,000 cfs, when lockages are halted on the Illinois Waterway at Brandon Road Lock.

### **3.1 Flow Duration Flows & Elevations**

The 50% Duration was originally used for a medium flow based on ranking daily data from the past 10 years of record. As a comparison, the 1940-1976 Flow Duration for 50% is 3200 cfs (versus 3160 cfs for the past 10 years), and the stage duration for 1935-2011 is 505.2 ft which matched the past 10 years of data. While the USGS gage has a short record, it is in line with past data on file. The medium flow was changed from the 50% to the 2.5% duration to have a wider

distribution of flows, and the high flow was changed from the 0.2% annual chance event to the maximum flow where navigation halts.

Based on the USGS gage daily mean record for DES PLAINES RIVER AT ROUTE 53 AT JOLIET, IL (Station ID 5537980) 02/2005 - 10/2014

2.5% = 11200 cfs (506.6 ft 1929 datum) (Recommended “Medium” flow for analyses)  
5.0% = 8790 cfs (506.2 ft)  
25.0% = 4630 cfs (505.5 ft)  
50.0% = 3160 cfs (505.2 ft)  
75.0% = 2380 cfs (504.9 ft)  
95.0% = 1350 cfs (504.7 ft)  
97.5% = 1260 cfs (504.5 ft) (Recommended “Low” flow for analyses)

### 3.2 Annual Chance Exceedance (ACE) Flows & Elevations

Brandon Rd Lock is unique in that it does not close during high events, so barges may still lock through during a 0.2% Annual Chance Exceedance (500-year) event. At this frequency the head difference between pool and tail is still greater than 20 ft. Navigation stops at 15,000 cfs however due to traffic constraints (no lockages) upstream and downstream of Brandon Road. The frequency data below is from the 2004 Flood Frequency Study, located at River Mile 285.95 just downstream of the dam.

#### Frequency Information

0.2% = 500-year = 36,000 cfs (514.5 ft 1929 datum)  
0.5% = 200-year = 33,000 cfs (513.5 ft)  
1.0% = 100-year = 30,000 cfs (512.6 ft)  
2.0% = 50-year = 28,000 cfs (512.0 ft)  
4.0% = 25-year = 24,000 cfs (511.2 ft)  
10% = 10-year = 21,000 cfs (510.8 ft)  
20% = 5-year = 17,000 cfs (510.2 ft)  
32% = 3.8-year = 15,000 cfs (509.9 ft)\*  
50% = 2-year = 12,000 cfs (509.5 ft)

\* 15,000 cfs is the recommended “High” flow for analyses, as 15,000 cfs is the maximum flow for upstream lockages

## 4 HEAD GATE VELOCITIES

This analysis was performed because of the concern that ANS swimmers might be able to pass upstream through the head gates at Brandon Road Dam. The concern at debris passage was also considered because of the thought that large debris might prevent the head gates from closing. To be able to address these concerns, the water velocity of the jet coming through the opened head gate must be estimated and compared to the estimated burst speed of the ANS swimmers, especially Asian Carp. It was concluded by a panel of experts (November 2015) that the velocity

coming through the head gates (28 ft/s) was too strong for ANS passage. Details of the analysis are below.

Lock and dam personnel should utilize the tainter gates to maintain the upstream pool within the authorized limits. After all tainter gates have been opened then the Head Gates are used to pass additional flow. Head Gate velocities and velocities downstream of the lock were estimated using the as-built drawings and hand calculations. Figure 1 is a drawing of the Head Gate geometry after the major rehabilitation work in the 1980's. There are currently eight head gates that are 15 ft wide by 16 ft high, five of which are raised and lowered by a mobile crane. The opening height is 15.75 ft high, and the gate sill elevation is 510.5 ft.

The recommended low, medium and high flows for modeling/analyses all have tailwater elevations below the head gate sill (the tailwater is 509.9 ft at a high flow of 15,000 cfs), so any potential for upstream passage of aquatic nuisance species (ANS) would be confined to times of larger flood events when the tailwater depths are higher than the head gate sill elevation of 510.5 ft. The depth of water on the head gate sill is shown on Table 1 below for various Annual Chance Exceedance (ACE) floods:

*Table 1 Depth of Water on the Head Gate Sill during Frequency Event Flooding*

Depth on Sill (ft)	Annual Chance Exceedance (ACE)	Recurrence Interval (1/ACE)
0.3	10%	10-year
0.7	4%	25-year
1.5	2%	50-year
2.1	1%	100-year
3.0	0.5%	200-year
4.0	0.2%	500-year



Normal Pool Elevation: 538.5 ft 1929 datum

Top of Gate Opening = 526.75 ft (1912 datum) or 526.3 ft (1929 datum)

Sill Elevation of Head Gates = 511 ft (1912 datum) or 510.55 ft (1929 datum)

Tailwater at High Flow Elevation (3.8-year ACE or 15,000 cfs) = 509.9 ft (1929)

Initial estimates of velocity through head gates at 20 ft head are 28 to 42 ft/s depending where in the water column from the Head Gate sill to the Top of the gate opening. Calculations appear on Table 2 below).

**Table 2: Velocity Calculations for Head Gates at Brandon Road Dam**

**head gate  
computations**

RI	freq elevs	depth (ft) on sill
500	514.5	4
200	513.5	3
100	512.6	2.1
50	512	1.5
25	511.2	0.7
10	510.8	0.3

**head gate computations**

Flow Equation Q	$CA\sqrt{2gH}$	
=		
Qcoef (C)	0.8	
Height Gate	15.75	ft
Width Gate	15	ft
Area of Opening	236.25	ft <sup>2</sup>
2g	64.4	ft/s <sup>2</sup>
pool	538.55	ft 1929
sill	510.5	ft 1929
Head ave	20.1	ft
Q (head gate discharge full open)	<b>6800</b>	<b>cfs</b>

Vertical Profile of Velocity from sill to bottom of fully open head gate

	Head (ft)		Velocity (ft/s)
bottom of fully open head gate	12.3	upper	28.1
middle of fully open sill elevation	20.55	mid	<b>36.4</b>
Head Gate	28.05	lower	42.5

Gate Opening (ft)	Coef	A	H (ft)	Total Q (cfs)	Ave Q per foot opening	<u>frequency (ACE)</u>	Average Velocity (ft/s)
0	0.73	0	28.05	0	0		0
0.3	0.73	4.5	27.90	139	464	10.0%	30.9
0.7	0.73	10.5	27.70	324	462	4.0%	30.8
1	0.73	15	27.55	461	461		30.7
1.5	0.73	22.5	27.30	689	459	2.0%	30.6
2	0.73	30	27.05	914	457		30.5
2.1	0.73	31.5	27.00	959	457	1.0%	30.4
3	0.74	45	26.55	1377	459	0.5%	30.6
4	0.74	60	26.05	1819	455	0.2%	30.3
5	0.74	75	25.55	2251	450		30.0
6	0.75	90	25.05	2711	452		30.1
7	0.76	105	24.55	3173	453		30.2
8	0.77	120	24.05	3636	455		30.3
9	0.77	135	23.55	4048	450		30.0
10	0.78	150	23.05	4508	451		30.1
11	0.79	165	22.55	4967	452		30.1
12	0.8	180	22.05	5426	452		30.1
13	0.81	195	21.55	5884	453		30.2
14	0.82	210	21.05	6340	453		30.2
15	0.81	225	20.55	6630	442		29.5
16	0.8	236.25	20.175	6813	426		28.8

*rule-of-thumb at site 450 cfs/ft*

The average velocity through the head gates using a conservative water depth (H) of 20 ft is 30 ft/s. A maximum velocity threshold for ANS transfer has not yet been specified, so it is currently unknown what velocity is too great for ANS transfer. Therefore, Head Gate velocities were looked at more closely to determine if initial velocity estimates could at all be lowered by such factors as debris, downstream submergence, and gate operations. These further analyses found that 28 ft/s is the lowest spot velocity possible through the head gates (see details below).

## 4.1 Debris Concern

The consideration of debris causing pockets of lower velocity has been examined. The head gates are 15 ft wide and 16 ft tall. They can be operated with partial openings and the approximate discharge is 450 cfs per foot of opening. From experience at the site, there has never been trouble with debris in the head gates; debris gets caught on the tainter gates because the debris is floating and a debris and ice wall is in place at this dam. If debris was pulled downward and through the head gates it would most likely occur during a time the gates are fully opened and able to pass such debris. A 16 ft gate opening could then pass debris below it due to the high velocities produced by the head pressure.

## 4.2 Head Gate Tailwater Submergence

A literature search was conducted to address the condition where tailwater submergence would decrease the velocities through the head gates. The following three journal articles were used to conduct a submerged velocity analysis given the geometry at Brandon Road Dam:

(i) Gumus V.; Simsek O.; Soydan N. G.; Akoz M. S.; and Kirkgoz M. S. (2015). “*Numerical Modeling of Submerged Hydraulic Jump from a Sluice Gate*”, Journal of Irrigation and Drainage Engineering, ASCE, August 2015.

(ii) Cassan L. and Belaud G. (2011). “*Experimental and Numerical Investigation of Flow under Sluice Gates*”, Journal of Hydraulic Engineering, ASCE, September 2011.

(iii) Shammaa Y.; Zhu D. Z.; and Rajaratnam N. (2005). “*Flow Upstream of Orifices and Sluice Gates*”, Journal of Hydraulic Engineering, ASCE, February 2005.

Figure 2 below shows the location of submergence at  $h_1$  in the upper portion of the head gate opening.

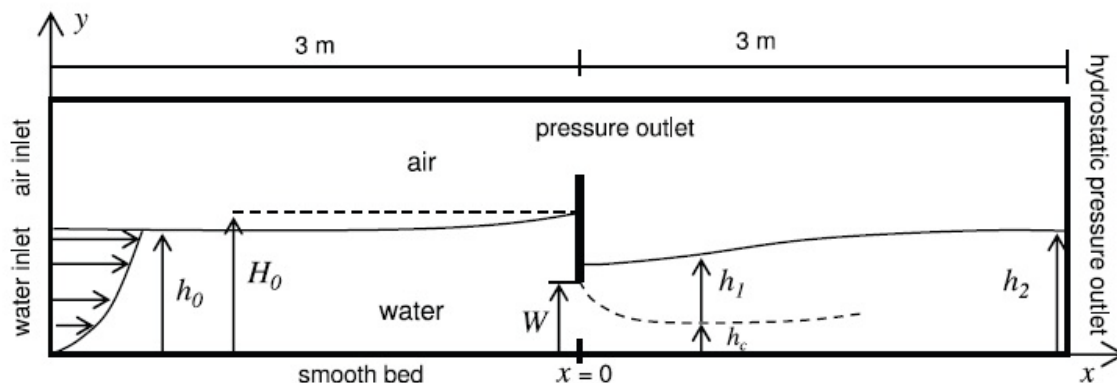


**Figure 2: Domain and Boundary Conditions for 2D RANS simulation of the submerged sluice gate**

Spreadsheet calculations show that as the tailwater rises and submerges the head gate jets, the average velocity through the gate becomes smaller. Also, as the difference between Pool and Tail decreases, the average velocity through the gate decreases. However, site conditions at Brandon Road do not permit this difference to become too small to significantly decrease velocities through the head gates. Velocity decreases of 2 ft/s were seen at various elevations through the water column. The minimum velocity through the Head Gates at Brandon Road Dam should be considered to be 28 ft/s.

During the literature research for sluice gate discharge under submerged tail conditions, all the figures showed that the maximum velocity on the vertical velocity distribution curves is near the channel bottom both upstream and downstream of the sluice gate. Therefore, it is possible to increase the average velocity through the head gates by opening more head gates and keeping them at smaller openings; however the increase in average velocity through these head gates would be small (approximately 2 ft/s). The maximum burst velocity of ANS must be 28 ft/s or higher for upstream passage of ANS to occur through the Head Gates of Brandon Road Dam.

## **5 FILLING VALVES**

The purpose of this analysis is to quantify the amount of water that enters the lock chamber during lockage and flushing operations. These calculations were made manually and were verified by direct measurement by the USGS on December 9, 2014. This information was given to ERDC to help their modeling of 3D flushing of ANS particles (floaters) in the lock chamber.

Valve height 8.5 ft in valve assembly drawing (and 7' - 9" in the water control manual)

Drawing "Valve Well Steelwork General" shows 9' - 0" high. 9' x 9'

Culvert width under the valve is 9 ft

Valve type: vertical lift gate (sluice gate), sill elevation, Flat Pool elevation 538.5 ft

Sill elevation of lift gate 506 ft (upper valve) and 492.7 ft (lower valve).

When the upper valves are greater than 1/4 open and there is a normal tailwater elevation, head pressure on the upstream side of the valve cause the gate to vibrate or get stuck when closing. This will need to be addressed during final design.

Typically the lock filling valve is under 32.5 ft of head (538.5 – 506.0), and the tailwater is at its flat pool elevation of 504.5 ft 1929 datum. A simplified diagram appears in Figure 3, along with equations and discharge calculations in Table 3. The discharge coefficients are taken from the Hydraulic Design Criteria (HDC) 320-1 and shown in the graph on Figure 4.

Free Discharge Equation:  $Q = C * A * \text{SQRT}(2gH) * (\% \text{ Gate Opening})$

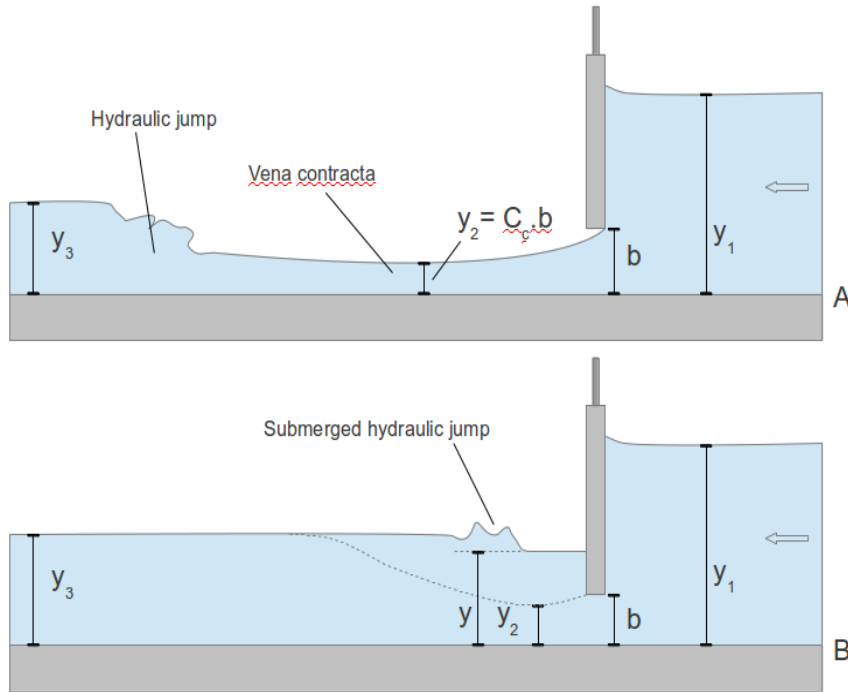


Figure 3: Sluice Gate Discharge, free discharge and submerged discharge

Table 3: Discharge Calculations of Lock Chamber Filling Valves at Brandon Road Lock

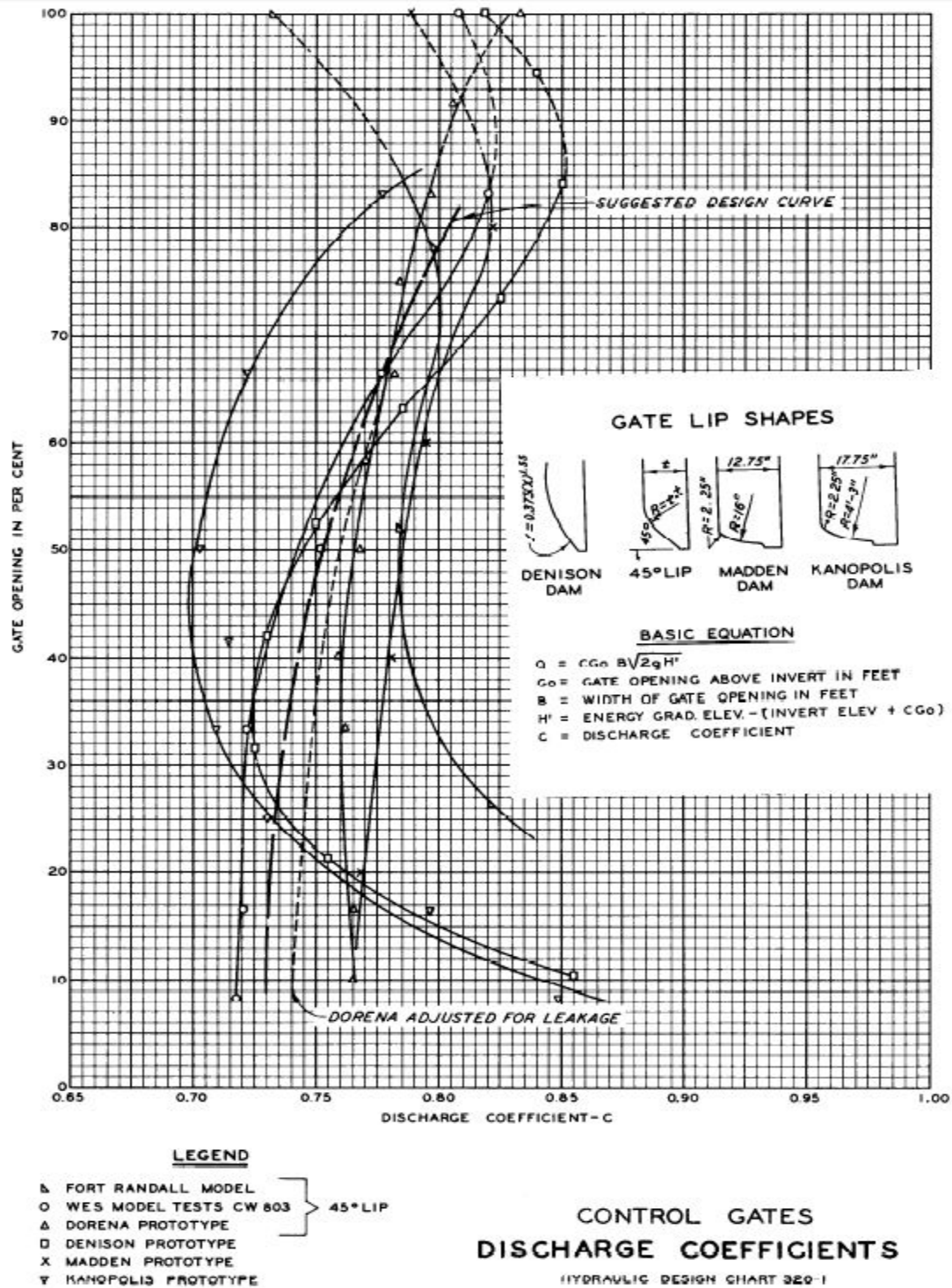
Brandon Road Lock, Filling Valve Sluice Flow							
$Q$ (cfs)	C	A	H to sill 32.5 H	Go Opening percent	Opening ft	ho/h1	
0	0.73	0	32.50	0.0%	0	0.00	
335	0.73	10.125	31.99	12.5%	1.125	0.03	
665	0.73	20.25	31.43	25.0%	2.25	0.07	
1002	0.74	30.375	30.86	37.5%	3.375	0.10	
1342	0.75	40.5	30.30	50.0%	4.5	0.14	
1706	0.77	50.625	29.74	62.5%	5.625	0.17	
2080	0.79	60.75	29.18	75.0%	6.75	0.21	
2495	0.82	70.875	28.61	87.5%	7.875	0.24	
2754	0.80	81	28.05	100.0%	9	0.28	

The average velocity in the chamber would be approximately 0.85 ft/s when flushing continuously using a valve opening of 25%. At this valve opening each filling culvert has a

discharge of 665 cfs. The valve opening of 25% is used because, by experience, this is the maximum opening the valve can be before pinning forces on the gate become a concern during existing debris flushing operations. It is possible for these valves to be re-designed to accommodate larger openings, which will be looked at by the design team in the future.

Flushing is accomplished through the existing side filling ports of the lock, which directs flow into the chamber and out of the opened miter gates downstream. This procedure leaves a “recirculation zone” at the upstream portion of the lock chamber that may not be able to be flushed. Various alternatives were considered by the study team to reduce or eliminate this recirculation zone, and a 3D model was used by ERDC to give recommendations of the best alternatives.

During flushing operations, the lower miter gates must be secured in their recesses using straps or latches to avert the possibility of being pulled into the current and off their hinges. (Miter gates falling off in this fashion are rare but have occurred resulting in long periods of navigation shutdown while the gates are being replaced and gate connections are being repaired.) Securing the miters was done during the USGS data collection period Dec 8-10, 2014. It is recommended that future anti-ANS flushing operations use a permanent latching system for the downstream miter gates (which must be constructed).



WES 4-1-53

Figure 4: Discharge Coefficients of Lock Filling Valve Conduits, Hydraulic Design Criteria (HDC) 320-1

## 6 ANS TRANSFER VIA I&M CANAL

The I&M Canal was built to increase commerce by connecting Lake Michigan to the Mississippi River. The canal was 6 ft deep, 60 ft wide, 96 miles long, and had 15 locks. Construction was completed in 1848. Its function was largely replaced by the wider and shorter Chicago Sanitary and Ship Canal in 1900 and it ceased transportation operations with the completion of the Illinois Waterway in 1933. Since then, the canal has been developed for recreation. The I&M Canal Lock has been closed with a permanent concrete bulkhead placed where the former lock miter gates were located. Current photos of the I&M Canal Lock are shown below; Photo 1 is looking upstream and Photo 2 is looking downstream.

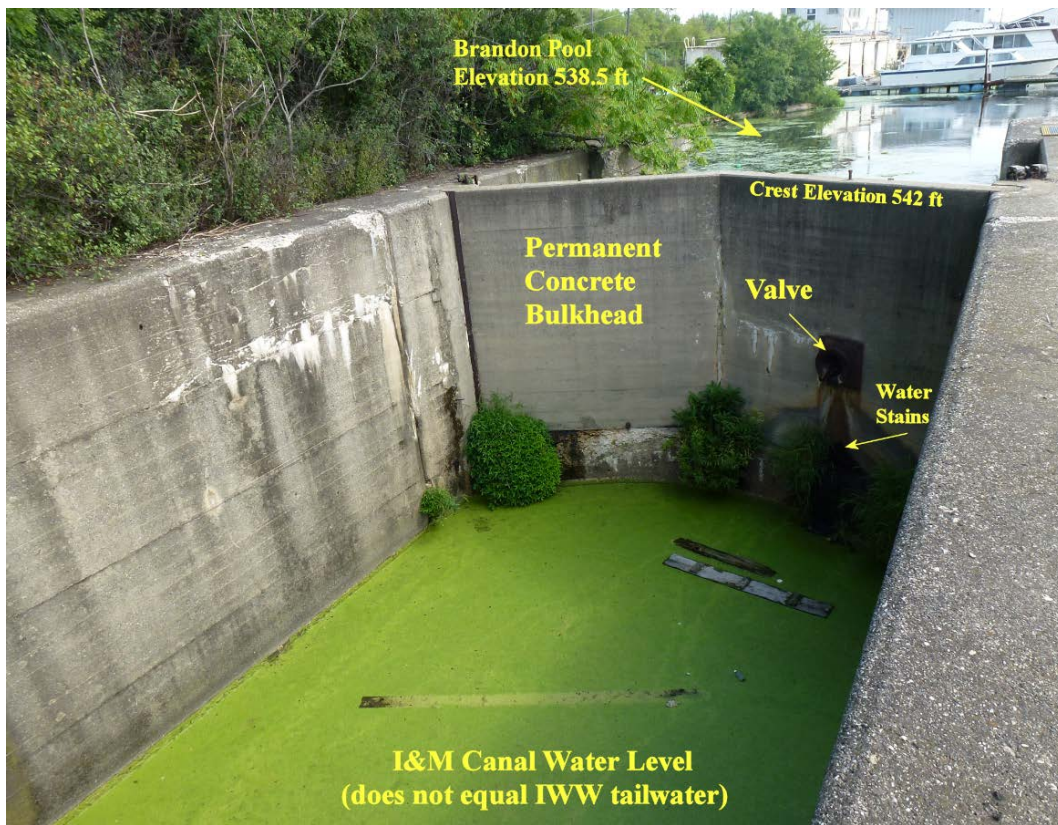


*Photo 1: I&M Canal Lock at Brandon Road closed by a permanent concrete bulkhead*



*Photo 2: I&M Canal Lock at Brandon Road (looking downstream)*

The purpose of this analysis is to investigate whether or not ANS transfer at the I&M Canal Lock is possible from any of three locations. All of these pathways have been found to be highly unlikely but will be further analyzed during PED (preconstruction, engineering, & design). Details of these analyses are given in the following sections below.

The possibility of ANS has been investigated to determine:

- 1) whether the Brandon Road Pool can rise and overtop the I&M Canal's Lock Bulkhead providing a pathway for ANS,
- 2) whether a high tailwater on the Illinois Waterway can bring the water level in the I&M Canal above the invert elevation of a valve that penetrates the permanent concrete bulkhead, assuming this valve would be open at the time, or
- 3) whether overland flow could allow fish access from the I&M Canal to the pool during extreme flood conditions, either over the I&M Canal Lock bulkhead or around it.

## **6.1 Brandon Road Pool Fluctuations**

The Brandon Road pool is held at elevation 538.5 ft throughout the year, and even during flood events. It is possible at this site to hold pool during flood events because there are an adequate number of head gates that can be opened to pass incoming flood flows. A large flood flow of 36,000 cfs (1/500 ACE event) can be passed by four head gates fully open, and there are eight

head gates available on the dam. Therefore, the pool rising and overtopping the I&M Canal bulkhead (crest 542 ft) will not occur. See Photo 2 for level of Brandon Road Pool compared to the crest of the I&M Lock Bulkhead.

## 6.2 High Tailwater on the Illinois Waterway

Normal tailwater is at an elevation of 504.5 ft and can rise ten feet to 514.5 during the 1/500 Annual Chance Exceedance (ACE) Flood. The I&M Canal is separated from the Illinois Waterway by a canal berm and a roadway berm; the I&M Canal does not have a direct connection to the Illinois Waterway near Brandon Road, and does not experience the same fluctuations in water levels. The tailwater on the Illinois Waterway connects to the I&M Canal approximately 10 miles downstream from Brandon Road Lock, and water would have back up into the I&M Canal 10 miles for water levels to be impacted near the I&M Canal Lock; this cannot occur even during a 1/500 ACE flood.

The separation of the I&M Canal from the IWW can be seen in Figure 5. This figure is a GIS generated map of 1 ft LIDAR data showing a close-up view of the elevations in the area of Brandon Road Lock and Dam. Highway 6 is approximately 6 ft higher than the 1/500 ACE event in the IWW tailwater at its lowest point (see Figure 6).

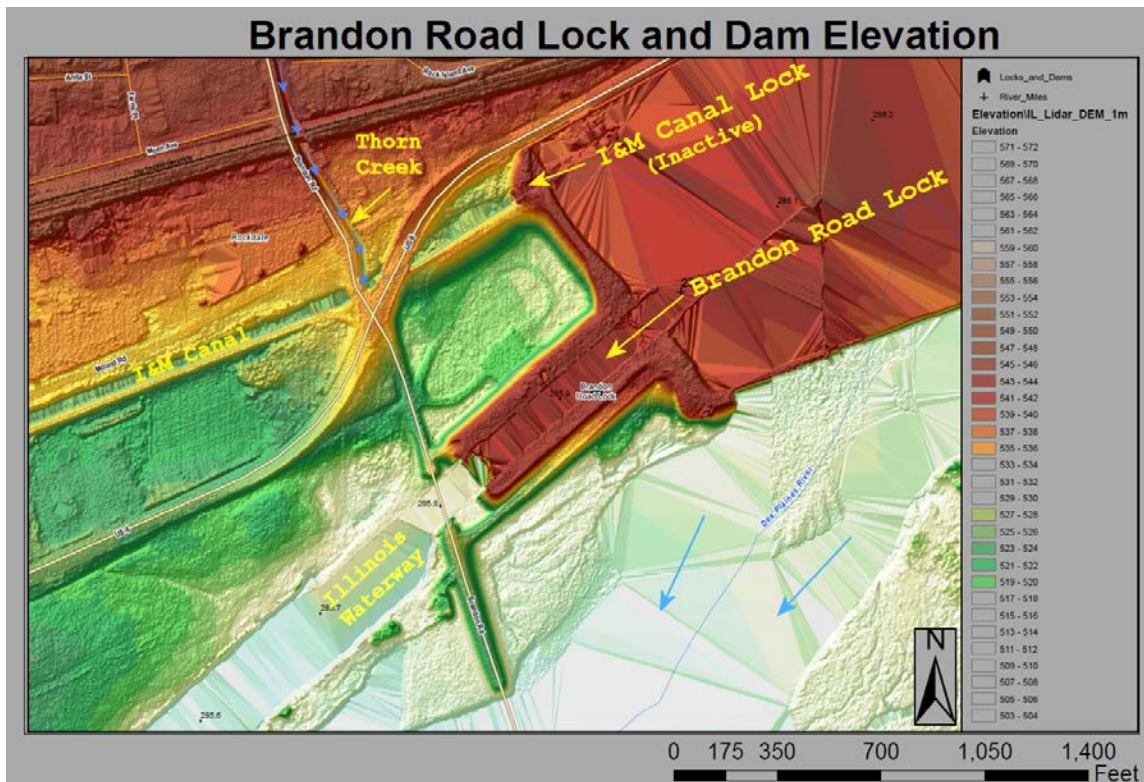
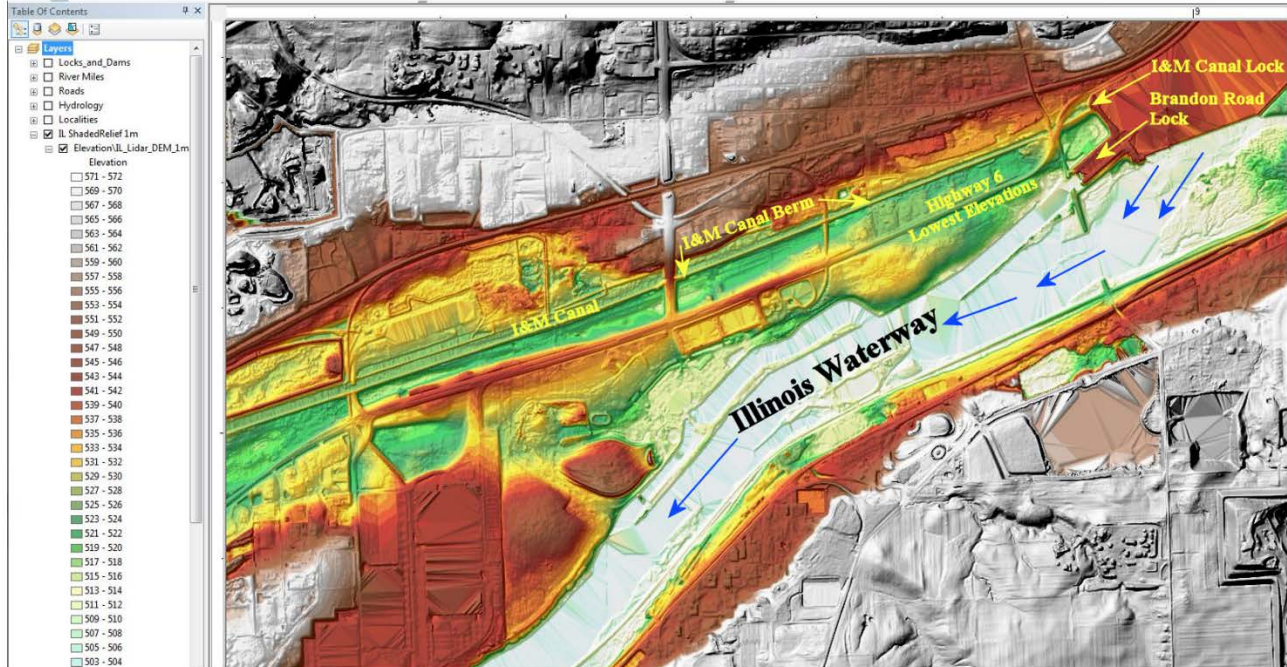


Figure 5: LIDAR elevations near Brandon Road Lock and the I&M Canal Lock



**Figure 6: Regional View of I&M Canal elevations being much greater than Illinois Waterway elevations**

### 6.3 I&M Canal Overland Flow

The potential pathway of ANS using overland flow on Thorne Creek to bypass Brandon Road Lock & Dam at the I&M Canal lock was investigated. The Flood Insurance Rate Map shows a flood elevation of 537 ft (1/100 ACE event) at the junction of Thorne Creek and the I&M Canal (Figure 7). The 1/500 ACE event is 537.2 ft on the corresponding profile graph (Figure 8).

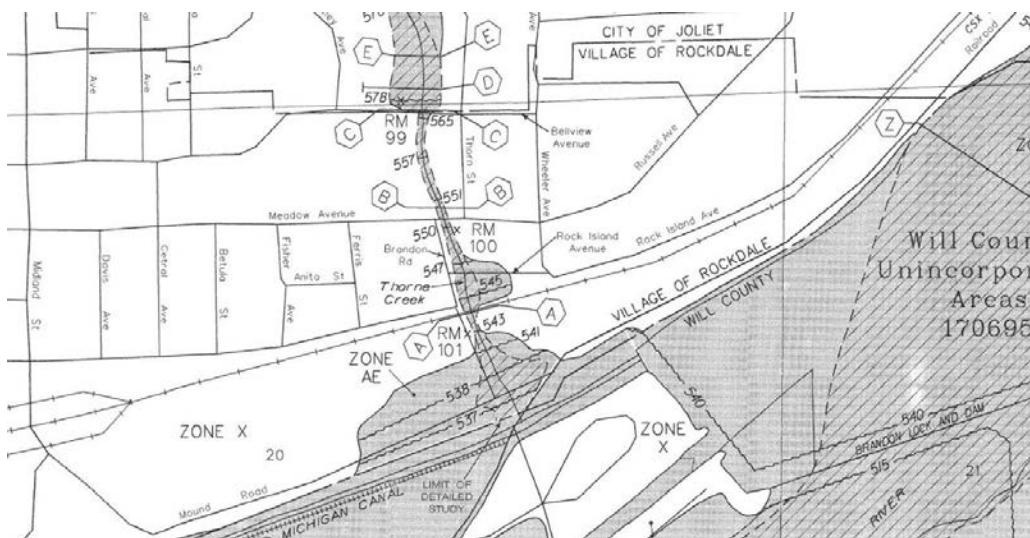


**Figure 7: FEMA FIRM near Brandon Road Lock and Dam (Thorne Creek)**

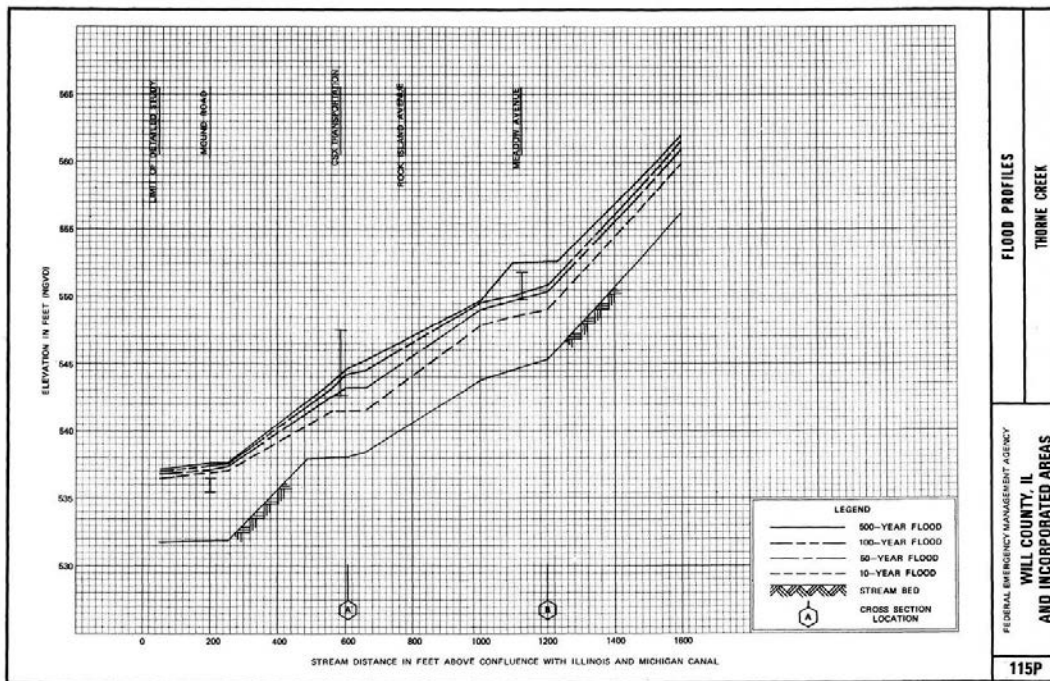


*Figure 8: FEMA FIRM Thorn Creek Flood Profile*

The crest elevation of the permanent concrete bulkhead on the I&M Canal Lock is 542 ft, so a major flood from Thorn Creek cannot overtop it (537.2 ft is the 0.2% Annual Chance Flood on FIRM profile) and this pathway is not viable.

From Photo 2, the invert of the culvert is well below 537.2, so a 0.2% annual chance flood on Thorn Creek, for example, could raise water levels in the I&M Canal above the invert of this culvert. This could lead to a direct pathway for ANS if the valve inside the culvert is operational. Little information exists about this valve but from Photo 2 it is known that the valve is currently closed. Further investigation about the condition of the valve is being conducted by Chicago District COE.

The analysis above does not evaluate the stormwater drainage network adjacent to the I&M canal. An interior drainage study would need to be conducted to accurately assess the I&M canal water levels during different precipitation events and how the storm drainage network might function as a pathway. However, such a study is not expected to produce a pathway for upstream transport of ANS because of the high elevation of the physical embankment separating the Brandon road pool (539 ft) from the I&M canal. Such overland floodwater is likely to enter the I&M Canal and not allow a direct connection during extreme flood events.

## 7 WATER SUPPLY DURING LOW FLOW PERIODS

Brandon Road Lock and Dam is a navigation dam and is not authorized or designed to store water for other purposes. The term “water supply” in this document refers to the inflow of water from the Illinois Waterway plus the possible use of natural water volume within a 0.5 foot operational band for maintaining navigable depths in the pool. A major portion of the inflow to Brandon Road Dam comes from releases from the hydropower plant at Lockport, located five miles upstream of Brandon Road Lock and Dam. The Lockport Hydropower Plant is operated by the Metropolitan Water Reclamation District of Greater Chicago (MWRDGC). The pool extends from Brandon Road Lock and Dam to Lockport Lock and Dam. If the flushing demand is less than the water supply, water can be used to flush ANS neutrally buoyant particles (floaters) out of the chamber prior to each lockage.

Daily average discharges in low flow periods vary, but 1400 cfs is considered a typical value for low flow discharge at Brandon Road (see Table 6). The month of November has the greatest potential for low flows, and 981 cfs is considered a minimum daily average during this month (although lower flows can occur for short periods of time). Table 6 shows monthly values and other statistics based on the USGS gaging station at Ruby Street upstream of Brandon Road Lock and Dam.

**Table 4: USGS Flow Statistics at the Ruby Street Gaging Station**

(USGS 05537980 DES PLAINES RIVER AT ROUTE 53 AT JOLIET, IL 2005-2014 data)

	Jan	Feb	Mar	Apr	May	Jun	Jul	Aug	Sep	Oct	Nov	Dec
Min Daily Ave	1412	1519	2209	1886	1913	1811	1774	1642	1652	1442	981	1434
10th Percentile Ave	n/a	1540	2209	1886	1913	1811	1774	1642	1652	n/a	n/a	n/a
25th Percentile Ave.	1816	1960	2879	2808	2492	2550	2318	2296	2109	1753	1303	1787
Mean of Monthly	3060	3410	4820	4920	4080	4300	3660	4230	3810	2720	2110	3300
75th Percentile Ave	4061	4774	6325	7072	5208	5962	4824	5546	4834	3103	2642	4288
90th Percentile Ave	n/a	9194	10112	10597	9042	9287	7465	9976	9747	n/a	n/a	n/a
Max Daily Ave	6659	8071	10112	10597	9042	9287	7465	9976	9747	6442	4628	8368

## 7.1 Navigation during Low Flow Periods

The Brandon Road pool is very narrow and does not have overbank areas. Because of this, water supply is limited and it is possible for the water level to drop even if all of the Tainter gates at the dam are closed. Flushing of the lock chamber prior to each lockage requires a certain volume of water depending on the duration of flushing and the size of valve opening made to discharge water to the lock chamber. The pool must be controlled within a maximum of 0.5 ft from normal pool (elev 538.5 ft) to stay within authorized navigational limits. Tainter gate operations on the dam need to be coordinated with ANS flushes, especially in times of low flow or drought.

The maximum flushing discharge is currently of 1350 cfs (currently the valve opening maximum is 25% during flushing operations). This flow was measured by the USGS on Dec 9, 2014. This represents the flushing demand, so any river discharge below 1350 cfs will not meet this demand. A new valve design is being considered to allow larger valve openings during flushing, which could reduce the flush time needed prior to each lockage.

The average filling discharge of 1700 cfs was calculated using a 19 minute fill time and the dimensions of the lock chamber containing a 3x3 barge cut assembly drafting 9 ft. During this portion of the lockage, any river discharge below 1700 cfs will not meet this demand.

Flushing during periods of low flow conditions may be difficult if the flushing demand is greater than the water supply. In times of prolonged low flow periods, it may be necessary to reduce the duration of flushing (to less than 15 minutes) or reduce the valve opening (to less than 25% open), if not preclude flushing altogether. The number of vessels that can be flushed and locked were analyzed for different flow conditions. The results of that analysis are shown in Table 7.

**Table 5: Water Supply Analysis Results (water budget spreadsheet calculations)**

<b>River Discharge</b>	<b>Effect on Water Supply</b>
0 cfs (no flow)	Approx. 2 lockages can be made before cutting back on flushing duration or valve opening. No Flow occurrences are short duration events.
981 cfs (November Min Daily Ave flow)	Approx. 6 lockages can be made before cutting back on flushing duration or valve opening
1400 cfs (Typical Low Flow)	Approx. 22 lockages can be made before cutting back on flushing duration or valve opening
1700 cfs and higher	Adequate water supply for 15-min flushing operations

Brandon Rd Lock and Dam has a high head compared to the rest of the dams on the Illinois Waterway. It never shuts down during high flow, although barges may tie off upstream of the lock during high flows because the upstream lock (Lockport) is closed. 15,000 cfs is typically when navigation ties off and lockages cease at Brandon Road Lock. More information on Navigation Traffic is located in the PCX Navigation Economics appendix.

Downstream tie off locations for tows are necessary during flushing periods so that ANS floaters can be pushed out of the lock chamber and further downstream. The closer to the lock the tow ties off, the less volume of water that is needed to be flushed. The potential location of an electric barrier may limit where the tie-off locations can be, and future tests of the electric field will likely need to be done to determine this. More information to be found in the PCX Navigation Economics appendix.

## **7.2 Required Number of Flushes**

The required number of flushes is the number of upbound lockages, both commercial and recreational lockages, plus the number of downbound double lockages. The reason for flushing downbound traffic is due to “return water” that comes into the chamber when the first downbound cut exits the lock. The return water can carry ANS floaters which could then be transported upstream when the second half of the vessel enters the chamber.

The lowest flow month is typically November (Table 6) when hydropower operations change upstream. Based on past navigation traffic during this month, there are typically between 5-7 lockages per day. Navigation statistics are located in the PCX Navigation Economics appendix.

## **7.3 USGS Lock Chamber Velocity and Discharge Measurements**

During the data collection on Dec 8-9, 2014, two tainter gates were opened at the beginning of the collection. When the pool fell to its lower limit, gate #2 was shut; however, gate #1 could not be shut due to a large tree stuck in the gate. The tree was too large for small scale removal techniques so a crane will be needed. Debris on the tainter gates occurs frequently at this site, so it is recommended that at least two gates be sheltered by a debris boom so they can be reliably operated in the future during ANS flushing.

The stage hydrograph in Figure 9 shows the water levels in Brandon Road Pool during the USGS site visit December 8-9, 2014. The drop in pool from Max operation to Min operation in less than 2 hours can be best seen on Dec 9<sup>th</sup> from 4:00 pm to 6:00 pm. Valve discharge of 1350 cfs was continuously flushing through chamber during this time while the USGS collected velocity data in the lock chamber. One Tainter gate was stuck open during this test due to a large stump which could not be removed. The discharge through this gate was approximately 500 cfs

(estimated visually from 550 cfs per tainter that is typically discharged by one gates). The total discharge, loss to the pool, was 1850 cfs during the USGS tests. The pool can drop from maximum to minimum (0.5 ft operational band) in 2 hours with 1850 cfs.

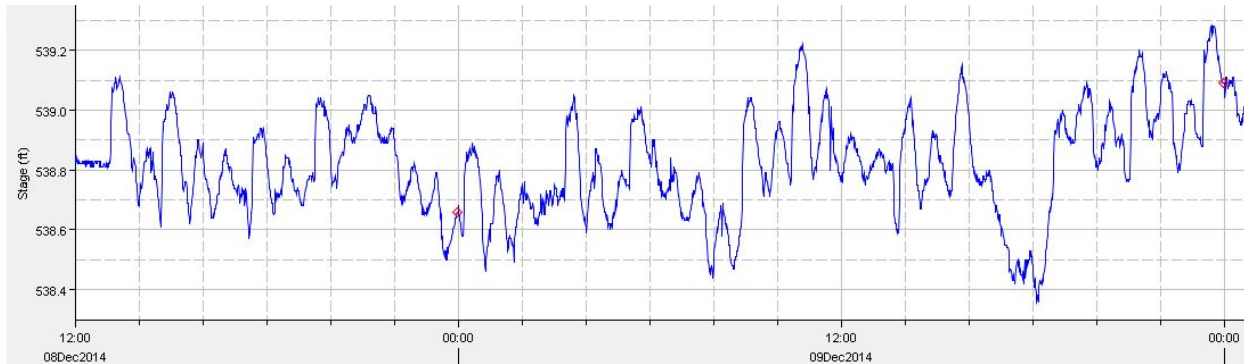


*Figure 9: Pool Hydrograph at Ruby Street Gaging Station upstream of Brandon Road Dam during time of USGS field tests, December 8-9, 2014*

#### **7.4 Conclusions on Water Supply**

Flushing the lock chamber before each lockage at Brandon Road Lock is being considered to reduce the likelihood of Aquatic Nuisance Species (ANS) passing upstream into the Great Lakes. The effectiveness of flushing increases with both the flushing duration and flushing discharge. There may be periods of low flow in which flushing operations must be reduced in order to preserve navigation or ceased altogether (Ref Table 3). These procedures would preserve the available water supply in order to preserve (or extend) navigation in times of drought. It is recommended that at least two gates be sheltered by a debris boom so they can be reliably operated in the future during ANS flushing.

**GLMRIS - Brandon Road  
Appendix E - Hydrology and Hydraulics**

**GLMRIS Lock, Reducing Risk of Aquatic  
Nuisance Species Transfer through Brandon  
Road Lock , Analytical and Numerical Model  
Study**



**US Army Corps  
of Engineers®**  
Engineer Research and  
Development Center



*Great Lakes and Mississippi River Interbasin Study*

## **GLMRIS Lock, Reducing Risk of Aquatic Nuisance Species Transfer through Brandon Road Lock, Analytical and Numerical Model Study**

E. Allen Hammack, David S. Smith, Richard Styles,  
and Richard L. Stockstill

January 2016



This is a draft report and currently in the process of final review and editing. This report will be published as an ERDC Technical Report in FY18 and available at <http://www.erd.c.usace.army.mil/Library.aspx>



Approved for public release; distribution is unlimited.

**The U.S. Army Engineer Research and Development Center (ERDC)** solves the nation's toughest engineering and environmental challenges. ERDC develops innovative solutions in civil and military engineering, geospatial sciences, water resources, and environmental sciences for the Army, the Department of Defense, civilian agencies, and our nation's public good. Find out more at [www.erdcl.usace.army.mil](http://www.erdcl.usace.army.mil).

To search for other technical reports published by ERDC, visit the ERDC online library at <http://acwc.sdp.sirsi.net/client/default>.

# **GLMRIS Lock, Reducing Risk of Aquatic Nuisance Species Transfer through Brandon Road Lock, Analytical and Numerical Model Study**

E. Allen Hammack, David S. Smith, Richard Styles, and Richard L. Stockstill

*Coastal and Hydraulics Laboratory  
U.S. Army Engineer Research and Development Center  
3909 Halls Ferry Rd.  
Vicksburg, MS 39180-FOUR*

Final report

Approved for public release; distribution is unlimited.

Prepared for U.S. Army Corps of Engineers  
Washington, DC 20314-1000

Monitored by Coastal and Hydraulics Laboratory  
U.S. Army Engineer Research and Development Center  
3909 Halls Ferry Rd. 39180-6199

## Abstract

As a next step in the Great Lakes and Mississippi River Interbasin Study (GLMRIS), the Assistant Secretary of the Army (Civil Works) has directed the U.S. Army Corps of Engineers (USACE) to proceed with a formal evaluation of potential aquatic nuisance species (ANS) control technologies.

This report is an assemblage of ideas and preliminary hydraulic calculations as part of the development of an ANS flushing system for Brandon Road Lock on the Illinois Waterway. The design ideas were generated during discussions between personnel of the U. S. Army Corps of Engineers, Chicago District (LRC), Rock Island District (MVR), Inland Navigation Design Center (INDC), and Coastal and Hydraulics Laboratory (CHL).

Four flushing system designs and operations are presented. The Type 1 design uses the existing culvert system. Types 2 and 3 designs require modifications to the lock structure. The Type 4 design is not actually a lock flushing system, but rather a design that provides a continuous supply of clean water in the lower lock approach to prevent ANS from reaching the lock chamber.

This report is not a comprehensive answer to the questions raised in this study. Rather, it is an overall commentary on design ideas and considerations for modeling the flushing rate of the lock chamber. The mechanics of hydraulic

**DISCLAIMER:** The contents of this report are not to be used for advertising, publication, or promotional purposes. Citation of trade names does not constitute an official endorsement or approval of the use of such commercial products. All product names and trademarks cited are the property of their respective owners. The findings of this report are not to be construed as an official Department of the Army position unless so designated by other authorized documents.

**DESTROY THIS REPORT WHEN NO LONGER NEEDED. DO NOT RETURN IT TO THE ORIGINATOR.**

Page Numbers Referenced Appear at Top Right

# Contents

<b>Abstract</b> .....	<b>ii</b>
<b>Figures and Tables</b> .....	<b>v</b>
<b>Preface</b> .....	<b>viii</b>
<b>Unit Conversion Factors</b> .....	<b>ix</b>
<b>1 Introduction</b> .....	<b>1</b>
1.1 Background.....	1
1.2 Previous research .....	3
1.3 Brandon Road Lock.....	4
<b>2 Lock Flushing – Analytical Description</b> .....	<b>9</b>
2.1 Advection-Diffusion Equation.....	10
2.1.1 Turbulence and mixing .....	12
2.1.2 Momentum jets .....	16
2.1.3 Stagnant regions (dead zones) .....	18
<b>3 Lock flushing concepts</b> .....	<b>19</b>
3.1 Hydraulic design of flushing systems .....	19
3.1.1 Hydraulic coefficients .....	19
3.2 Lock flushing systems .....	19
3.2.1 Type 1 lock flushing concept (existing filling and emptying system) .....	19
3.2.2 Type 2 lock flushing concept (lateral flushing manifold).....	23
3.2.3 Type 3 lock flushing concept (culverts through sill).....	25
3.2.4 Type 4 lock flushing concept (continuous flow below chamber).....	28
3.2.5 Type 5 lock flushing concept (redesigned filling and emptying system).....	29
<b>4 Numerical Modeling Process</b> .....	<b>31</b>
4.1 Governing Equations .....	31
4.2 Modeling Procedure .....	33
<b>5 Numerical Model Setup</b> .....	<b>34</b>
5.1 Type 1 lock flushing concept model geometry .....	35
5.2 Type 2 lock flushing concept model geometry .....	36
5.3 Type 3 lock flushing concept model geometry .....	37
5.4 Type 3r lock flushing concept model geometry .....	38
5.5 Type 5 lock flushing concept.....	39
<b>6 Numerical Model Results</b> .....	<b>40</b>
6.1 Type 1 lock flushing concept.....	43
6.2 Type 2 lock flushing concept.....	52
6.3 Type 3 lock flushing concept.....	52

6.4	Type 3r lock flushing concept .....	62
6.5	Type 5 lock flushing concept.....	71
<b>7</b>	<b>Physical Model .....</b>	<b>80</b>
7.1	Kinematic Similitude .....	80
7.2	Dynamic Similitude.....	81
7.3	Similitude for Lock Models.....	81
7.4	Model-Prototype Comparison.....	84
7.5	Similitude for mixing models .....	85
<b>8</b>	<b>Hawser Forces during Flushing.....</b>	<b>86</b>
<b>9</b>	<b>Further Research – Prototype and Physical Model Testing .....</b>	<b>89</b>
9.1	Prototype Tests .....	89
9.2	Physical Model Experiments .....	89
9.2.1	<i>Safety</i> .....	89
9.2.2	<i>USACE regulations</i> .....	90
9.2.3	<i>Numerical modeling uncertainties</i> .....	90
9.3	Tow Effects .....	92
<b>10</b>	<b>Summary and Recommendations.....</b>	<b>94</b>
<b>11</b>	<b>References.....</b>	<b>97</b>
	<b>Appendix A – Eisenhower Lock Flushing System Drawings.....</b>	<b>100</b>
	<b>Appendix B – Computational Meshes.....</b>	<b>102</b>
	<b>Appendix C – Type 2 fixed lid model results.....</b>	<b>111</b>
	<b>Report Documentation Page</b>	

## Figures and Tables

### Figures

Figure 1. Brandon Road Lock, sidewall port filling and emptying system (elevations are in feet referred to msl1912).....	6
Figure 2. Schematic of inflow source descriptions. ....	10
Figure 3. Advection-dominated, plug flow. ....	13
Figure 4. Dispersion-dominated, well-mixed flow. ....	15
Figure 5. Concentration resulting from transport and dispersion. ....	16
Figure 6. Circular jet issuing into a reservoir.....	16
Figure 7. Jet diffusion sketch.....	17
Figure 8. Two-dimensional jet issuing into a reservoir. ....	18
Figure 9. Type 1 (existing) lock flushing concept schematic. ....	20
Figure 10. Well-mixed lock chamber concentration histories.....	22
Figure 11. Well-mixed system flushing times for various dilutions.....	23
Figure 12. Type 2 design flushing system schematic. ....	24
Figure 13. Type 3 lock flushing concept schematic.....	26
Figure 14. Plug-flow system flushing time for various tailwater elevations .....	28
Figure 15. Type 4 concept schematic.....	29
Figure 16. Type 5 concept schematic.....	30
Figure 17. CAD model of Type 1 lock flushing concept.....	35
Figure 18. CAD model of Type 2 lock flushing concept .....	36
Figure 19. CAD model of Type 3 lock flushing concept .....	37
Figure 20. CAD model of Type 3r lock flushing concept.....	38
Figure 21. CAD model of Type 5 lock flushing concept .....	39
Figure 22. Simulation contour plot elevations.....	41
Figure 23. Sample lock flushing volume plot – single curve explanation .....	42
Figure 24. Sample lock flushing volume plot – single flushing time explanation.....	43
Figure 25. Type 1 velocity magnitude contours at el. 493.....	45
Figure 26. Type 1 velocity magnitude contours at el. 499.6.....	46
Figure 27. Type 1 velocity magnitude contours at lock chamber surface.....	47
Figure 28. Type 1 original lock chamber water concentration contours at el. 493.....	48
Figure 29. Type 1 original lock chamber water concentration contours at el. 499.6.....	49
Figure 30. Type 1 original lock chamber water concentration contours at el. lock chamber surface .....	50
Figure 31. Type 1 lock chamber flushing performance .....	51
Figure 32. Type 3 velocity magnitude contours at el. 493.....	54
Figure 33. Type 3 velocity magnitude contours at el. 499.6.....	55

Figure 34. Type 3 velocity magnitude contours at lock chamber surface .....	56
Figure 35. Type 3 original lock chamber water concentration contours at el. 493 .....	57
Figure 36. Type 3 original lock chamber water concentration contours at el. 499.6 .....	58
Figure 37. Type 3 original lock chamber water concentration contours at lock chamber surface .....	59
Figure 38. Type 3 lock chamber flushing performance .....	61
Figure 39. Type 3r velocity magnitude contours at el. 493 .....	63
Figure 40. Type 3r velocity magnitude contours at el. 499.6 .....	64
Figure 41. Type 3r velocity magnitude contours at lock chamber surface .....	65
Figure 42. Type 3r original lock chamber water concentration contours at el. 493 .....	66
Figure 43. Type 3r original lock chamber water concentration contours at el. 499.6 .....	67
Figure 44. Type 3r original lock chamber water concentration contours at lock chamber surface .....	68
Figure 45. Type 3r lock chamber flushing performance .....	70
Figure 46. Type 5 velocity magnitude contours at el. 493 .....	72
Figure 47. Type 5 velocity magnitude contours at el. 499.6 .....	73
Figure 48. Type 5 velocity magnitude contours at lock chamber surface .....	74
Figure 49. Type 5 original lock chamber water concentration contours at el. 493 .....	75
Figure 50. Type 5 original lock chamber water concentration contours at el. 499.6 .....	76
Figure 51. Type 5 original lock chamber water concentration contours at lock chamber surface .....	77
Figure 52. Type 5 lock chamber flushing performance .....	79
Figure 53. Whitten (Bay Springs) Lock filling curves .....	82
Figure 54. Currents generated as an upbound tow enters a lock chamber .....	93
Figure 55. Currents generated as a downbound tow leaves a lock chamber .....	93
Figure 56. Plan and section of ice flushing system added to Eisenhower Lock, St. Lawrence Seaway .....	100
Figure 57. Section and elevation of ice flushing system added to Eisenhower Lock, St. Lawrence Seaway .....	101
Figure 58. Type 1 geometry and computational mesh .....	103
Figure 59. Type 1 geometry and computational mesh – Zoom 1 .....	103
Figure 60. Type 1 geometry and computational mesh – Zoom 2 .....	104
Figure 61. Type 2 geometry and computational mesh .....	104
Figure 62. Type 2 geometry and computational mesh – Zoom 1 .....	105
Figure 63. Type 2 geometry and computational mesh – Zoom 2 .....	105
Figure 64. Type 3 geometry and computational mesh .....	106
Figure 65. Type 3 geometry and computational mesh – Zoom 1 .....	106
Figure 66. Type 3 geometry and computational mesh – Zoom 2 .....	107

Figure 67. Type 3r geometry and computational mesh.....	107
Figure 68. Type 3r geometry and computational mesh - Zoom 1 .....	108
Figure 69. Type 3r geometry and computational mesh - Zoom 2 .....	108
Figure 70. Type 5 geometry and computational mesh.....	109
Figure 71. Type 5 geometry and computational mesh – Zoom 1 .....	109
Figure 72. Type 5 geometry and computational mesh – Zoom 2 .....	110
Figure 73. Type 2 velocity magnitude contours at el. 494.6.....	112
Figure 74. Type 2 velocity magnitude contours at el. 499.6 .....	113

## Tables

Table 1. Brandon Road Lock, elevation information.....	7
Table 2. Brandon Road Lock, lock particulars.....	8
Table 3. Loss coefficients for Brandon Road Lock filling system.....	21
Table 4. Loss coefficients for Type 2 lock flushing concept. ....	25
Table 5. Loss coefficients for Type 3 lock flushing concept. ....	26
Table 6. Calculated discharge for Type 3 lock flushing concept, 34 ft normal lift. ....	27
Table 7. Lock flushing model discharges .....	34
Table 8. Type 1 chamber flushing performance – 5-minute intervals .....	52
Table 9. Type 3 chamber flushing performance – 5-minute intervals .....	61
Table 10. Type 3r chamber flushing performance – 5-minute intervals.....	70
Table 11. Type 5 chamber flushing performance – 5-minute intervals.....	79
Table 12. Model-prototype scale relations.....	81
Table 13. Lock coefficient, $C_L$ , for various projects .....	85
Table 14. Computational mesh sizes .....	102

## Unit Conversion Factors

<b>Multiply</b>	<b>By</b>	<b>To Obtain</b>
cubic feet	0.02831685	cubic meters
degrees (angle)	0.01745329	radians
feet	0.3048	meters
miles (U.S. statute)	1,609.347	meters
square feet	0.09290304	square meters

# 1 Introduction

## 1.1 Background

As a next step in the Great Lakes and Mississippi River Interbasin Study (GLMRIS), the Assistant Secretary of the Army (Civil Works) has directed the U.S. Army Corps of Engineers (USACE) to proceed with a formal evaluation of potential aquatic nuisance species (ANS) control technologies. The following project description is from the GLMRIS web site <http://glmr.is.anl.gov/brandon-rd/>.

The GLMRIS - Brandon Road effort is an assessment of the viability of establishing a single point to control the one-way, upstream transfer of ANS from the Mississippi River basin into the Great Lakes basin near Brandon Road Lock and Dam located in Joliet, Illinois. The Brandon Road control point was identified in the GLMRIS analyses as the only single location that can address upstream transfer of Mississippi River species through all Chicago Area Waterway System (CAWS) pathways. Implementation of technologies at the Brandon Road control point was a feature of three of the six structural alternatives presented in the GLMRIS Report (<http://glmr.is.anl.gov/glmris-report/>).

The Brandon Road site is located downstream of the confluence of the Des Plaines River and the Chicago Sanitary and Ship Canal (CSSC). Previous investigations have indicated that a potential hydrologic bypass can occur during periods of high precipitation from the Des Plaines River to the CSSC. A one-way control point at the Brandon Road site would significantly lessen the likelihood of bypass of Mississippi River ANS into the Great Lakes basin during flood events.

A project at the Brandon Road site is likely to significantly reduce a number of previously identified adverse impacts to existing waterway uses and users, such as increased potential for flooding or degradation of water quality. These impacts contributed significantly to the lengthy timeframes and significant costs of the structural alternatives presented by the GLMRIS Report.

The physical configuration of Brandon Road Dam prevents the upstream transfer of Mississippi River ANS. There is a minimum 25-foot difference

in water elevation from the downstream side of the dam to the upstream side, which effectively limits upstream transfer and promotes the use of gravity for flushing operations. Lock operation at this location currently provides the only known aquatic pathway that allows transfer of Mississippi River ANS to the Great Lakes through the CAWS.

Preventing ANS, present in the lower pool, from reaching the upper pool requires that the chamber be flushed prior to each lock filling operation. The empty chamber (water-surface at tailwater elevation) must be flushed prior to filling regardless of the presence of a tow in the chamber. Once a lock chamber is flushed and the miter gates and operation valves are closed, the chamber can be filled in a normal manner with clean water from the upper pool entering the chamber. Filling the lock in preparation for a down-bound tow approaching the lock must be preceded by a flushing cycle. Safety assurance will most likely require longer flushing times when a tow is in the chamber as compared to an empty chamber. These questions are best answered with a physical model study that includes hawser force measurements.

This report presents design concepts for flushing Brandon Road Lock as part of the overall study to answer how a navigation lock and dam can be used as a barrier to the upstream passage of ANS. These ideas were generated during discussions between personnel of the U. S. Army Corps of Engineers, Chicago District (LRC); Rock Island District (MVR); Inland Navigation Design Center (INDC); and the Engineering Research and Development Center (ERDC), Coastal and Hydraulics Laboratory (CHL). Initial estimates of flushing efficiency for various design ideas are provided. Before implementation, any chosen design should be further evaluated during a physical model study. The physical model will provide the flushing information and ensure that navigation safety is maintained after modifications are made to the lock's filling and emptying system. Therefore, a description of the physical model is also provided in this report.

This report is a commentary on design ideas and considerations for modeling the flushing of a lock chamber. First, previous studies that may provide design ideas are reviewed. This literature review is followed by a brief description of Brandon Road Lock. Then the mechanics of hydraulic mixing with application to flushing a lock chamber are discussed. Four design and operation ideas are presented with estimates of component sizes and

efficiencies. Finally, descriptions of further evaluation needed for design refinement are presented.

## 1.2 Previous research

Operations of navigation locks are hindered when floating or submerged substances in the water require consideration. The most common substances are floating objects such as debris and ice, which must be flushed from the chamber to allow room for vessel passage. Salt water is another substance that must be addressed daily at certain projects. Locks are used to arrest salt-water wedges at some projects that separate the forebay's fresh water from salt water comprising the tailwater. Studies have been directed toward developing operation strategies for flushing ice and debris. Salt water advance is halted with bubble plumes and various structures placed on the lock floor.

Prohibiting passage of neutrally-buoyant particles, such as ANS, presents a new challenge to lock operators. The ANS "floaters" as they are called are assumed to occupy the lower pool, and Brandon Road Lock and Dam will be used to prevent ANS from entering the CAWS.

Ice and debris floating on the water surface will be transported from the chamber once enough flow is introduced into the chamber to develop a water-surface gradient. However, ANS flushing is more complicated because the turbulent flow will disperse the entities. Therefore, previous studies are of limited benefit to the problem faced by USACE operators of the Illinois Waterway navigation projects. However, modifications made to the Eisenhower and Snell Locks on the St. Lawrence Seaway are used in this report to demonstrate the feasibility of adding culverts in the lock upper sill and tied into one of the filling culverts.

Investigations have been conducted to determine how a navigation lock may be used as a conduit to facilitate passage of substances such as ice and debris. Ice and debris studies (e.g. Tuthill et al. 2004, Tuthill 2003, and Tuthill and Gooch 1997) have focused on passing materials which tend to float on the water surface. Numerous studies are documented in the literature regarding how a lock may serve as a barrier to salt water intrusion. Salt water intrusion studies (e.g. Parchure et al. 2000, Mausshardt and Singleton 1995, Abraham et al. 1973, Bastian 1971, Wood 1970, and Boggess 1970) have focused on preventing salt water from entering the

lock chamber. The salt water problem focuses on the density differences of the fresh and salt water bodies which are to remain separated.

The current study differs from previous research in that the objective is to prevent passage of aquatic nuisance species (ANS) which, for the purposes of the current study, are assumed to be neutrally-buoyant particles. The exchange of upstream and downstream waters for the CAWS is complicated by the fact that the mixing of water from these bodies is to be limited even though natural mixing processes occur during normal operations. The simple act of opening the lock gates generates turbulent mixing of the fluids on either side of the gate. Also, vessels entering and exiting the chamber generate mixing as return currents and propeller wash mix large quantities of water. These mixing processes make maintaining the ANS concentration at near zero levels difficult.

### **1.3 Brandon Road Lock**

Brandon Road Lock and Dam is being considered for modification to make the project serve as a “barrier” to ANS. Brandon Road Lock and Dam is the first project downstream of the Lockport Lock and Dam, and the ANS are assumed to exist on the downstream side of Brandon Road Lock. The objective of the GLMRIS is to prevent ANS from entering the CAWS from the Lower Des Plaines River via Brandon Road Lock.

Brandon Road Lock and Dam is 286 miles above the confluence of the Illinois River with the Mississippi River. Brandon Road Dam, located on the Des Plaines River just below the city of Joliet, Illinois (about 27 miles southwest of Chicago), is a fixed concrete structure, 1,569 feet (ft) long. The water-surface elevation of the pool and discharge past the dam are controlled by twenty-one 50-foot tainter-type crest gates which hold the normal pool 27 inches above the crest of the masonry. Six openings through the dam, previously controlled by sluice gates, have been sealed and are no longer used. A 320-foot section of head gates, which was designed for future addition of a powerhouse, contains eight operating head gates used for passing water. An ice chute and two sections of earth embankment complete the dam. The major portion of the short pool is the city of Joliet and is in part contained between flood walls varying in height to a maximum of 35 ft.

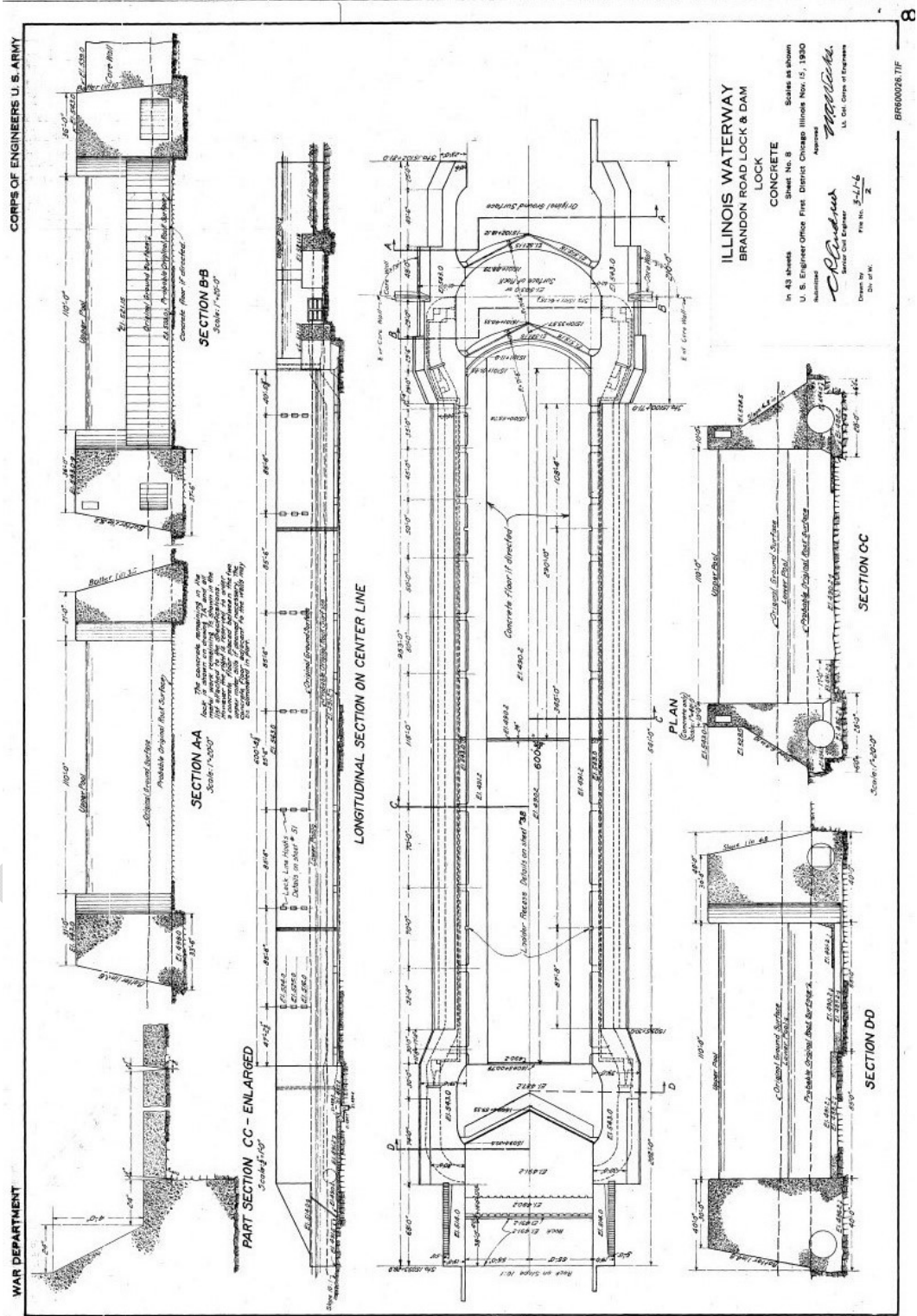
The lock which opened in 1933 is nominally 600 ft long and 110 ft wide. It operates under a nominal lift of 34 ft with an average 19-minute (min) lock

chamber fill time and a 15-min emptying time. The dam is 2,391 ft long (exclusive of fixed embankment and river wall). It contains twenty-one operational tainter gates, six sluice gates (bulkheaded closed), and sixteen pairs of headgates (eight operational, eight bulkheaded closed).

Brandon Road Lock, as the majority of locks operated by the USACE, is of the sidewall port design filling and emptying system. The layout of the lock filling and emptying system is shown in Figure 1. The lock features a redundant upstream miter gate, vertical-lift valves for flow control, with intakes and outlets immediately upstream and downstream of the upper and lower miter gates, respectively. The chamber is filled and emptied with 12-ft-diameter culverts in each lock wall. Each sidewall manifold has ten ports, 5.0 ft wide by 3.5 ft tall, which means the ratio of the sum of the cross-sectional area of the ports to the cross-sectional area of the culvert (port-to-culvert area ratio) is 1.55, whereas 0.95 is the current design criteria for sidewall port systems given in EM 1110-2-1604 “Hydraulic Design of Navigation Locks” (Headquarters, US Army Corps of Engineers 2006). The port spacing varies from 35 ft to 115 ft along the chamber length. The ports in each wall are positioned directly opposite rather than staggered as specified in current lock design criteria (Headquarters, US Army Corps of Engineers 2006). The chamber floor is at el. 489.7 ft with 19-ft-wide aprons at elevation 490.7 adjacent to either lock wall.

In each culvert the ratio of the total cross-sectional area of the ports to the cross-sectional area of culvert should be about 0.95. If the sum of the cross-sectional area of the ports is larger than the cross-sectional area of the culvert, poor distribution of flow from the port manifold will result. During peak discharge of a filling operation, flow can be drawn from the lock chamber by the upstream ports (Headquarters, US Army Corps of Engineers 2006). Conversely, if the port-to-culvert area ratio is too small, filling time will be sacrificed without a noticeable improvement in conditions in the lock chamber.

Figure 1. Brandon Road Lock, sidewall port filling and emptying system (elevations are in feet referred to msl1912).



Simple volume exchange calculations can provide order-of-magnitude estimates of mixing attributed to a vessel entering or leaving a lock chamber. For the case in which a tow exits the lock into ANS contaminated water, a first approximation is to assume the volume of water displaced by the tow in the lock will be replaced by ANS-contaminated water as the barge leaves the chamber. The upcoming calculations are based on geometrical parameters of the lock chamber and the design vessel such as those listed in Tables 1 and 2.

**Table 1. Brandon Road Lock, elevation information.**

Elevations (ft NGVD)	
Upper Pool Normal	538.5
Upper Pool Minimum	537.2
Upper Pool Maximum	540.5
Lower Pool Normal (no flow)	504.5
Lower Pool Minimum	501.1
Lower Pool Maximum	513.5
Chamber Floor (Average)	490.0

The floor of Brandon Road Lock chamber is rock at el 489.7 with a concrete apron at el 490.7\* that is 19 ft wide adjacent and along either chamber wall. The average elevation of the chamber floor is el 490.0 (72 ft at el 489.7 and 38 ft at el 490.7). The chamber is 110 ft wide by 671 ft long pintle-to-pintle.

Although the volume to be exchanged will be less when the tailwater is at normal or minimum lower pool elevation, the higher head may be most critical regarding hawser forces if a tow is present. River conditions that provide maximum lower pool elevation will have the largest volume and the least head, both of which result in a longer flushing time. This report does not consider the volume of water in the culverts, but the volume of

---

\* All elevations are referenced to NGVD 1929 datum.

potentially contaminated water residing in the culverts will be included in the exchange-time determinations of the physical model study.

**Table 2. Brandon Road Lock, lock particulars.**

<b>Lock Information at Normal Upper Pool (el 538.5) and Lower Pool (el 504.5)</b>	
Lock Filling and Emptying System	Sidewall Port
Chamber Width	110 ft
Chamber Length	671 ft
Culvert Diameter	12 ft
Port Size	5.0 ft wide by 3.5 ft tall
Number of Ports (each culvert)	10
Port-to-Culvert Area Ratio	1.55
Filling Time	19 min
Emptying Time	15 min
Chamber Depth when Filled	48.5 ft
Volume of "Filled" Lock	3,579,785 ft <sup>3</sup>
Chamber Depth when Empty	14.5 ft
Volume of "Empty" Lock	1,070,245 ft <sup>3</sup>
Normal Lift	34 ft
Normal Lift Volume	2,509,540 ft <sup>3</sup>

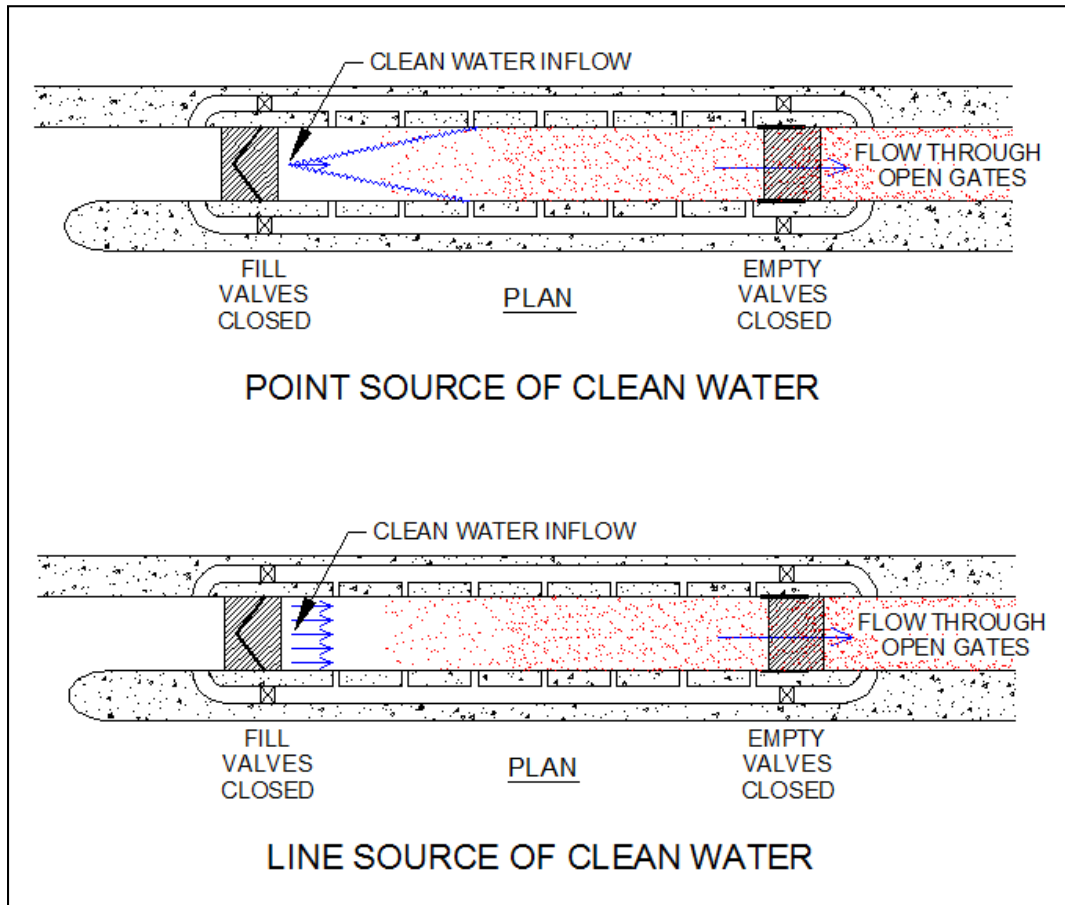
## 2 Lock Flushing – Analytical Description

Flushing of Brandon Road Lock chamber will be accomplished by introducing clean water from the upper pool into the chamber, diluting ANS-contaminated water by mixing, and transporting ANS contaminated water from the chamber through opened lower miter gates. This chapter provides the analytical evaluation required to estimate the time and space consequences of flushing the lock chamber.

This report outlines concepts for flushing the lock using gravity thus avoiding the large expenses of mechanical pumping. The energy and other operation costs as well as construction and maintenance costs over the pump lives can be avoided if a gravitational system can be developed. Flushing will bring upper pool water into the chamber, which will be at lower pool level, so the energy available will be the head from the pool differences.

The introduction of clean upper pool water at the upstream end of the chamber can be considered as a point or line source. Schematics of each of these systems are provided in Figure 2. The red dots indicate the presence of ANS, and the blue lines indicate clean water. Modeling the point source conditions requires knowledge of both the lateral and the longitudinal dispersion coefficients. Point source evaluation further requires the inclusion of lateral diffusion and a multidimensional advection-diffusion equation for analysis. Rather than speculating about the effectiveness of a single outlet, this analytical evaluation will consider the clean water inflow as a steady-state line source as illustrated in Figure 2. The alternatives will be further evaluated by the design team to compare cost, operation and maintenance issues, and overall efficiency of the alternatives.

Figure 2. Schematic of inflow source descriptions.



## 2.1 Advection-Diffusion Equation

Flushing of the lock chamber using a line source of clean water can be considered a one-dimensional (1-D) transport problem. The concentration relative to position is quantified with the 1-D advection-diffusion equation. The advection-diffusion equation with a conservative constituent is used to estimate the rate of longitudinal dispersion. The 1-D advection-diffusion equation is

$$\frac{\partial C}{\partial t} + U \frac{\partial C}{\partial x} - D \frac{\partial^2 C}{\partial x^2} = 0 \quad (0)$$

where  $C$  = cross-sectional average concentration [ML<sup>-3</sup>]

$t$  = time [T]

$U$  = cross-sectional average velocity [LT<sup>-1</sup>]

$x$  = longitudinal direction of flow [L]

$D = D_x + D_t + E_x$  = the longitudinal dispersion coefficient [L<sup>2</sup>T<sup>-1</sup>]

$D_x$  =  $x$ -direction molecular diffusion

$D_t$  = turbulent (eddy) diffusion (time-averaged)

$E_x$  = x-direction dispersion coefficient (space-averaged)

The molecular diffusion is the random motion of particles, the eddy diffusion is the turbulent mixing of particles, and the mechanical dispersion is the mixing caused by variations in velocities. Diffusion is the process where a constituent moves from a higher concentration to a lower concentration, whereas dispersion is mixing caused by physical processes.

The flushing process consists of the initial condition that at  $t = 0$ ,  $C = C_0$  for all  $x$  and the boundary condition that the concentration at the inflow boundary is constant,  $C = 0$  at  $x = 0$  or

$$C(x, 0) = C_0 \text{ for } x \geq 0 \quad (0)$$

$$C(0, t) = 0 \text{ for } t \geq 0 \quad (0)$$

$$C(\infty, t) = C_0 \text{ for } t \geq 0 \quad (0)$$

The analytical solution for the advection-diffusion equation with these initial and boundary conditions is (e.g. Jainswal et al. 2011, Socolofsky and Jirka 2005, and Runkel 1996) is

$$C(x, t) = \frac{C_0}{2} \left[ 1 - \operatorname{erf} \left( \frac{x-Ut}{\sqrt{4D_t}} \right) \right] \quad (0)$$

The difficulty of solving the spatial and temporal concentration variation using this equation is that the longitudinal dispersion coefficient is unknown. Numerous researchers have developed methods to quantify the longitudinal dispersion coefficient. Yet, the discrepancies between the values of the observed and predicted longitudinal dispersion coefficients range from one to three orders of magnitude, and existing methods, in general, underestimate the dispersion coefficient (Deng et al. 2002).

Mixing in the lock chamber will be driven by free shear such as a jet from the clean-water source. Farther from the clean-water source, the flushing will approach uniform flow and boundary friction will then be the primary source of shear. The longitudinal dispersion coefficient for boundary shear is estimated from the friction velocity,  $U_*$  which is

$$U_* = \sqrt{gRS_f} = \sqrt{\frac{f}{8}U^2} \quad (0)$$

where  $S_f = \text{friction slope} = \frac{f}{D_h} \frac{U^2}{2g} = \frac{fU^2}{8Rg}$   
 $f = \text{Darcy friction factor.}$

The most commonly used method of determining the longitudinal dispersion coefficient is the Fischer equation (Fischer et al. 1979), which is

$$\frac{D}{hU_*} = 0.011 \left(\frac{B}{h}\right)^2 \left(\frac{U}{U_*}\right)^2 \quad (0)$$

This equation is popular because it gives the longitudinal dispersion coefficient,  $D$ , in terms of readily available hydraulic variables, the width-to-depth ratio ( $B/h$ ), and friction term ( $U/U_*$ ). The left-hand side of the Fischer equation is commonly referred to as the dimensionless dispersion coefficient. Seo and Cheong (1998) used regression analysis to develop an empirical form of the hydraulic and geometric variables of the Fischer equation to better represent observed values.

$$\frac{D}{hU_*} = 5.915 \left(\frac{B}{h}\right)^{0.62} \left(\frac{U}{U_*}\right)^{1.428} \quad (0)$$

### 2.1.1 Turbulence and mixing

Without knowledge of the longitudinal dispersion coefficient, the problem can be bounded as one of advection-dominated flow and one in which the flow is better characterized as dispersion dominated. Evaluation requires determination of the importance of dispersion relative to the transport of a concentration (ANS). This is done using the Peclet number, which is the relative advection-to-dispersion ratio and is given as

$$Pe = \frac{UL}{D} = \frac{U^2t}{D} \quad (0)$$

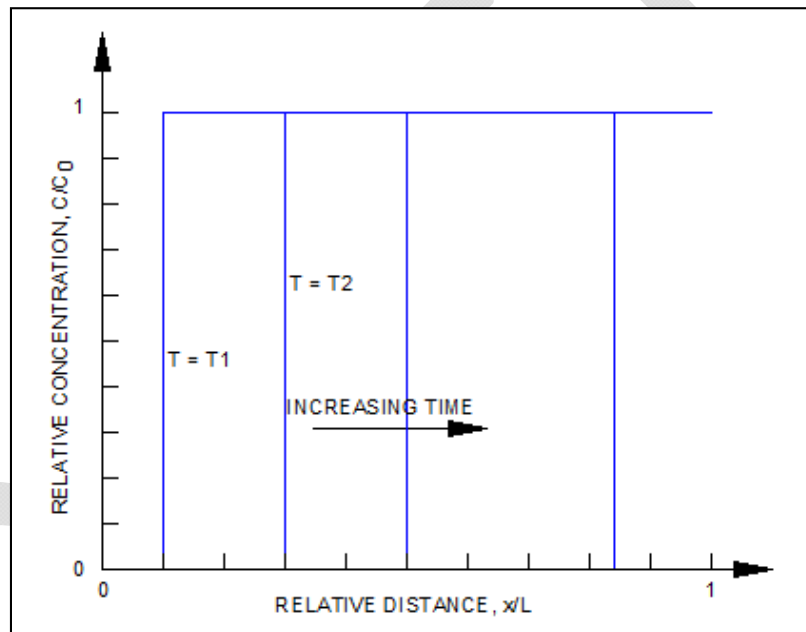
Note that the Peclet number is sometimes given as the ratio of dispersion to advection (reciprocal of what is defined here). As presented here the Peclet number is large when the flow is advection-dominated and small when dispersion dominates. If the flow is dispersion-dominated, the Peclet number goes to zero. In the case of advection domination, the Peclet goes toward infinity, and the transport is similar to plug flow.

Some simple water quality models can be developed for special cases where either advection or dispersion is dominant. As the Peclet number becomes large, the longitudinal dispersion can be neglected and the system behaves as a plug-flow chamber

#### 2.1.1.1 Plug flow

The plug-flow concentration is shown at a particular position for various times in Figure 3. The concentration,  $C$ , is normalized by the initial concentration,  $C_0$ , and the distance from the clean water source,  $x$ , is related to the lock chamber length,  $L$ .

Figure 3. Advection-dominated, plug flow.



The time required flushing water into and from the chamber,  $T_f$ , is the volume to be exchanged,  $V_c$ , divided by the volumetric flow rate,  $Q$ .

$$T_f = \frac{V_c}{Q} \quad (0)$$

where  $T_f$  = time required to flush the lock chamber assuming plug flow  
 $V_c$  = the volume of the lock chamber when the water surface is at tailwater

The fastest time is limited by the maximum allowable discharge. Of course the actual flow conditions in the lock chamber will not be plug flow, but

the plug-flow equation provides the absolute shortest time and least volume of water required to flush the lock chamber. The actual flow volume required to flush Brandon Road Lock chamber in a reasonable time will produce high-shear turbulent conditions in the lock chamber. The turbulent dispersion in the lock chamber will require a longer time and larger volume of water to flush as compared to the plug-flow condition.

#### 2.1.1.2 Well-mixed flow

Dispersion-dominated problems can be treated as a well-mixed system. The dispersion-dominated case is analogous to a continuously-stirred tank. Flow that enters the chamber is assumed to instantaneously mix throughout the full chamber volume. This situation is referred to as the well-mixed case wherein conservation of mass means that

$$\frac{\partial(CV)}{\partial t} = -Q(C_{in} - C_{out}) \quad (0)$$

In the case at hand where the chamber has an ANS concentration of  $C(t)$ , the chamber is flushed with clean inflow having a concentration of  $C_{in} = 0$ . The volume of water in the chamber is constant because the volumetric flow rate into the chamber equals that flowing from the chamber, so

$$\frac{\partial C}{\partial t} = -\frac{Q}{V}C_{out} \quad (0)$$

The well-mixed case means that the concentration of water flowing from the chamber is equal to the concentration in the chamber,  $C(t)$ . The solution of this differential equation is

$$C(t) = \exp\left(-\frac{Q}{V}t\right) \quad (0)$$

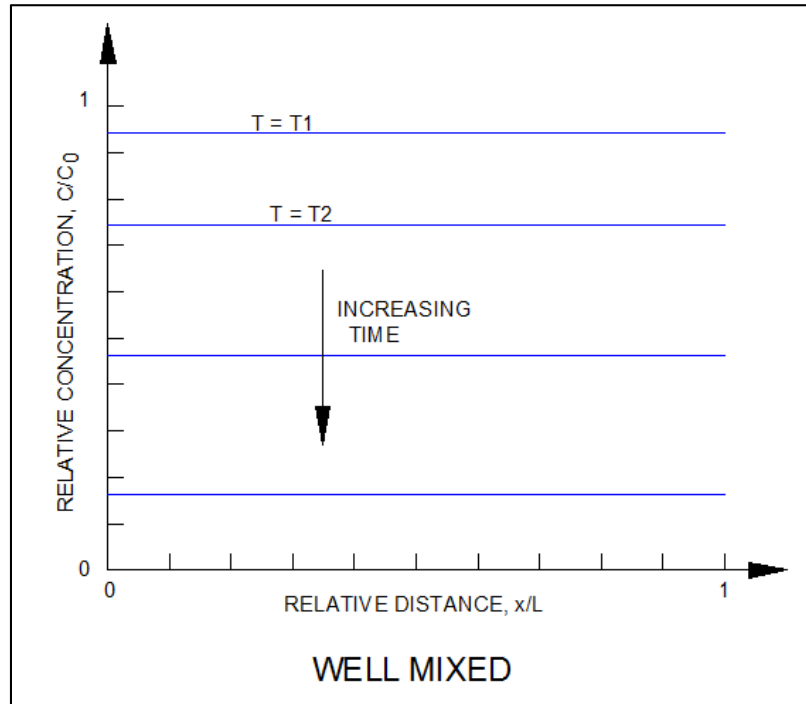
For an inflow concentration of zero, the concentration in the chamber decreases exponentially for the well-mixed case wherein dispersion dominates advection.

The time required to flush 95% is the time required to reduce the concentration from 1.0 to 0.05. The time required is

$$t = -\frac{V}{Q}\ln C = -\frac{V}{Q}\ln(0.05) \quad (0)$$

Temporal variation of relative concentration at a particular distance from the clean-water source is illustrated for the well-mixed case in Figure 4.

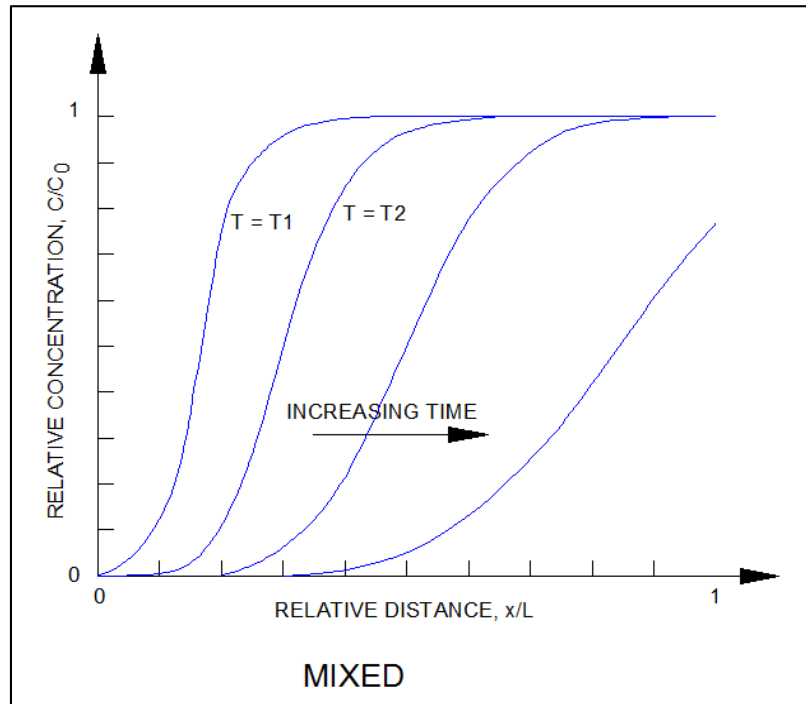
Figure 4. Dispersion-dominated, well-mixed flow.



### 2.1.1.3 Advection-dispersion flow

A third case of flushing the lock chamber will cause the ANS to be transported downstream and their concentration dispersed. The problem is theoretically bound between the plug-flow situation which is the quickest flushing time and the well-mixed case which requires the most time to flush. The actual response to the introduction of clean water via momentum jets will be as the concentrations illustrated in Figure 5.

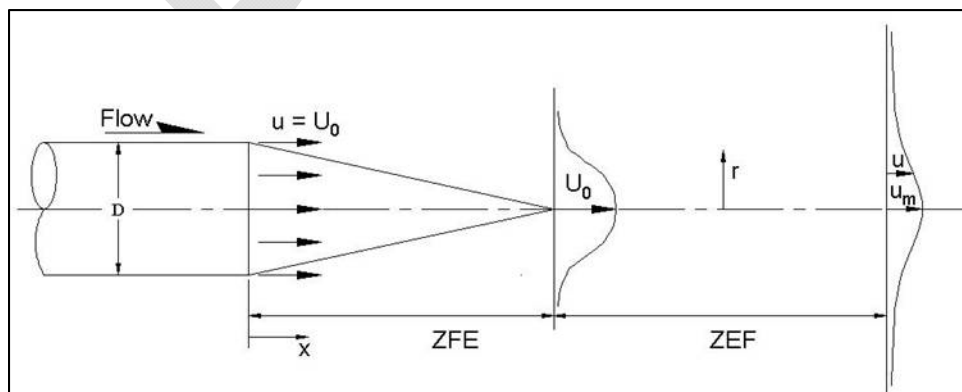
Figure 5. Concentration resulting from transport and dispersion.



### 2.1.2 Momentum jets

Regardless of how clean water is introduced into Brandon Road Lock chamber, the flow will enter the chamber as momentum jet(s). Albertson et al. (1950) describe the mechanics of a submerged jet using the assumptions of steady (but turbulent) flow, quiescent ambient fluid, and that the receiving fluid has the same density as the discharge fluid. The jet development is classified as being in two zones, the zone of flow establishment (ZFE) and the zone of established flow (ZEF) as illustrated in Figure 6. Further assumptions are that the jet grows linearly, that the pressure distribution is hydrostatic, and that the velocity profile is Gaussian.

Figure 6. Circular jet issuing into a reservoir.



The Albertson et al. (1950) experiments were conducted at  $Re \approx 5 \times 10^4$ , so the results are valid for turbulent flow.

### 2.1.2.1 Round (Circular) Jet

Expressions for velocity and discharge in the ZEF are

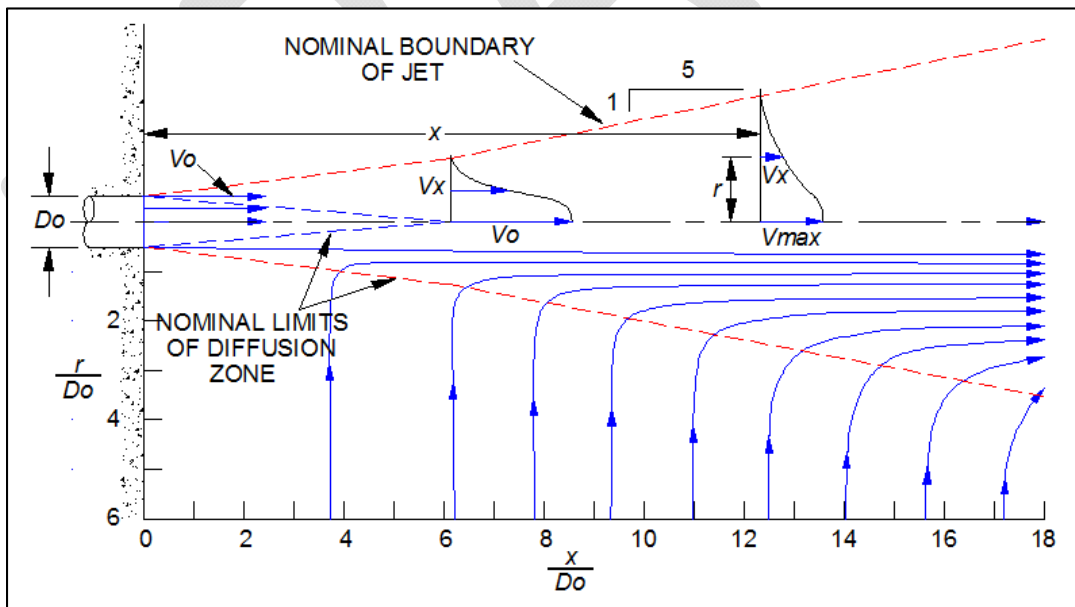
$$\frac{u_m}{U_o} = 6.2 \left( \frac{D_o}{x} \right) \quad (0)$$

$$\frac{Q}{Q_o} = 0.32 \left( \frac{x}{D_o} \right) \quad (0)$$

where  $u_m$  = maximum velocity within the jet  
 $U_o$  = jet velocity at the port face  
 $D_o$  = inflow culvert diameter  
 $x$  = distance from the port face

The centerline velocity and discharge grow linearly, entraining flow in the jet as illustrated in Figure 7. Note that nominal boundaries of the submerged circular jet expand by a ratio of 1 lateral to 5 longitudinal.

Figure 7. Jet diffusion sketch.



### Two-Dimensional Momentum Jet

The velocity distribution for a 2-D jet produced from a channel of width  $B_o$  is illustrated in Figure 8. Albertson et al. (1950) determined the upstream

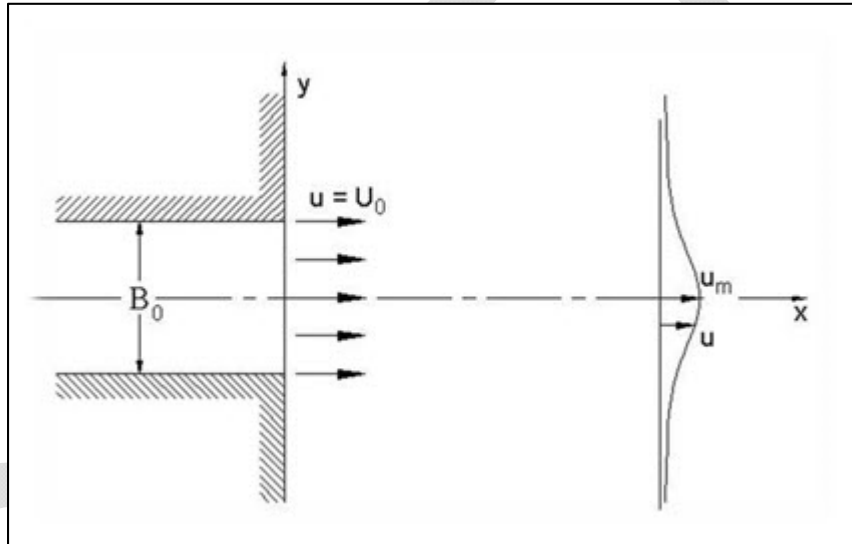
limit of the ZEF to be  $\frac{x}{B_0} = 5.2$  and that the velocity and discharge are given as

$$\frac{u_m}{U_0} = 2.28 \sqrt{\frac{B_0}{x}} \quad (0)$$

$$\frac{Q}{Q_0} = 0.62 \sqrt{\frac{x}{B_0}} \quad (0)$$

The free shear attributed to submerged jets will be the primary source of dispersion during lock flushing operations.

Figure 8. Two-dimensional jet issuing into a reservoir.



### 2.1.3 Stagnant regions (dead zones)

The jet diffusion sketches illustrate that, even with the entrainment currents induced by the jet shear, there can be regions within the ambient fluid that remain unmoved. ANS will be trapped in stagnant regions referred to as dead zones or storage zones (Fernando 2012). Therefore, reduction of dead zones will in turn provide a more efficient flushing system.

## 3 Lock flushing concepts

### 3.1 Hydraulic design of flushing systems

#### 3.1.1 Hydraulic coefficients

The energy loss  $H_L$  through each component can be expressed as

$$H_{L_i} = K_i \frac{V_i^2}{2g} \quad (0)$$

where  $K_i$  = loss coefficient for component  $i$   
 $V_i$  = velocity through component  $i$

Loss coefficients for many hydraulic components are well established and are readily available in the literature (e.g. Miller 1990). However, lock culvert system components are often unique to a particular project and the loss coefficients have not been determined.

### 3.2 Lock flushing systems

The flushing process can be described as introducing clean water from the upper pool into an empty chamber (chamber water-surface at lower pool elevation) either using the existing filling and emptying system or a new culvert system designed specifically for flushing ANS.

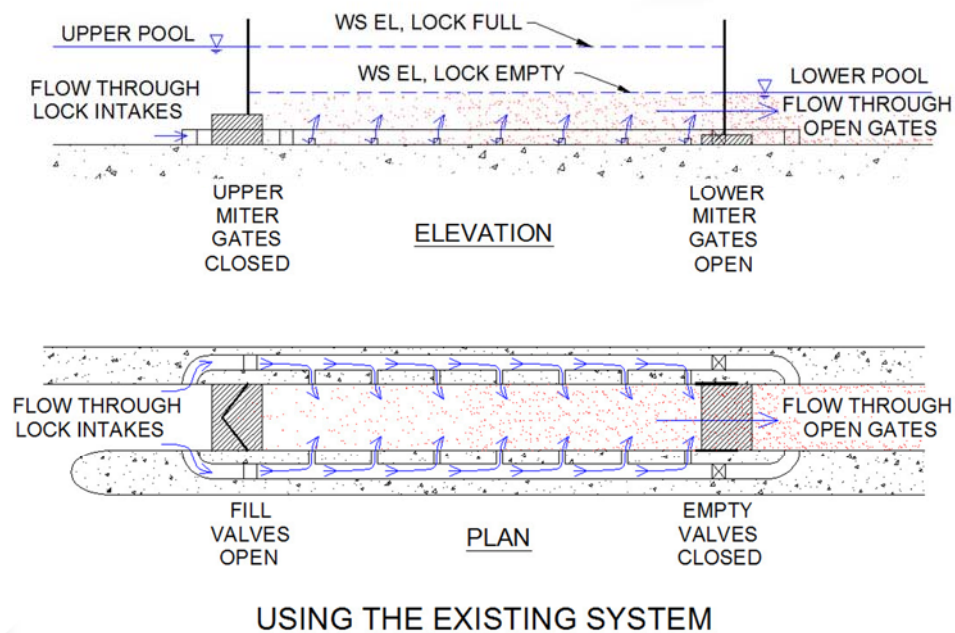
Four basic concepts have been identified. The first lock flushing concept (Type 1) relies on the existing filling and emptying system to flush the lock. The second lock flushing concept (Type 2) adds a lateral manifold from one of the filling culverts across the lock chamber immediately downstream of the upper sill. The third lock flushing concept (Type 3) adds culverts from the upper pool to the chamber through the upper sill. A final concept considered herein is not designed to flush the lock chamber, but rather provides a continuous flow of clean water flushing the lower lock approach in order to prevent ANS from entering the lock chamber (Type 4 design flushing system).

#### 3.2.1 Type 1 lock flushing concept (existing filling and emptying system)

The Type 1 lock flushing concept (shown in Figure 9) uses the existing lock filling and emptying system to flush the lock chamber. The system setup would have the upper miter gates closed, the lower miter gates open, the

fill valves opened (perhaps partially), and the emptying valves closed. This scheme would input clean water with zero concentration along the length of the chamber which would respond more as a well-mixed system wherein dispersion dominates the flow. The movement of flushing flow through the system is indicated by the blue arrows in the figure. The lower miter gates may need to be retrofitted with a means to secure them in the open position as the chamber is flushed.

Figure 9. Type 1 (existing) lock flushing concept schematic.



The lock coefficient for a standard design sidewall port filling system is about 0.80 (McCartney et al. 1998). Loss coefficients for lock filling and emptying systems are customarily given in terms of the velocity head in the culvert at the valve (i.e. valve fully open). Estimates of loss coefficient values for Brandon Road Lock filling system components are provided in Table 3. These coefficients are for a standard sidewall port filling system (e.g. Murphy 1975, McCartney et al. 1998, and Headquarters, US Army Corps of Engineers 2006). Since the design standards were not developed until decades after Brandon Road Lock was constructed, the loss coefficient values will need to be validated with field or laboratory data. The head loss as flow passes a partially-opened vertical-lift valve is a function of the shape of the valve lip and the valve opening. So, the head loss varies during a valve operation. The Hydraulic Design Chart 320-1 (Headquarters, US Army Corps of Engineers 1988) is a plot of discharge coefficient as

a function of valve position. The relation between the discharge coefficient,  $C_v$ , and a head loss coefficient for the valve,  $K_v$ , can be determined by equating the change in head across the valve

$$K_v = \left(\frac{b}{B}\right)^{-2} C_v^{-2} \quad (0)$$

where  $b$  = valve opening  
 $B$  = culvert height at the valve, 9 ft

The discharge coefficient for a valve opening of 25% is given in Hydraulic Design Criteria 320-1 as 0.73. This yields a loss coefficient of 30, which is the same valve given in Miller (1990) for vertical lift valves opened 25%.

Table 3. Loss coefficients for Brandon Road Lock filling system.

Lock Component	Representative area (valve area), $A_v$	Loss Coefficient, $K$
Upper pool to valve	9 ft by 9 ft = 81 ft <sup>2</sup>	0.45
Through open valve	81 ft <sup>2</sup>	0.11
Through valve 25% open	81 ft <sup>2</sup>	30
Valve to lock chamber	81 ft <sup>2</sup>	1.05

The sum of head loss at normal pool conditions is 34 ft. So, the discharge is estimated to be

$$Q = A_v \sqrt{\frac{2gH}{K_T}} = 81 \text{ ft}^2 \sqrt{\frac{2(32.2 \text{ ft}/\text{sec}^2)(34 \text{ ft})}{1.61}} = 2987 \text{ ft}^3/\text{sec} \quad (0)$$

This is the estimated discharge per culvert with the vertical-lift gates fully open. The total discharge into the chamber is estimated to be 5,970 ft<sup>3</sup>/sec. This method of flushing will require that the filling valves are able to close in flowing water at the project's full head. Project operation personnel have indicated that the filling valves can only be opened 25% during

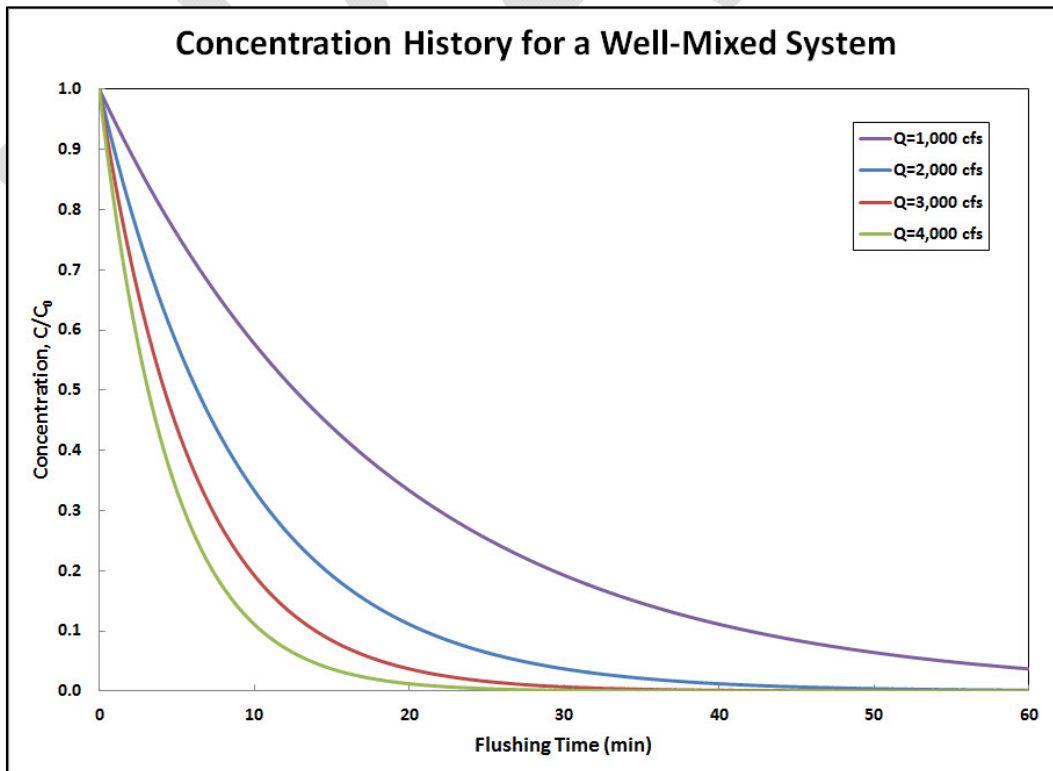
flushing. One reason for concern is that during flushing, the open lower miter gates may slam shut. Therefore, a device to hold the lower miter gates open will need to be installed. Another consideration is that the existing vertical-lift valves may either require modification or replacement with valves that are designed specifically for flow control and are heavy enough to close under full flow. The flushing discharge with the fill valves opened 25% rather than 100% is calculated using the head loss coefficient for a vertical-lift valve opened 25% as  $K_v = 30$  (Miller 1990). Then, the total loss coefficient with the valve opened 25% is 31.15. So the discharge through each culvert is estimated to be

$$Q_{25\%} = A_v \sqrt{\frac{2gH}{K_T}} = 81 \text{ ft}^2 \sqrt{\frac{2(32.2 \text{ ft}/\text{sec}^2)(34 \text{ ft})}{31.15}} = 679 \text{ ft}^3/\text{sec} \quad (0)$$

per culvert for a total flushing discharge of about 1,360 ft<sup>3</sup>/sec.

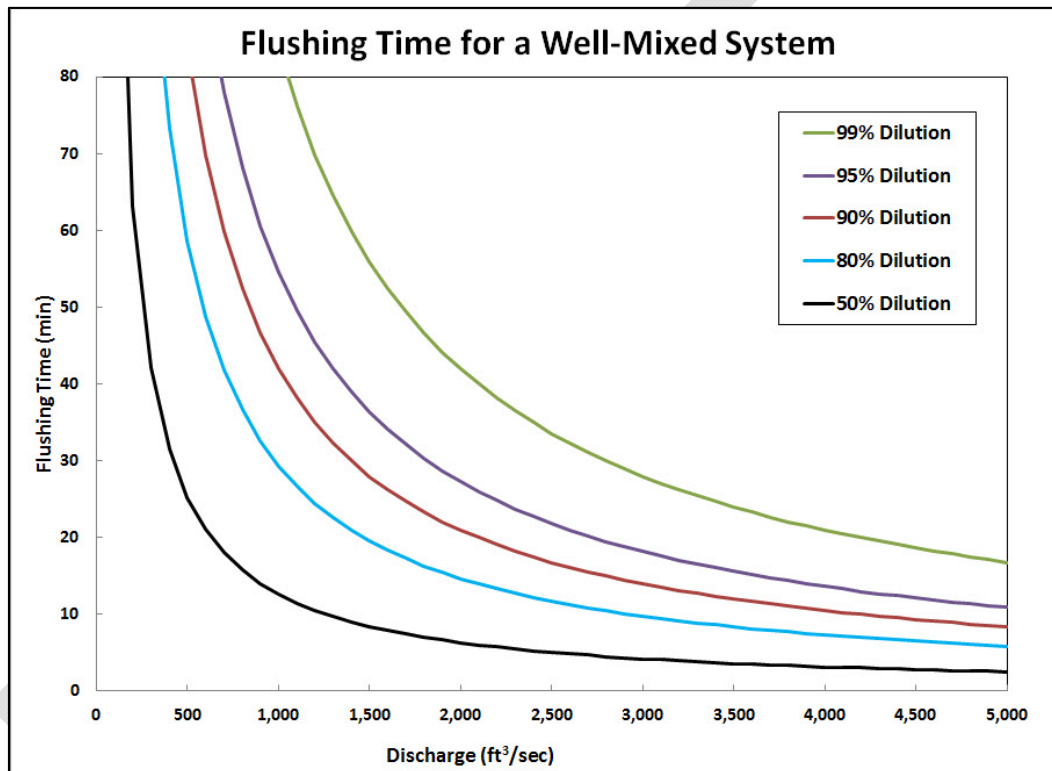
Concentration histories for various discharges are shown in Figure 10. These concentrations presented correspond to a normal tailwater el 504.5 where  $C = \exp\left(-\frac{Q}{V}t\right)$ .

Figure 10. Well-mixed lock chamber concentration histories



The Type 1 concept will perform more as a well-mixed flow field wherein the flushing times for various discharges are illustrated in Figure 10. Flushing of the well-mixed chamber can be evaluated as the time required for dilution to a particular concentration. The flushing times required to reduce the ANS concentration by various amounts ranging from 50% to 99% are shown in Figure 11. The flushing times shown correspond to various dilutions at the normal tailwater el. 504.5 where  $t = -\frac{V}{Q} \ln(C)$ .

Figure 11. Well-mixed system flushing times for various dilutions

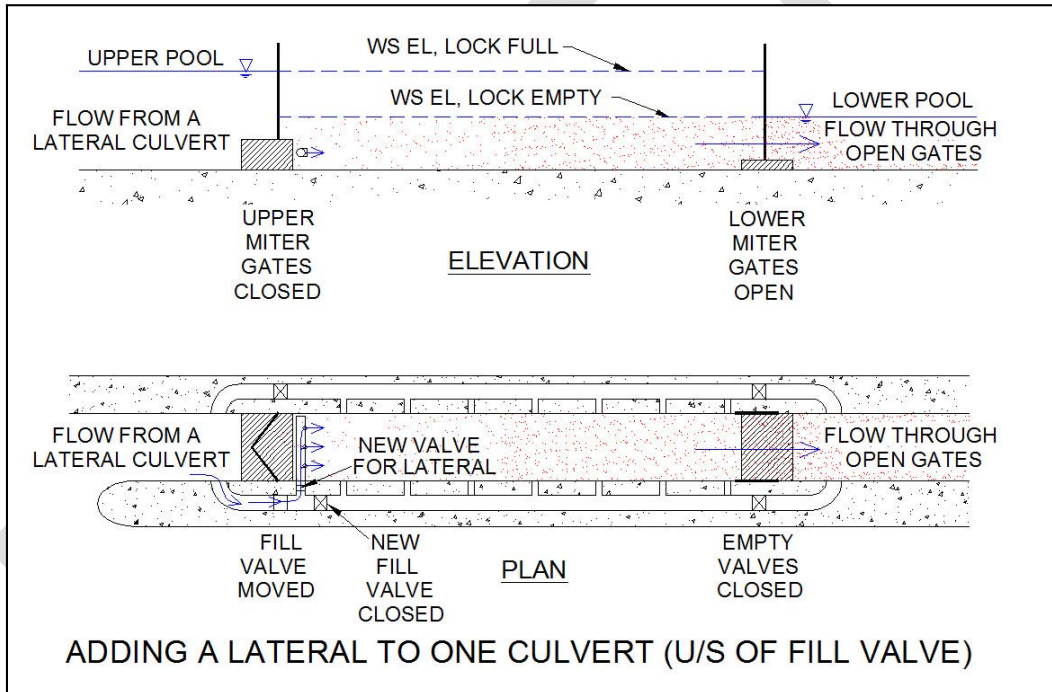


### 3.2.2 Type 2 lock flushing concept (lateral flushing manifold)

The Type 2 lock flushing concept (Figure 12) is a new culvert and manifold perpendicular to the lock walls. The movement of flushing flow through the system is indicated by the blue arrows in the figure. The flushing operation would have the upper miter gates closed, the lower miter gates open and the filling and emptying valves closed. This scheme would require a valve on the flushing lateral that would be opened during the flushing operation. The flushing manifold would be placed immediately downstream of the upper sill so that most of the chamber is downstream of the lateral's discharge. This culvert would join one of the filling culverts (either right or left wall) upstream of that culvert's fill valve. The existing culvert system of

Brandon Road Lock would have to be significantly altered to accommodate this design. Fitting this configuration into Brandon Road Lock filling system will be a challenge. The culverts make rectangular-to-circular transition and the fill valve will have to be moved downstream. The first port on the lock manifold will perhaps have to be closed to make room for the new fill valve and lateral culvert. Closing the first port may actually have beneficial consequences since the sum of the port areas is about 1.5 times that of the culvert area. Sidewall port design criteria calls for a ratio of 0.95. Chamber performance during filling is enhanced when the flow control is at the ports. This requires that the port to culvert area ratio be less than or equal to 1.0.

Figure 12. Type 2 design flushing system schematic.



For the purposes of this report, culvert sizes and configurations were taken from the St. Lawrence Seaway Development Corporation's design for the Eisenhower Lock (Figure 56 in Appendix A). The flushing culvert is 10 ft in diameter and the lateral manifold has five pipes that tee into the lateral. Each pipe is 4 ft in diameter and serves as a port resulting in a sum of the port-to-culvert area ratio of 0.8.

The sum of head loss at normal pool conditions is 34 ft. Equating this head loss to the losses listed in Table 4, the discharge is calculated to be 3,540 ft<sup>3</sup>/sec. This is the estimated discharge from the Type 2 concept at normal

pool conditions with the flow-control valve (vertical-lift valve) fully open. This concept will act somewhat as an advection-dominated system wherein the water moves downstream as plug flow.

Table 4. Loss coefficients for Type 2 lock flushing concept.

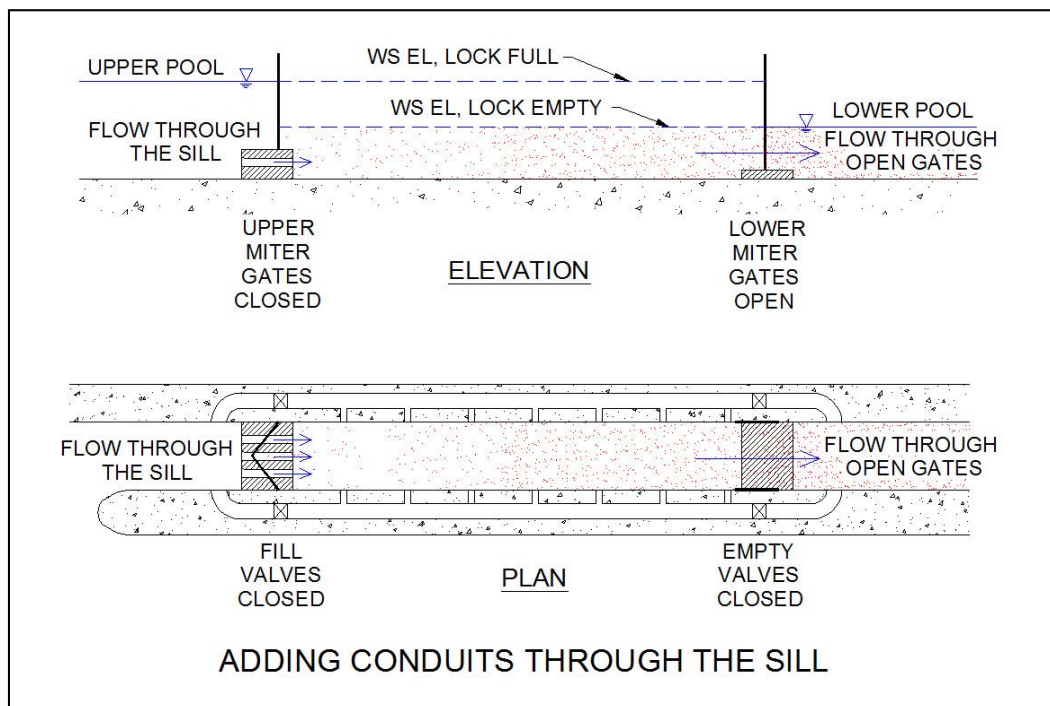
System Component	Loss Coefficient, $K$	Representative area, ft <sup>2</sup>	Coefficient Value
Lock Intake	$K_i$	216	0.24
90 deg bend	$K_b$	216	0.24
Open vertical-lift valve (old)	$K_{gv}$	81	0.11
90 deg T junction	$K_{tee}$	78.5	0.23
Open flow-control (butterfly) valve	$K_{bv}$	78.5	0.2
Dividing flow manifold	$K_m$	78.5	1.5
Outlets	$K_o$	12.6	1.0

The Type 2 design will require at least 10.5 ft of excavation below the existing lock floor elevation. This limestone excavation is required for placement of the lateral culvert beneath the lock floor.

### 3.2.3 Type 3 lock flushing concept (culverts through sill)

The Type 3 lock flushing concept (Figure 13) would be the addition of conduits through the upper sill. These pipes would require valves to control the flushing flow. The movement of flushing flow through the system is indicated by the blue arrows in the figure. Snell Lock on the St. Lawrence Seaway has undergone similar modifications to facilitate ice flushing from the chamber. The plug-flow analogy would be a more reasonable representative of the flushing than the well-mixed case.

Figure 13. Type 3 lock flushing concept schematic.



The new pipes will be long enough to pass from the upstream to downstream face of the upper sill (approximately 85 ft). Culverts passing through the sill will experience intake losses, friction losses, loss at the opened valve (e.g. butterfly), and exit losses. The pertinent loss coefficient characteristics and values for the Type 3 lock flushing concept are shown in Table 5. Multiple pipes are required to prevent reverse eddies and motionless areas in the upper corners of the chamber (Oswalt 1976). The total discharges possible for Type 3 with a 34 ft lift are shown in Table 6.

Table 5. Loss coefficients for Type 3 lock flushing concept.

Conduit Segment	Loss Coefficient, K	Characteristic Dimension(s)	Coefficient Value
Inlet	$K_i$	$A = \frac{\pi D^2}{4}$	0.1
Wall friction	$f L/D$	$L = 85 \text{ ft}$	$0.014 * 85/D$
Open butterfly valve	$K_v$	$A = \frac{\pi D^2}{4}$	0.2
Exit	$K_e$	$A = \frac{\pi D^2}{4}$	1.0

Table 6. Calculated discharge for Type 3 lock flushing concept, 34 ft normal lift.

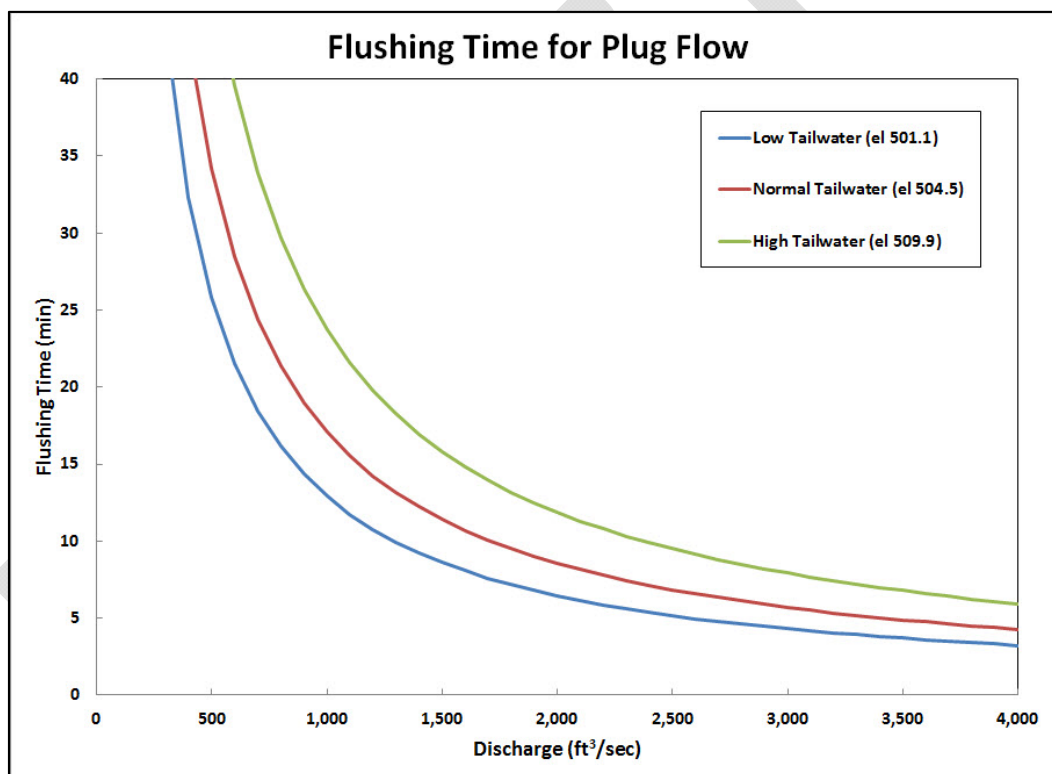
Pipe Diameter, $D$ , ft	Number of Pipes	Total Discharge, ft <sup>3</sup> /sec
4	1	460
	2	930
	3	1,390
	4	1,860
	5	2,320
5	1	740
	2	1,480
	3	2,230
	4	2,970
	5	3,710
6	1	1,080
	2	2,170
	3	3,250
	4	4,340
	5	5,420

Intakes in the upper sills of locks have led to vortex formations during lock filling. Numerous physical model studies have been conducted to reduce vortex tendencies (e.g. Ables 1979, Hite 1999, Hite 2000, Hite and Tuthill 2005, and Hite 2012). During previous model studies, conducted with through-the-sill intakes, modifications in the approach were developed to reduce the tendency for strong vortices to form. Streamlining the flow into the intakes by modifying the miter gate recesses have helped reduce vortex formation. Reducing the approach velocities by deepening the approach also helps improve flow conditions. Therefore, the Type 3 concept will most likely induce vortices in the upper approach during flushing operations. The tendency for vortex formation is due to the relatively small intake area in conjunction with the culvert intakes being relatively shallow.

Vortices will not only inhibit the efficiency of the culverts thereby reducing the discharge, they can also be a safety hazard and draw debris down to the culvert intakes. Intake trash racks can then become clogged with submerged debris, further restricting in the intake area and discharge.

The Type 2 and Type 3 concepts will serve more as advection-dominated flow fields and the plug-flow analogy provides an order of magnitude estimate of the time required to flush ANS from the lock chamber. The flushing times for multiple flushing discharges are shown in Figure 14. The discharges shown are given by  $t = -\frac{V}{Q}$ .

Figure 14. Plug-flow system flushing time for various tailwater elevations

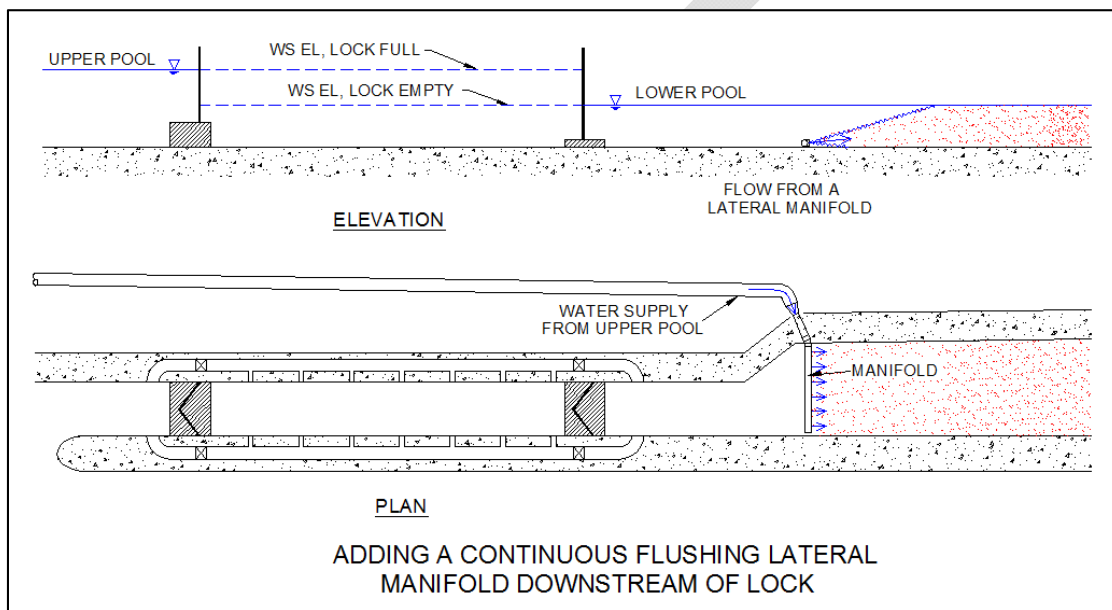


### 3.2.4 Type 4 lock flushing concept (continuous flow below chamber)

The Type 4 concept is not a configuration of Brandon Road Lock, but rather relies on keeping ANS from entering the lock chamber. The barrier is a lateral manifold across the lower approach channel downstream of the lock providing continuous flow. The clean water is taken from the upper pool and the flow is distributed across the channel with a multiported manifold as illustrated by the sketch in Figure 15.

One short coming of this concept is that it does not address the ANS that can be carried into the lock chamber as upbound and downbound tows traverse the lock. Propeller wash from tow boats and return currents generated as downbound tows leave the chamber may transport ANS over the continuous flow manifold. Also, the water pushed ahead of upbound tows may also overcome the hydraulic gradient that the manifold maintains. Once ANS are upstream of the manifold, there is no means to flush them using the Type 4 concept.

Figure 15. Type 4 concept schematic.



The physical model could be designed to accommodate experiments to evaluate the Type 4 concept. Particular questions could be answered such as the effectiveness of the Type 4 concept as tows pass over it.

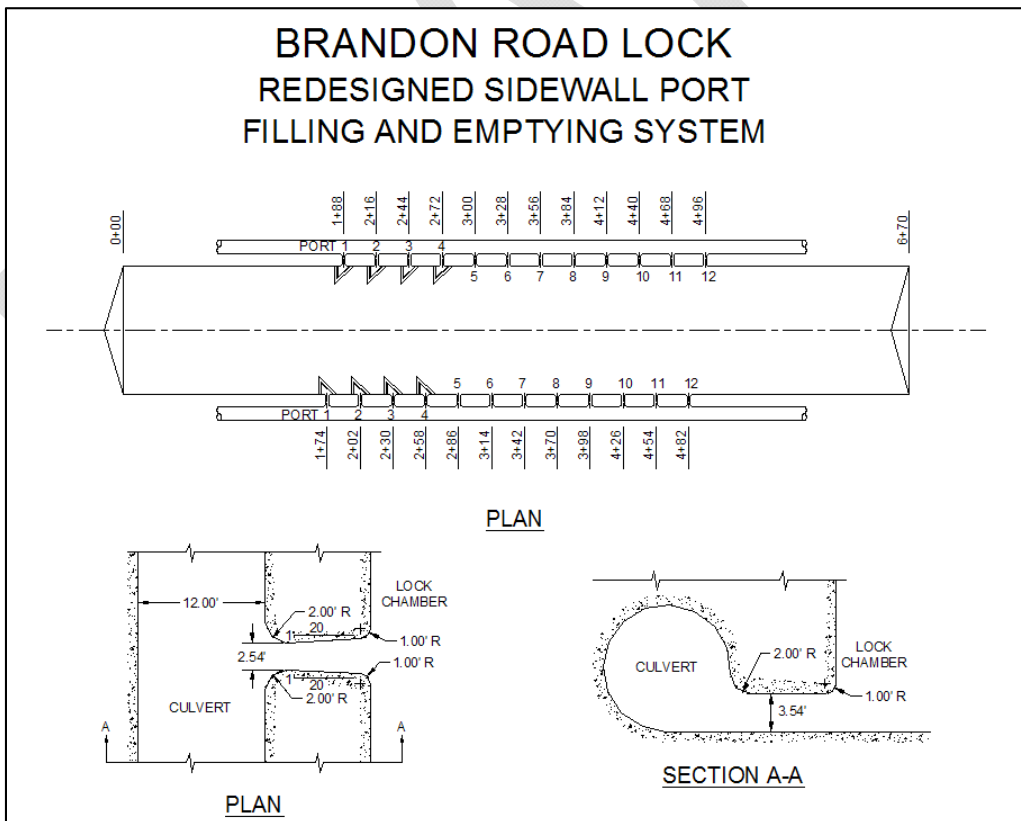
### 3.2.5 Type 5 lock flushing concept (redesigned filling and emptying system)

The Type 5 lock flushing concept, shown in Figure 16, uses a redesigned lock filling and emptying system to flush the lock chamber. This system would be set up and operate similarly to the Type 1 system. For details of this setup, see Section 3.2.1. This concept basically adheres to the current USACE hydraulic design guidance for lock filling and emptying systems (Engineer Manual 1110-2-1604, “Hydraulic Design of Navigation Locks”). Each culvert consists of twelve 3.54-ft tall ports that are 2.54 ft wide at the culvert with a 1 on 20 taper to the culvert. These ports have a 28-ft spacing

(center to center). Unlike the ports with the existing design that face one another directly, the ports in the redesigned system are offset by 14 ft. This offset is included so the jets extending from the ports on one culvert do not interfere with those from the ports in the opposite culvert. Removing any such interference should reduce any bulking at the chamber water surface. Triangular flow deflectors are included in the lock chamber for the first four ports on each culvert. These deflectors are included on the upstream third of the culverts on each port to have jets that have a downstream component. That is, to produce jets that point toward the opposite lock chamber wall instead of more toward the downstream gates.

The only deviation from the current design guidance is the inclusion of a 6x6-ft port (shown in Figure 21 in Chapter 5) at the upstream end of each filling and emptying culvert. These two ports are included in the design solely to improve the flushing performance of the upstream end of the lock chamber. These ports are positioned at the location of the first port in the existing filling and emptying system (Figure 17 in Chapter 5).

Figure 16. Type 5 concept schematic



## 4 Numerical Modeling Process

Dead zones, defined as regions that are not directly affected by the momentum exchange from the flushing jets, can be recreated with numerical models. Therefore, a numerical model has been developed for each of three lock flushing concepts to determine the location and size of dead zones produced by each lock flushing concept. Each numerical model includes details of the flushing evaluation such as the complete geometry that are not used in the purely analytical approach. Also, the numerical model produces flow distributions and patterns that are needed to evaluate flushing efficiency.

A three-dimensional (3-D) Navier-Stokes (non-hydrostatic) numerical flow model of the lock is a useful predictive tool to explore lock flushing concepts. The ERDC's 3-D Navier-Stokes module of the Adaptive Hydraulics (AdH) code has been used to model the complicated turbulent exchange processes as flow passes into and from the lock chamber and is an appropriate tool for this modeling effort. AdH produces time-varying flow solutions, and steady-state solutions are obtained by simulating time until the dynamic variation in the flow field ceases.

### 4.1 Governing Equations

The Reynolds-Averaged Navier-Stokes (RANS) equations are employed to model the flow field approaching, interacting with, and passing by hydraulic structures. The RANS equations are three-dimensional (3-D) with four degrees of freedom: the pressure and the three components of fluid velocity. These equations make no assumptions about pressure distributions. Since many hydraulic flow models assume the flow is hydrostatic, RANS models are referred to as non-hydrostatic models.

The RANS equations are derived from the conservation of mass and conservation of momentum applied to fluid flow by decomposing the instantaneous flow velocity into a mean component,  $\mathbf{U}$ , and a fluctuating component,  $\mathbf{u}$ , and averaging these equations over time periods that are long compared to the periods of fluctuations. Following the velocity decomposition, the conservation of mass for an incompressible fluid, described as

$$\nabla \cdot \mathbf{U} = 0 \quad (0)$$

and, the conservation of momentum is given as

$$\rho \left( \frac{\partial \mathbf{U}}{\partial t} + \mathbf{U} \cdot \nabla \mathbf{U} \right) - \nabla \cdot \boldsymbol{\sigma} + \nabla \cdot (\rho \mathbf{u} \mathbf{u}) = 0 \quad (0)$$

where  $t =$  time

$\rho =$  fluid density

$\boldsymbol{\sigma} = -p\mathbf{I} + \boldsymbol{\tau}$

$\mathbf{I} =$  identity matrix

$\boldsymbol{\tau} = 2\mu\boldsymbol{\Gamma}$

$\boldsymbol{\Gamma} = \frac{1}{2}(\nabla \mathbf{u} + \nabla \mathbf{u}^T)$

$\mu =$  fluid viscosity

The RANS equations are written in terms of the mean velocity,  $\mathbf{U}(x, t)$  and pressure  $p(x, t)$  to reduce the modeling of turbulence to a set of quasi-steady-state equations that incorporate terms to model the effects of turbulence on the main flow. In a RANS approach, the term  $\nabla \cdot (\rho \mathbf{u} \mathbf{u})$  is used to represent the effect of turbulence on the mean flow.

Following the suggestion of Boussinesq, an eddy viscosity is added to the molecular viscosity in the momentum equations to account for the effects of turbulence. A constant eddy viscosity model was used to replicate the turbulent effects. The eddy viscosity value was reduced until the velocity magnitudes no longer changed with decreasing values of the eddy viscosity. This threshold value of eddy viscosity was used for all simulations.

The effectiveness and efficiency of each lock flushing concept was modeled by direct calculation of the concentration of the flushing flow throughout the flow domain. These concentrations were treated as being composed of neutrally-buoyant concentrations. The behavior of the concentration is described by the advection-diffusion equation as indicated in Section 2.1 (Equations 1). For the numerical modeling the three-dimensional form of the advection-diffusion equations assuming a constant diffusion coefficient is used

$$\frac{\partial C}{\partial t} + \mathbf{U} \cdot (\nabla C) - D \nabla^2 C = 0 \quad (0)$$

where  $\mathbf{U} =$  mean velocity vector at a point

The diffusion coefficient  $D$  is assumed to be equal in all directions.

## 4.2 Modeling Procedure

Before the equations of motion can be applied, the domain must be discretized into numerical elements. This process includes the construction of a 3-D CAD representation of the flow boundaries including the geometric features of the hydraulic structure, the bathymetry of the approaching river, and the water surface. The CAD model is then used as input for a mesh generator.

A computational mesh is constructed to fill the volume enclosed by the CAD model surfaces. For AdH simulations, the computational mesh must only sufficiently describe the boundaries of the flow domain because automatic mesh refinement is used to ensure that the flow features interior to the domain are reproduced correctly. The mesh of the CAD surface will be composed of individual faces of the elements that form the lock's boundaries and the water surface. The boundary conditions such as velocity, discharge and pressure, are needed on these faces and their nodes to determine a particular solution to the governing partial differential (RANS) equations.

## 5 Numerical Model Setup

A numerical model was created for each lock flushing concept. For each lock flushing concept the upper pool elevation is 538.5 ft NGVD, and the lower pool (chamber) elevation is 504.5 ft NGVD. These elevations are the average normal pool elevations present at Brandon Road Lock from 2005-2014. Additional information about the computational meshes such is included in Appendix B.

Each model has two flux boundaries – one inflow and one outflow. The model discharge, listed in Table 7, was applied as an average inflow velocity at the inflow boundary. Initially for Type 3, a flushing discharge of 3,000 ft<sup>3</sup>/sec was used. This discharge was based on the maximum available flushing discharge outlined in Chapter 4 (Table 6). However, this discharge produced such high velocities in the upstream end of the chamber near the flushing pipe outlets that the water surface drawdown in that area was around 5 ft. Such a large drawdown would likely not satisfy safety concerns when barges are moored in the lock chamber, so the flushing discharge was reduced to 1,000 ft<sup>3</sup>/s. The new flushing discharge produced average velocities in the flushing pipes that are similar to the largest average velocities through the filling and emptying ports in Type 1.

The 2,600 ft<sup>3</sup>/sec flushing discharge for Type 5 is based on a redesigned (stronger) intake valve and gate that can be opened to half open when under full head; currently the existing valves can only be lifted a quarter open under full head without excessive vibration and chance of being pinned shut.

**Table 7. Lock flushing model discharges**

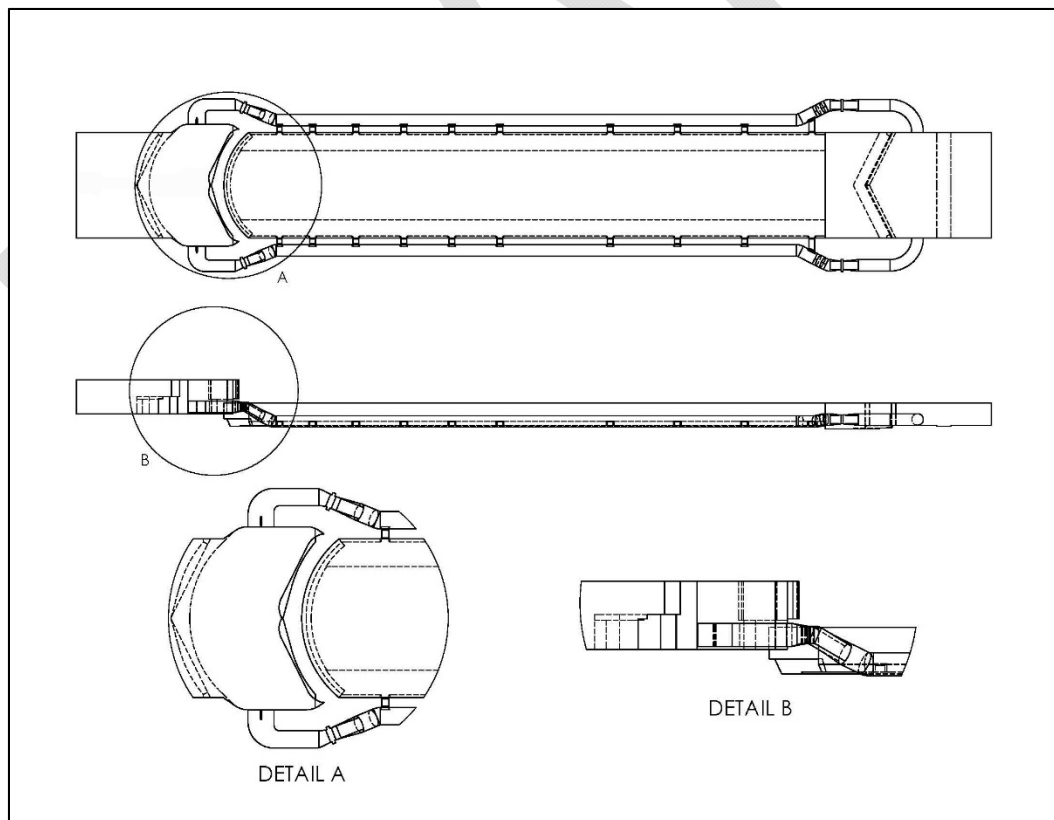
Flushing Concept	Flushing Discharge (ft <sup>3</sup> /sec)
Type 1	1,350
Type 2	3,540
Type 3	1,000
Type 3r	3,000
Type 5	2,600

For each model a hydrostatic pressure distribution was applied to the nodes on the downstream boundary such that zero pressure was applied to the nodes at the water surface on the downstream boundary. Further details of each lock flushing concept geometry are discussed in the proceeding sections. The diffusion coefficient of  $0.0003 \text{ ft}^2/\text{sec}$  was used for all simulations.

### 5.1 Type 1 lock flushing concept model geometry

The Type 1 lock flushing concept is the existing filling and emptying system. Figure 17 shows a CAD model of Brandon Road Lock filling and emptying system. The CAD model was constructed from the line drawings provided by the INDC (e.g. “Brandon Road - Lock & Dam - 3-L1-6-2 - Dated 1930.pdf”). The flow domain includes a portion of the lock upstream of the upper miter gates, both filling and emptying culverts with both the intakes and ports, and the lock chamber. The downstream end of the flow domain is located at the pintle of the downstream miter gates. The culvert is terminated downstream of the last (tenth) port.

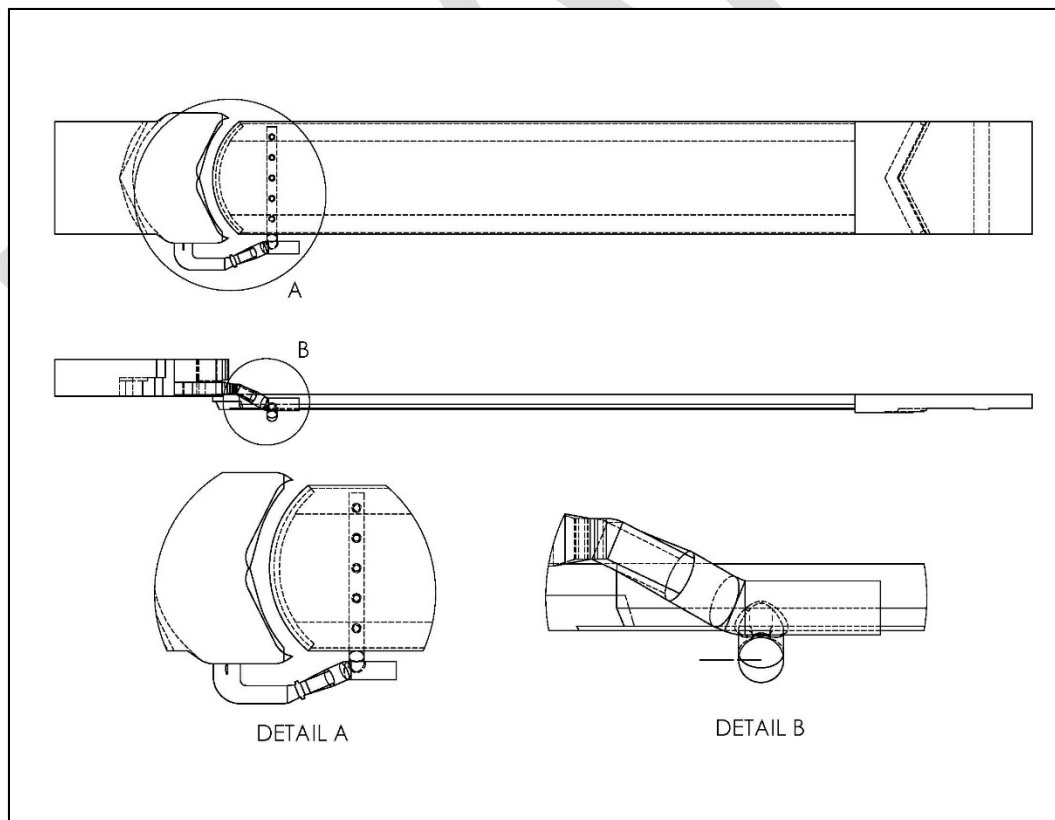
Figure 17. CAD model of Type 1 lock flushing concept



## 5.2 Type 2 lock flushing concept model geometry

The Type 2 lock flushing concept is an additional lateral flushing manifold positioned near the upstream end of the lock chamber. The CAD model for this concept is shown in Figure 18. The flushing manifold is connected to the right of the existing filling and emptying culvert at the first port. This manifold culvert has a uniform 10-ft circular diameter cross-section with five 4-ft diameter ports. These ports are connected to the top of the flushing culvert and are directed vertically. The center of the first port is 15 ft from the lock wall, and the ports are at 20-ft spacings (center to center). To satisfy USACE design criteria on clearance, the lock flushing culvert is 10.5 ft below the lock chamber floor. The flushing ports connect the top of the flushing culvert to the lock floor. The flushing manifold would require all the flow entering one of the existing filling and emptying culverts to be directed completely through the manifold, so the filling and emptying culvert downstream of the flushing manifold was not included in the flow domain. The opposite filling and emptying culvert (the one not involved in the lock chamber flushing) was also excluded from the flow domain.

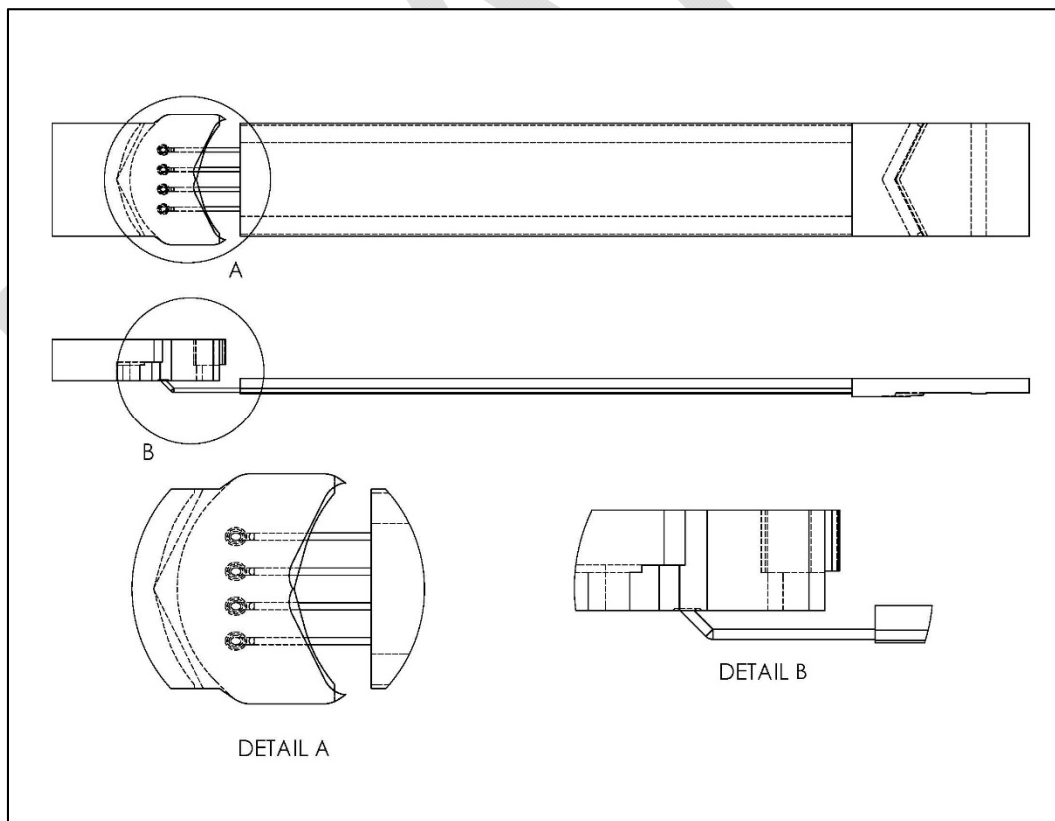
Figure 18. CAD model of Type 2 lock flushing concept



### 5.3 Type 3 lock flushing concept model geometry

The Type 3 lock flushing concept is a series of pipes in the upstream gate sill that connect the upper pool with the lock chamber. The configuration chosen for the computation model, shown in Figure 19, has four 5-ft diameter pipes positioned laterally at a 19.2-ft spacing (center to center) along the gate sill over the deepest portion of the lock chamber. The center of these pipes is at el. 494, which corresponds to a submergence of 10.4 ft when the lower pool water surface is at el. 504.5. The filling and emptying culverts play no role in the lock flushing for this concept, so they were not included in the flow domain. The Type 3 numerical model flow domain includes a portion of the lock upstream of the upper miter gates, the gate sill pipes, and the lock chamber terminated at the downstream miter gates. The lock chamber for the Type 3 concept differed from that of the Types 1 and 5 in that a portion of the upstream end (upstream of the first port in the existing filling and emptying system) was removed. This removal is a structural requirement for the flushing pipes.

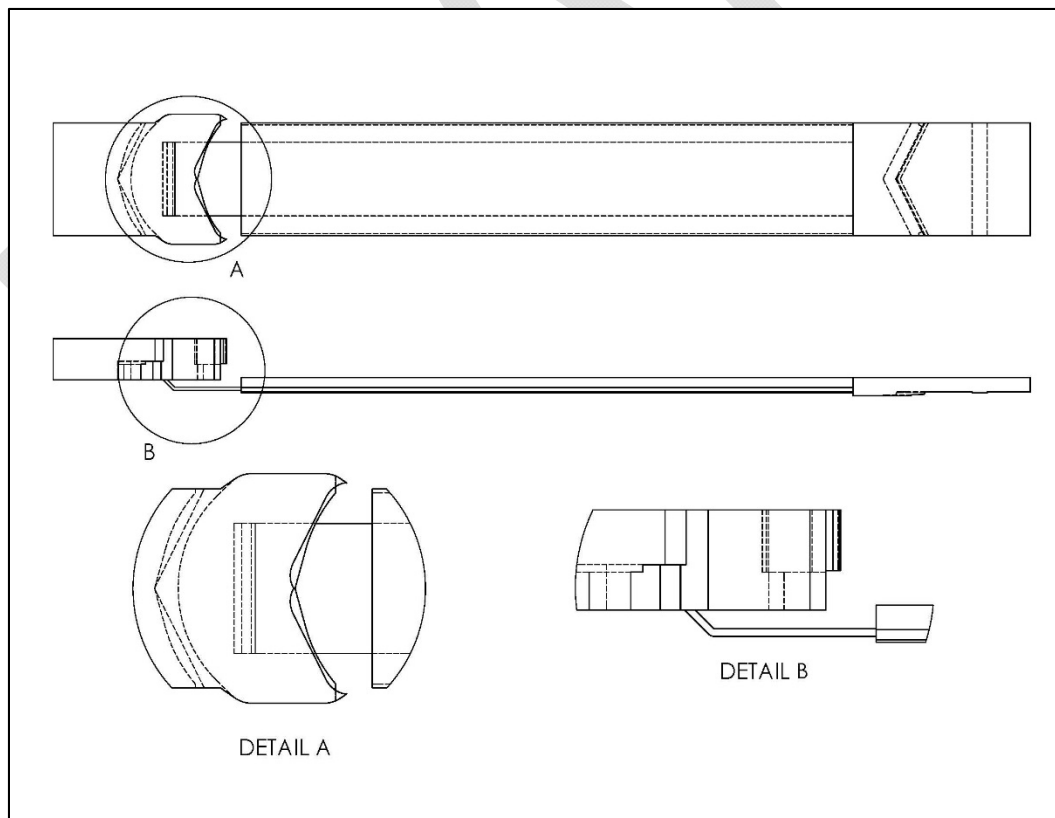
Figure 19. CAD model of Type 3 lock flushing concept



## 5.4 Type 3r lock flushing concept model geometry

The Type 3r lock flushing concept, shown in Figure 20, was developed as a result of the reduced discharge in the Type 3 model. For the Type 3 numerical model, the discharge was reduced because of the high velocities in the upstream side of the lock chamber. For the Type 3r model, the size of the conduit that introduces flushing flow into the lock chamber was increased such that the average flushing velocity introduced into the lock chamber is close to 15ft/sec. This average velocity corresponds to the largest average velocity of flow through the filling and emptying ports in the Type 1 lock flushing concept. This new conduit, referred to as the “rectangular slot,” is a constant 72 ft wide by 3 ft tall cross-section that connects to the lock chamber at the same centerline elevation as the gate sill pipes in Type 3. The rectangular slot is centered laterally in the lock chamber. Constructing such a large conduit through the gate upstream gate sill is highly improbable, so this lock flushing concept is largely just to show how well a gate sill lock flushing concept could perform if only the hydraulics of the system are considered.

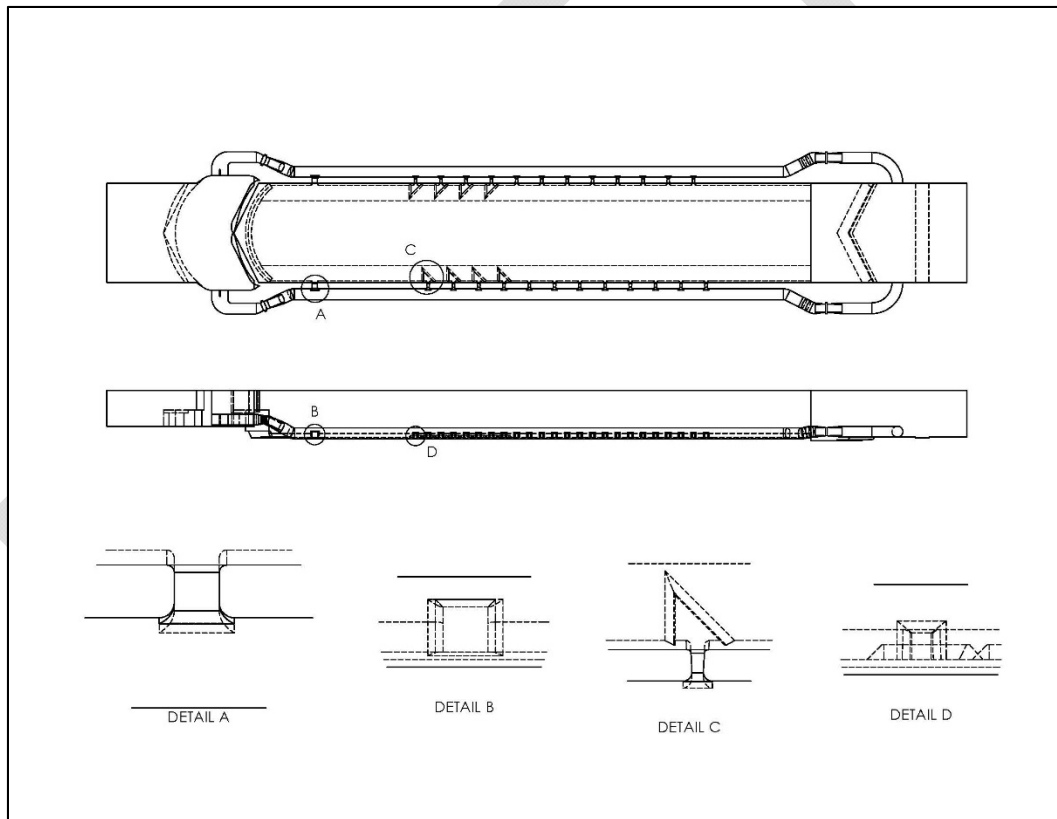
Figure 20. CAD model of Type 3r lock flushing concept



## 5.5 Type 5 lock flushing concept

The Type 5 lock flushing concept, shown in Figure 21, is a redesign of the filling and emptying system at Brandon Road Lock. The flow domain includes a portion of the lock upstream of the upper miter gates, both filling and emptying culverts with both the intakes and ports, and the lock chamber. The downstream end of the flow domain is located at the pintle of the downstream miter gates. The culvert is terminated downstream of the last (twelfth) port. One of the flushing ports mentioned in Section 3.2.5 is shown in Detail A of Figure 21. The upstream four ports on either side of the lock include deflectors as shown in Detail C. The port positioning and deflector geometry follow the guidelines set forth in EM 1110-2-1604.

Figure 21. CAD model of Type 5 lock flushing concept



## 6 Numerical Model Results

The results of each numerical model are shown and discussed in this chapter. Contour plots of the flow velocity and the original lock water concentration of each lock flushing concept during a simulated lock flushing operation are presented.

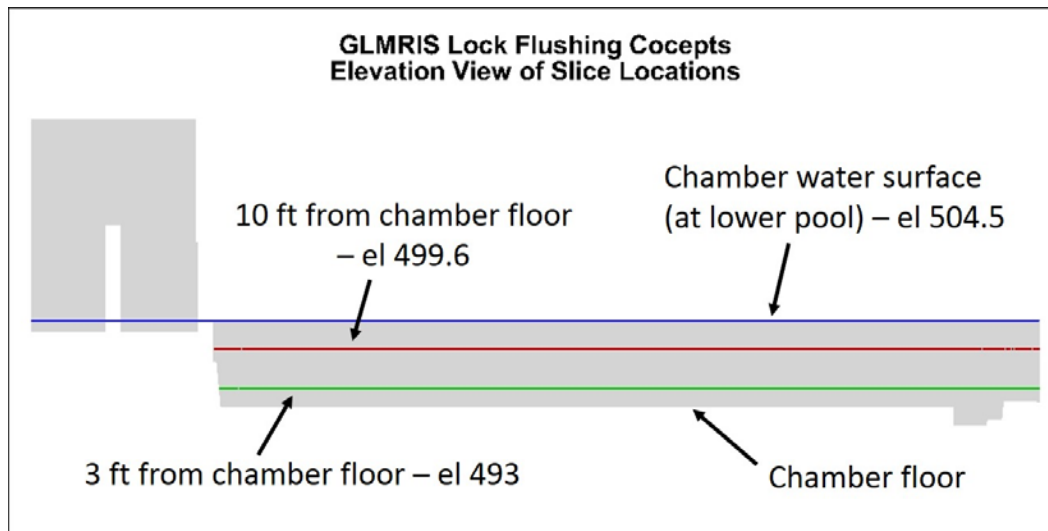
The flow results are presented with the velocity magnitude  $V$ , which is defined as

$$V = \sqrt{u^2 + v^2 + w^2}$$

where  $u$  = x-component of flow velocity  
 $v$  = y-component of flow velocity  
 $w$  = z-component of flow velocity

The simulation results are shown via contour plots that show the spatial distribution of the flow variables during lock flushing. These contour plots are presented for each of three different vertical slices in the lock chamber. As indicated in Figure 22, these three slices are a location three feet from the lock chamber floor, ten feet from the lock chamber floor, and at the lock chamber surface. Figure 22 has been stretched vertically by a factor of five, so the different slice locations could be seen more easily.

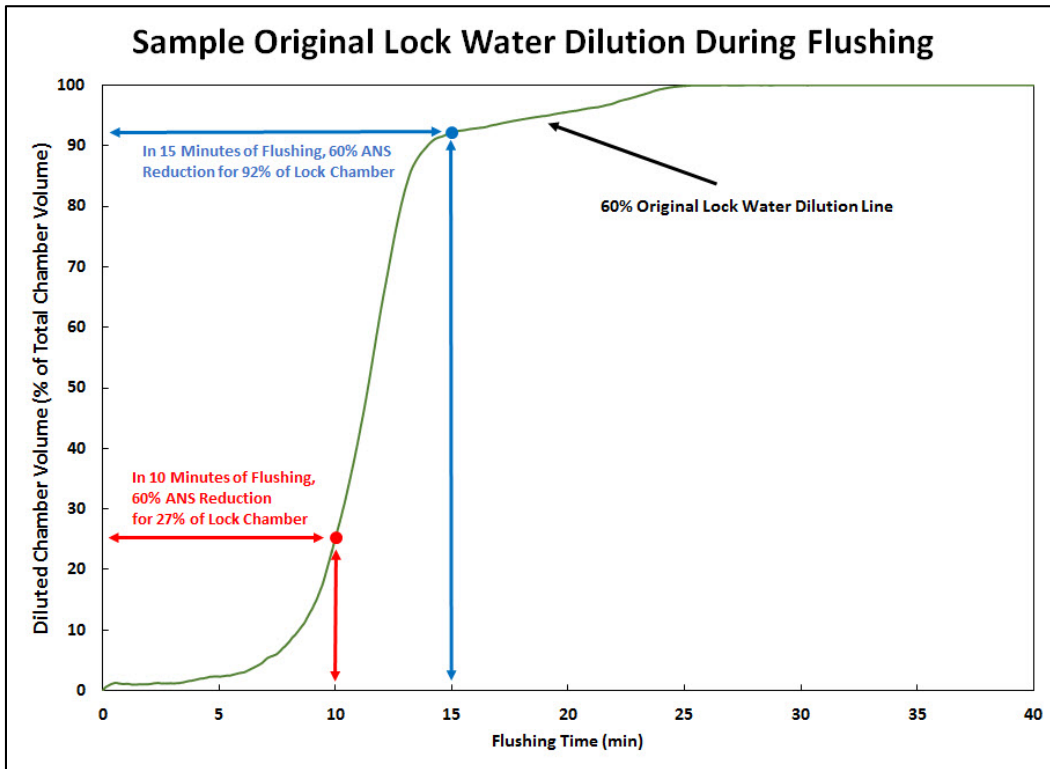
Figure 22. Simulation contour plot elevations



The effectiveness and efficiency of each flushing operation was quantified by calculating the reduction of the original lock chamber water concentration during the flushing operation. The volume of the lock chamber where the original lock chamber water concentration reduced to pre-chosen levels is shown as different curves on the dilution plots. These flushing volume results are reported as percentages of the total lock chamber volume throughout the lock flushing operation.

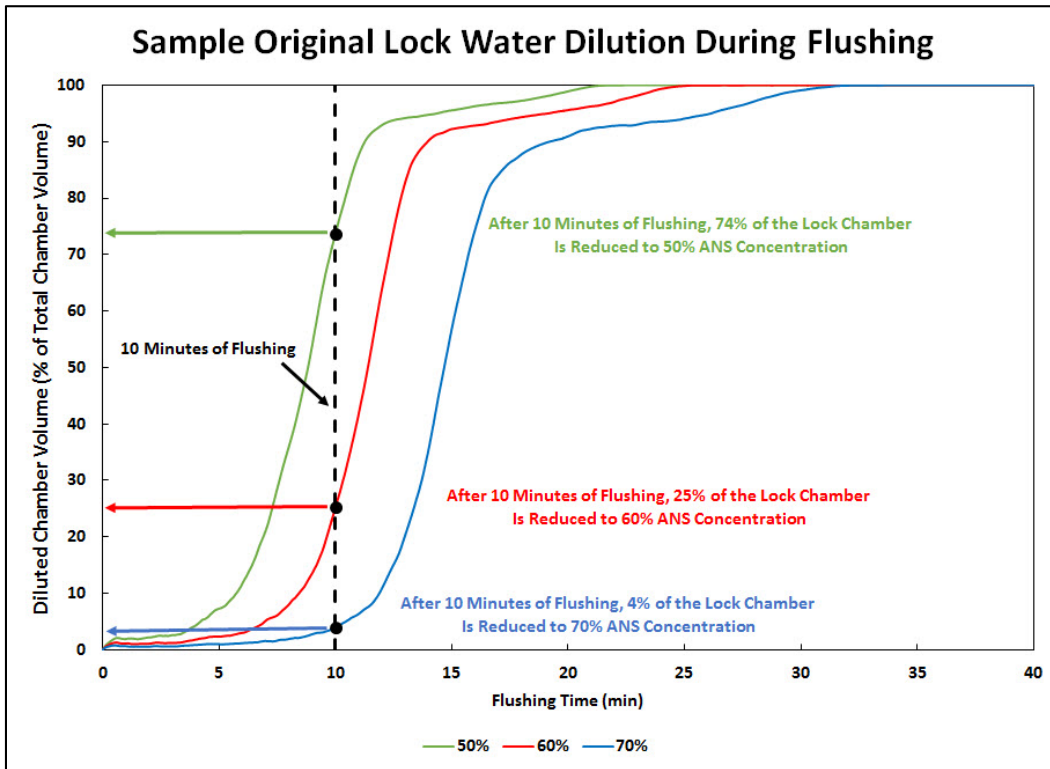
Figure 23 shows an example plot of how the lock flushing performance is quantified. The horizontal axis represents the flushing time and the vertical axis represents the percentage of the lock chamber volume that is reduced to certain concentration levels. In the example plot, the green curve shows the volume of the lock chamber that has been flushed to 60% of the concentration of water in the lock chamber during flushing. Two points on the curve are indicated. The red point on the plot represents ten minutes of flushing flow. Moving vertically from the horizontal axis at ten minutes to the red point, then proceeding to the left to the vertical axis shows that 27% of the lock chamber volume has been reduced to 60% concentration of the original lock chamber water. The blue point on the plot represents fifteen minutes of flushing flow. Moving vertically from the horizontal axis at fifteen minutes to the blue point, then proceeding to the left to the vertical axis shows that 92% of the lock chamber volume has been reduced to 60% concentration of the original lock chamber water.

Figure 23. Sample lock flushing volume plot – single curve explanation



Additionally, the plots can be read to show how much of the lock chamber has been reduced to multiple concentration levels at a single flushing time. In Figure 24, the blue, red, and green curves represent 70%, 60%, and 50% concentrations of water in the lock chamber during flushing. The black dashed line indicates ten minutes of flushing flow. The plot is read by picking a flushing time, moving vertically from the horizontal, flushing time axis, and each time the black dashed line intersects a concentration curve moving left to the horizontal axis to read the percentage of the lock chamber that has been flushed to the concentration indicated by the intersected curve. For instance, the black dashed line first intersects the blue line which indicates that after ten minutes of flushing flow, 4% of the lock chamber has been reduced to 70% of the original concentration. Similarly, the red curve indicates that 25% of the chamber is reduced to 60% of the original concentration in ten minutes of flushing. Also, the green curve indicates that 74% of the lock chamber has been reduced to 50% of the original concentration in ten minutes of flushing.

Figure 24. Sample lock flushing volume plot – single flushing time explanation



## 6.1 Type 1 lock flushing concept

The contour plots of the velocity magnitudes for the Type 1 lock flushing concept is shown in Figure 25-Figure 27. In each figure, the velocity contours shown at the beginning of flushing, at five minutes of flushing, and at ten minutes of flushing. The flushing discharge is remains constant throughout the simulation. Flushing flow is introduced into the lock chamber at several locations via the filling and emptying ports. Viewing the contours closest to the chamber floor, the velocity magnitudes vary in both time and space. The jets that extend from each port have a maximum velocity of about 4 ft/sec. Each jet extends roughly halfway across the lock chamber. The jets are directed more toward the downstream miter gates for the ports that are furthest downstream. The contours ten feet from the chamber floor show that the variation in velocity magnitudes is much smaller further away from the ports. At that elevation the maximum velocity magnitude is about 3 ft/sec. At the lock chamber surface, the velocity magnitudes vary more that near the center of the lock chamber water column. The largest velocity magnitudes at the water surfaces are about 3 ft/sec.

Contour plots of the original lock chamber water concentration for the Type 1 flushing concept are shown in Figure 28-Figure 30. At the beginning of flushing (flushing time = 0), the entire lock chamber is orange/red indicating a uniform concentration of 100% of the original lock chamber water. During flushing, the contours in the lock chamber change from orange/red to green to blue. These changes show that the lock chamber flushing is reducing the concentration of original lock chamber water. Since flushing flow is introduced at multiple locations in the lock chamber, the original lock chamber water concentration is reduced gradually throughout the lock chamber. Three feet from the chamber floor, the effect of the ports is noticeable and the reduction in chamber concentration varies dramatically in both time and space. Moving further up the lock chamber, the reduction in concentration is more gradual. After fifteen minutes of lock flushing, the concentration of original lock chamber water for each elevation is around 50% for the entire chamber. Upstream of the first filling port, the original lock chamber concentration is even higher.

Figure 25. Type 1 velocity magnitude contours at el. 493.

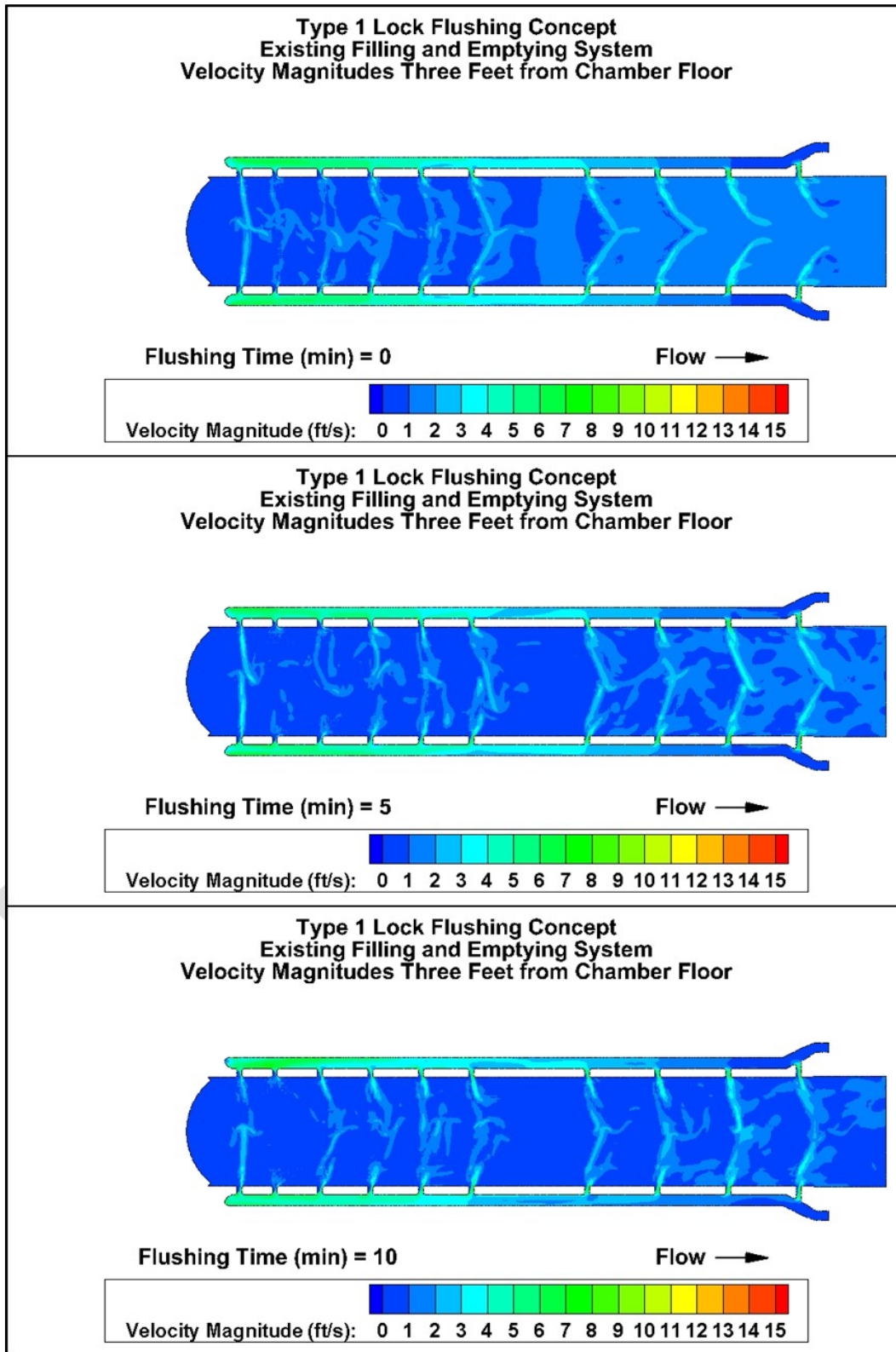


Figure 26. Type 1 velocity magnitude contours at el. 499.6.

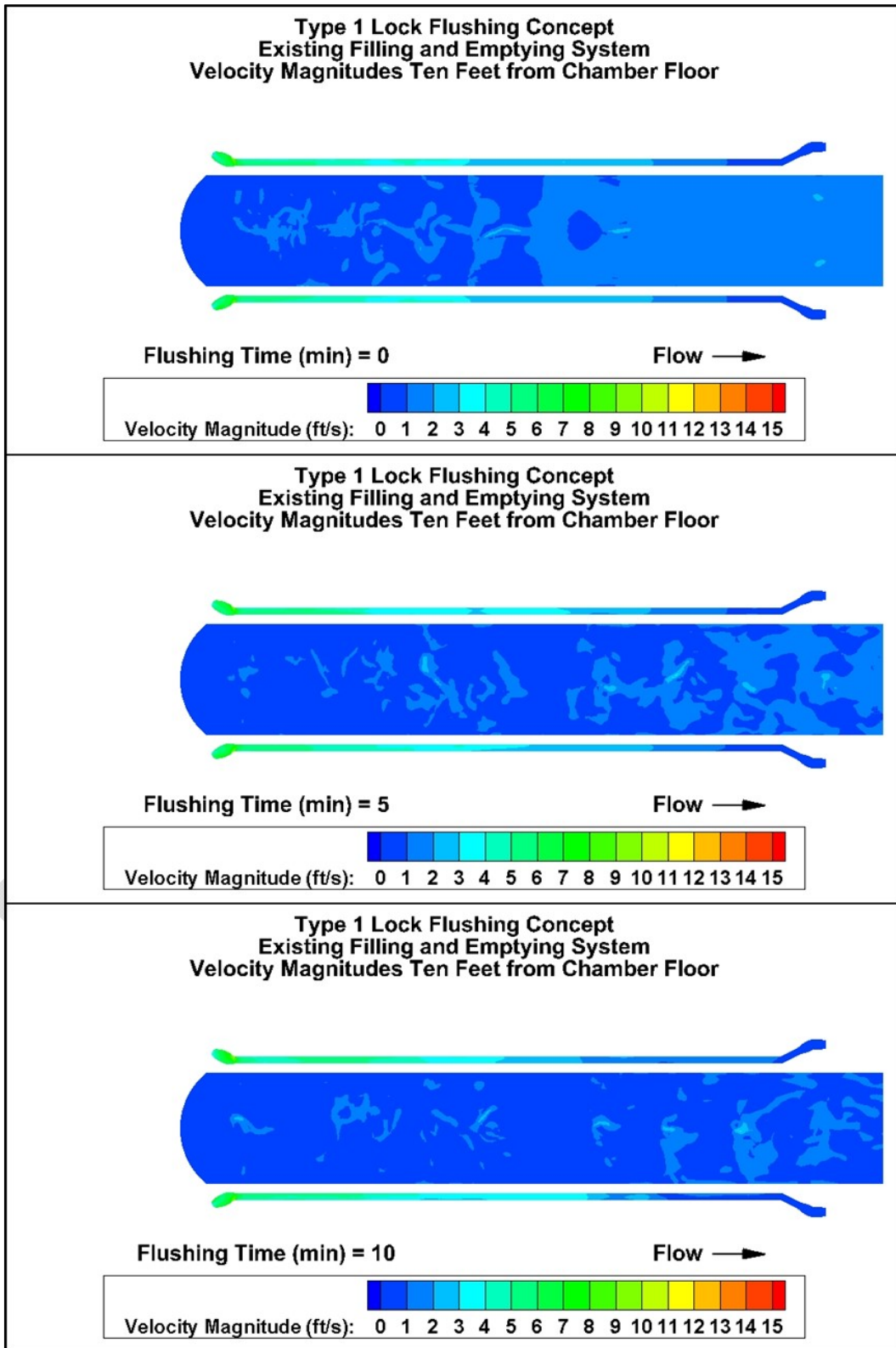


Figure 27. Type 1 velocity magnitude contours at lock chamber surface

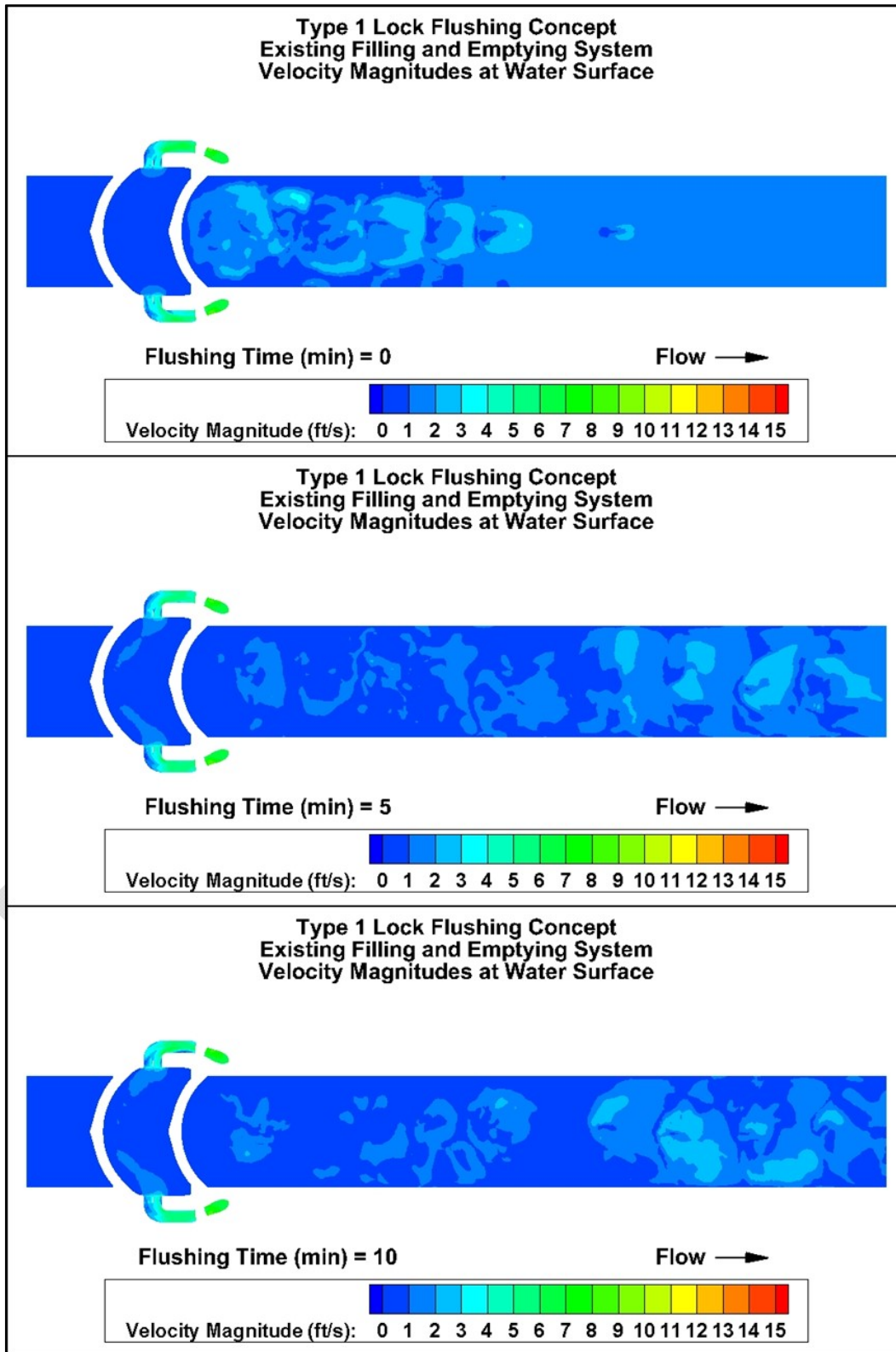


Figure 28. Type 1 original lock chamber water concentration contours at el. 493.

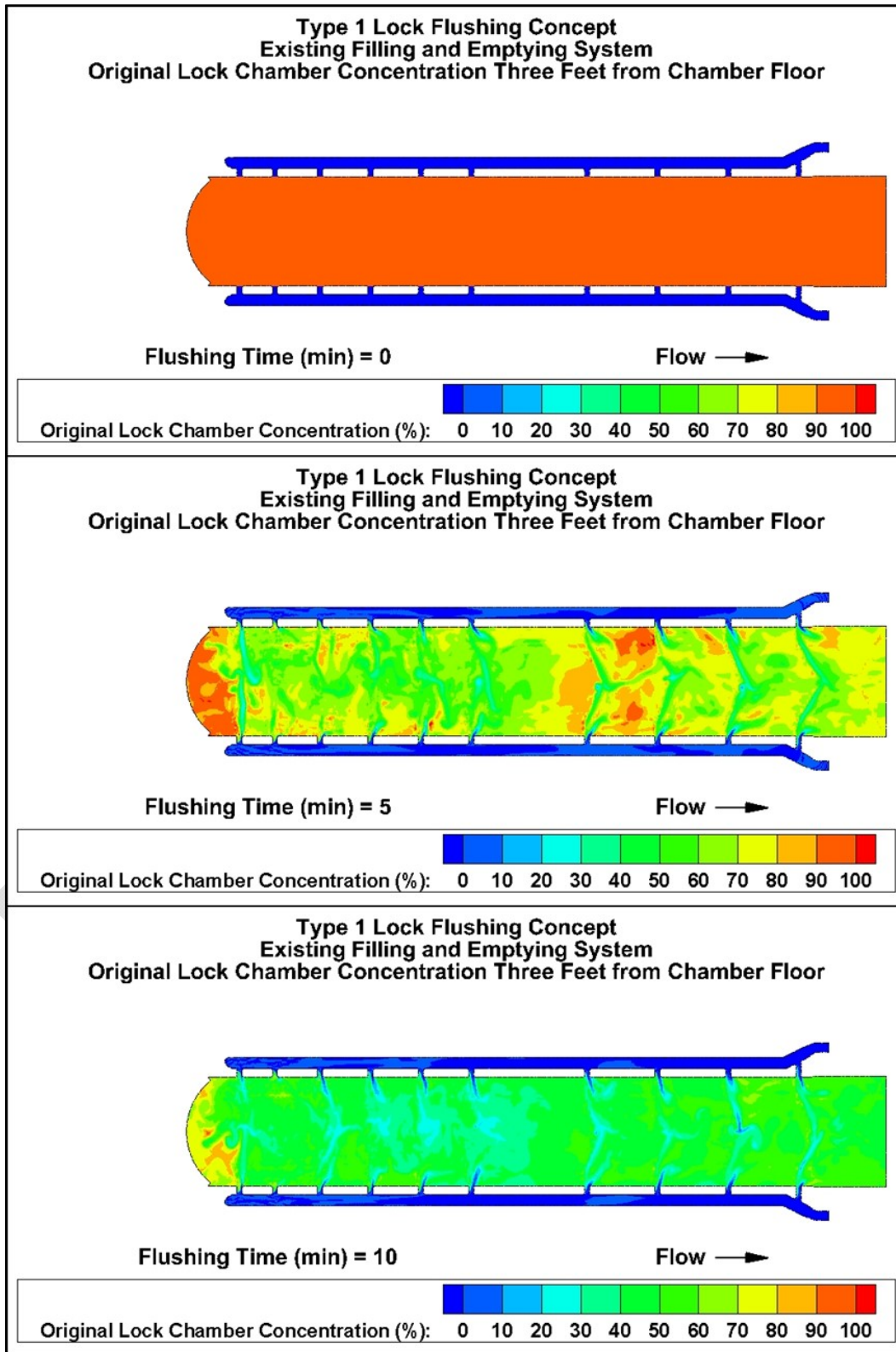


Figure 29. Type 1 original lock chamber water concentration contours at el. 499.6.

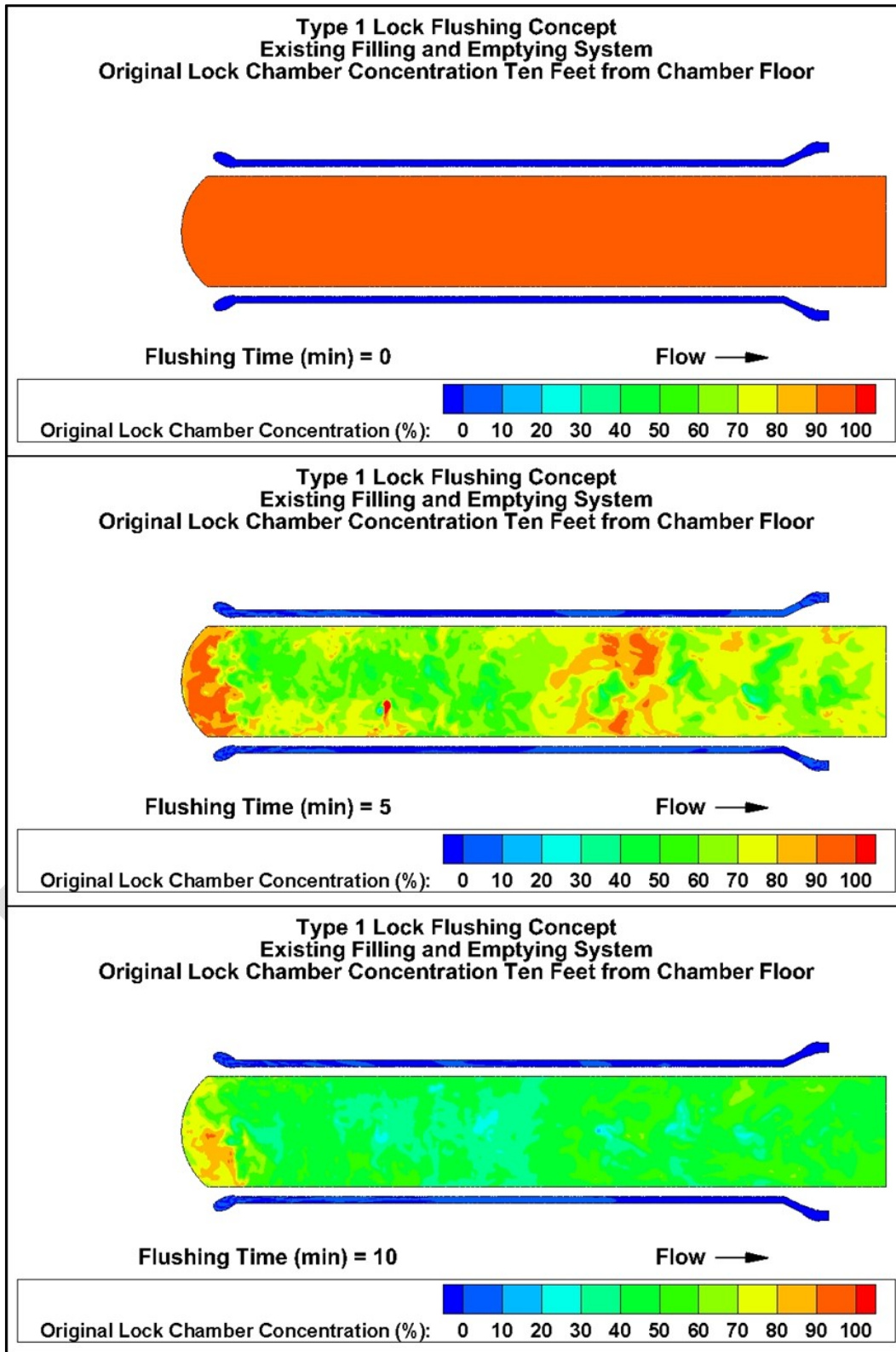
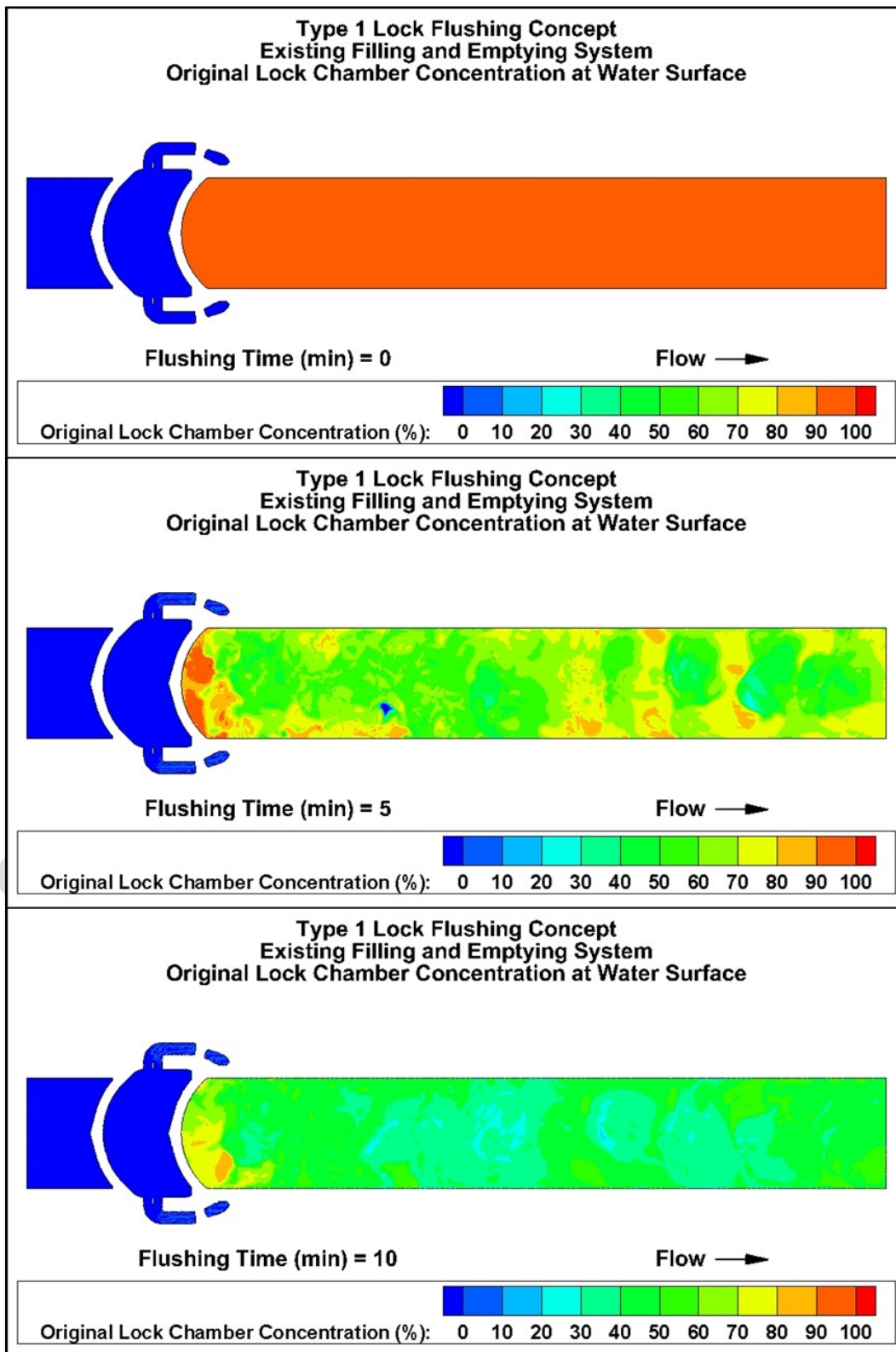


Figure 30. Type 1 original lock chamber water concentration contours at el. lock chamber surface



The flushing effectiveness and efficiency for Type 1 are shown in Figure 31 and Table 8. In the figure, the original lock water concentration is plotted against the flushing time. The different curves indicate how much of the lock chamber has reach different levels of original lock chamber water concentration during a flushing operation, with red indicating at most a 10% reduction in the original lock chamber concentration, green indicating at most a 50% reduction, and dark blue indicating a 99.9% reduction (essentially portions of the chamber where the water has been completely replaced by flushing water). Most of the curves show a slow volume change initially, a period of rapid volume change, and finally a return to a slow volume change as the curves approach 100% of the lock chamber. The desired amount of flushing (99.9% reduction) as indicated by the dark blue line (which is essentially on top of the horizontal axis) is not attained in forty minutes of flushing. After fifteen minutes (indicated by the dashed black line) even 80% reduction of the flow has only occurred in 4% of the lock chamber. Lock chamber volume percentages at five minute increments of flushing are shown in Table 8. The values listed correspond to values that can be read directly from Figure 31. Type 1 lock chamber flushing performance, but the table values provide more precision in the percent volumes.

Figure 31. Type 1 lock chamber flushing performance

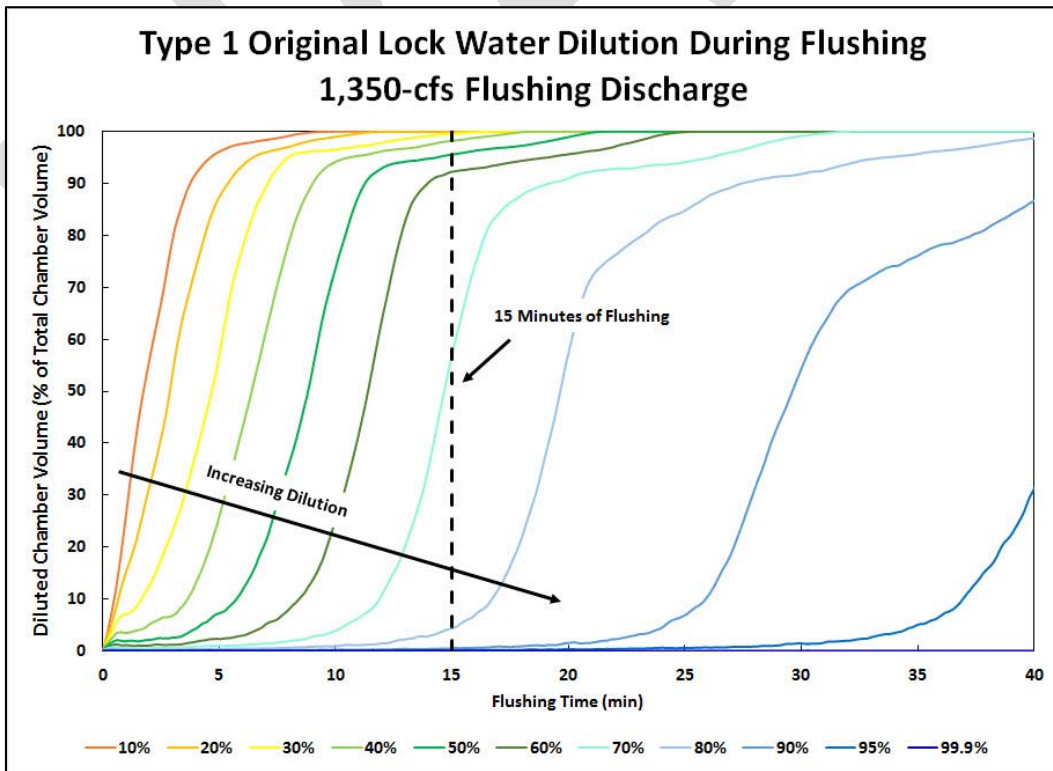


Table 8. Type 1 chamber flushing performance – 5-minute intervals

Flushing Time (min)		Flushed chamber volume (% of total lock chamber volume)							
		5	10	15	20	25	30	35	40
Dilution of original lock chamber water	99.9%	<1	<1	<1	<1	<1	<1	<1	<1
	90%	<1	<1	1	2	7	54	76	87
	80%	<1	1	4	57	85	92	96	99
	70%	1	4	57	91	94	99	100	100
	60%	2	25	92	96	100	100	100	100
	50%	7	74	96	99	100	100	100	100
	40%	26	94	98	100	100	100	100	100
	30%	57	97	100	100	100	100	100	100
	20%	87	99	100	100	100	100	100	100
	10%	96	100	100	100	100	100	100	100

## 6.2 Type 2 lock flushing concept

The Type 2 lock flushing concept was simulated in a previous phase of numerical modeling work for the GLMRIS project. The numerical modeling process during that phase included fixed lid models of the lock flushing concepts with no direct calculation of original lock water concentration. The velocity magnitude contour plots are included in Appendix C to give an idea of how the Type 2 concept would perform, but these results should be used as a direct comparison with the results shown and discussed in this chapter because extra degrees of freedom were included in those models, which can significantly affect the flow solution.

## 6.3 Type 3 lock flushing concept

The contour plots of the velocity magnitudes for Type 3 concept is shown in Figure 32-Figure 34. In each figure, the velocity contours shown at the beginning of flushing, at five minutes of flushing, and at ten minutes of flushing. The flushing discharge is constant throughout the simulation. Flushing flow is introduced into the lock chamber at the upstream end via four pipes through the gate sill. The outlets of these pipes are near the lock

chamber floor. The jets that extend from each pipe have a maximum velocity of about 15 ft/sec. The contours closest to the chamber floor show that the velocity magnitudes vary in both time and space in the upstream third of the lock chamber. Further downstream, the variation of velocity magnitude is much smaller, and the maximum flow velocities are about 2 ft/sec. The contours ten feet from the chamber floor show that the variation in velocity magnitudes is smaller further away from the ports, but is still largely restricted to the upstream third of the lock chamber. At that elevation, the maximum velocity magnitude is about 7 ft/sec. At the lock chamber surface, the velocity magnitudes vary more than near the center of the lock chamber water column. The strong effect of introducing the flushing flow through the pipes is still very apparent at the chamber surface. The largest velocity magnitudes at the water surfaces are about 7 ft/sec.

Contour plots of the original lock chamber water concentration for Type 3 are shown in Figure 35-Figure 37. At the beginning of flushing (flushing time = 0), the entire lock chamber is orange/red indicating a uniform concentration of 100% of the original lock chamber water. During flushing, the contours in the lock chamber change from orange/red to green to blue. These changes show that the lock chamber flushing is reducing the concentration of original lock chamber water during flushing. Since flushing flow is introduced at the upstream end of the lock chamber, the original lock chamber water concentration is reduced first at the upstream end of the lock chamber. The original lock chamber water concentration is reduced throughout the lock chamber as the flushing flow moves toward the downstream miter gates. There is no strong vertical variation in the original lock chamber water concentration. After fifteen minutes of lock flushing, the original lock chamber concentration at upstream end of the lock chamber has already been reduced to around 10%. These concentration contours indicate that Type 3 is more efficient than Type 1. Further, Type 3 does not produce any areas of the lock chamber that take significantly longer to flush than other areas.

Figure 32. Type 3 velocity magnitude contours at el. 493

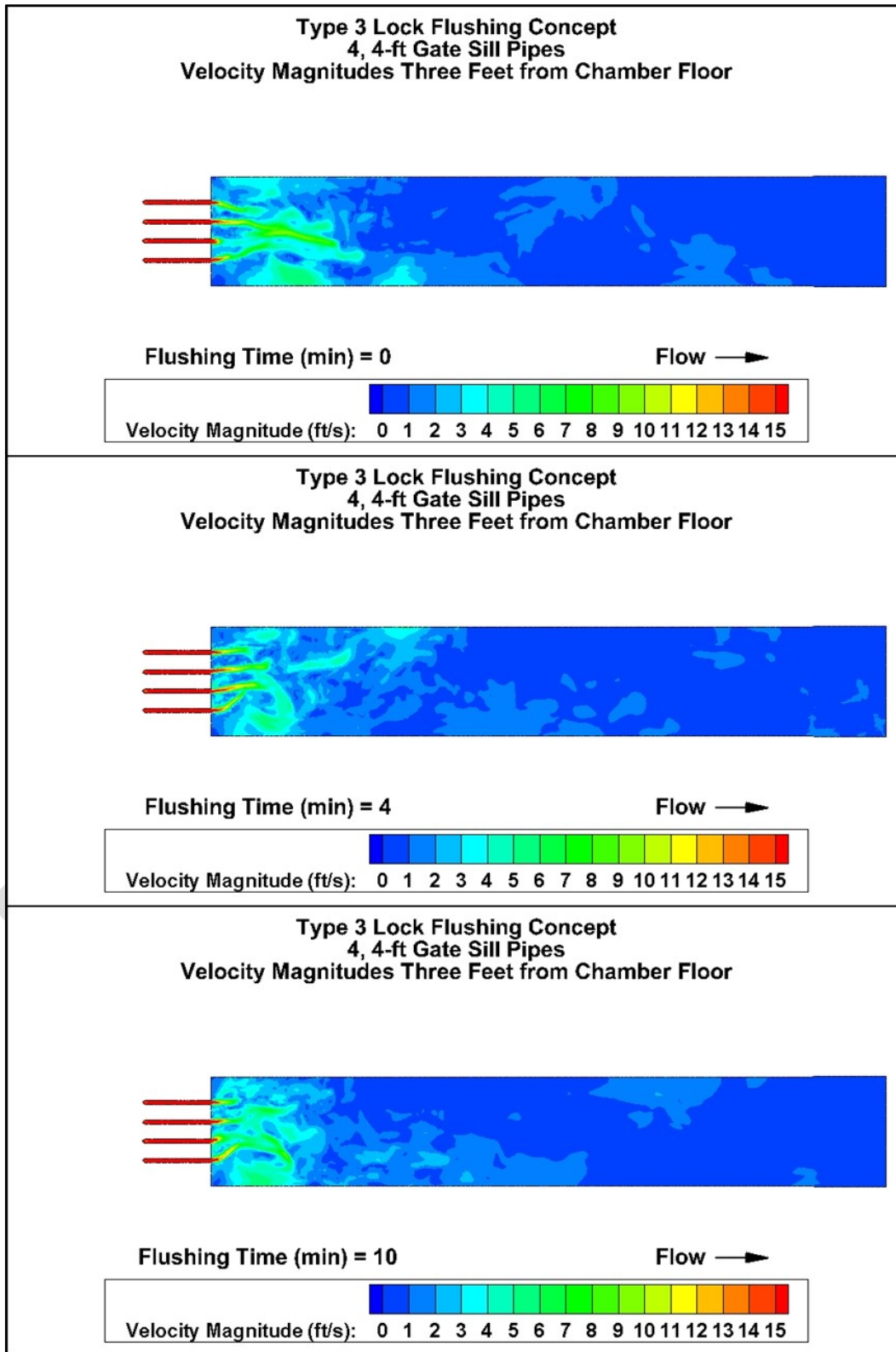


Figure 33. Type 3 velocity magnitude contours at el. 499.6

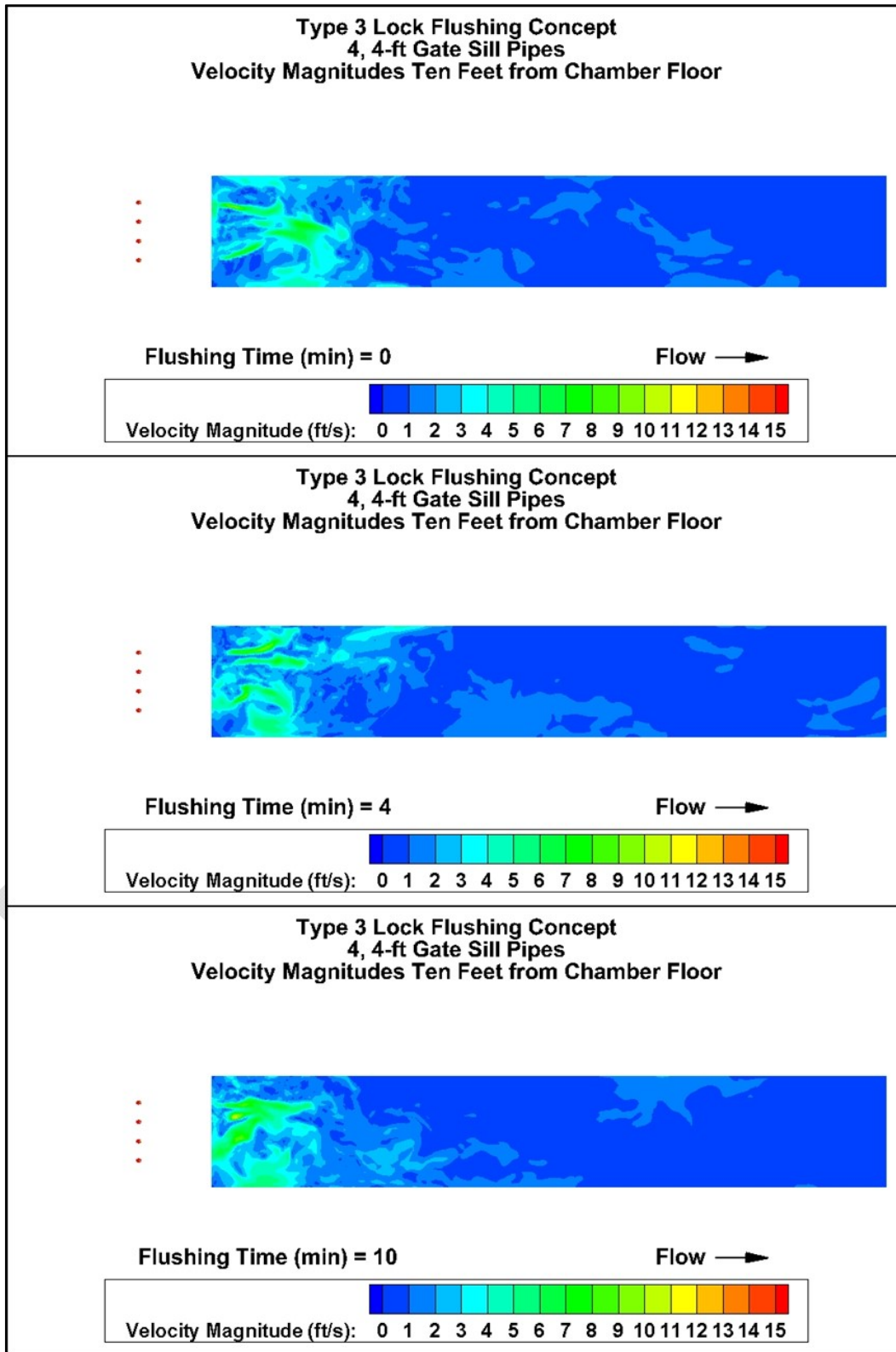


Figure 34. Type 3 velocity magnitude contours at lock chamber surface

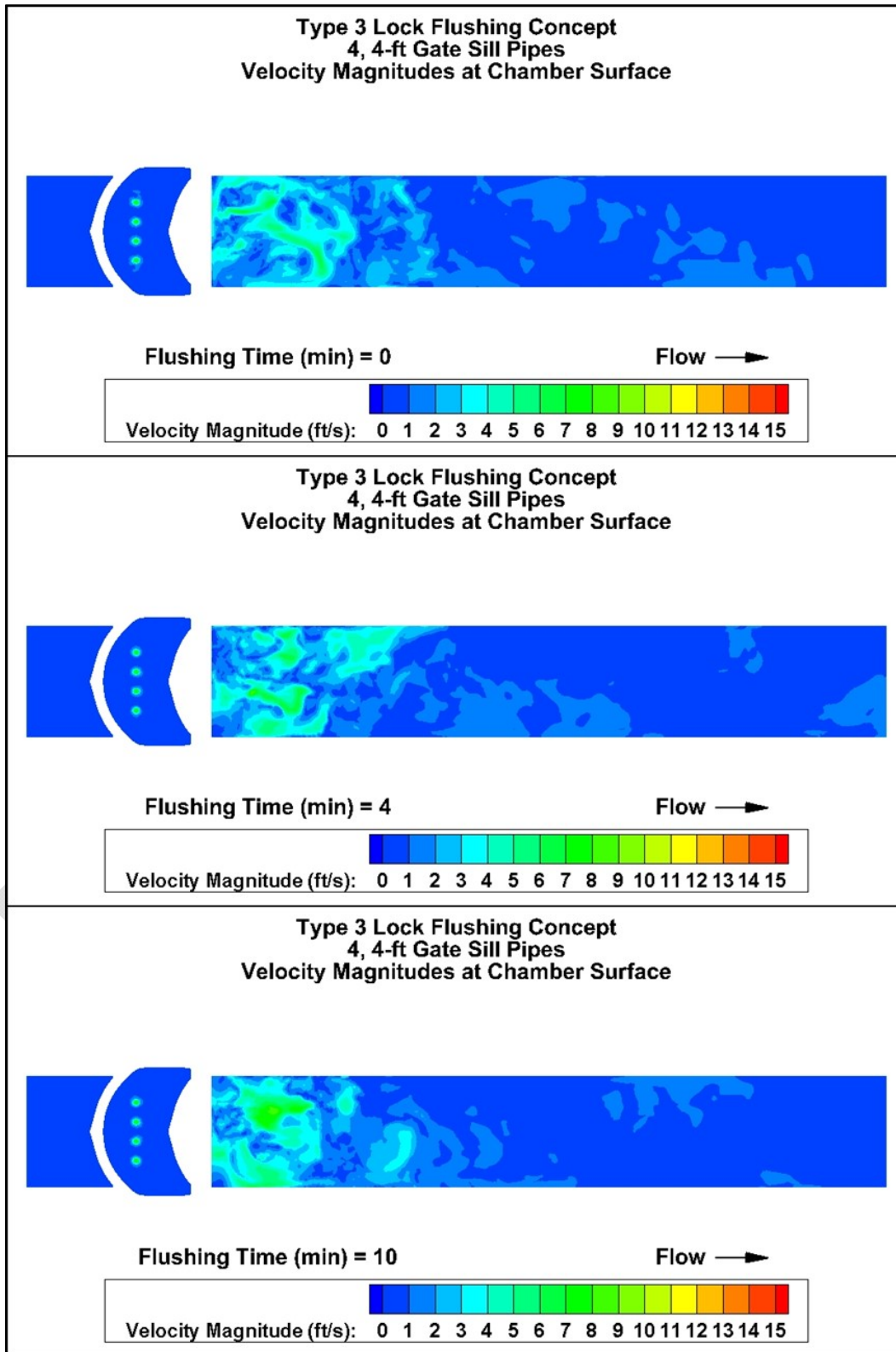


Figure 35. Type 3 original lock chamber water concentration contours at el. 493

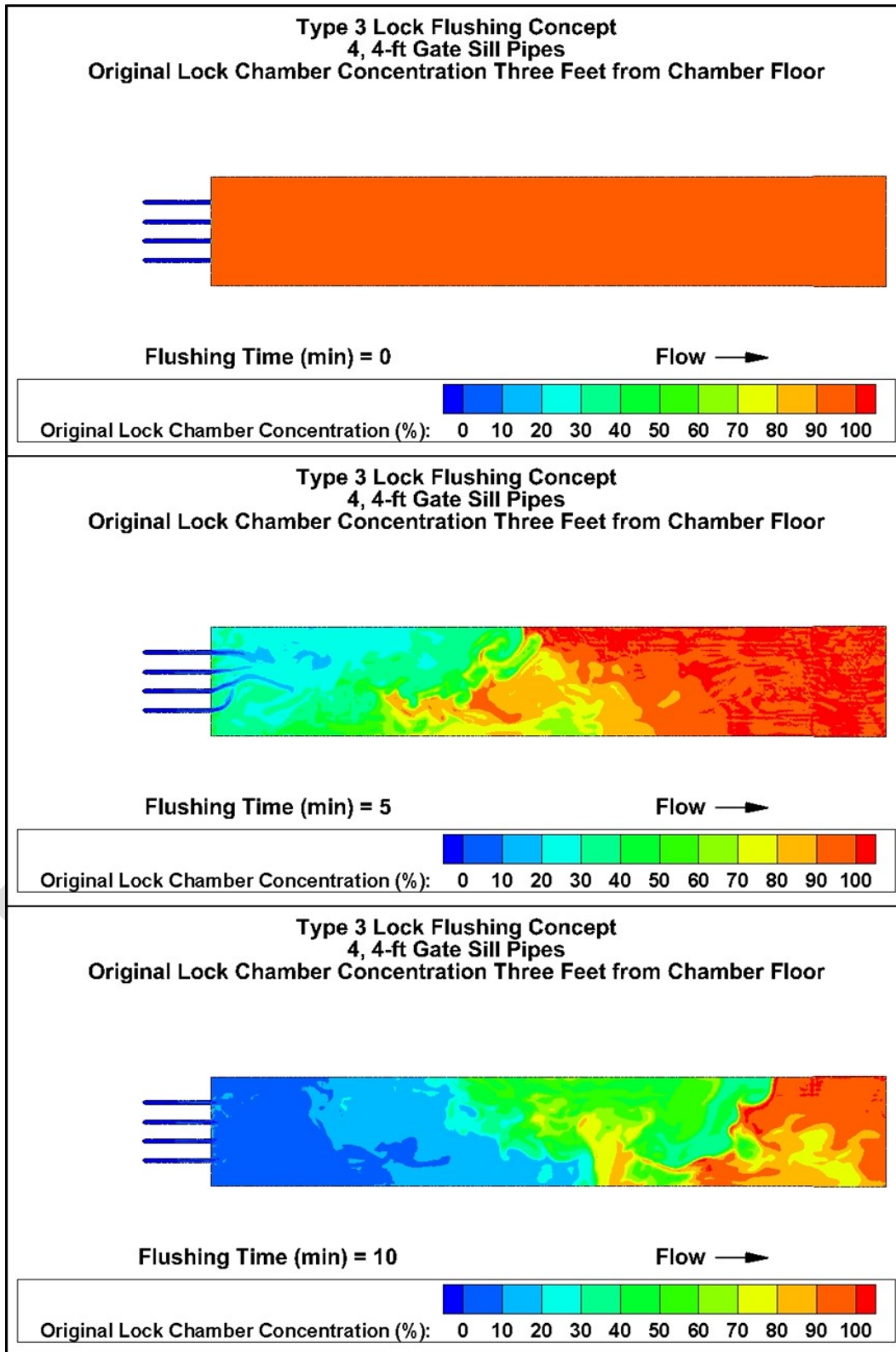


Figure 36. Type 3 original lock chamber water concentration contours at el. 499.6

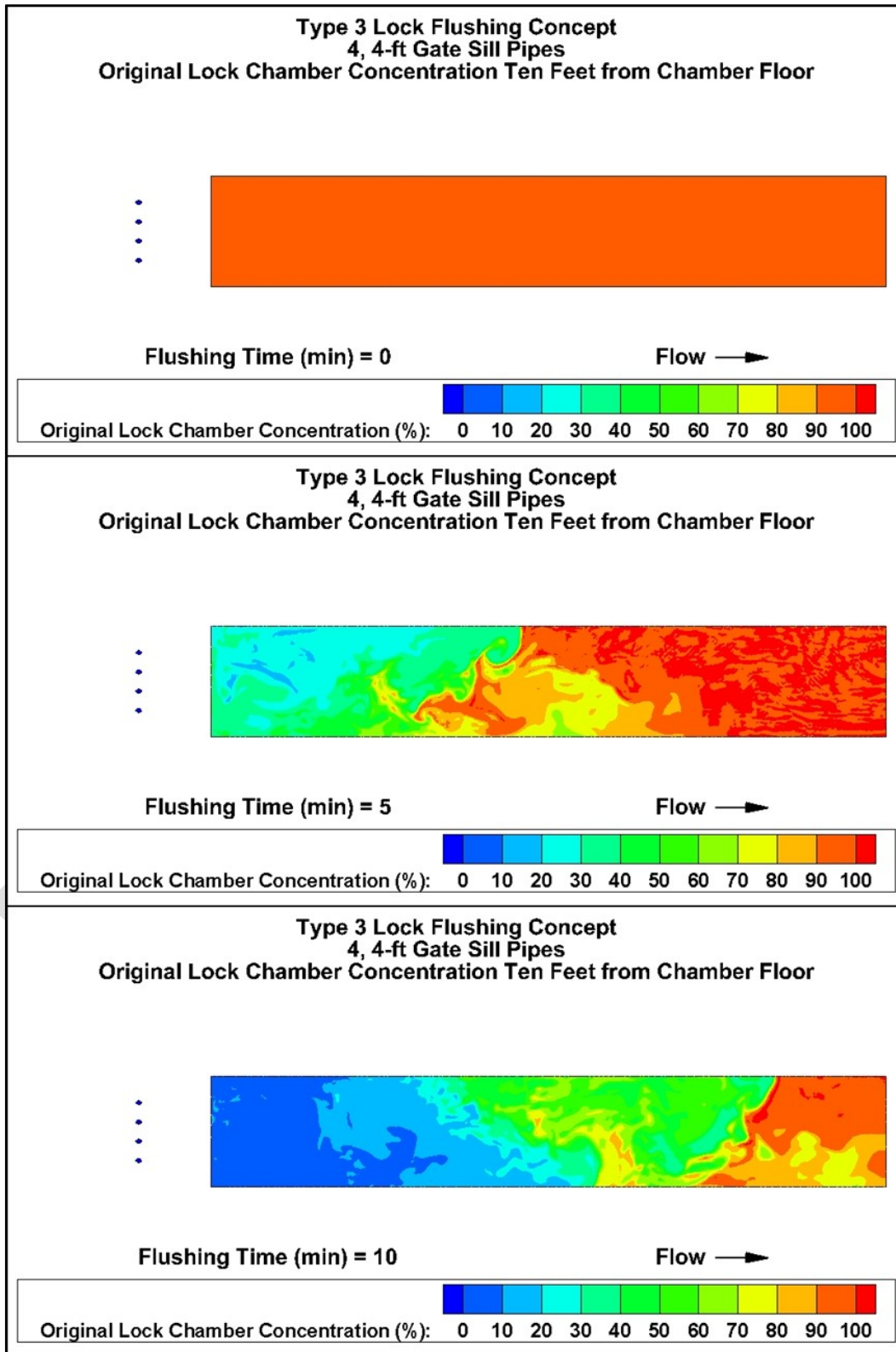
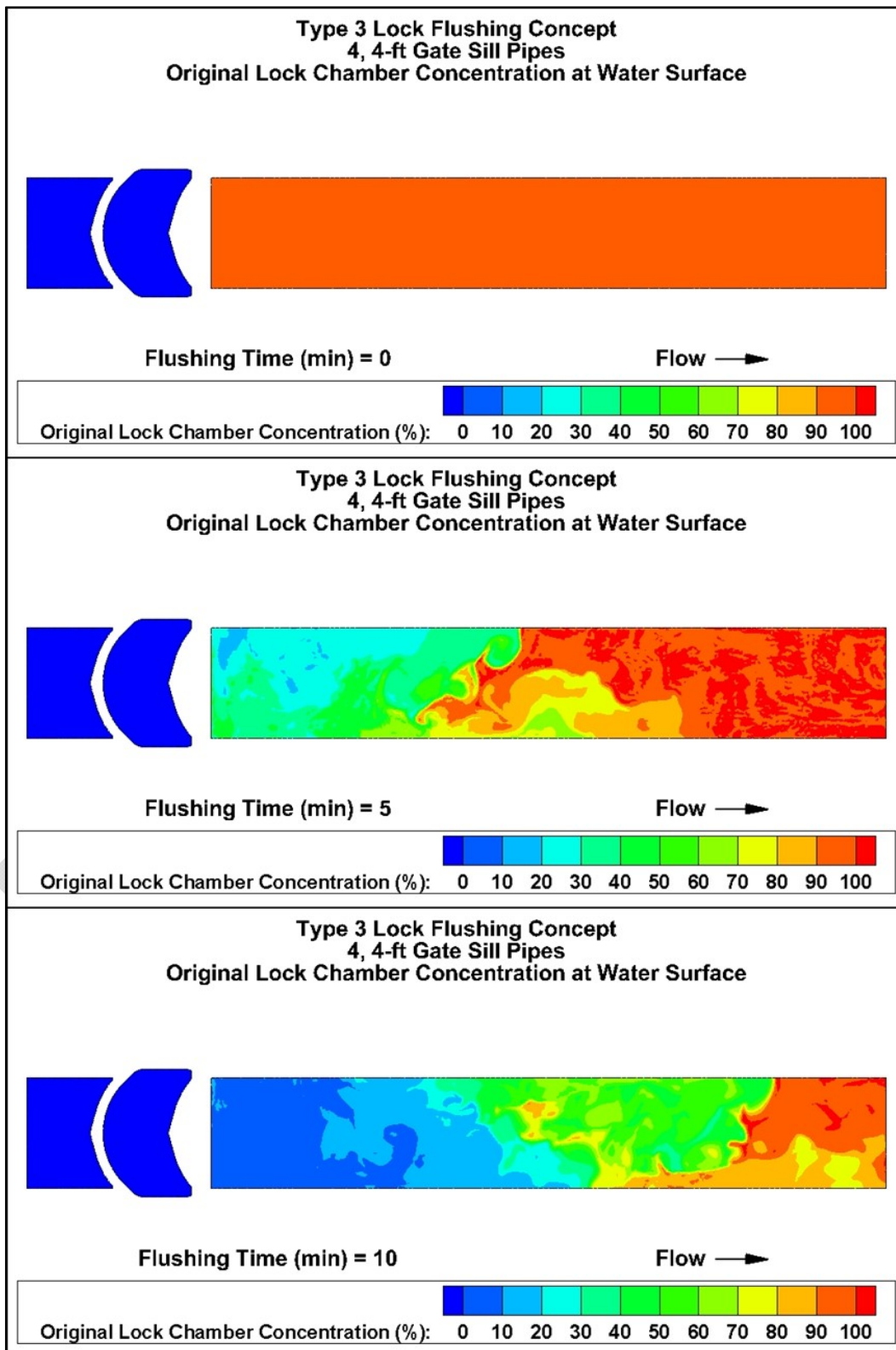


Figure 37. Type 3 original lock chamber water concentration contours at lock chamber surface



The flushing effectiveness and efficiency for Type 3 are shown in Figure 38 and Table 9. In the figure, the original lock water concentration is plotted against the flushing time. The different curves indicate how much of the lock chamber has been flushed to different levels of original lock chamber water concentration during a flushing operation with red indicating at most a 10% reduction in the original lock chamber concentration, green indicating at most a 50% reduction, and dark blue indicating a 99.9% reduction (essentially portions of the chamber where the water has been completely replaced by flushing water).

The curves corresponding to at least 70% dilution show a slow volume change initially, a period of rapid volume change, and finally a return to a slow volume change as the curves approach 100% of the lock chamber. Essentially complete flushing (99.9% reduction) as indicated by the dark blue furthest to the right is only been achieved in over 1% of the lock chamber after twenty minutes of flushing. However, 90% reduction of the original lock chamber concentration has occurred in 44% of the lock chamber after fifteen minutes of flushing (indicated by the dashed black line). Lock chamber volume percentages at five minute increments of flushing are shown in Table 9. The values listed correspond to values that can be read directly from Figure 38, but the table values provide more precision in the percent volumes.

Figure 38. Type 3 lock chamber flushing performance

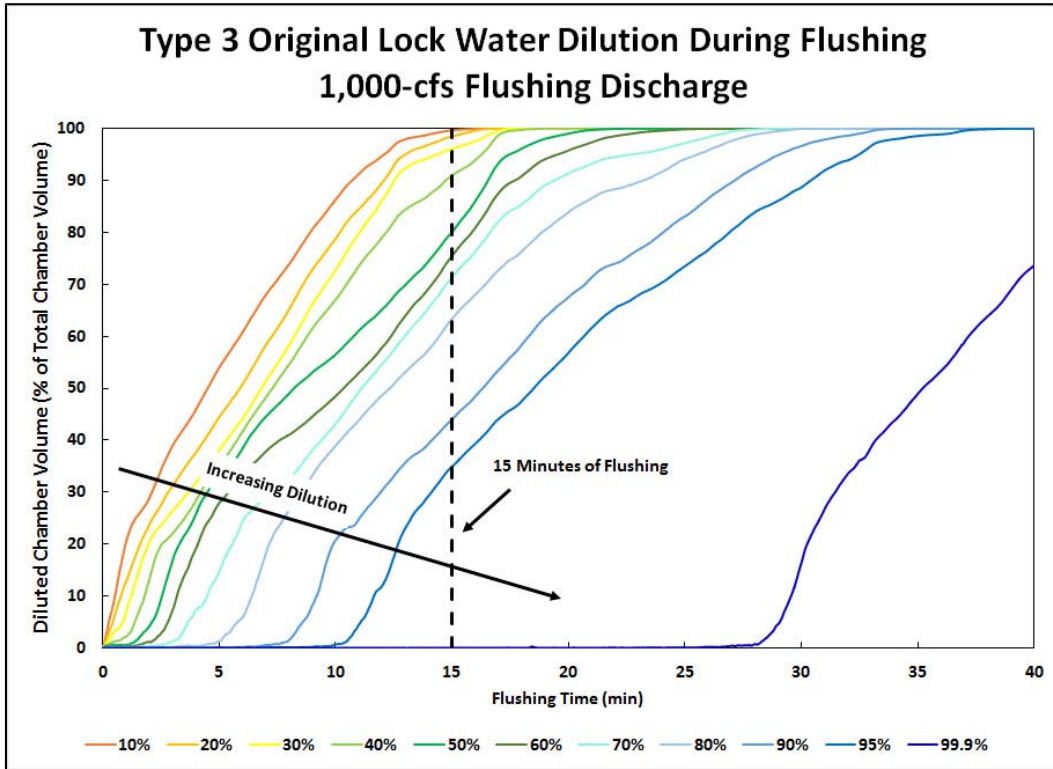


Table 9. Type 3 chamber flushing performance - 5-minute intervals

Flushing Time (min)		Flushed chamber volume (% of total lock chamber volume)							
		5	10	15	20	25	30	35	40
Dilution of original lock chamber water	99.9%	<1	<1	<1	<1	<1	16	49	74
	90%	<1	21	44	68	83	97	100	100
	80%	1	39	63	84	94	100	100	100
	70%	15	43	71	91	97	100	100	100
	60%	28	48	75	96	100	100	100	100
	50%	33	56	80	99	100	100	100	100
	40%	35	67	91	100	100	100	100	100
	30%	38	73	96	100	100	100	100	100
	20%	44	79	98	100	100	100	100	100
	10%	54	86	100	100	100	100	100	100

## 6.4 Type 3r lock flushing concept

The contour plots of the velocity magnitudes for the Type 3r lock flushing concept is shown in Figure 39-Figure 41. In each figure, the velocity contours shown at the beginning of flushing, at five minutes of flushing, and at ten minutes of flushing. The flushing discharge is constant throughout the simulation. Flushing flow is introduced into the lock chamber at the upstream end via a rectangular slot through the gate sill. The jet that extends from the rectangular slot has a maximum velocity of about 15 ft/sec. Viewing the contours closest to the chamber floor, the velocity magnitudes vary in both time and space in roughly the upstream half of the lock chamber. The flow velocity in the jet halfway down the lock chamber is about 7 ft/sec. Further downstream, the variation of velocity magnitude is much smaller, and the maximum flow velocities are about 4 ft/sec. The contours ten feet from the chamber floor show that the velocity magnitudes are much smaller further away from the rectangular slot, but is still largely restricted to the upstream half of the lock chamber. At that elevation, the maximum velocity magnitude is about 7 ft/sec in the upstream half of the chamber and 4 ft/sec further downstream. At the lock chamber surface, the velocity magnitudes vary more that near the center of the lock chamber water column. The jet issuing from the rectangular slot reaches the surface roughly halfway down the lock chamber creating 7 ft/sec flows at the surface.

Contour plots of the original lock chamber water concentration the Type 3r are shown in Figure 42-Figure 44. At the beginning of flushing (flushing time = 0), the entire lock chamber is orange/red indicating a uniform concentration of 100% of the original lock chamber water. During flushing, the contours in the lock chamber change from orange/red to green to blue. These changes show that the lock chamber flushing is reducing the concentration of original lock chamber water. Since flushing flow is introduced at the upstream end of the lock chamber, the original lock chamber water concentration is reduced first at the upstream end of the lock chamber. The original lock chamber water concentration is reduced throughout the lock chamber as the flushing flow moves toward the downstream miter gates. There is no strong vertical variation in the original lock chamber water concentration. After fifteen minutes of lock flushing, the original lock chamber concentration at upstream end of the lock chamber has already been reduced to around 10%.

Figure 39. Type 3r velocity magnitude contours at el. 493

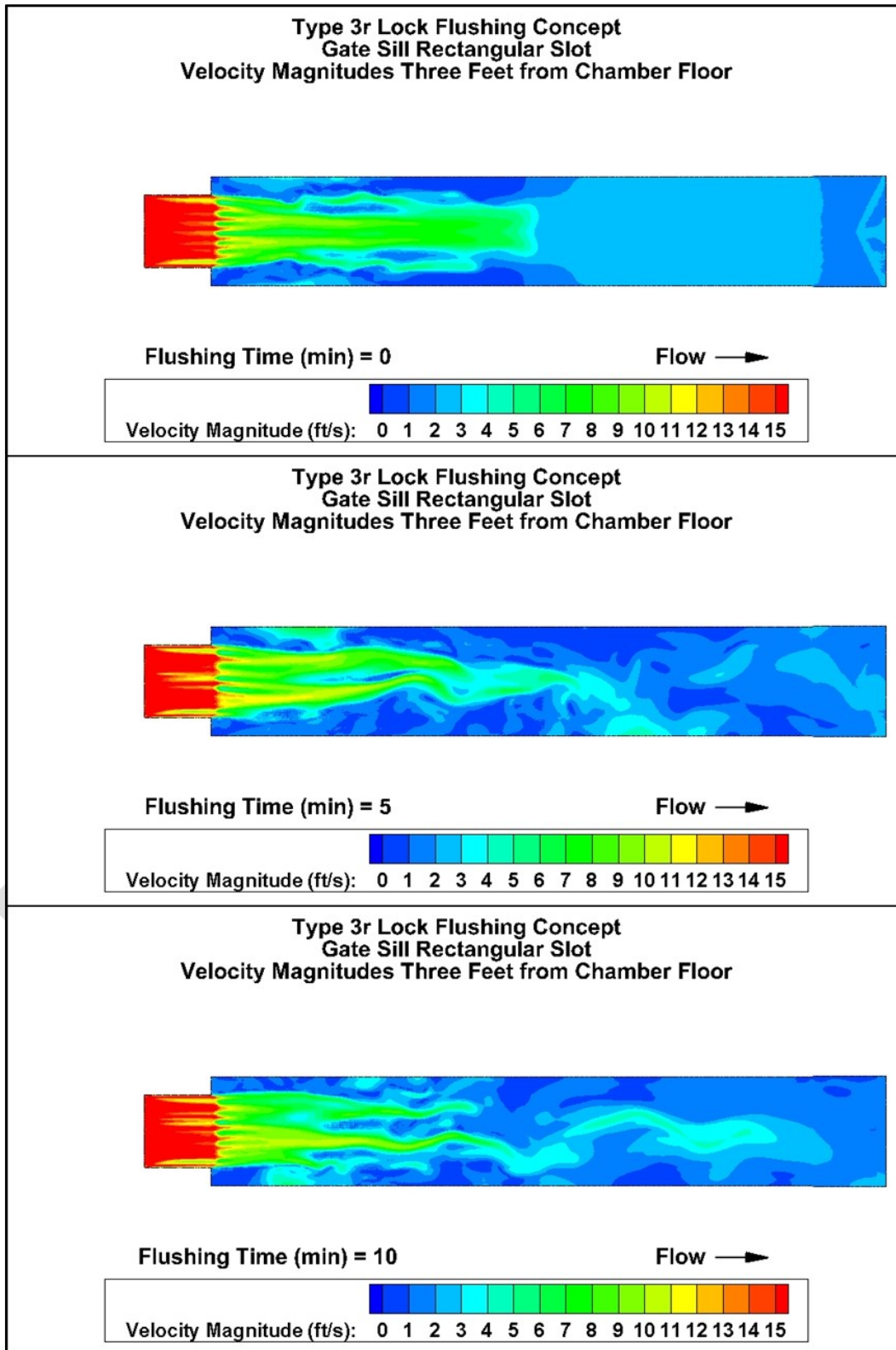


Figure 40. Type 3r velocity magnitude contours at el. 499.6

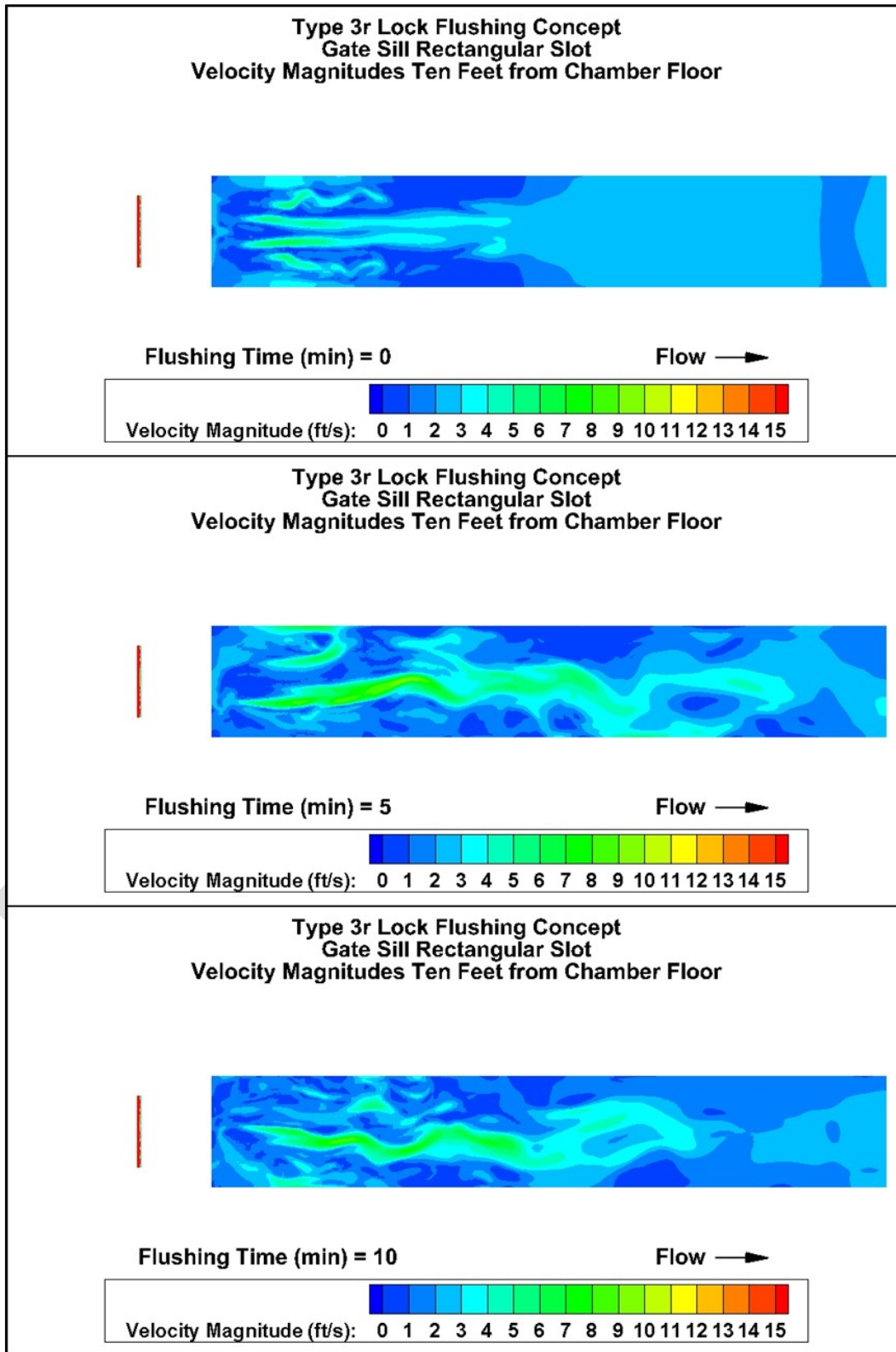


Figure 41. Type 3r velocity magnitude contours at lock chamber surface

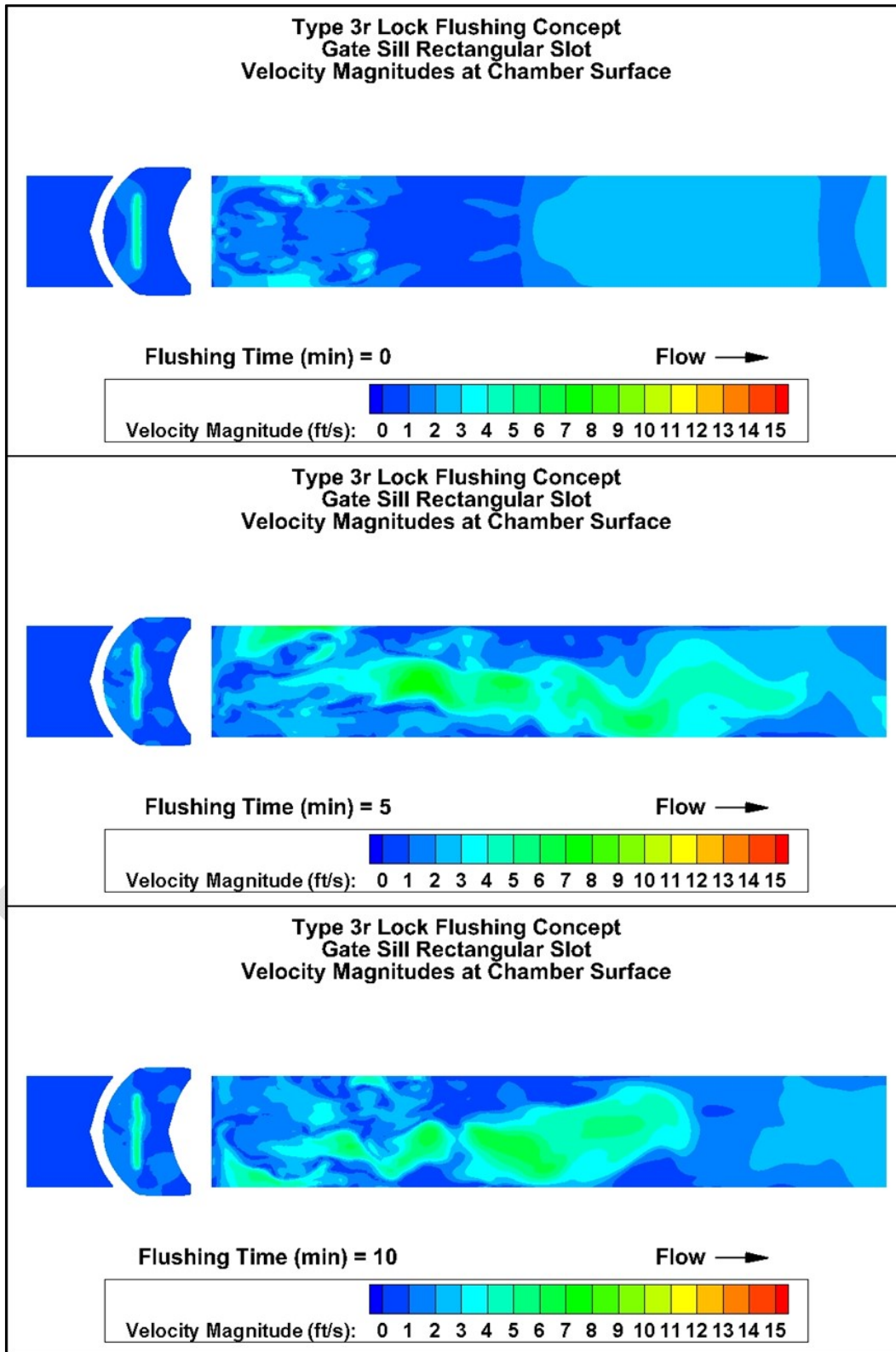


Figure 42. Type 3r original lock chamber water concentration contours at el. 493

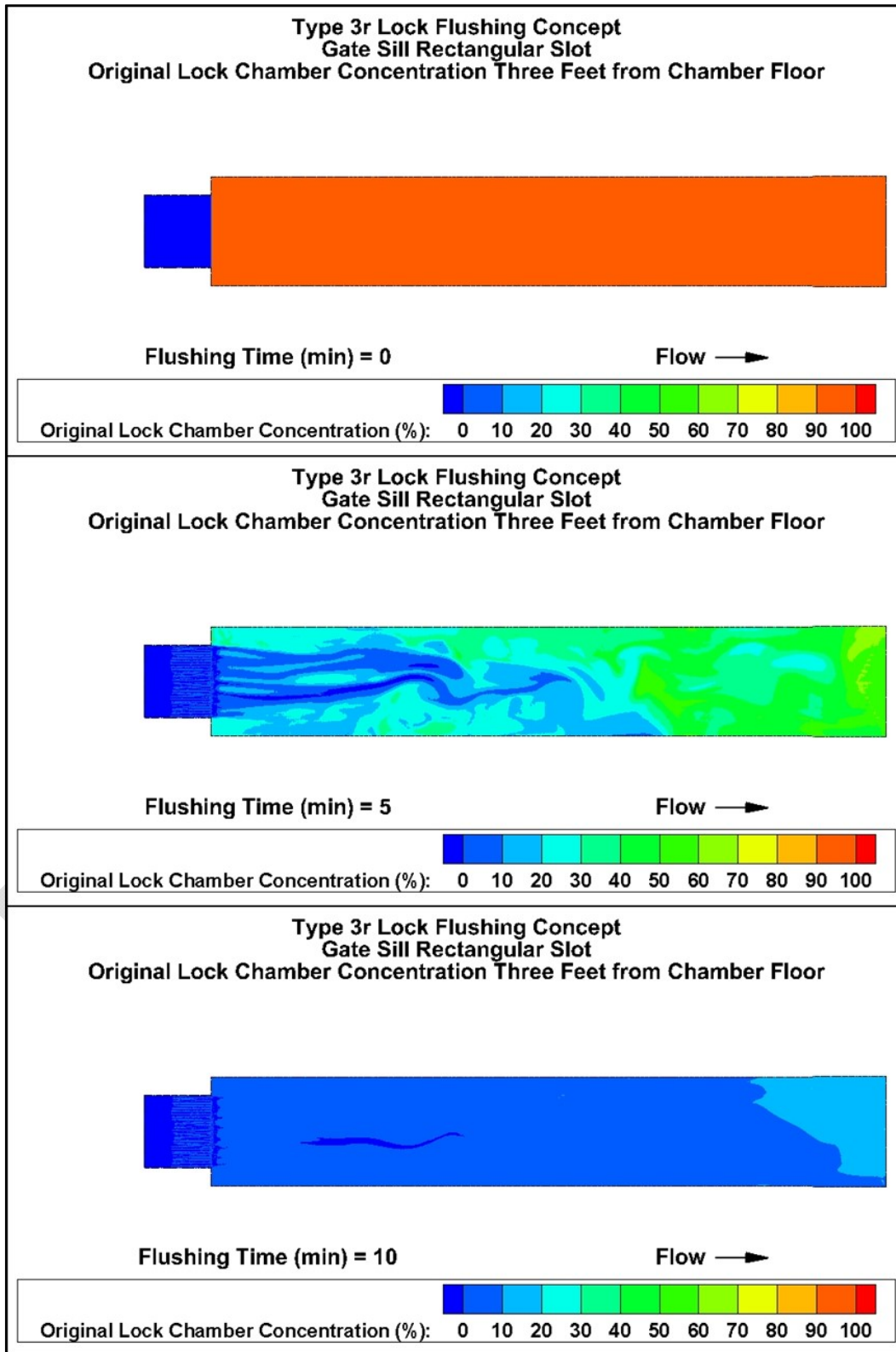


Figure 43. Type 3r original lock chamber water concentration contours at el. 499.6

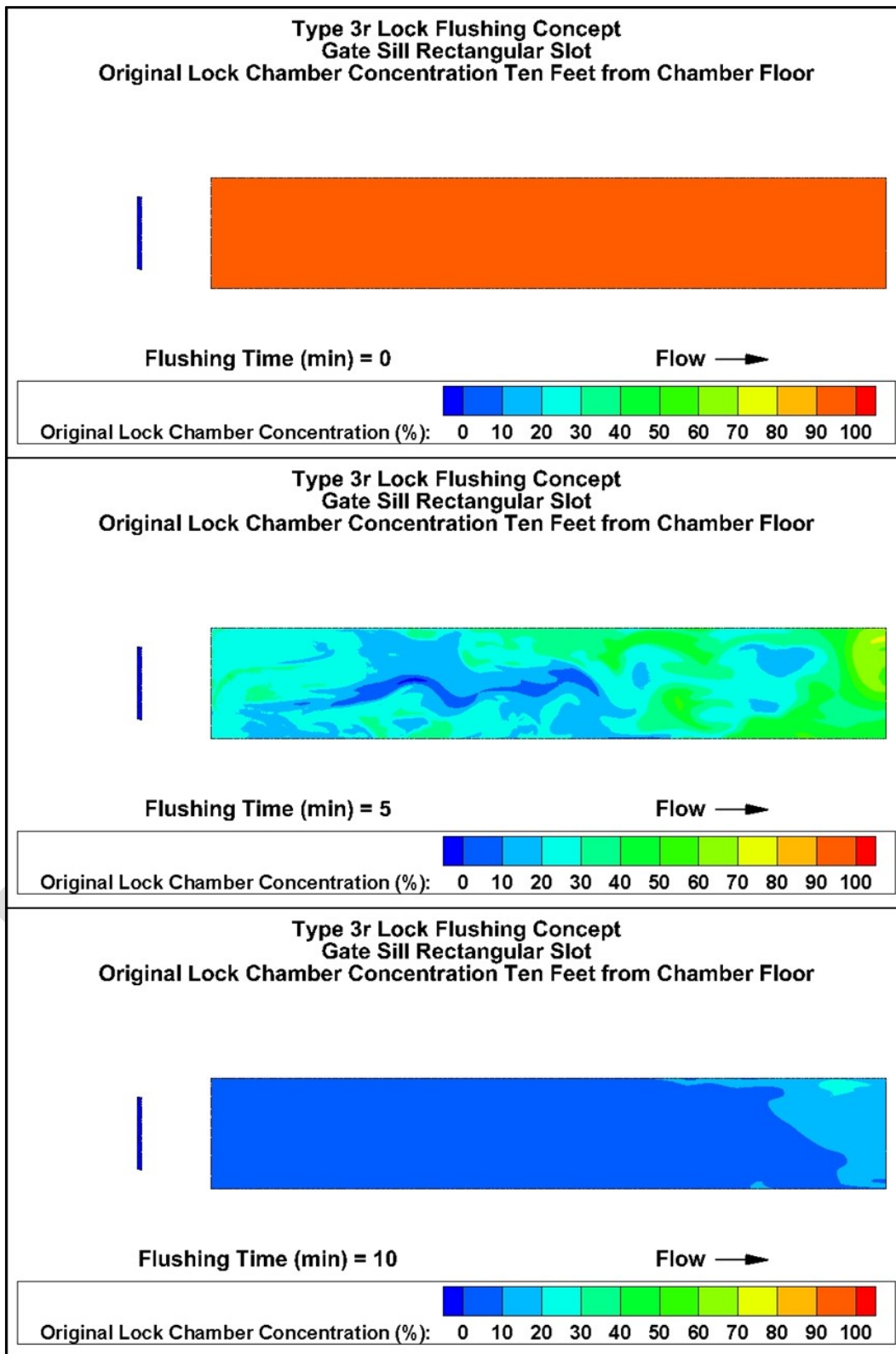
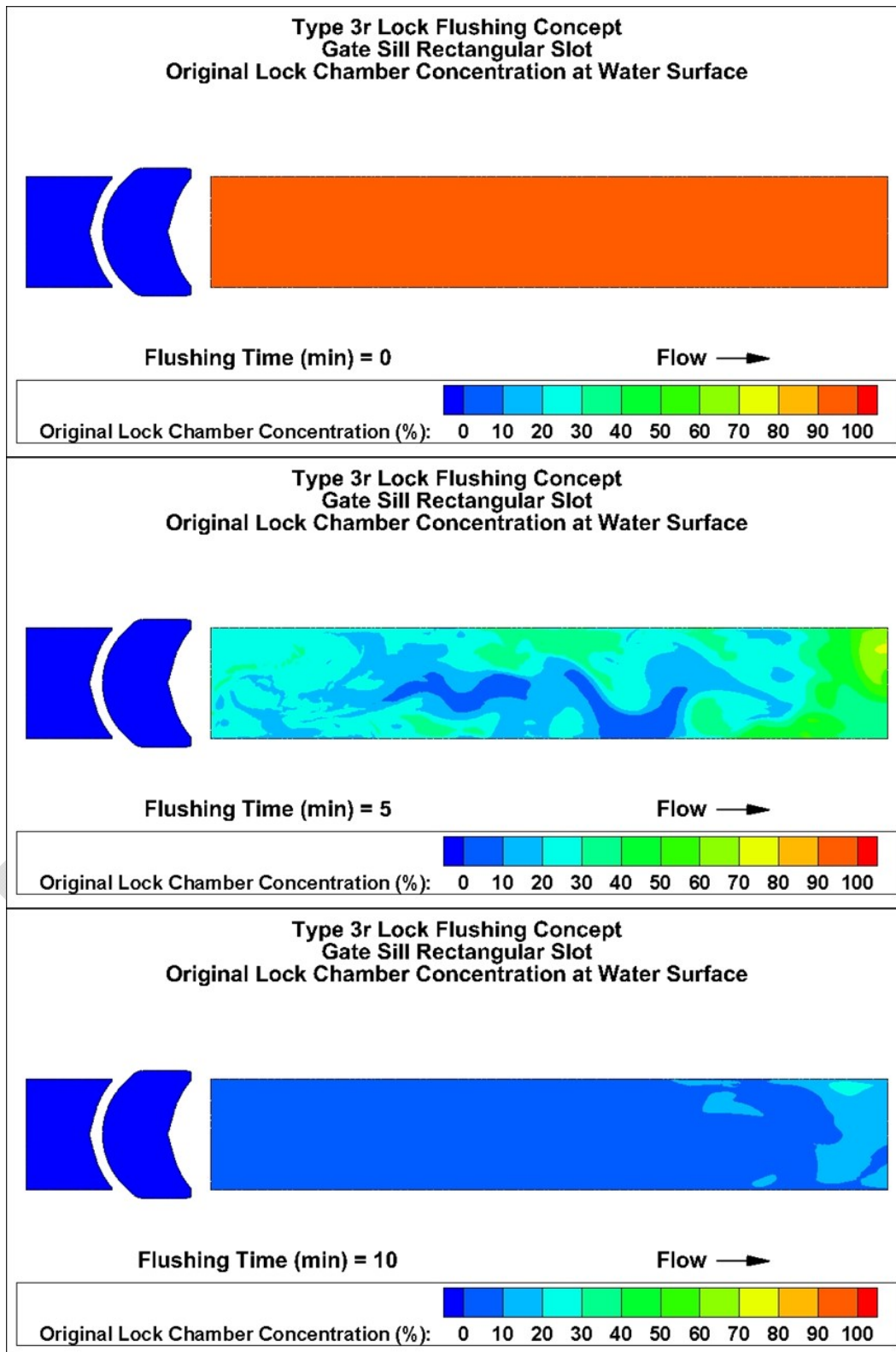


Figure 44. Type 3r original lock chamber water concentration contours at lock chamber surface



The flushing effectiveness and efficiency for Type 3r are shown in Figure 45 and Table 10. In the figure, the original lock water concentration is plotted against the flushing time. The different curves indicate how much of the lock chamber has been flushed to different levels of the original lock chamber water concentration during a flushing operation with red indicating at most a 10% reduction in the original lock chamber concentration, green indicating at most a 50% reduction, and dark blue indicating a 99.9% reduction (essentially portions of the chamber where the water has been completely replaced by flushing water).

The curves corresponding to at least 70% dilution show a slow volume change initially, a period of rapid volume change, and finally a return to a slow volume change as the curves approach 100% of the lock chamber. Essentially complete flushing (99.9% reduction) as indicated by the dark blue furthest to the right is only been achieved in about 4% of the lock chamber after twenty minutes of flushing. However, 95% reduction of the concentration has occurred in the entire lock chamber after fifteen minutes of flushing (indicated by the dashed black line). Lock chamber volume percentages at five minute increments of flushing are shown in Table 10. The values listed correspond to values that can be read directly from Figure 45, but the table values provide more precision in the percent volumes.

Figure 45. Type 3r lock chamber flushing performance

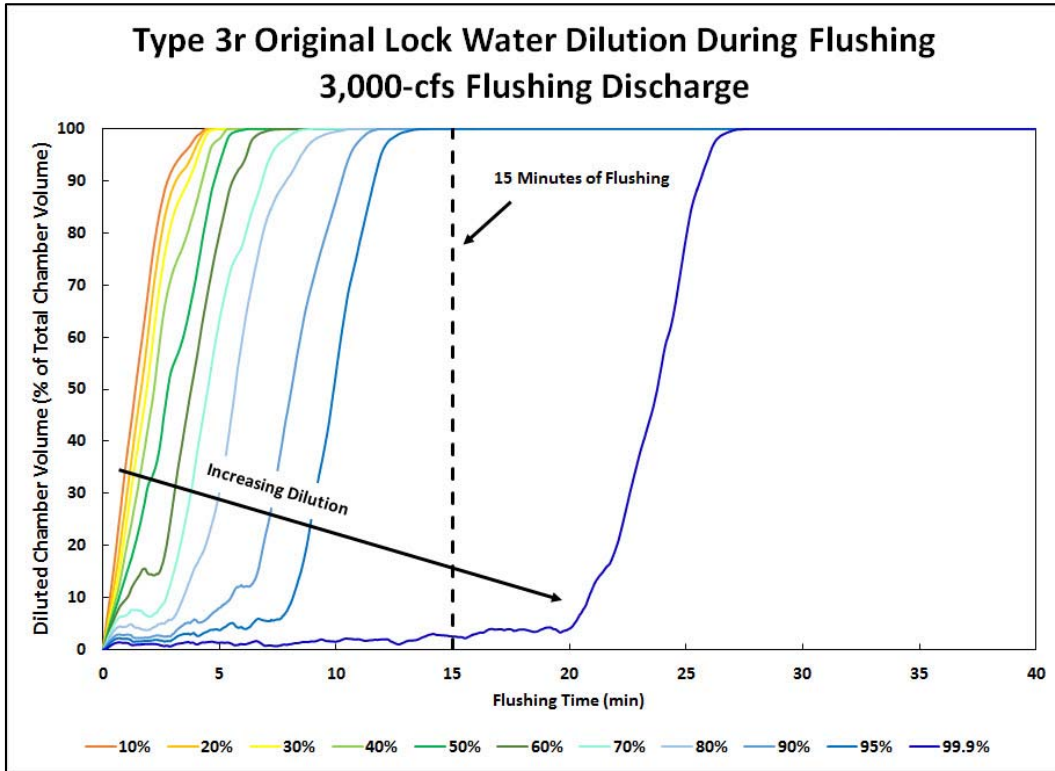


Table 10. Type 3r chamber flushing performance – 5-minute intervals

Flushing Time (min)		Flushed chamber volume (% of total lock chamber volume)							
		5	10	15	20	25	30	35	40
Dilution of original lock chamber water	99.9%	1	2	3	4	79	100	100	100
	90%	8	86	100	100	100	100	100	100
	80%	30	99	100	100	100	100	100	100
	70%	63	100	100	100	100	100	100	100
	60%	80	100	100	100	100	100	100	100
	50%	93	100	100	100	100	100	100	100
	40%	98	100	100	100	100	100	100	100
	30%	100	100	100	100	100	100	100	100
	20%	100	100	100	100	100	100	100	100
	10%	100	100	100	100	100	100	100	100

## 6.5 Type 5 lock flushing concept

The contour plots of the velocity magnitudes for the Type 5 lock flushing concept is shown in Figure 46-Figure 48. In each figure, the velocity contours shown at the beginning of flushing, at five minutes of flushing, and at ten minutes of flushing. The flushing discharge remains constant throughout the simulation. Flushing flow is introduced into the lock chamber at several locations via the filling and emptying ports. Viewing the contours closest to the chamber floor, the velocity magnitudes vary in both time and space. The jets that extend from each port have a maximum velocity of about 5 ft/sec. Each jet extends roughly halfway across the lock chamber. The jets are directed more toward the downstream miter gates for the ports that are furthest downstream. The flow deflectors on the first four ports on each culvert drastically reduce the distance the corresponding jets extend toward the opposite lock chamber wall. The contours ten feet from the chamber floor show that the variation in velocity magnitudes is much smaller further away from the ports. At that elevation, the maximum velocity magnitude is about 3 ft/sec. At the lock chamber surface, the velocity magnitudes vary more than near the center of the lock chamber water column. The largest velocity magnitudes at the water surfaces are about 3 ft/sec. The velocity magnitudes in the lock chamber for Type 5 are noticeably larger throughout the lock chamber than with Type 1.

Contour plots of the original lock chamber water concentration for Type 5 are shown in Figure 49-Figure 51. At the beginning of flushing (flushing time = 0), the entire lock chamber is orange/red indicating a uniform concentration of 100% of the original lock chamber water. During flushing, the contours in the lock chamber change from orange/red to green to blue. These changes show that the lock chamber flushing is reducing the concentration of original lock chamber water during flushing. Since flushing flow is introduced at multiple locations in the lock chamber, the original lock chamber water concentration is reduced gradually throughout the lock chamber. Three feet from the chamber floor, the effect of the ports is noticeable and the reduction in chamber concentration varies dramatically in both time and space. Moving further up the lock chamber, the reduction in concentration is more gradual. Note that after fifteen minutes of lock flushing, the concentration of original lock chamber water for each elevation is around 30% for the entire chamber. Upstream of the flushing port upstream of the filling ports, the original lock chamber concentration is even higher.

Figure 46. Type 5 velocity magnitude contours at el. 493

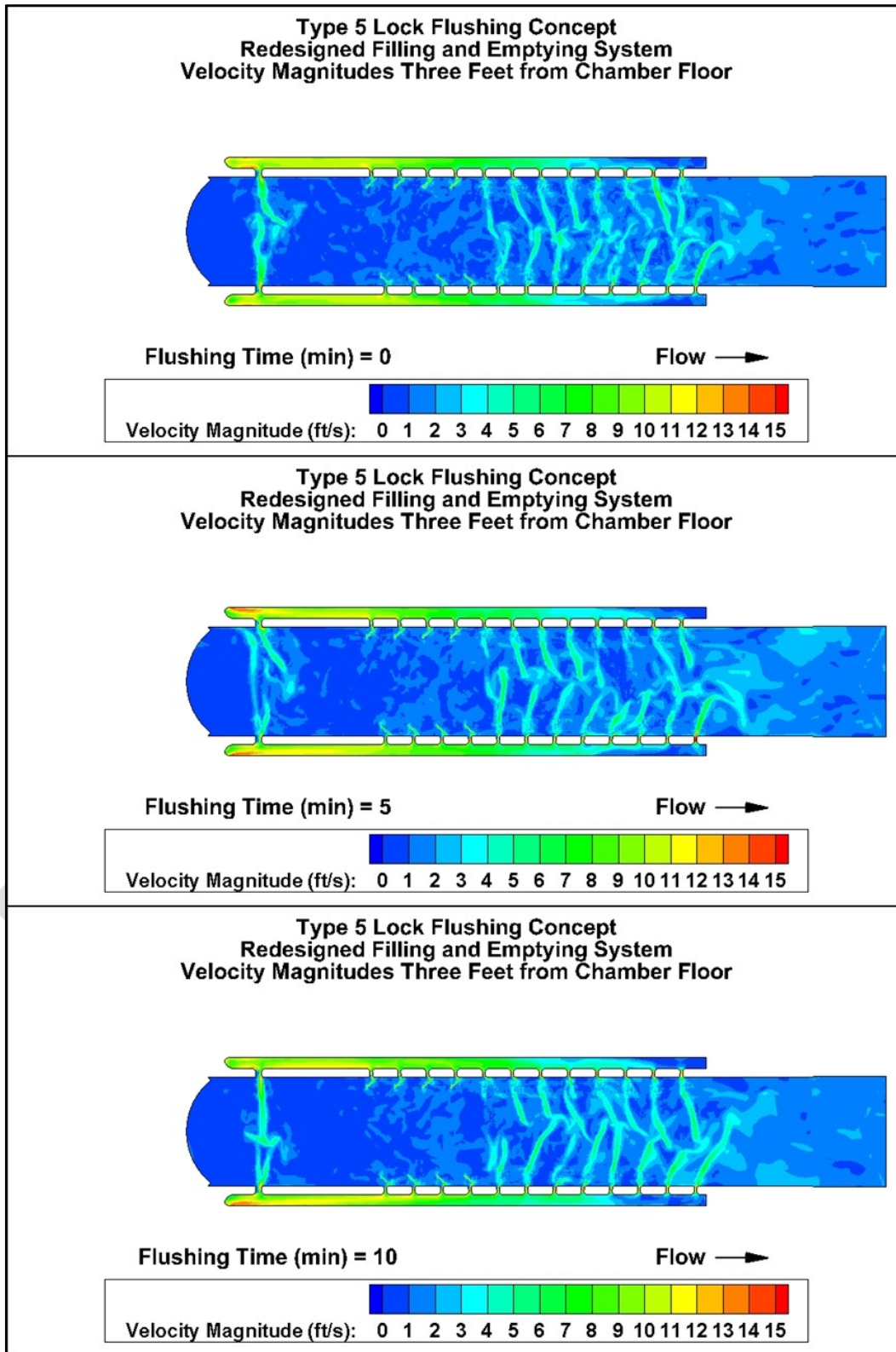


Figure 47. Type 5 velocity magnitude contours at el. 499.6

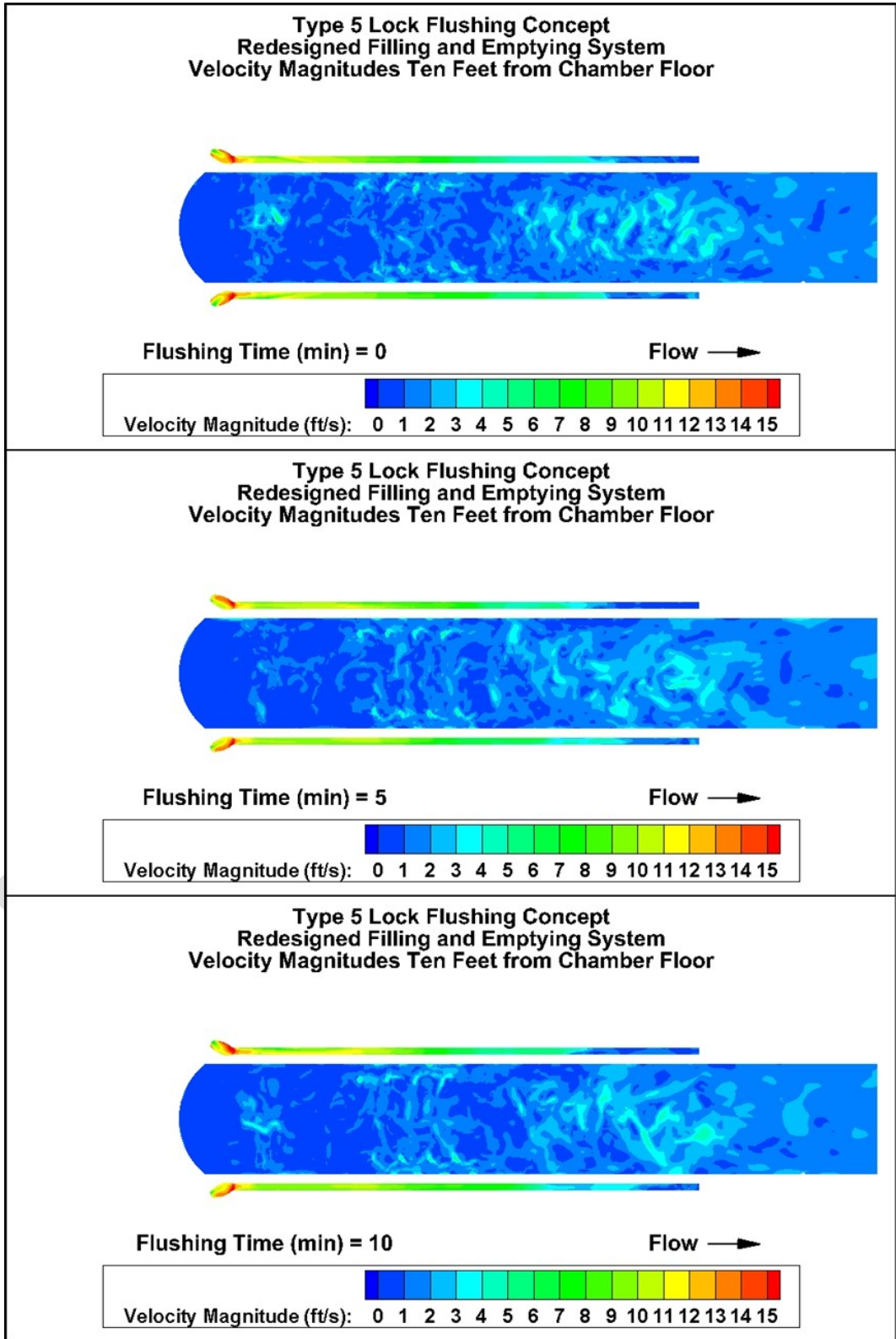


Figure 48. Type 5 velocity magnitude contours at lock chamber surface

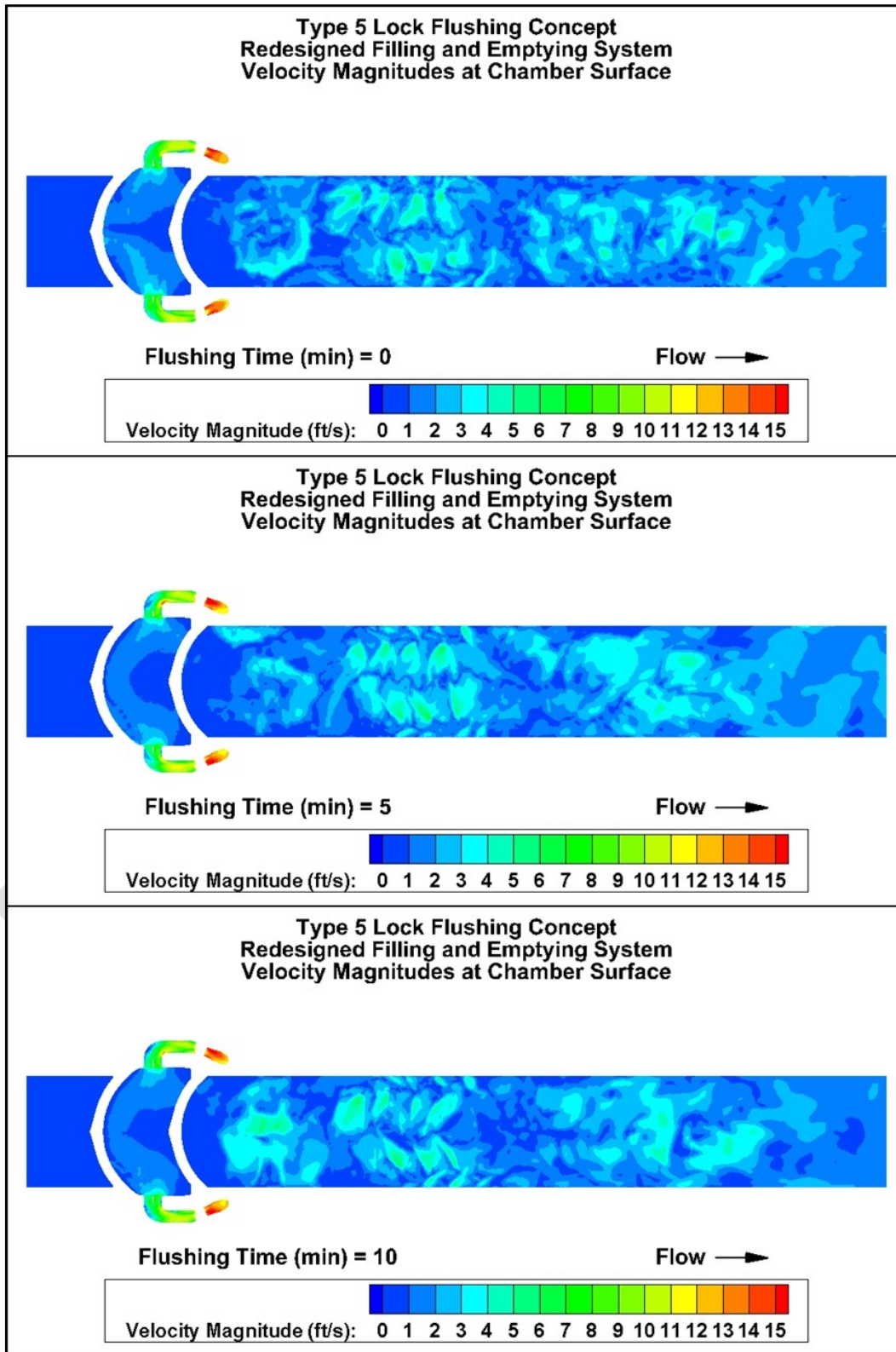


Figure 49. Type 5 original lock chamber water concentration contours at el. 493

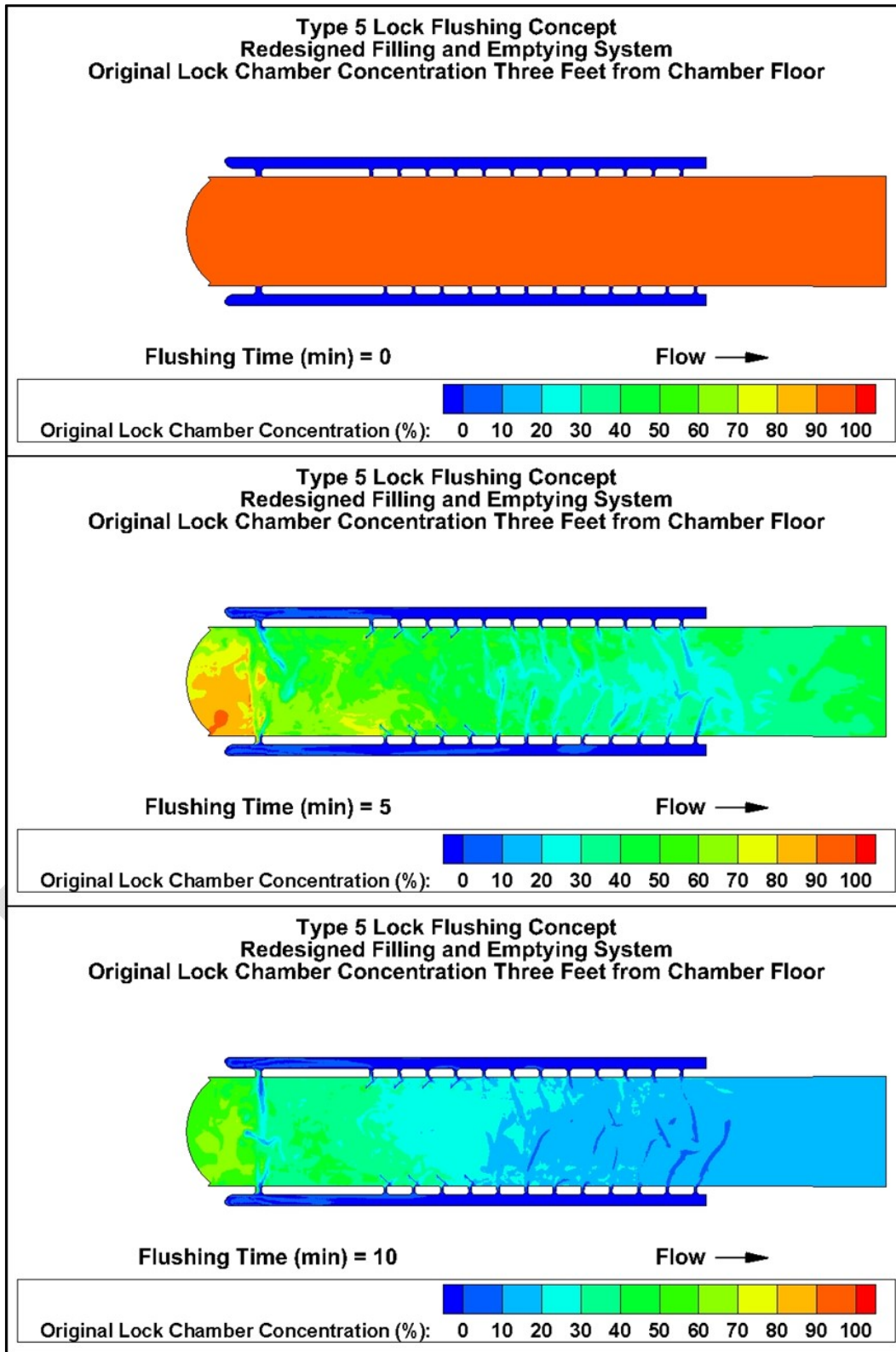


Figure 50. Type 5 original lock chamber water concentration contours at el. 499.6

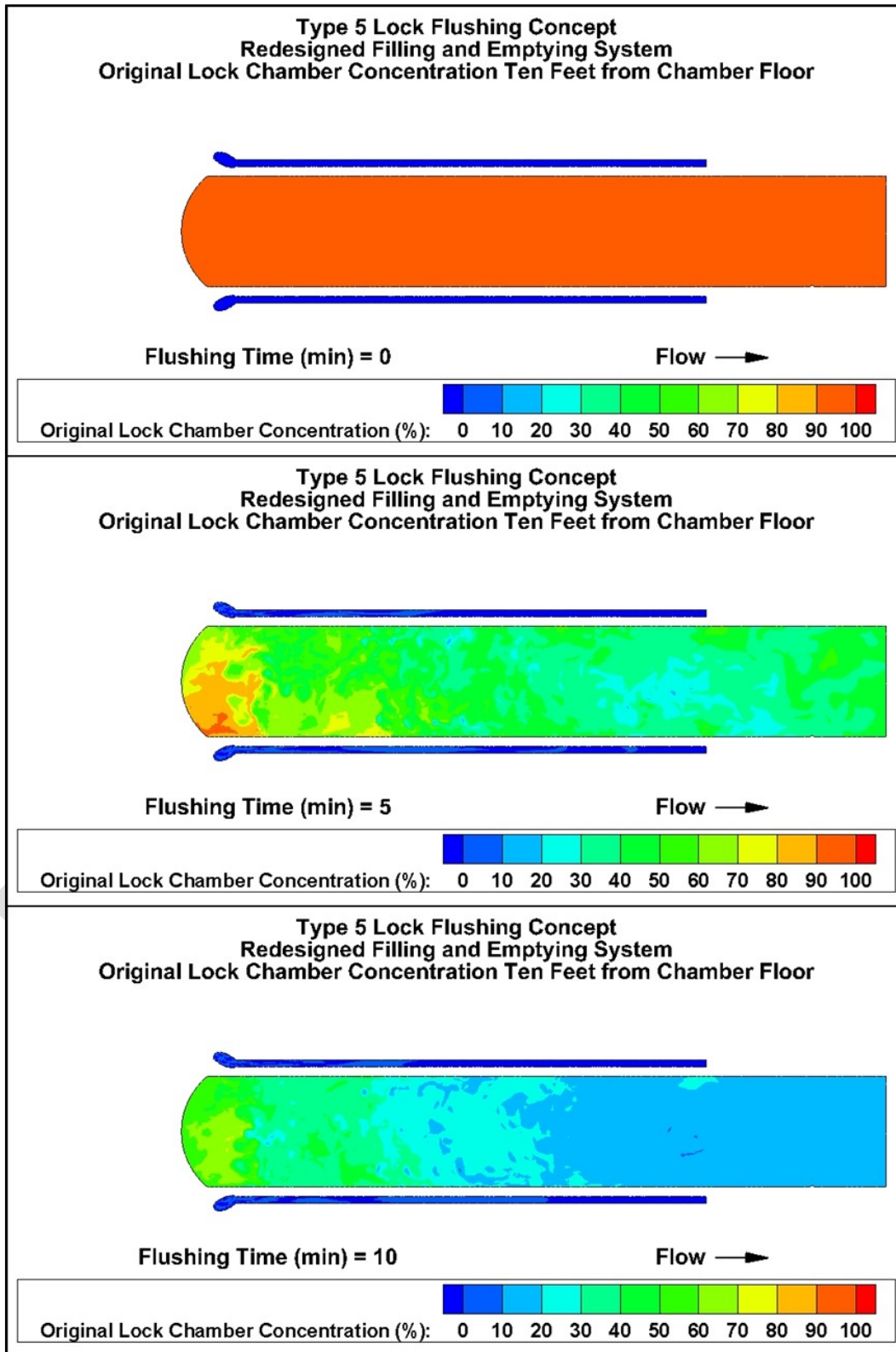
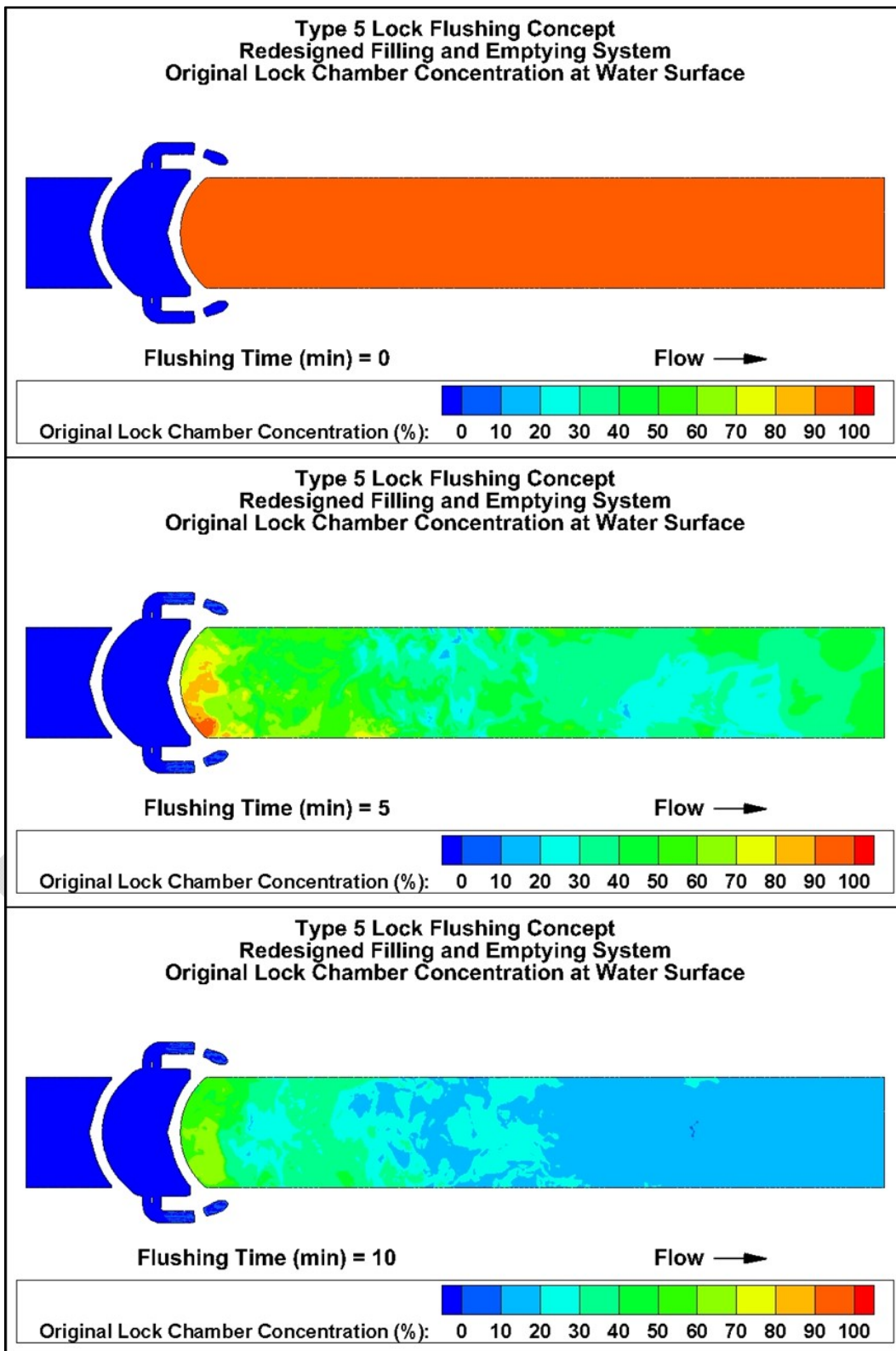


Figure 51. Type 5 original lock chamber water concentration contours at lock chamber surface



The flushing effectiveness and efficiency for Type 5 are shown in Figure 52 and Table 11. In the figure, the original lock water concentration is plotted against the flushing time. The different curves indicate how much of the lock chamber has been flushed to different levels of the original lock chamber water concentration during a flushing operation with red indicating at most a 10% reduction in the original lock chamber concentration, green indicating at most a 50% reduction, and dark blue indicating a 99.9% reduction (essentially portions of the chamber where the water has been completely replaced by flushing water).

The curves below a reduction of 50% of the original lock chamber concentration show a slow volume increase initially, a period of rapid volume increase, and finally a return to a slow volume increase as the curves approach 100% of the lock chamber. This improvement in efficiency is indicated in the concentration volume plot (Figure 52) being further to the left and above the analogous curves for Type 1 (Figure 31). The desired amount of flushing (99.9% reduction) as indicated by the dark blue line that is essentially on top of the horizontal axis is not attained even in forty minutes of flushing. After fifteen minutes (indicated by the dashed black line) even 90% reduction of the flow has only occurred in 4% of the lock chamber. Lock chamber volume percentages at five minute increments of flushing are shown in Table 11. The values listed correspond to values that can be read directly from Figure 52, but the table values provide more precision in the percent volumes.

Figure 52. Type 5 lock chamber flushing performance

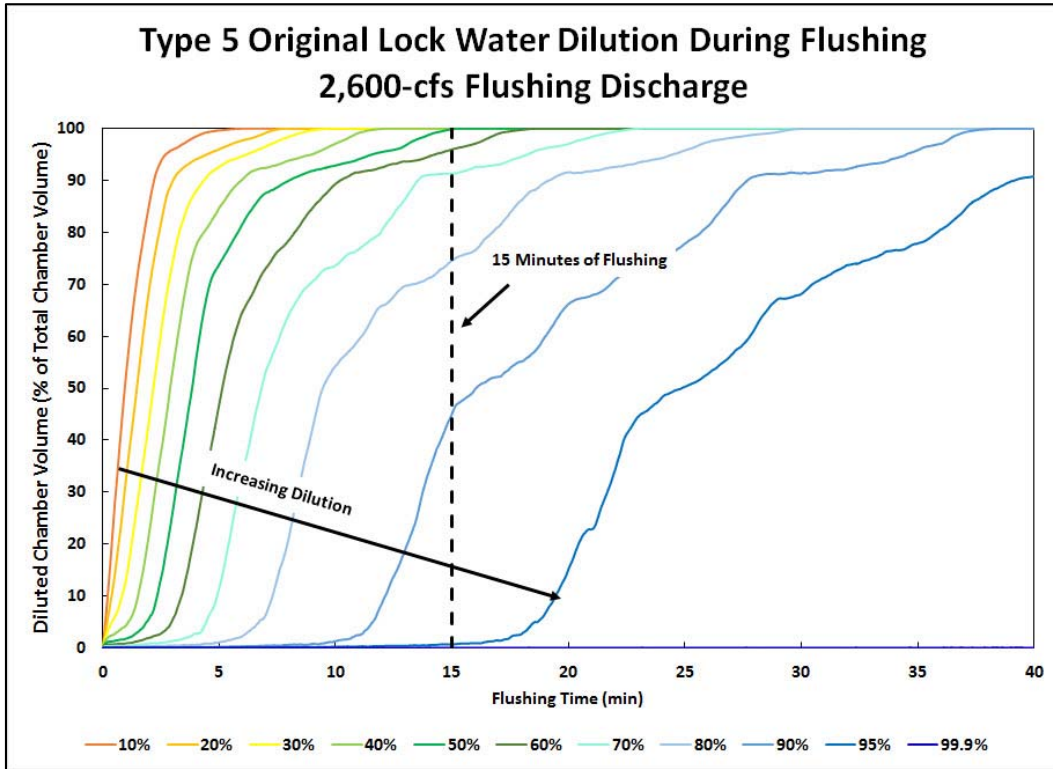


Table 11. Type 5 chamber flushing performance – 5-minute intervals

Flushing Time (min)		Flushed chamber volume (% of total lock chamber volume)							
		5	10	15	20	25	30	35	40
Dilution of original lock chamber water	99.9%	<1	<1	<1	<1	<1	<1	<1	<1
	90%	<1	1	45	66	78	91	96	100
	80%	1	54	75	92	96	100	100	100
	70%	12	74	91	97	100	100	100	100
	60%	47	89	96	100	100	100	100	100
	50%	74	93	100	100	100	100	100	100
	40%	85	97	100	100	100	100	100	100
	30%	93	100	100	100	100	100	100	100
	20%	96	100	100	100	100	100	100	100
	10%	100	100	100	100	100	100	100	100

## 7 Physical Model

The primary similitude consideration in hydraulic modeling of navigation locks is that the scale is large enough to reduce the scale effects to an understandable level. A 1:25-scale model is the current practice for evaluating the performance of a lock chamber (Headquarters, US Army Corps of Engineers 2006).

### 7.1 Kinematic Similitude

Kinematic similarity is an appropriate method of modeling free-surface flows in which the viscous stresses are negligible. Kinematic similitude requires that the ratio of the inertial forces ( $\rho V^2 L^2$ ) to the gravitational forces ( $\rho g L^3$ ) in the model are equal to those of the prototype. Here,  $\rho$  = fluid density,  $V$  = fluid velocity,  $L$  = a characteristic length, and  $g$  = acceleration due to gravity. This ratio is generally expressed as the Froude number,  $Fr$ .

$$Fr = \frac{V}{\sqrt{gL}} \quad (0)$$

Here,  $L$ , the characteristic length, is usually taken as the flow depth in open-channel flow.

The Froude number can be viewed in terms of the flow characteristics. Because a surface disturbance travels at the celerity of a gravity wave,  $\sqrt{gh}$  where  $h$  = flow depth, the Froude number describes the ratio of advection speed to the gravity wave celerity. Evaluation of the lock chamber performance primarily concerns modeling the hawser forces on moored barges during filling and emptying operations. During normal locking operations, the skin friction drag on the vessel is insignificant because horizontal fluid velocities are minute. Hawser forces are generated primarily by slopes of the lock chamber water surface. The tow's bow-to-stern water-surface differentials are the result of long period seiches in the lock chamber. Seiching is the process of gravity waves traveling in the longitudinal direction from the upper service gates to the lower service gates. Therefore, equating Froude numbers in the model and prototype is an appropriate means of modeling the lock chamber.

## 7.2 Dynamic Similitude

Modeling forces is a significant purpose of the laboratory investigation. Appropriate scaling of viscous forces requires the model be dynamically similar to the prototype. Dynamic similarity is accomplished when the ratios of the inertia forces to viscous forces ( $\rho vVL$ ) of the model and the prototype are equal. Here,  $\nu$  is the kinematic viscosity of the fluid. This ratio of inertia to viscous forces is usually expressed as the Reynolds number

$$Re = \frac{VL}{\nu} \quad (0)$$

and, in pressure flow analysis, the culvert hydraulic diameter is usually chosen as the characteristic length,  $L$ . The Reynolds number quantifies the flow's viscous forces relative to advection forces. As the Reynolds number increases, the flow is less affected by viscous shear.

## 7.3 Similitude for Lock Models

Modeling lock filling and emptying systems is not entirely quantitative. The system is composed of pressure flow conduits and open-channel flow components. Further complicating matters, the flow is unsteady. Discharges (therefore  $Re$  and  $Fr$ ) vary from no flow at the beginning of an operation to peak flows within a few minutes and return to no flow at the end of the cycle. Current laboratory studies of lock designs employ 1:25-scale Froudian models in which the viscous differences (model and prototype) are small and can be estimated based on previously reported model-to-prototype comparisons. Setting the model and prototype Froude numbers equal yields the relations between the dimensions and hydraulic quantities shown in Table 12.

Table 12. Model-prototype scale relations

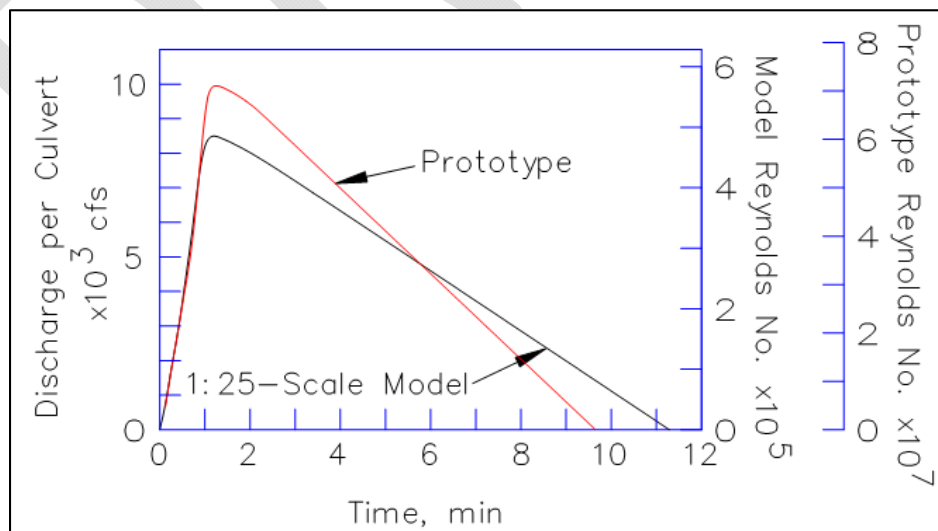
Characteristic	Dimension	Scale Relation Model:Prototype
Length	$L_r = L_r$	1:25
Pressure	$P_r = L_r$	1:25
Area	$A_r = L_r^2$	1:625
Velocity	$V_r = L_r^{1/2}$	1:5
Discharge	$Q_r = L_r^{5/2}$	1:3,125

Time	$T_r = L_r^{1/2}$	1:5
Force	$F_r = L_r^3$	1:15,625
Reynolds Number	$Re_r = L_r^{3/2}$	1:125

These relations are used to transfer model data to prototype equivalents and vice versa.

Complete similitude in a laboratory model is attained when geometric, kinematic, and dynamic similitudes are satisfied. Physical models of hydraulic structures with both internal flow (pressure flow) and external flow (free-surface flow) typically are scaled using kinematic (Froudian) similitude at a large enough scale that the viscous effects in the scaled model can be neglected. The USACE has investigated more than fifty model and ten prototype studies of lock filling and emptying systems (Pickett and Neilson 1988). The majority of these physical model studies were conducted at a scale of 1:25, although early studies sometimes used a 3:100 scale. Lock models constructed to a scale of 1:25 have maximum Reynolds numbers at peak discharges on the order of  $10^5$ , while the corresponding prototype values are on the order of  $10^7$ . This difference is illustrated in results from laboratory (Ables 1978) and field (McGee 1989) experiments on the Whitten (Bay Springs) Lock presented on the filling curves in Figure 53.

Figure 53. Whitten (Bay Springs) Lock filling curves.



Boundary friction losses in lock culverts are empirically described using the “smooth-pipe” curve of the Darcy-Weisbach friction factor where the head loss is expressed as

$$H_f = f \frac{L V^2}{D 2g} \quad (0)$$

where  $H_f$  = head loss due to boundary friction  
 $f$  = Darcy-Weisbach friction factor  
 $L$  = culvert length  
 $D$  = culvert diameter

The Darcy-Weisbach friction factor for turbulent flow in smooth pipes is given in an implicit form as (Vennard and Street 1982):

$$\frac{1}{\sqrt{f}} = 2.0 \log(Re \sqrt{f}) - 0.8 \quad (0)$$

Because the friction factor decreases with increasing Reynolds number, the model is hydraulically “too rough” as compared to the prototype. The scaled friction losses in the model will, therefore, be larger than those experienced by the prototype structure. Consequently, the scaled velocities (and discharges) in the model will be lower and the scaled pressures within the culverts will be higher than those of the prototype. Lower discharges result in longer filling and emptying times in the model than the prototype. Prototype filling and emptying times for similar designs will be smaller than those measured in a 1:25-scale lock model.

Boundary friction decreases with increasing Reynolds number. As mentioned previously, lock model velocities scaled using kinematic similitude (model Froude number equal to prototype Froude number) in a 1:25-scale model have maximum Reynolds numbers at peak discharges on the order of  $10^5$  yet the corresponding prototype values are on the order of  $10^7$ . Therefore, scaled friction losses in the model are larger than those experienced by the prototype structure. (The model is said to be hydraulically “too rough”.) Consequently, the scaled velocities (and discharges) in the model are smaller and the scaled pressures within the culverts are higher than those of the prototype. Even in lock systems in which low pressures are not a particular concern, the lower discharges cause longer scaled filling and emptying times in the model than those experienced by the prototype.

Even though a prototype lock filling-and-emptying system is normally more efficient than predicted by its hydraulic model, EM 1110-2-1604 (Headquarters, US Army Corps of Engineers 2006) states that the difference in efficiency is acceptable as far as most of the modeled quantities are concerned (hawser forces, for example) and can be accommodated empirically for others (filling time and overtravel, specifically).

#### 7.4 Model-Prototype Comparison

Direct component-to-component comparison of differences in model and prototype performance is difficult due to the lack of accurate data of the turbulent, unsteady flow. However, comparison of the overall lock coefficient,  $C_L$ , for model and prototype structures provides a dimensionless parameter that describes the hydraulic efficiency integrated over the flow cycle of locking operations. The nondimensional term is also convenient because rarely do data exist for the same pools in model and prototype. The lock coefficient is defined by the relation commonly referred to as the Pillsbury equation (Pillsbury 1915):

$$T - k_v t_v = \frac{2A_L}{\sqrt{2gC_L A_c}} (\sqrt{H + d} - \sqrt{d}) \quad (0)$$

or

$$C_L = \frac{2A_L}{\sqrt{2gA_c(T - k_v t_v)}} (\sqrt{H + d} - \sqrt{d}) \quad (0)$$

where,  $C_L$  = overall lock coefficient

$A_L$  = plan area of the lock chamber

$H$  = initial head or lift

$d$  = lock-chamber water level over-travel (under-travel for lock emptying)

$A_c$  = sum of culvert area at each operation valve

$T$  = filling or emptying time

$t_v$  = valve operation time

$k_v$  = valve coefficient (which generally ranges from 0.45 to 0.55 and is taken as 0.5 for the present study)

The lock coefficient for existing locks ranges from about 0.45 for relatively slow operation to about 0.90 for very efficient systems that provide rapid operation (Headquarters, US Army Corps of Engineers 2006).

Laboratory and field data suggest that the coefficient from a 1:25-scale model can range from 11% to 17% less than the prototype equivalent during filling and 12% to 19% less during emptying. As previously discussed, the prototype structures are relatively more efficient because of the differences in viscous forces. Some examples from studies listed in the references are presented in Table 13.

Table 13. Lock coefficient,  $C_L$ , for various projects

Lock Project	Filling Operations			Emptying Operations		
	Model	Prototype	Difference	Model	Prototype	Difference
Bankhead	0.66	0.78	15%	0.56	0.69	19%
Lower Granite	0.77	0.93	17%	0.66	0.78	15%
Bay Springs	0.63	0.75	16%	0.52	0.59	12%
Bonneville	0.61	0.72	15%	0.47	0.56	16%
Barkley*	0.75	0.84	11%	N/A	0.62	N/A
Greenup*	0.57	0.62	8%	0.51	0.59	14%

\*Barkley and Greenup locks were tested in 3:100-scale models.

## 7.5 Similitude for mixing models

Hydraulic modeling of mixing requires not only geometric and kinematic similitude but also dynamic similitude so that model observations are representative of prototype behavior. The most important phenomenon which must be modeled is the interplay between momentum of the issuing jet and the ambient fluid. This behavior dominates the flow both near and to some distance from the discharge point. To achieve dynamic similitude, the values of Reynolds number and Froude numbers in the model and prototype must be the same. This cannot be achieved unless the model is full scale (1:1-scale) or a different fluid is used in the model. The Reynolds number is always relegated to secondary importance with the provision that its value in the model is sufficiently large to achieve turbulent flow (Fischer et al. 1979). This turbulent flow requirement means that the Reynolds number of the discharge jet based on the jet flushing velocity and diameter should be larger than approximately 2,000 (Fischer et al. 1979). This would result in a turbulent jet in the model. A 1:25-scale Froude-scaled model with Reynolds number of 100,000 will be large enough to provide a reasonable representation of prototype mixing.

## 8 Hawser Forces during Flushing

Navigation locks are designed and operated to ensure safety for vessel operators and project personnel. Safety is viewed in terms of lock chamber performance. Chamber performance is evaluated based on surface currents and turbulence such that conditions cannot be hazardous to small craft and on hawser forces, the mooring line forces required to hold the design vessel in place. USACE lock design criteria (Headquarters, US Army Corps of Engineers 2006 and Headquarters, US Army Corps of Engineers 1995) limits hawser forces to 5 tons.

If the buoyant force balances the barge weight and if the pitch motion is assumed negligible, then the single-degree-of-freedom equation of motion for the moored system is

$$(1 + C_a)m_v\ddot{s} + C_h\dot{s} + (K_0 + k)s = F \quad (0)$$

where  $s$  = surge displacement of the barge

$C_a$  = added mass coefficient

$m_v$  = mass of the barge tow

$C_h$  = hydrodynamic damping coefficient

$K_0$  = initial tension in the hawser

$k$  = hawser spring constant,

$F = F_s + F_\tau + F_p$

$F_s$  = difference in hydrostatic force between the bow and stern

$F_\tau$  = force due to shear stress

$F_p$  = hydrodynamic response (force required to accelerate the fluid) (Kalkwijk 1973)

The overscript dot indicates differentiation with respect to time.

Steady-state forces acting on a moored vessel can be determined from the right-hand side of (31), which is the sum of the external forces acting on the system with. In equation form

$$F_s = \rho g b d l S_s \quad (0)$$

$$F_r = \frac{1}{2} C_f \rho A V |V| \quad (0)$$

$$F_p = \frac{1}{2} \rho b d C_p V |V| \quad (0)$$

where  $b$  = beam width of barge  
 $d$  = barge draft  
 $l$  = barge length  
 $S_s$  = slope of the water surface  
 $g$  = acceleration due to gravity  
 $\rho$  = fluid density  
 $C_f$  = friction coefficient  
 $A$  = wetted area of the hull  
 $C_p$  = pressure coefficient  
 $V$  = mean velocity of fluid relative to the vessel

Although this single-degree-of-freedom model only simulates the vessel's surge, Natale and Savi (1994) demonstrate its accuracy in modeling barges moored in a lock chamber. The single-degree-of-freedom equation of motion (31) is a second-order, nonhomogeneous, ordinary differential equation for a damped system with external forcing. In mooring applications, the system is generally underdamped and the displacement of the moored vessel oscillates with an exponential decay in amplitude.

A model of forces exerted in hawsers mooring a vessel in a lock chamber has been used in conjunction with a numerical flow model of lock filling systems to optimize lock operations (Natale and Savi 2000 and 1994). Information on such parameters as the hawser spring constant is available (e.g. Naval Facilities Engineering Command 1986a, 1986b). Added mass and hydrodynamic damping coefficients needed to model the mooring of a barge tow in a lock chamber are given in Stockstill (2000).

Often, the only force considered is the hydrostatic force since it is much larger than the shear due to friction or the hydrodynamic response. However, using the equation of motion provides a more accurate answer. Equation (31) can be used in conjunction with a numerical flow solution to estimate the forces exerted during flushing operations when a tow is moored in the chamber. This modeling system could also be used to estimate hawser forces on vessels moored downstream of the lock in the lower approach during flushing. This process would require values for the added mass and damping coefficients, which could be determined using physical model experiments.

If the inertia is neglected, then the longitudinal flow is uniform from one end of the chamber to the other. The water-surface slope in the lock chamber can be estimated using the Darcy-Weisbach equation.

$$\frac{H_L}{L} = S_f = S_s = \frac{f}{8R} \frac{Q^2}{gA^2} \quad (0)$$

where  $Q$  = discharge

$A$  = flow area =  $Bh$

$R$  = hydraulic radius =  $\frac{Bh}{2h+B}$  (flow area divided by wetted perimeter)

The dimensions of Brandon Road Lock are the depth,  $h = 13.9$  ft, width,  $B = 110$  ft, and length,  $L = 671$  ft. The design tow is assumed to be a 3 by 3 flotilla of jumbo barges, each barge being 35 ft wide by 195 ft long and drafted at 9 ft. The 3 by 3 tow dimensions are the beam width,  $b = 105$  ft, the length,  $l = 585$  ft, and draft,  $d = 9$  ft.

The water-surface slope can also be estimated using the Manning's Equation.

$$S_s = \frac{n^2}{C_m R^{\frac{4}{3}}} \left(\frac{Q}{A}\right)^2 \quad (0)$$

where  $n$  = Manning's roughness coefficient

$C_m$  = a dimensional constant ( $C_m = 1$  for SI units and 2.208 for US Customary units).

A reasonable value of Manning's coefficient for a lock chamber with concrete walls and rock floor is 0.015, depending on the roughness of the lock floor.

## 9 Further Research – Prototype and Physical Model Testing

### 9.1 Prototype Tests

A field study of Brandon Road Lock has been proposed by the U.S. Geological Survey. The prototype test plan includes measuring velocities in the lock chamber during steady flow conditions through the filling system, similar to the Type 1 lock flushing concept. To avoid any safety issues, these experiments will be conducted without tows in the lock chamber. These field data will be used to validate future numerical and physical models. If the validation results find that the physical model reproduces field conditions with an empty chamber, then experiments with a tow present in the chamber can be conducted with confidence.

### 9.2 Physical Model Experiments

A physical model is required for the lock flushing concept that is being considered for implementation after the numerical modeling phase. Before a final decision is made on the lock flushing concept to be constructed at Brandon Road Lock, a physical model would be needed to answer questions related to safety, because of existing USACE regulations, and uncertainties that currently exist in numerical modeling navigation locks and the related flow situations.

#### 9.2.1 Safety

Vessel movement within the lock chamber during flushing is the primary safety concern. Fluid and vessel forces are derived from many sources including hydraulic forces acting on the vessel and mooring line forces. The processes involved in calculating vessel movement within the lock chamber during flushing are very complex and include poorly constrained parameters, e.g., added mass, hydraulic damping coefficients, turbulence intensity, scales of motion, etc. Further research is needed, especially with regard to large vessels operating in confined spaces as well as vessel displacement sensitivities to some input parameters, to determine appropriate values for use in other types of models.

Hawser criteria are based on the hydrodynamic vessel forces and are designed to provide a high degree of safety during lock operations. The vessel

is expected to experience the maximum safe forces for an extended period during the flushing process. Flushing produces a longitudinal water surface slope that will generate substantial forces on vessels. Since the hawser forces must be known for safe lock operation when vessels are in the chamber, the only way to develop safe operating criteria is to measure these forces in a physical model.

### **9.2.2 USACE regulations**

USACE regulations require physical models for lock designs which do not follow the design criteria directly. EM 1110-2-1604 "Hydraulic Design of Navigation Locks" and EM 1110-2-2602 "Planning and Design of Navigation Locks" describe USACE's requirements for lock design and construction including navigation criteria. EM1110-2-1604 defines the criteria for maximum hawser forces on moored vessels based on physical model studies. Therefore, USACE guidance standards require a physical model to determine the maximum safe force. EM 1110-2-2602 states that "physical model studies... are a traditional and necessary part of the planning and design phase for most navigation facilities". While the document mentions the use of numerical models, they currently cannot sufficiently reproduce the flow conditions and subsequent physical quantities to address new designs or extensive modifications to existing projects. The hydraulic engineering community does not have a thoroughly validated modeling system capable of providing the accuracy required to meet the USACE hawser safety criteria prescribed in EM 1110-2-1604. Existing numerical models are appropriate for low-level screening to determine relative differences (not absolute) between some design alternatives but are inappropriate for exploring the extensive modifications proposed in the Brandon Road lock flushing study.

### **9.2.3 Numerical modeling uncertainties**

Tracer and dye studies are the only practical method to quantify lock flushing with high certainty. Numerical models can include a tracer or particle tracking feature to simulate chamber flushing. The tracer algorithms are based on turbulent diffusion theory that includes diffusion coefficients. These diffusion coefficients are derived from turbulence closure methods and are subject to some degree of uncertainty as the mixing algorithm is specific to a particular set of equations, which are discretized in a particular manner. These equations include empirically-determined coefficients and scaling parameters that are calculated from laboratory or field data

and often must be adjusted when applied in a new situation. There is no real randomness in the numerical model, so the result is an average or synthetic representation of the real world. Furthermore, the added complexity of the alternative flushing systems combined with the presence of a vessel in the chamber has not been explored previously. Numerical model results cannot be verified to be representative of Brandon Road Lock because of the uncertainty in the coefficients.

A physical model could be constructed at the ERDC with which a suite of filling and emptying tests would be conducted to determine flushing rates for the lock chamber. A 1:25-scale physical model of Brandon Road Lock filling and emptying system could be used to measure flushing with and without tows to directly determine residence time within the lock chamber and the culverts. This would unequivocally establish the lock operation procedures required to reduce the lock ANS concentration to various dilution levels (e.g. 95%, 99%). In addition to emptying and filling without vessels, experiments using a remote-controlled tow with different barge configurations could determine the effects of vessel lockage on exchange. Vessel blockage during the locking process can either increase (exiting) or decrease (entering) the volume within the lock. Localized mixing along the hull as well as propeller wash can further complicate the exchange mechanism, so the case with tows is significantly more complex and critical to understanding the role of navigation in lock flushing. Vessel effects such as “What is the role of vessels during the locking process in enhancing/hindering the exchange flow?” and “How does vessel-induced turbulence and propeller wash modify residence time?” and “What role does vessel blockage play in modifying the exchange flow rate?” could be quantified. Experiments could explore the consequences of upbound and downbound tows with different barge configurations.

Rhodamine dye could be used to track the water mass within the lock chamber to quantify turbulent dispersion coefficients and flushing rates. Rhodamine dye has been used extensively in the marine environment as a water mass tracer and accurate methodologies to measure the mixing rates and dispersion are well developed. Rhodamine fluorescence can be easily measured using inexpensive fluorometers, thus providing residence time and flushing efficiency within the lock chamber and culvert. Confetti can be used to measure surface water exchange and flow visualization tech-

niques, such as high speed digital photography, provide direct measurements of particle velocity and rotation to evaluate water mass exchange dynamics.

Experiments with a 1:25-scale lock model would include running multiple lock filling and emptying scenarios with and without tows to measure flushing times and to determine optimal lock operations. Several methods would be used to quantify volume exchange time including dye tracers and confetti combined with digital camera systems to determine flow trajectories, mixing rates and turbulence.

Particular attention could be paid to evaluating the Type 1 concept (existing filling and emptying system). If Brandon Road Lock could serve as the necessary barrier using the existing filling and emptying system, then the project modification expenses would be limited to insuring that the filling valves can close under flowing conditions and that the lower miter gates are secured open during flushing. The barrier expense would then be limited to the additional flushing time required prior to each filling operation, which is common to each design alternative considered.

The effectiveness of the Type 4 concept (continuous flushing downstream of the lock) could be evaluated in the same physical model if it was constructed to include a sufficient reach of the lower approach. Experiments with tows passing over the Type 4 concept manifold could determine how the flushing currents interact with the tow's return currents and propeller wash for both upbound and downbound tows.

### **9.3 Tow Effects**

The currents generated as an upbound tow enters a lock chamber are illustrated in Figure 54. As the vessel enters the chamber, the displacement forces the same volume of water from the chamber. The resulting flow is referred to as the return current. A barge tow leaving the lock draws water into the chamber to replace the vessels displacement volume (Figure 55). Vessel speed and squat, and thus the return currents, are influenced by the depth over the sill and chamber floor (Maynard 2000).

Figure 54. Currents generated as an upbound tow enters a lock chamber.

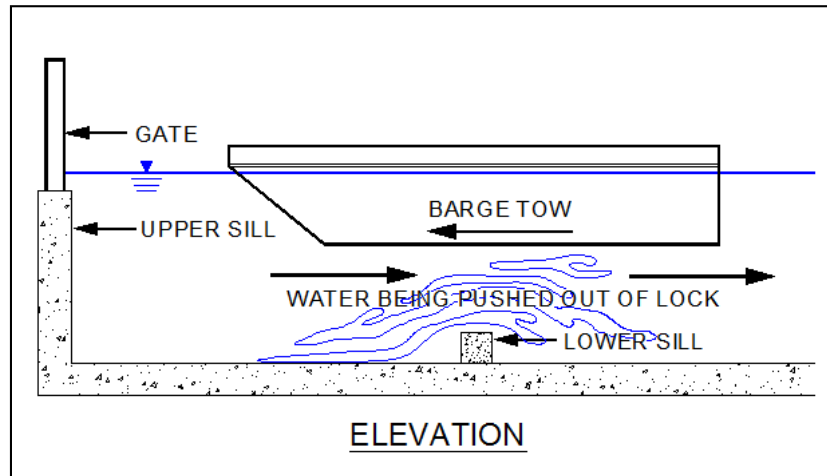
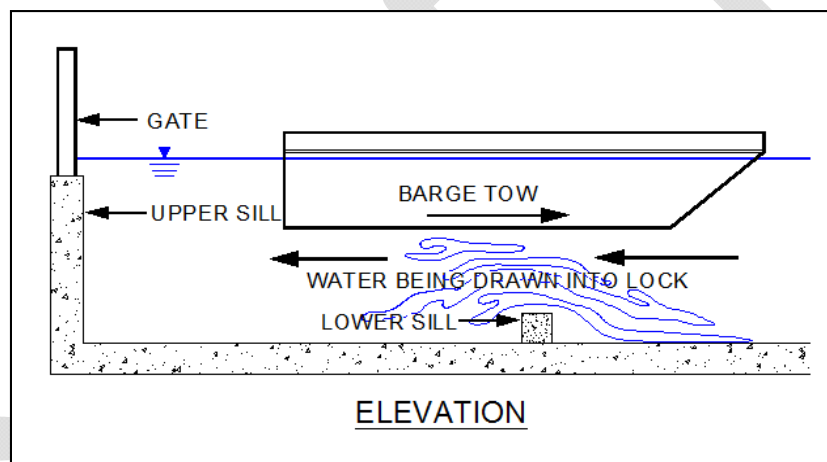


Figure 55. Currents generated as a downbound tow leaves a lock chamber.



For the case where the vessel is exiting the lock into ANS contaminated water, a rough approximation is to assume that the volume of water initially displaced by the tow will be replaced by ANS-contaminated water as the tow exits the chamber. In practice, the propeller wash will contribute significantly to mixing and increase the risk of ANS-contaminated water entering the chamber, particularly as the tow exits the chamber.

## 10 Summary and Recommendations

Ideas and preliminary hydraulic calculations have been presented as part of the development of an ANS flushing system for Brandon Road Lock. Four flushing system designs and operations have been drafted. The Type 1 lock flushing concept uses the existing culvert system. Types 2 and 3 lock flushing concepts require modifications to the lock structure. The Type 4 idea is not actually a lock flushing concept, but rather a design that provides a continuous supply of clean water in the lower lock approach thus preventing ANS from reaching the lock chamber.

Five lock flushing concepts (Types 1, 2, 3, 3r, and 5) have been tested in a 3-D numerical model. Each model has a lock chamber without tows only. The Type 1 lock flushing concept shows highly unsteady flow fields. Original lock chamber water dilution happens throughout the lock chamber. The area upstream of the first filling and emptying ports flushes considerably less slowly than the other areas of the chamber.

The Type 2 flushing concept was simulated in the first phase of modeling work but was removed from further consideration because of construction and construction cost concerns. The numerical models of this concept did not include direct calculation of original lock dilution.

In the Type 3 lock flushing concept flow is introduced at the upstream end of the chamber, and lock flushing occurs generally upstream to downstream. Because of lock chamber surface drawdown, the flushing discharge for the Type 3 concept must be significantly reduced from what flushing discharge is possible given the difference in head differential between the upper and lower pools. If tows are not present in the lock chamber during flushing, the flushing discharge could remain at the maximum possible value. Flushing flow is also introduced in the upstream end of the lock chamber for the Type 3r concept. The conduit through which this flushing flow is introduced into the chamber is much larger than with the Type 3 concept in order to reduce the flushing velocities inside the chamber. The flushing behavior for this concept is also generally upstream to downstream. However, the flushing is much faster for Type 3r due predominately to the higher flushing discharge. The introduction of flushing flow over a larger area of the upstream end of the lock chamber also increases the flushing efficiency. The main drawback to the Type 3r design is

that structural, mechanical, and construction considerations likely significantly limit how much space is available for the flushing conduit through the upstream gate sill.

The Type 5 flushing concept behaves similarly to the Type 1 concept in that flushing flow is introduced through the filling and emptying system ports at multiple areas of the lock chamber. In the Type 5 concept, the filling and emptying system conforms to current USACE hydraulic design guidance standards. The ports have been resized and repositioned. The only deviation in this flushing concept from current design guidance is the inclusion of flushing port on each culvert upstream of the filling and emptying ports. These flushing ports are located at the same station as the first filling and emptying port in the Type 1 concept. The sole purpose of these ports is to increase the flushing rate in the upstream end of the lock chamber. The Type 5 concept flushes the lock chamber more efficiently than the Type 1 concept, but not as efficiently or effectively as either the Type 3 or Type 3r flushing concepts.

The Type 1 lock flushing concept should be tested in a physical model. This concept would be the most economical one to implement because it would not require modifications to the lock structure and should be tested to determine the flushing efficiency using the existing filling system. A decision should be made whether the Type 3 (or some variation) or the Type 5 lock flushing concept should be tested. This decision should be based primarily on structural, mechanical, and cost engineering considerations. Placing pipes through the gate sill may require lower construction costs, but this concept (Type 3) may require flow control valves being submerged.

The Type 4 idea (lateral manifold downstream of lock) could be refined once information on the lock approach bathymetry and engineered channel is developed. The physical model should be designed to accommodate experiments to evaluate the Type 4 concept. Experiments could determine the effectiveness of the Type 4 concept as tows pass over it.

The Type 5 concept has the benefit of reducing the lock filling time due to the improved filling and emptying system performance. Such a reduction in filling time would at least partially offset any lockage time increases due to flushing and would be a benefit to navigation.

If a lock flushing concept is chosen for implementation at Brandon Road Lock, a physical model study must be performed to evaluate at least the safety concerns to navigation traffic during the flushing operation before a final decision is made.

DRAFT

## 11 References

- Ables, J. H. 1978. *Filling and emptying system for Bay Springs Lock, Tennessee-Tombigbee Waterway, Mississippi, hydraulic model investigation*, Technical Report HL-78-19, Vicksburg, MS: U.S. Army Engineer Waterways Experiment Station.
- Ables, J. H., Jr. 1979. *Vortex problem at intake Lower St. Anthony Falls Lock and Dam, Mississippi River, Minneapolis, Minnesota*. Technical Report HL-79-9. Vicksburg, MS: U.S. Army Engineer Waterways Experiment Station.
- Abraham, G., V. D. Burgh, and D. Vos. 1973. *Pneumatic barriers to reduce salt intrusion through locks*. Rijkswaterstaat Communications No. 17, The Hague: Government Publishing Office.
- Albertson, M. L., Y. B. Dai, R. A. Jensen, and H. Rouse. 1950. *Diffusion of submerged jets*, Transactions ASCE, 115, pp. 639-664.
- Bastian, D. F. 1971. *Calcasieu saltwater barrier prototype sector gate tests*. Miscellaneous Paper H-71-4, Vicksburg, MS: U.S. Army Engineer Waterways Experiment Station.
- Bogges, D. H. 1970. *A test of flushing procedures to control salt-water intrusion at the W.P. Franklin Dam near Ft. Myers, Florida*. Tallahassee, FL: Florida Department of Natural Resources, Bureau of Geology.
- Deng, Z. Q., L. Bengtsson, V. P. Singh, and D. D. Adrian. 2002. *Longitudinal dispersion coefficient in single-channel streams*, Journal of Hydraulic Engineering, vol. 128, no. 10, pp. 901-916.
- Fernando, H. J. S. 2012. *Handbook of Environmental Fluid Dynamics, Volume Two: Systems, Pollution, Modeling, and Measurements*, CRC Press.
- Fisher, H. B., E. J. List, R. C. Y. Koh, J. Imberger, and N. H. Brooks. 1979. *Mixing in Inland and Coastal Waters*, Academic Press.
- Headquarters, US Army Corps of Engineers. 2006. *Hydraulic design of navigation locks*. Engineer Manual No. 1110-2-1604, Washington, D.C.
- Headquarters, US Army Corps of Engineers. 1995. *Planning and design of navigation locks*. Engineer Manual No. 1110-2-2602, Washington, D.C.
- Headquarters, US Army Corps of Engineers. 1988. *Hydraulic design criteria*. Vicksburg, MS: US Army Engineer Waterways Experiment Station.
- Hite, J. E., Jr. 1999. *Model study of Marmet Lock filling and emptying system, Kanawha River, West Virginia*. Technical Report CHL-99-8. Vicksburg, MS: U.S. Army Engineer Waterways Experiment Station.
- Hite, J. E., Jr. 2000. *New McAlpine Lock filling and emptying system, Ohio River, Kentucky*. Technical Report ERDC/CHL-00-24. Vicksburg, MS: U.S. Army Engineer Research and Development Center.

- Hite, J. E., Jr. and A. M. Tuthill. 2005. New lock for Soo Locks and Dam, Sault Ste. Marie, Michigan, St. Mary's River. Technical Report ERDC/CHL-05-08. Vicksburg, MS: U.S. Army Engineer Research and Development Center.
- Hite, J. E., Jr. and C. Bislip-Morales. 2012. New lock for Soo Locks and Dam, model investigations during 2006-2010, Sault Ste. Marie, Michigan, St. Mary's River. Technical Report ERDC/CHL-12-1. Vicksburg, MS: U.S. Army Engineer Research and Development Center.
- Mausshardt, S., and G. Singleton. 1995. *Mitigating salt-water intrusion through Hiram M. Chittenden Locks*. Journal of Waterway, Port, Coastal, and Ocean Engineering, vol. 121, no. 4, pp. 224-227.
- Maynord, S. T. 2000. *Effects of lock sill and chamber depths on transit time of shallow draft navigation*. ERDC/CHL TR-00-13, Vicksburg, MS: U.S. Army Engineer Research and Development Center.
- McCartney, B. L., J. George, B. K. Lee, M. Lindgren, and F. Neilson. 1998. *Inland navigation: locks, dams, and channels*, Volume 94 of ASCE Manuals and Reports on Engineering Practice, ASCE Publications.
- McGee, R. G. 1989. *Prototype evaluation of Bay Springs Lock, Tennessee-Tombigbee Waterway, Mississippi*. Technical Report HL-89-15, Vicksburg, MS: U.S. Army Engineer Waterways Experiment Station.
- Miller, D. S. 1990. *Internal flow systems*, 2nd edition, Houston, TX: Gulf Publishing Co.
- Murphy, T. E. 1975. *Lock design, sidewall port filling and emptying system*. Miscellaneous Paper H-75-7, Vicksburg, MS: U.S. Army Engineer Waterways Experiment Station.
- Neilson, F. M. 1975. *Barkley Lock prototype tests, Cumberland River, Kentucky*. Technical Report H-75-11, Vicksburg, MS: U.S. Army Engineer Waterways Experiment Station.
- Oswalt, N. R. 1976. *Ice Flushing from St. Lawrence Seaway Locks*, Technical Report H-76-9, Vicksburg, MS: U.S. Army Engineer Waterways Experiment Station.
- Oswalt, N. R., J. H. Ables, and T. E. Murphy. 1972. *Navigation conditions and filling and emptying system, New Bankhead Lock, Black Warrior River, Alabama*. Technical Report H-72-6, Vicksburg, MS: U.S. Army Engineer Waterways Experiment Station.
- Parchure, T. M., S. C. Wilhelms, S. Sarruff, and W. H. McAnally. 2000. *Salinity intrusion in the Panama Canal*. ERDC/CHL TR-00-4, Vicksburg, MS: U.S. Army Engineer Research and Development Center.
- Pickett, E. B. and F. M. Neilson. 1988. *Lock hydraulic system model and prototype study data*. Miscellaneous Paper HL-88-1, Vicksburg, MS: U.S. Army Engineer Waterways Experiment Station.
- Pillsbury, G. B. 1915. *Excess head in the operation of large locks through the momentum of the column of water in the culverts*. U.S. Army Corps of Engineers, Professional Memoirs, vol. 7, no. 31, pp 206-212.

- Runkel, R. L. 1996. *Solution of the advection-dispersion equation: continuous load of finite duration*, Journal of Environmental Engineering, vol. 122, no. 9, pp. 830-832.
- Seo, J. W. and T. S. Cheong. 1998. *Longitudinal dispersion coefficient in straight rivers*, Journal of Hydraulic Engineering, vol. 127, no. 11, pp. 919-927.
- Seo, J. W. and T. S. Cheong. 1998. *Longitudinal dispersion coefficient in straight rivers*, Journal of Hydraulic Engineering, vol. 127, no. 11, pp. 919-927.
- Socolofsky, S. A. and G. H. Jerka. 2005. *CVEN 489-501 special topics in mixing and transport processes in the environment. Engineering – Lectures*, 5<sup>th</sup> Edition, College Station, TX: Coastal and Ocean Engineering Division, Texas A and M University.
- Stockstill, R. L. 2003. *Mooring Model Coefficients for Barge Tows in a Navigation Lock*, Journal of Waterway, Port, Coastal, and Ocean Engineering, vol. 129, no. 5, 233.
- Stockstill, R. L. and J. F. George. 1996. *Navigation lock for Bonneville Dam, Columbia River, Oregon, volume I: main text*. Technical Report HL-96-13, Vicksburg, MS: U.S. Army Engineer Waterways Experiment Station.
- Tool, A. R. 1980. *Prototype filling and emptying system measurements, New Bankhead Lock, Black Warrior River, Alabama*. Technical Report HL-80-13, Vicksburg, MS: U.S. Army Engineer Waterways Experiment Station.
- Tuthill, A. M. 2003. *Ice and debris passage for innovative lock designs*, ERDC/CRREL TR-03-2, Hanover, NH: U.S. Army Engineer Research and Development Center.
- Tuthill, A. and G. Gooch. 1997. *Modeling ice passage at Starved Rock Lock and Dam on Illinois Waterway*, Journal of Cold Regions Engineering, vol. 11, no. 3, pp. 232-243.
- Tuthill, A., L. Liu, and H. T. Shen. 2004. *Modeling ice passage at navigation locks*. Journal of Cold Regions Engineering, vol. 18, no. 3, pp. 89-109.
- U.S. Army Engineer Division Hydraulic Laboratory. 1979. *Navigation lock for Lower Granite Dam, Snake River, Washington, hydraulic model investigation*. Technical Report No. 126-1, Bonneville, Oregon: U.S. Army Engineer Division, North Pacific.
- Vennard, J. K. and R. L. Street. 1982. *Elementary fluid mechanics*, New York, NY: John Wiley and Sons.
- Waller, T. N. 1997. *Prototype evaluation of Bonneville Navigation Lock, Columbia River, Oregon*. Technical Report CHL-97-14, Vicksburg, MS: U.S. Army Engineer Waterways Experiment Station.
- Wood, I. R. 1970. *A lock exchange flow*. Journal of Fluid Mechanics, vol. 42, part 42, pp. 671-687.





## Appendix B – Computational Meshes

Before the lock flushing simulations could be conducted, the geometry defined by the CAD model of each lock flushing concept had to be divided into a computational mesh. Each geometry was divided into meshes that were composed of tetrahedral elements. The sizes of these elements differed throughout the flow domain for each geometry. Generally, the size of the element depended on the complexity and size of the component in that area of the geometry. For instance, the filling and emptying ports and culverts required smaller elements to define the wall curvatures than elements in the lock chamber and areas upstream of the upstream gate sill. The geometry and the computation mesh for each lock flushing concept are shown in Figure 58-Figure 72 on the following pages. The number of nodes and tetrahedral elements for each mesh is listed in Table 14.

**Table 14. Computational mesh sizes**

Flushing Concept	Nodes	Elements
Type 1	366,669	1,874,851
Type 2	226,285	1,138,554
Type 3	244,785	1,291,184
Type 3r	324,006	1,741,038
Type 5	365,312	1,865,316

Figure 58. Type 1 geometry and computational mesh

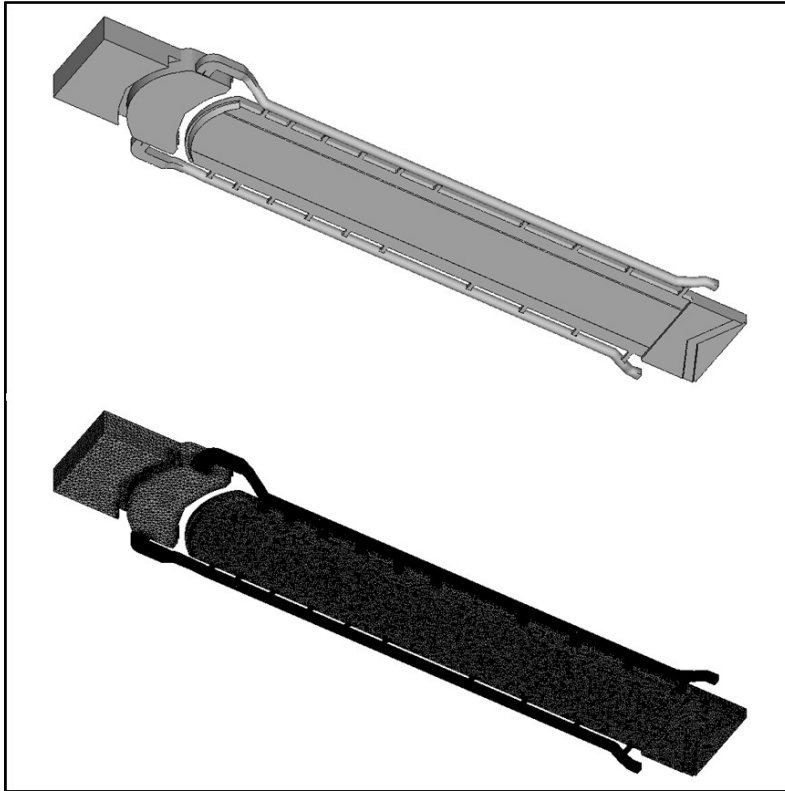


Figure 59. Type 1 geometry and computational mesh - Zoom 1

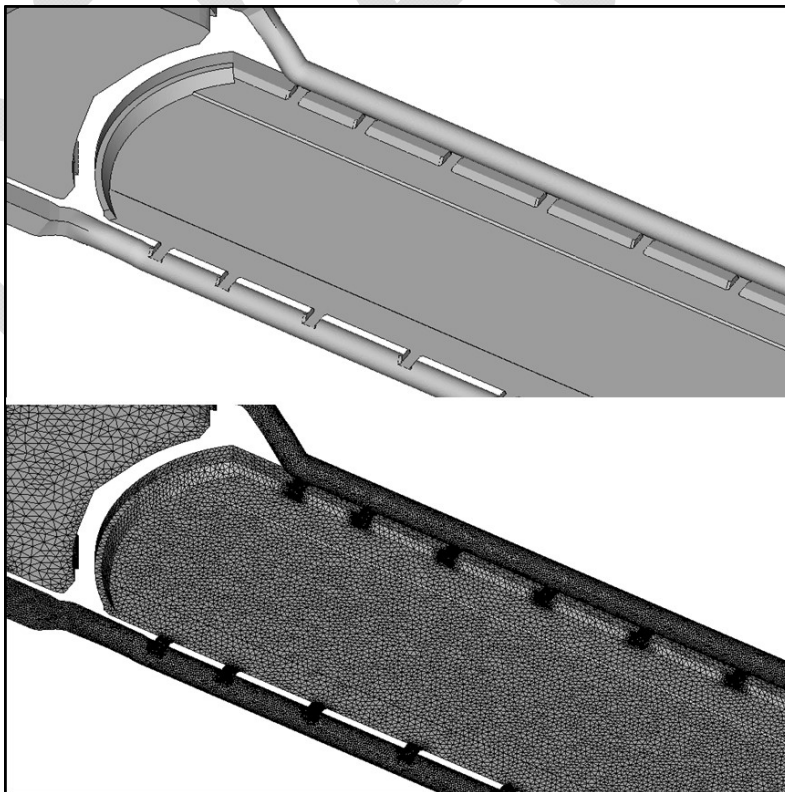


Figure 60. Type 1 geometry and computational mesh - Zoom 2

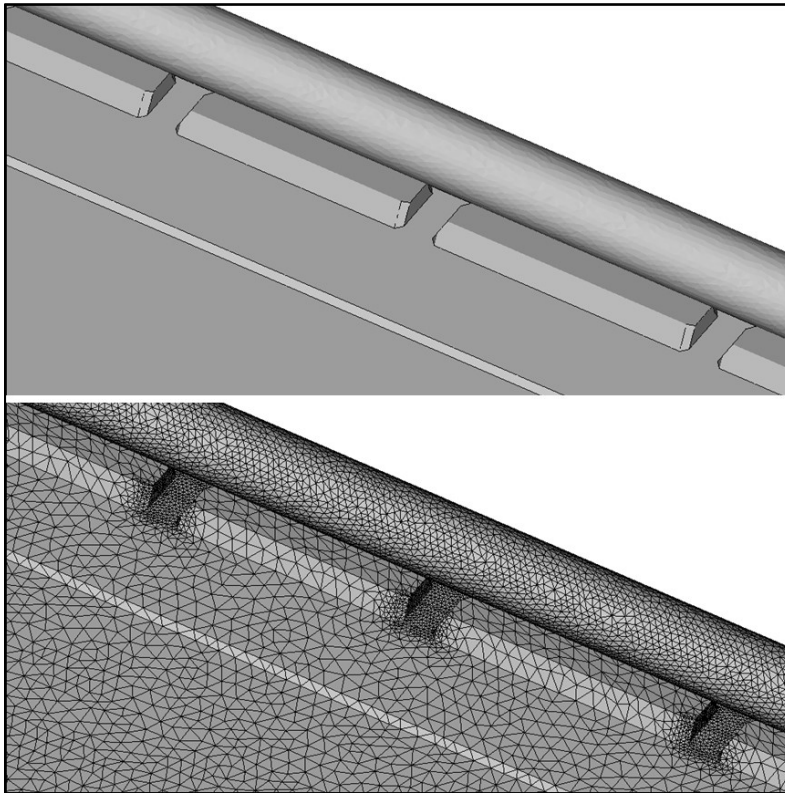


Figure 61. Type 2 geometry and computational mesh



Figure 62. Type 2 geometry and computational mesh - Zoom 1

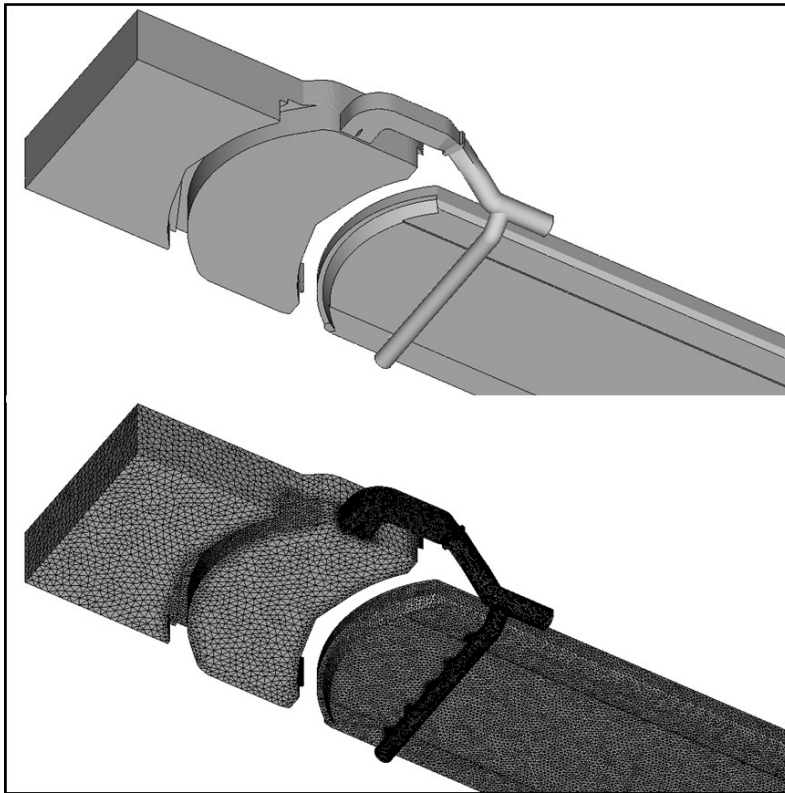


Figure 63. Type 2 geometry and computational mesh - Zoom 2

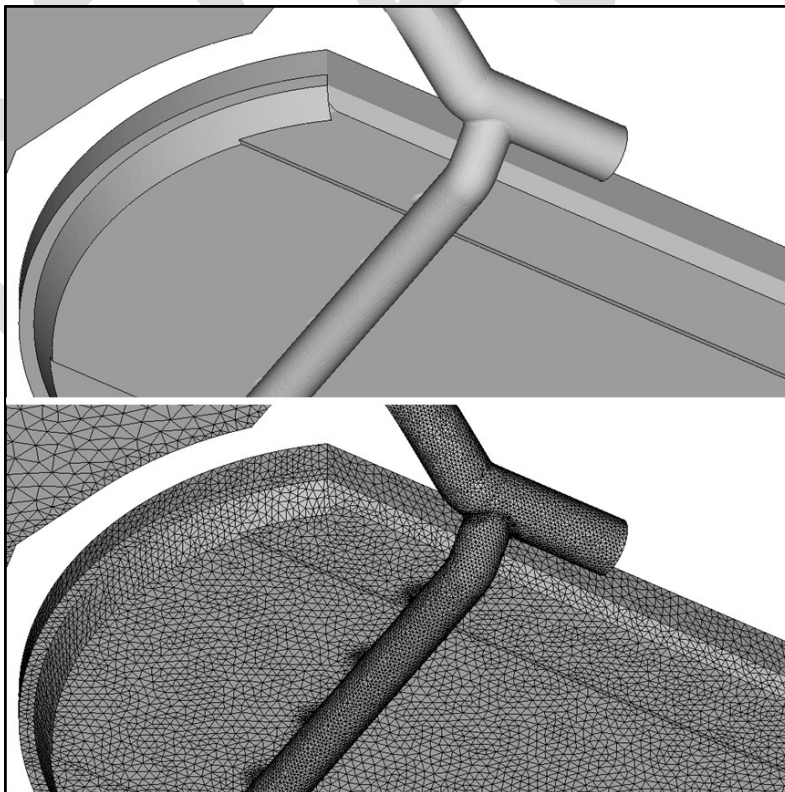


Figure 64. Type 3 geometry and computational mesh

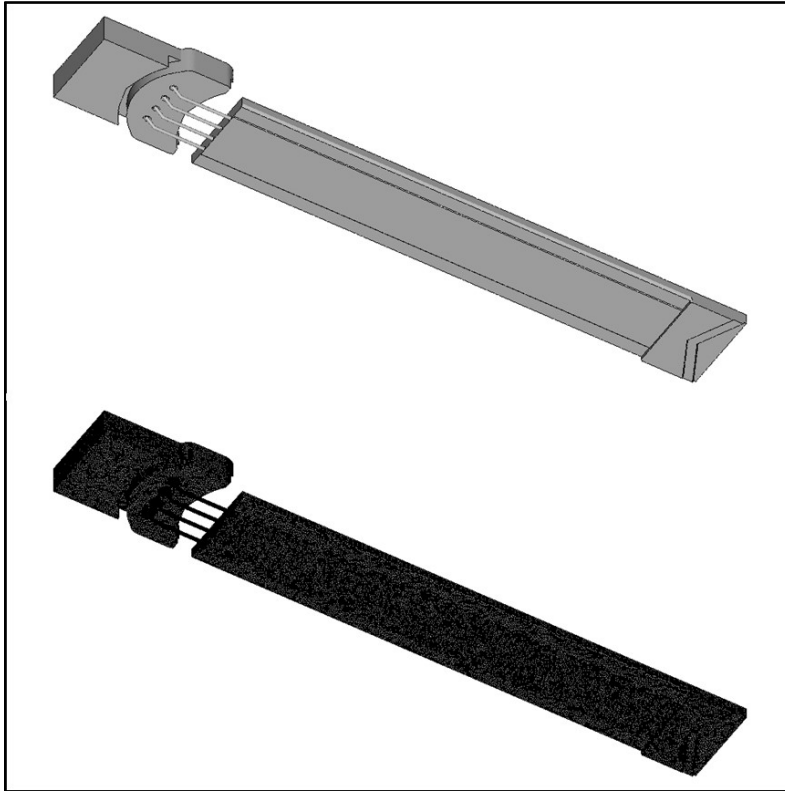


Figure 65. Type 3 geometry and computational mesh - Zoom 1

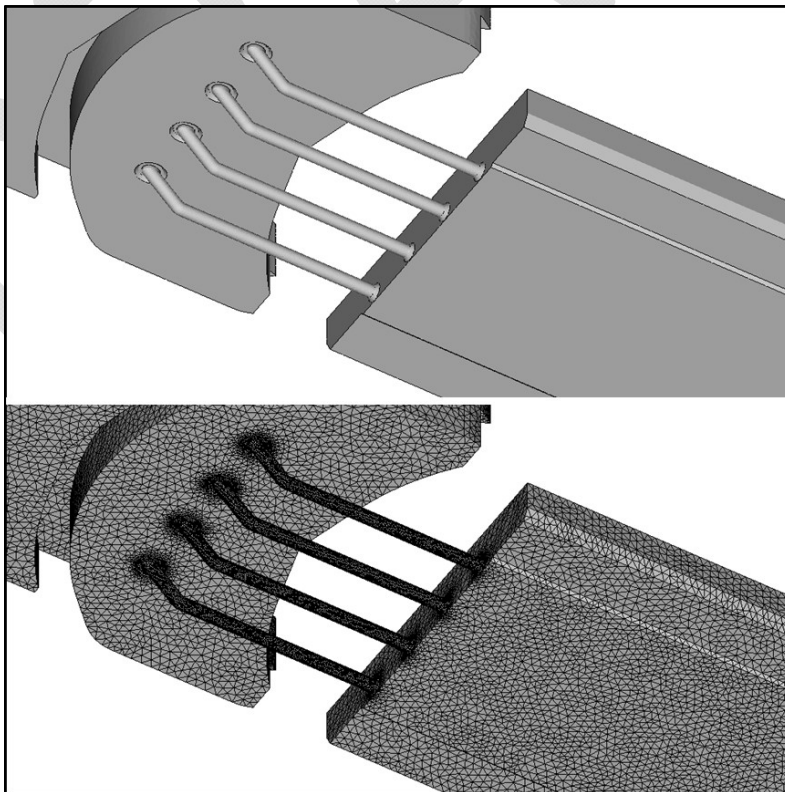


Figure 66. Type 3 geometry and computational mesh – Zoom 2

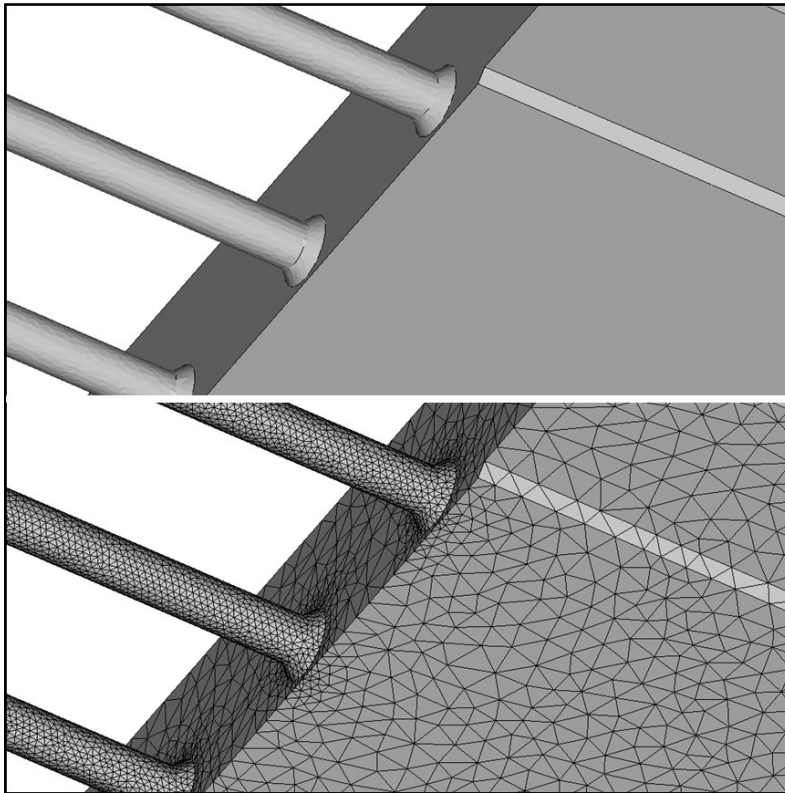


Figure 67. Type 3r geometry and computational mesh



Figure 68. Type 3r geometry and computational mesh - Zoom 1

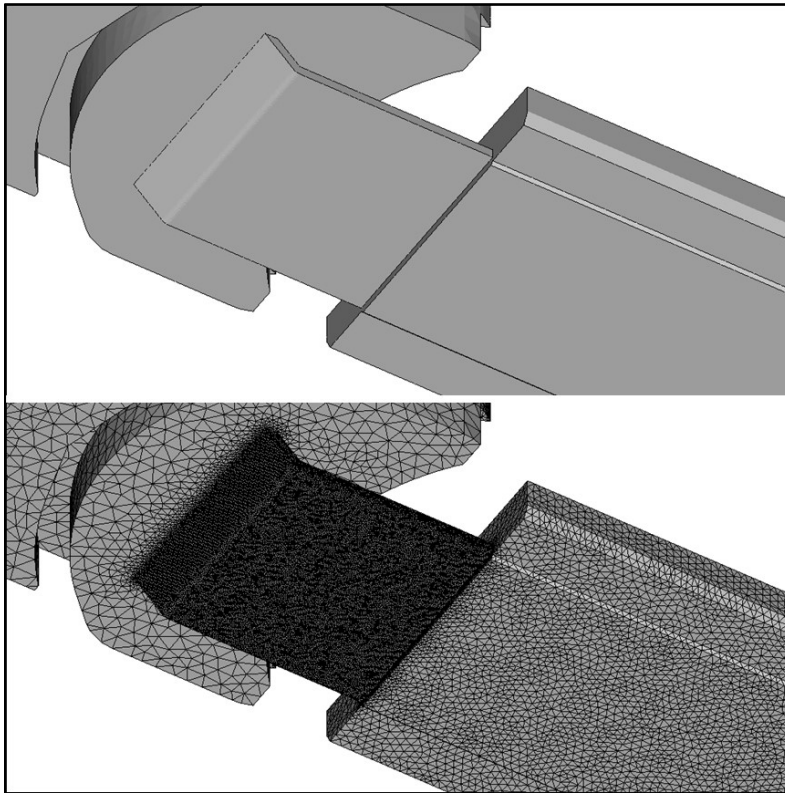


Figure 69. Type 3r geometry and computational mesh - Zoom 2

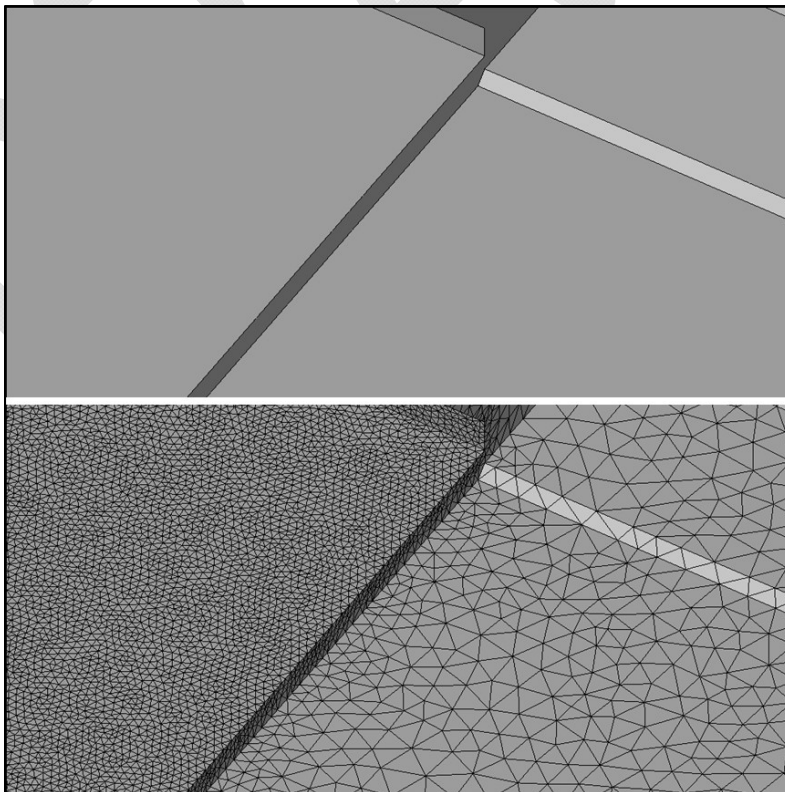


Figure 70. Type 5 geometry and computational mesh

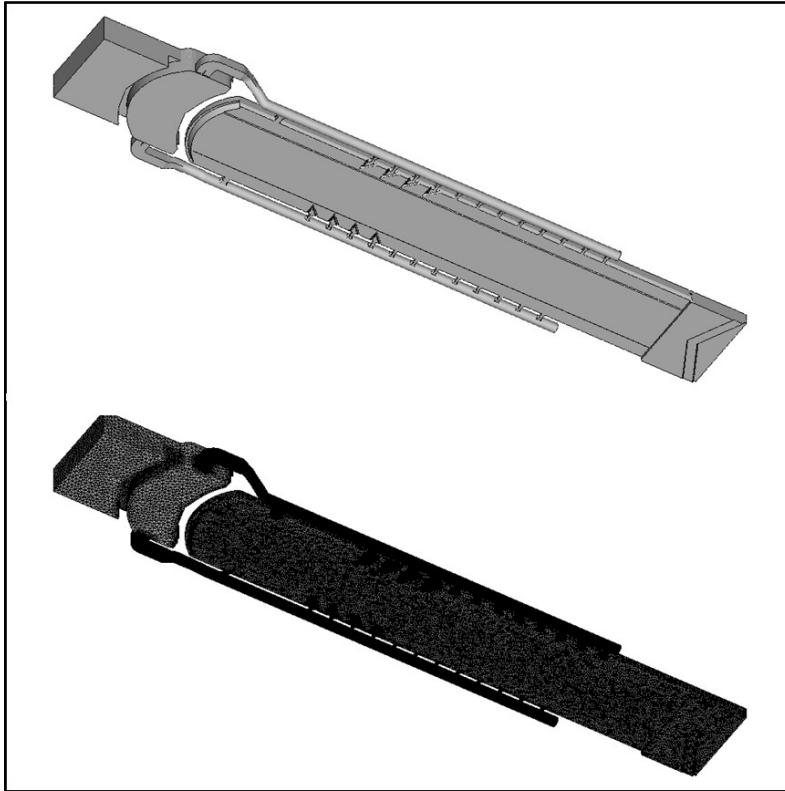


Figure 71. Type 5 geometry and computational mesh - Zoom 1

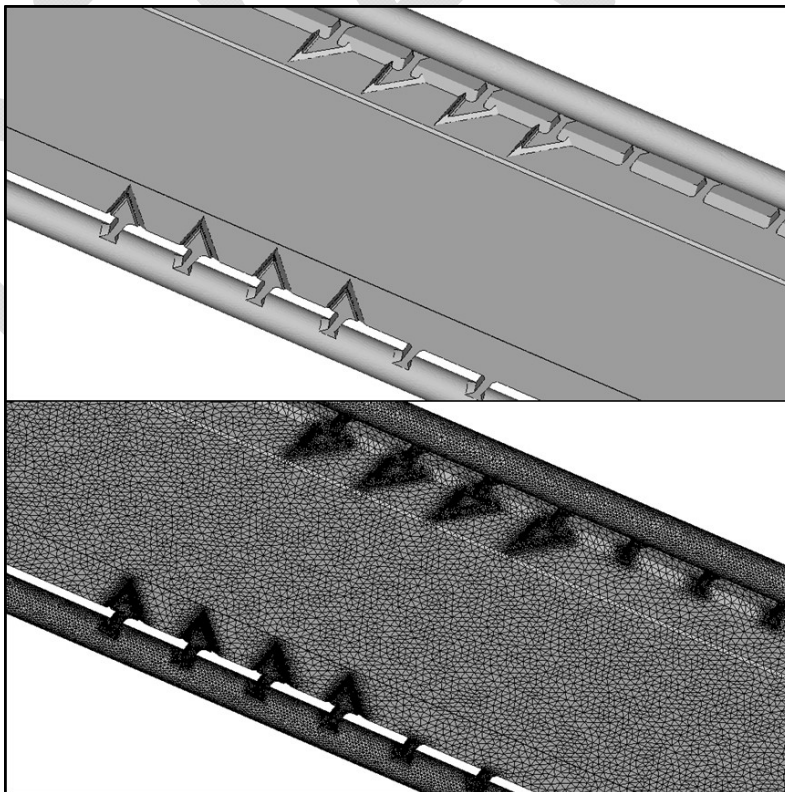
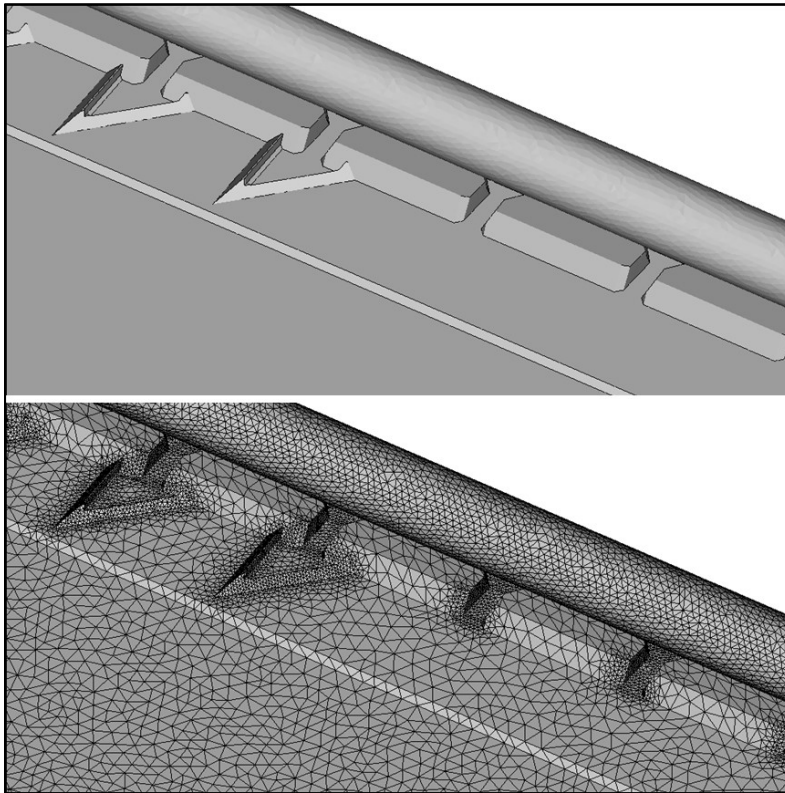


Figure 72. Type 5 geometry and computational mesh - Zoom 2



DRAFT

## **Appendix C – Type 2 fixed lid model results**

The Type 2 lock flushing concept was simulated in a previous phase of numerical modeling work for the GLMRIS project. The numerical modeling process during that phase included fixed lid models of the lock flushing concepts with no direct calculation of original lock water concentration. The velocity magnitude contour plots are included in this appendix to give an idea of how the Type 2 concept would perform, but these results should be used as a direct comparison with the results shown in Chapter 6 of this report because extra degrees of freedom were included in those models, which can significantly affect the flow solution.

Figure 73. Type 2 velocity magnitude contours at el. 494.6

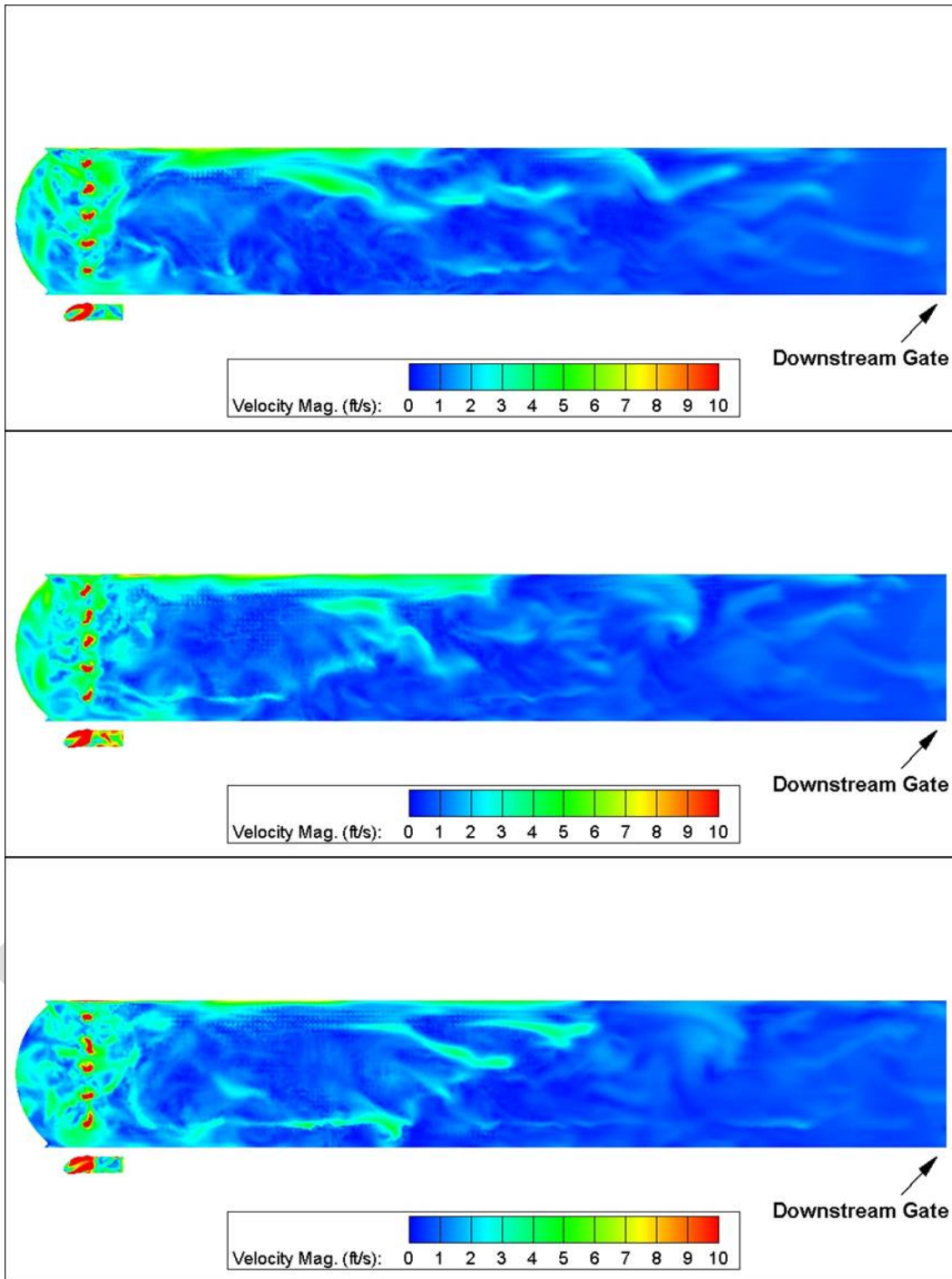
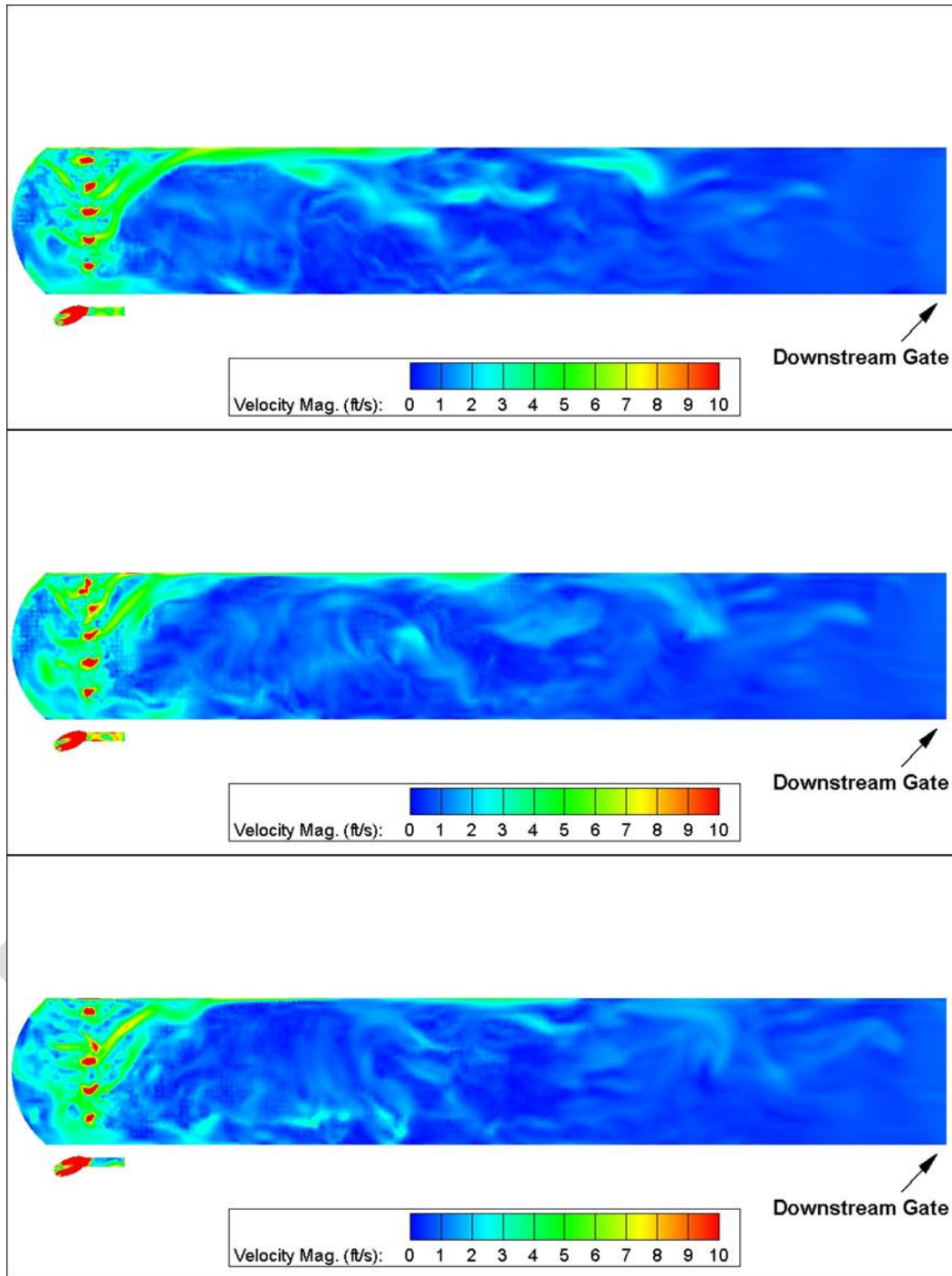


Figure 74. Type 2 velocity magnitude contours at el. 499.6



**GLMRIS - Brandon Road**  
**Appendix E - Hydrology and Hydraulics**

**Reverse Flows in Brandon Road Approach Channel**

## Table of Contents

<b>TABLE OF CONTENTS .....</b>	<b>E-167</b>
<b>LIST OF FIGURES .....</b>	<b>E-168</b>
<b>LIST OF TABLES .....</b>	<b>E-169</b>
<b>REVERSE FLOWS IN BRANDON ROAD LOCK APPROACH CHANNEL.....</b>	<b>E-170</b>
<b>1. Data Collection.....</b>	<b>E-170</b>
<b>2. Model Development.....</b>	<b>E-171</b>
2.1 Hydraulic Model.....	E-171
2.2 Hydrology.....	E-173
2.3 Continuous Simulation Model Runs .....	E-175
<b>3. Production Runs .....</b>	<b>E-181</b>
3.1 Lock Empty.....	E-181
3.2 Head Gate Operations.....	E-183
<b>4. Summary.....</b>	<b>E-184</b>

## List of Figures

<b>FIGURE 1: ACOUSTIC DOPPLER VELOCITY METER (ADVM) IN THE BRANDON ROAD APPROACH CHANNEL.....</b>	<b>E-170</b>
<b>FIGURE 2: PROVISIONAL ADVM 1-MINUTE DATA SHOWING THE X-VELOCITY IN THE APPROACH CHANNEL.....</b>	<b>E-171</b>
<b>FIGURE 3: MODEL EXTENT FOR THE HEC-RAS MODEL DEVELOPED FOR BRANDON ROAD TO EVALUATE FLOW REVERSALS IN THE APPROACH CHANNEL. ....</b>	<b>E-172</b>
<b>FIGURE 4: TWO-DIMENSIONAL FLOW AREA IN HEC-RAS MODEL DEVELOPED FOR BRANDON ROAD TO EVALUATE FLOW REVERSALS IN THE APPROACH CHNL.....</b>	<b>E-172</b>
<b>FIGURE 5: COMPUTED DISCHARGE FROM TWO LOCK EMPTIES ON JUN 14, 2015... </b>	<b>E-173</b>
<b>FIGURE 6: TERRAIN USED FOR THE TWO-DIMENSION FLOW AREA DOWNSTREAM OF BRANDON ROAD.....</b>	<b>E-175</b>
<b>FIGURE 7: MODEL RESULTS SHOWING THE COMPARISON OF CHANNEL VELOCITIES AT BIN 1 (NEAR MOORING STRUCTURE) BETWEEN THE HEC-RAS MODEL RESULTS (RED) AND THE OBSERVED ADVM DATA (BLUE). ....</b>	<b>E-176</b>
<b>FIGURE 8: MODEL RESULTS SHOWING THE COMPARISON OF CHANNEL VELOCITIES AT BIN 1 (B1) BETWEEN THE HEC-RAS MODEL RESULTS (RED) AND THE OBSERVED ADVM DATA (BLUE) FOR THE JUNE 2015 RUN. ....</b>	<b>E-176</b>
<b>FIGURE 9: MODEL RESULTS SHOWING THE COMPARISON OF CHANNEL VELOCITIES AT BIN 2 (B2) BETWEEN THE HEC-RAS MODEL RESULTS (RED) AND THE OBSERVED ADVM DATA (BLUE) FOR THE JUNE 2015 RUN. ....</b>	<b>E-177</b>
<b>FIGURE 10: MODEL RESULTS SHOWING THE COMPARISON OF CHANNEL VELOCITIES AT BIN 3 (B3) BETWEEN THE HEC-RAS MODEL RESULTS (RED) AND THE OBSERVED ADVM DATA (BLUE) FOR THE JUNE 2015 RUN. ....</b>	<b>E-177</b>
<b>FIGURE 11: MODEL RESULTS SHOWING THE COMPARISON OF CHANNEL VELOCITIES AT BIN 4 (B4) BETWEEN THE HEC-RAS MODEL RESULTS (RED) AND THE OBSERVED ADVM DATA (BLUE) FOR THE JUNE 2015 RUN. ....</b>	<b>E-178</b>
<b>FIGURE 12: MODEL RESULTS SHOWING THE COMPARISON OF CHANNEL VELOCITIES AT BIN 5 (B5) BETWEEN THE HEC-RAS MODEL RESULTS (RED) AND THE OBSERVED ADVM DATA (BLUE) FOR THE JUNE 2015 RUN. ....</b>	<b>E-178</b>
<b>FIGURE 13: MODEL RESULTS SHOWING THE COMPARISON OF CHANNEL VELOCITIES AT BIN 6 (B6) BETWEEN THE HEC-RAS MODEL RESULTS (RED) AND THE OBSERVED ADVM DATA (BLUE) FOR THE JUNE 2015 RUN. ....</b>	<b>E-179</b>
<b>FIGURE 14: MODEL RESULTS SHOWING THE COMPARISON OF CHANNEL VELOCITIES AT BIN 7 (B7) BETWEEN THE HEC-RAS MODEL RESULTS (RED) AND THE OBSERVED ADVM DATA (BLUE) FOR THE JUNE 2015 RUN. ....</b>	<b>E-179</b>
<b>FIGURE 15: MODEL RESULTS SHOWING THE COMPARISON OF CHANNEL VELOCITIES AT BIN 8 (B8) BETWEEN THE HEC-RAS MODEL RESULTS (RED) AND THE OBSERVED ADVM DATA (BLUE) FOR THE JUNE 2015 RUN. ....</b>	<b>E-180</b>
<b>FIGURE 16: MODEL RESULTS SHOWING THE COMPARISON OF CHANNEL VELOCITIES AT BIN 9 (B9) BETWEEN THE HEC-RAS MODEL RESULTS (RED) AND THE OBSERVED ADVM DATA (BLUE) FOR THE JUNE 2015 RUN. ....</b>	<b>E-180</b>

**FIGURE 17: FLOW HYDROGRAPH FOR A SIMPLIFIED LOCK EMPTY FROM THE BRANDON ROAD LOCK CHAMBER. IN THE HEC-RAS MODEL, THE HYDROGRAPH IS SPLIT EVENLY BETWEEN THE RIGHT AND LEFT EMPTY VALVES.....E-181**

**FIGURE 18: APPROXIMATELY 3 MINUTES AFTER THE LOCK EMPTY IS INITIATED, THE UPPER PORTION OF THE APPROACH CHANNEL IS APPROXIMATELY 1.5 FEET HIGHER THAN THE DOWNSTREAM END AND FLOW VELOCITIES ARE IN THE DOWNSTREAM DIRECTION ACROSS THE FULL CHANNEL CROSS-SECTION.....E-182**

**FIGURE 19: APPROXIMATELY 5 MINUTES AFTER THE LOCK EMPTY IS INITIATED, THE CHANNEL DOWNSTREAM OF THE APPROACH CHANNEL IS ELEVATED AND THE AT THE ELEVATED VELOCITIES HAVE MOVED DOWNSTREAM. ....E-182**

**FIGURE 20: APPROXIMATELY 2 MINUTES AFTER THE LOCK EMPTY COMPLETE, THE CHANNEL DOWNSTREAM OF THE REVERSE FLOWS IN THE APPROACH CHANNEL APPEAR. ....E-183**

**FIGURE 21: BEFORE THE HEAD GATES ARE OPENED WITH AVERAGE FLOW DOWNSTREAM OF BRANDON ROAD DAM.....E-183**

**FIGURE 22: APPROXIMATELY 8 MINUTES AFTER THE HEAD GATES ARE OPENED, CHANNEL DOWNSTREAM OF APPROACH CHANNEL BECOMES ELEVATED AND REVERSE FLOW THROUGH APPROACH CHANNEL IS OBSERVED IN THE SIMULATION. ....E-184**

**List of Tables**

**TABLE 1: HEC-RAS BOUNDARY CONDITIONS.....E-174**

## Reverse Flows in Brandon Road Lock Approach Channel

### 1. Data Collection

The GLMRIS Study Team recognized that water is frequently observed moving from the downstream end of the approach channel upstream toward the lock chamber. To better understand the frequency and magnitude of this, United States Geological Survey (USGS) installed an Acoustic Doppler Velocity Meter (ADVM) in the approach channel to detect and measure velocity reversals in the approach channel. The ADVM (USGS 05538020 Des Plaines River at Rockdale, IL) is located approximately 1,150 feet downstream of the downstream lock gates. The instrument is located on a mooring structure on the left side (looking downstream) of the approach channel. The ADVM measures velocity in nine bins to produce horizontal velocity profiles across the channel. Figure 1 shows the location of the ADVM.



**Figure 1: Acoustic Doppler Velocity Meter (ADVM) in the Brandon Road Approach Channel.**

The gage displays average stream velocity in the x and y direction at 5-minute intervals. USGS Illinois-Iowa Water Science Center provided provisional 1-minute data for time windows between 13-18 June 2015, and 8-11 December 2014. The June 2015 time window represents a high flow condition and the December 2014 time window represents a moderate flow condition. Figure 2 shows an example of the flow reversals observed in the approach channel for the bin closest to the mooring structure. The strong positive velocity in the approach channel is the immediate response to a lock empty. The short duration, large discharge through the approach channel creates a reverse gradient along the approach channel, resulting in the negative flow towards the lock chamber.

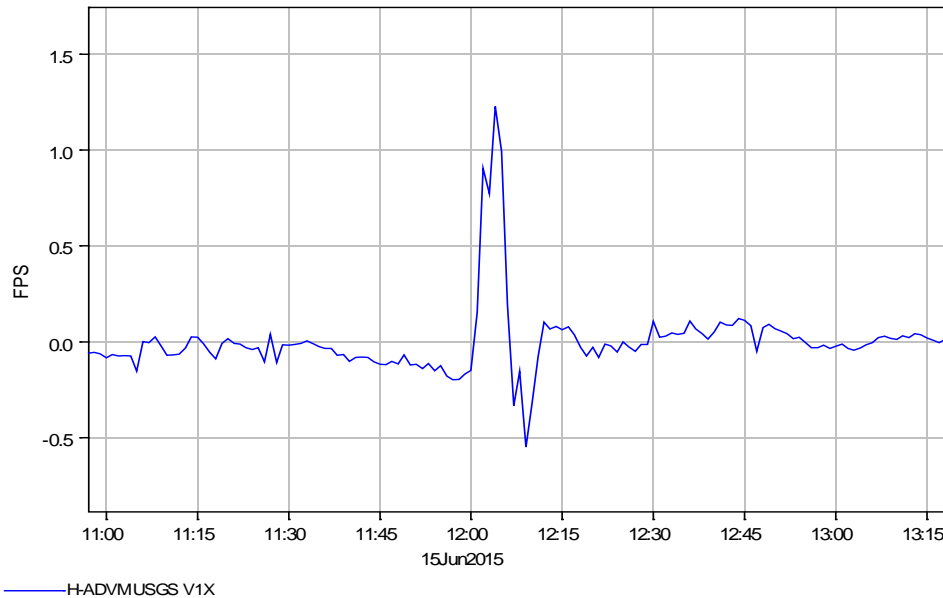


**Figure 2: Provisional ADVM 1-minute data showing the x-velocity in the approach channel.**

## 2. Model Development

### 2.1 Hydraulic Model

An integrated one-dimensional, two-dimensional model of the Des Plaines River downstream of Brandon Road Lock and Dam was created using HEC-RAS 5.0. The purpose of the model is to identify factors contributing to velocity reversals in the approach channel, and to evaluate how velocity reversals are affected by potential geometry changes. A one-dimensional HEC-RAS geometry developed by the US Army Corps of Engineers – Rock Island District was used to create the one-dimensional portion of the model. The one-dimension portion of the model extends from River Station 284.1 downstream to River Station 271.5 (Dresden Island Lock and Dam). This model domain fully encompasses the Dresden Island Pool. The cross-section at River Station 284.1 connects the one-dimensional and two-dimensional portions of the model. The computational mesh used in the two-dimensional area uses a variable grid mesh. In the approach channel where higher resolution required, the grid has a 10-foot spacing. Downstream of Brandon Road Dam and downstream of the approach channel, the grid size increases to 50 ft. In the two-dimensional flow area, a constant manning's n value of 0.022 was used to be consistent with the one-dimensional model developed by Rock Island District. Figure 3 shows the extent of the HEC-RAS model developed for Brandon Road Lock and Dam. Figure 4 shows the two-dimensional portion of the model.

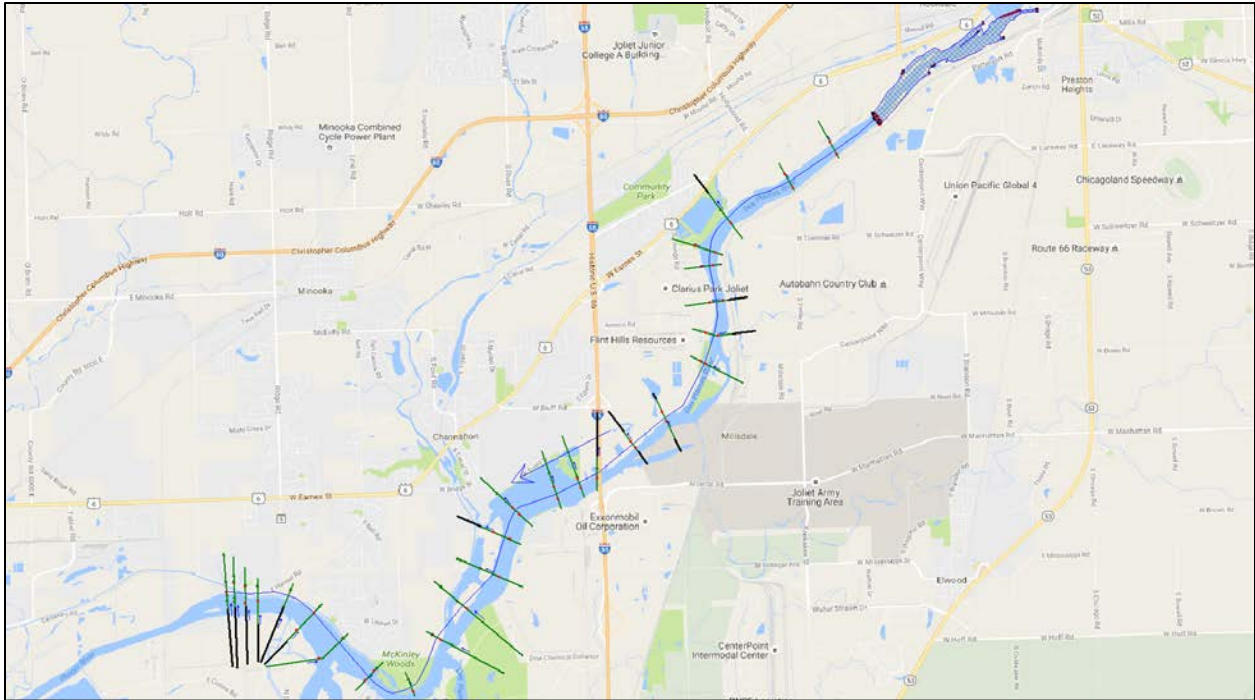


**Figure 3: Model extent for the HEC-RAS model developed for Brandon Road to evaluate flow reversals in the approach channel.**

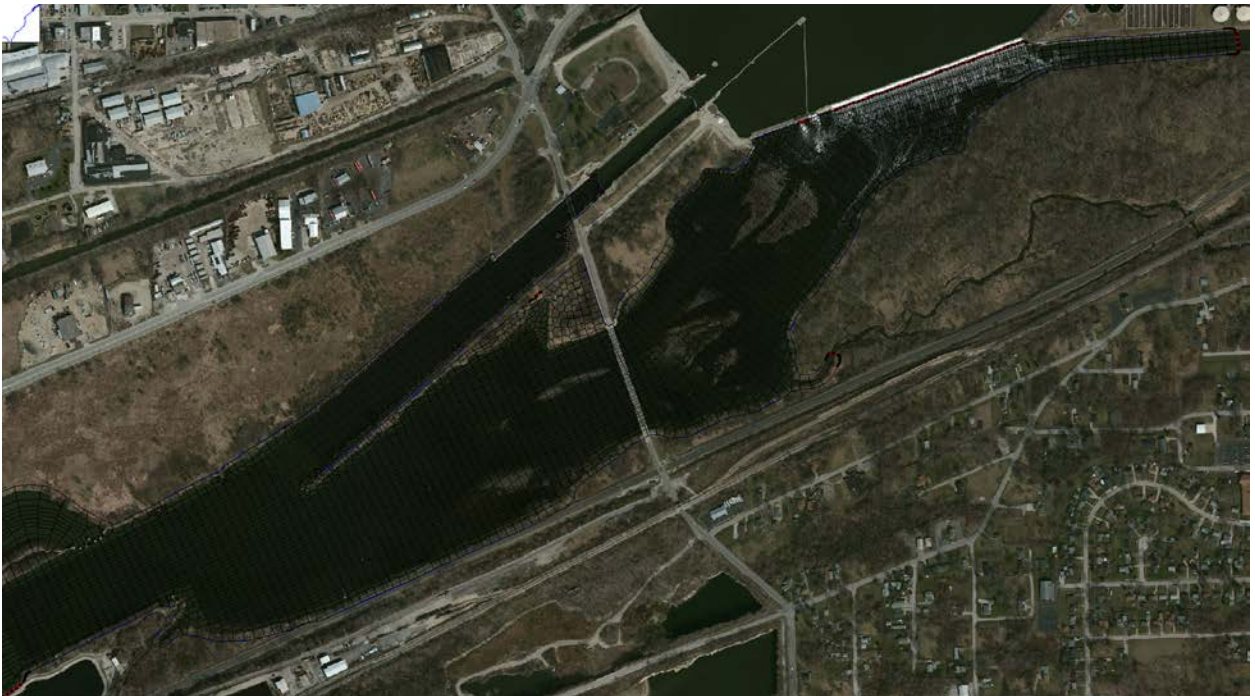


**Figure 4: Two-dimensional flow area in HEC-RAS model developed for Brandon Road to evaluate flow reversals in the approach channel.**

## 2.2 Hydrology

The model includes a large number of boundary conditions forcing flow into and out of the model domain. The major inflow into the upstream portion of the model domain is from releases at Lockport Lock and Dam upstream of Brandon Road. Discharges at Brandon Road Lock and Dam are regulated through 21 tainter gates and during flood flows, through 16 pairs of headgates. The approach channel experiences flow pulses through the empty valves during lock empties, and lower sustained discharges from the empty valve leakage. Boundary conditions were added to the two-dimensional mesh to represent each of the 21 tainter gates, head gates and lock empty valves. Two Joliet Generating Stations withdraw cooling water from the Des Plaines River and return the flow downstream. The larger station (on the north side of the river) withdrawals/discharges an average of 1,660 cfs. The smaller station (on the south side of the river) withdrawals/discharges an average of 588 cfs. Boundary conditions on the mesh domain represent these withdrawals and discharges. Unregulated discharges from Hickory Creek enter Dresden Pool immediately downstream of Brandon Road Dam on the left (looking downstream), and Sugar Run enters the pool 1700 feet downstream. Additional boundary conditions on the mesh domain represent these unregulated flows. The Kankakee and DuPage Rivers, along with Grant, Jackson and Cedar Creeks also enter Dresden Pool in the one-dimensional portion of the HEC-RAS model. A downstream stage boundary condition is used.

Boundary conditions come from a variety of sources. During the December 2014 and June 2015 data collection period, the USGS installed a stage hydrograph in the lock chamber. This stage time series was used, along with the lock chamber dimensions, to compute a flow time series for the lock empties. The time series generated with this data shows that the flow rates from each lockage can be highly variable (Figure 5). During the two time periods simulated, the left (looking downstream) empty valve was not operational due to maintenance, so the full lock empty was performed with the right empty valve. This operational change was modeled by using only the right valve boundary condition.

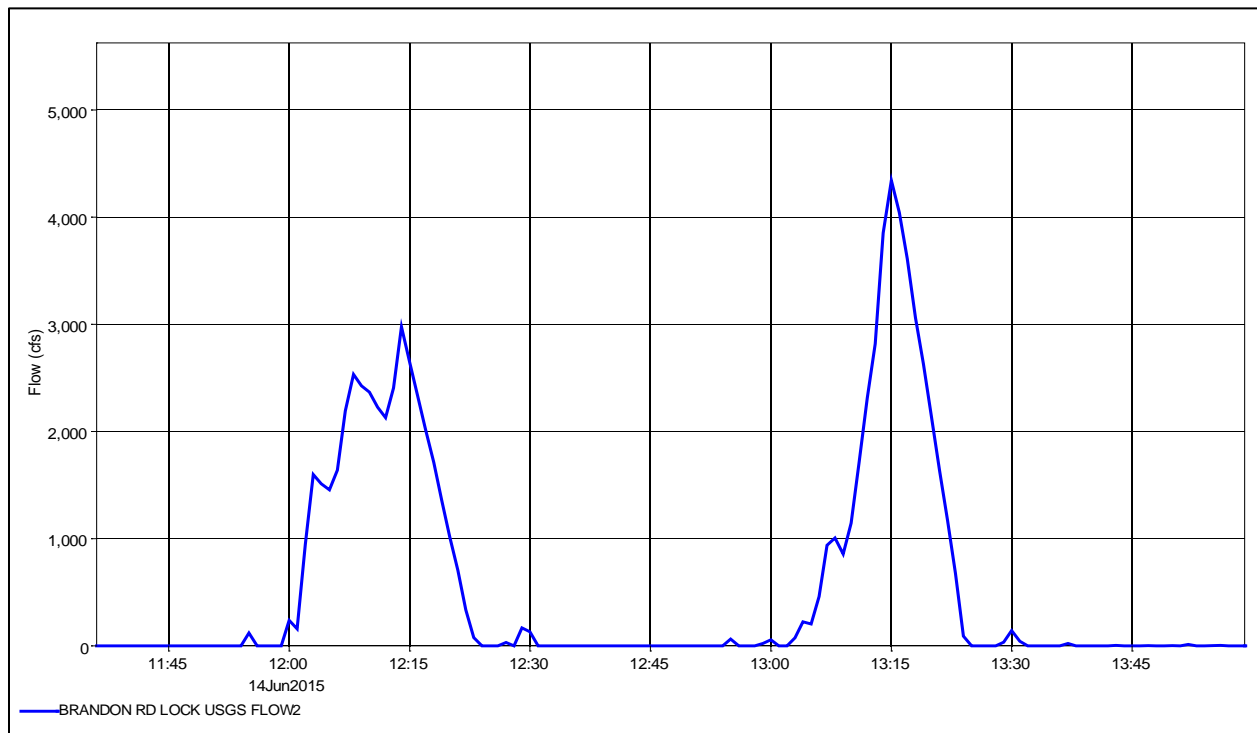


**Figure 5: Computed discharge from two lock empties on June 14, 2015.**

For the tainter gates and the and head gates, gate opening time series were used along with the gate rating curves, to generate flow hydrographs for each gate. Hickory Creek, the DuPage River and Hickory Creek are gaged, so gage data was used with a scaling factor to compensate for drainage area. Smaller ungaged tributaries were scaled from the Hickory Creek gage (05539000). Table 1 contains the inflow boundary conditions and the source for inflows.

**Table 1: HEC-RAS boundary conditions**

<b>Boundary Condition</b>	<b>Location</b>	<b>Source</b>	<b>Notes</b>
Tainter and Head Gates	2D mesh domain	Rivergages.com and Rating Curves	
Lock Empty Valves	2D mesh domain	Lock Chamber stage hydrograph with lock chamber dimensions	
Hickory Creek	2D mesh domain	USGS (05539000)	Scaled 1.01
Sugar Run	2D mesh domain	USGS (05539000)	Scaled 0.12
Joliet Generating Station (right)	2D mesh domain	NPDES Permit (monthly/average)	- for withdrawal, + for return
Joliet Generating Station (left)	2D mesh domain	NPDES Permit (monthly/average)	- for withdrawal, + for return
Kankakee River @ Wilmington	RS 272.65	USGS (05527500)	
DuPage River @ Shorewood	RS 276.5	USGS (05540500)	Scaled 1.16
Grant Creek	RS 275.0	USGS (05539000)	Scaled 0.16
Jackson Creek	RS 279.5	USGS (05539000)	Scaled 0.49
Cedar Creek	RS 280.2	USGS (05539000)	Scaled 0.13
Ungaged Uniform	Distributed uniform	USGS (05539000)	Scaled 0.25
Downstream Stage	RS 271.5	Rivergages.com	

The underlying terrain was developed from a variety of sources. A bathymetric survey performed by the Rock Island District is used for the channel bottom of the lock chamber, approach channel and the Des Plaines River downstream of the approach channel, and the scour area immediately downstream of Brandon Road Dam. A survey performed by the United States Geological Survey of the wide, flat section of the Des Plaines River between downstream of Brandon Road Dam and the approach channel was used for the bathymetry of this portion of the Des Plaines River. The survey was performed with an Acoustic Doppler Current Profiler (ADCP) and Real-Time Kinematic Global Positioning System (RTK-GPS) in shallow water depth areas. The Will County countywide LIDAR was used for overbank area, including the lock wall structures. Figure 6 shows the terrain used in the HEC-RAS two-dimensional flow area.



**Figure 6: Terrain used for the two-dimension flow area downstream of Brandon Road.**

### **2.3 Continuous Simulation Model Runs**

Model simulations were performed for two runs between 14JUN2015 00:00 and 18JUN2015 24:00 and 08DEC 2014 12:00 and 11DEC2014 24:00 to allow a comparison between simulated and observed velocities in the approach channel where the ADVM was installed. The current version of the model runs the two-dimension flow area with a 1-second time step with mixed flow regime. The current version of HEC-RAS 5.0 does not allow a user to directly access x and y velocity components from the results, so the application ‘h5Dump’ was used to extract the x and y velocity components from the hdf output file. The velocity components were rotated to align parallel (x) and perpendicular (y) to the approach channel. Figure 6 shows the model results for two lock empties on 14 June 2015. The model provides a good representation of velocities in the approach channel for some lock empties, but the comparison is not as favorable for others. It may be beneficial for future modeling to collect vessel positioning in the approach channel, to better understand how the presence of vessels may affect the hydrodynamics. Figure 7 through 16 shows a comparison of observed and modeled velocities across the approach channel for the June 2015 model run.

The comparison is not as favorable for Bin 9, on the side of the approach channel opposite the ADVM instrument. It is possible that the distance across the approach channel begins to approach the maximum distance for the instrument. The plots also shows quite a bit of disturbance in the approach channel outside of lock empties. From available data, it is not possible to know whether these disturbances are from waiting or moving vessels, wind, or other forces.

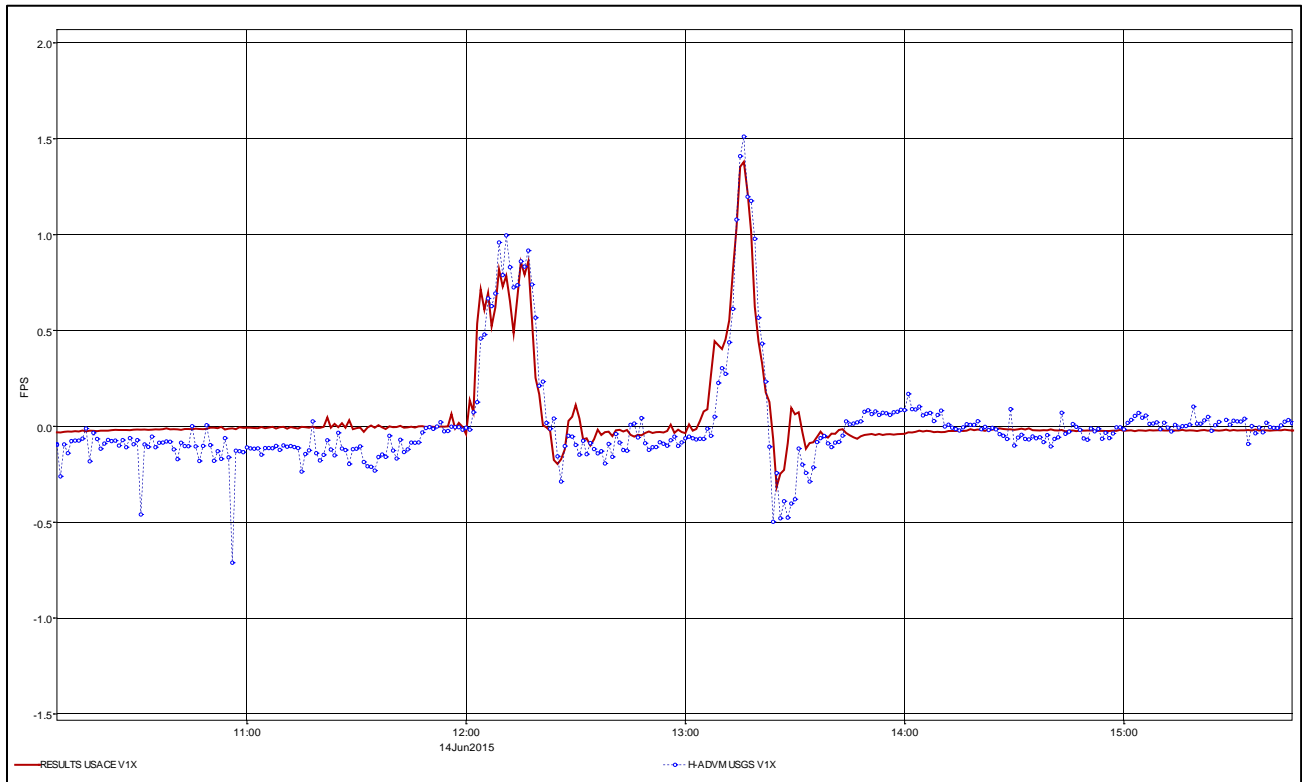


**Figure 7: Model results showing the comparison of channel velocities at Bin 1 (near mooring structure) between the HEC-RAS model results (red) and the observed ADVM data (blue).**

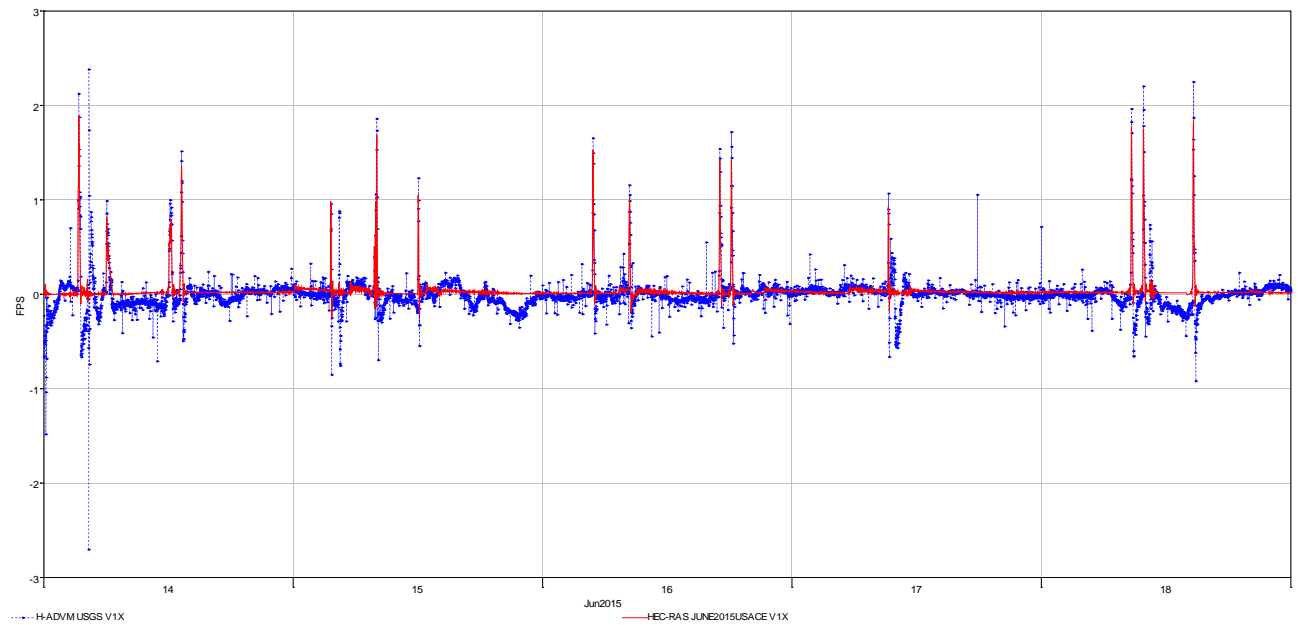


**Figure 8: Model results showing the comparison of channel velocities at Bin 1 (B1) between the HEC-RAS model results (red) and the observed ADVM data (blue) for the June 2015 run.**

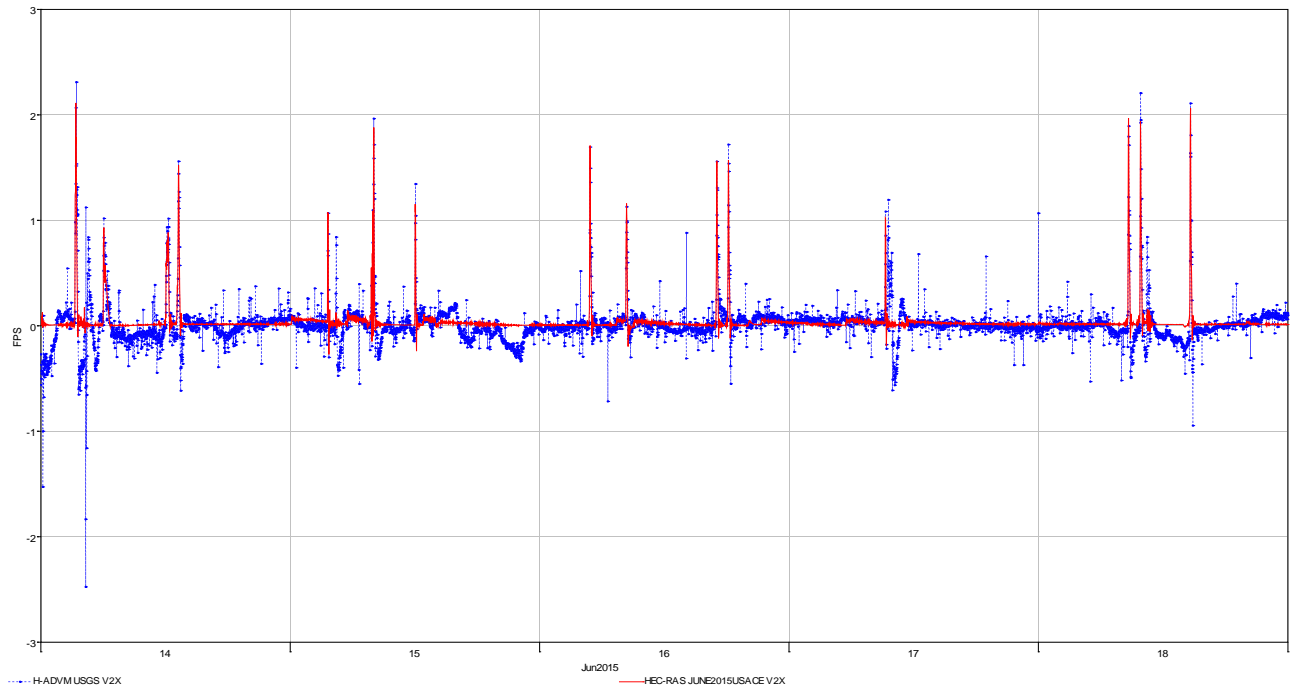


**Figure 9: Model results showing the comparison of channel velocities at Bin 2 (B2) between the HEC-RAS model results (red) and the observed ADVM data (blue) for the June 2015 run.**

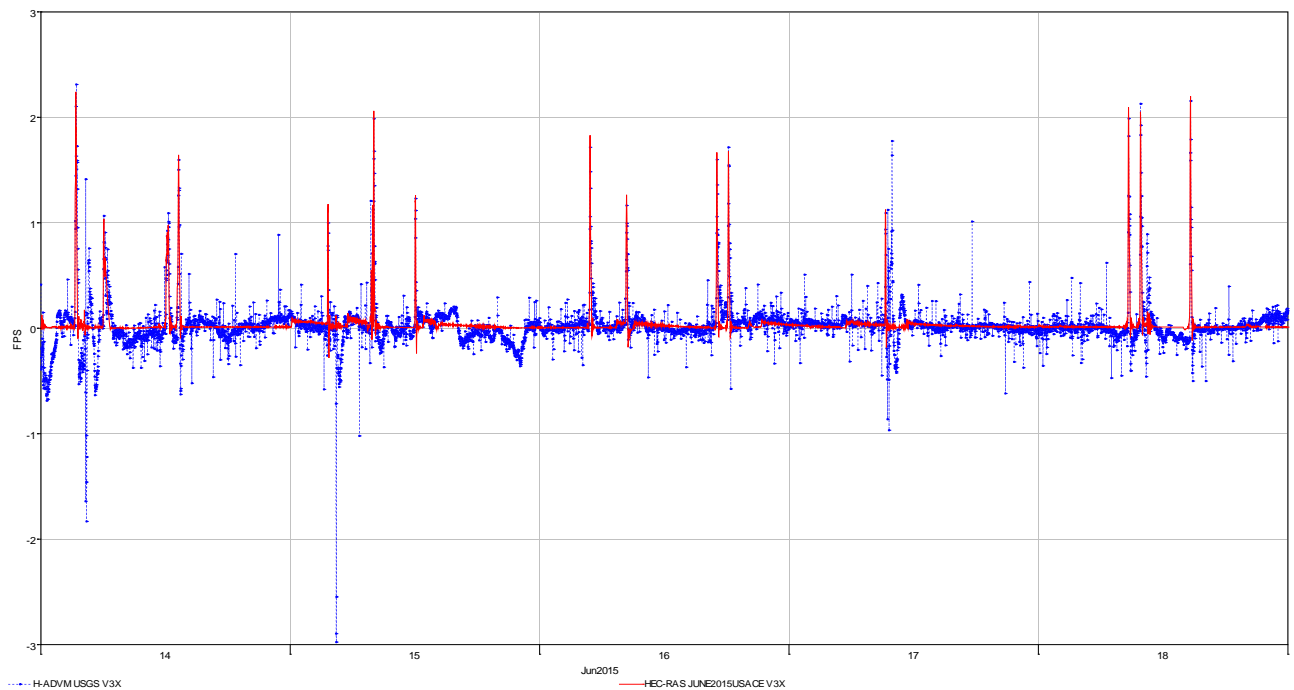


**Figure 10: Model results showing the comparison of channel velocities at Bin 3 (B3) between the HEC-RAS model results (red) and the observed ADVM data (blue) for the June 2015 run.**

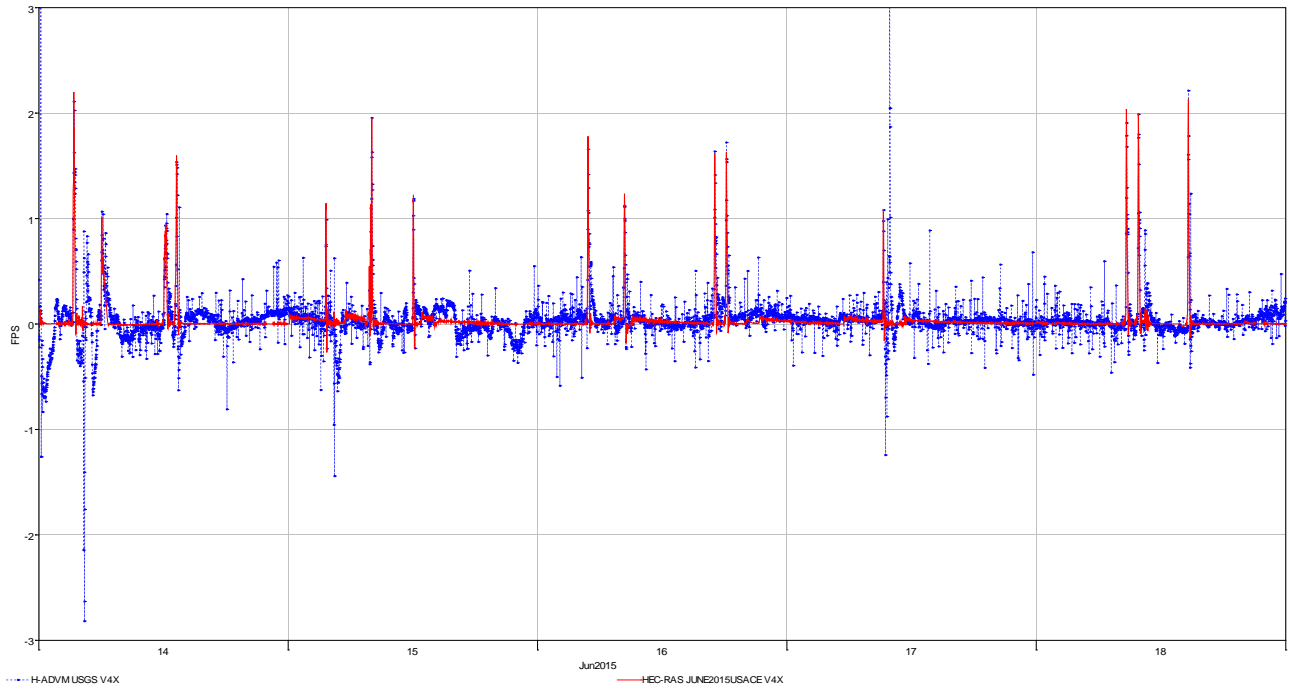


**Figure 11: Model results showing the comparison of channel velocities at Bin 4 (B4) between the HEC-RAS model results (red) and the observed ADVm data (blue) for the June 2015 run.**

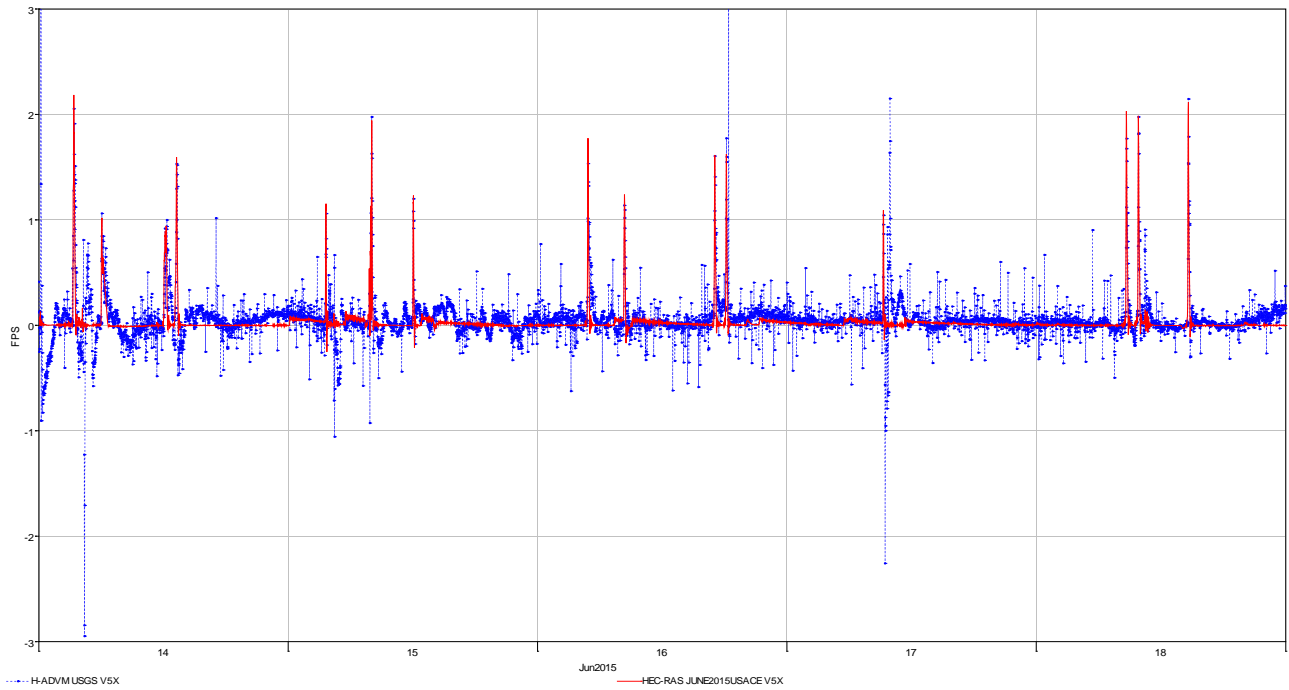


**Figure 12: Model results showing the comparison of channel velocities at Bin 5 (B5) between the HEC-RAS model results (red) and the observed ADVm data (blue) for the June 2015 run.**

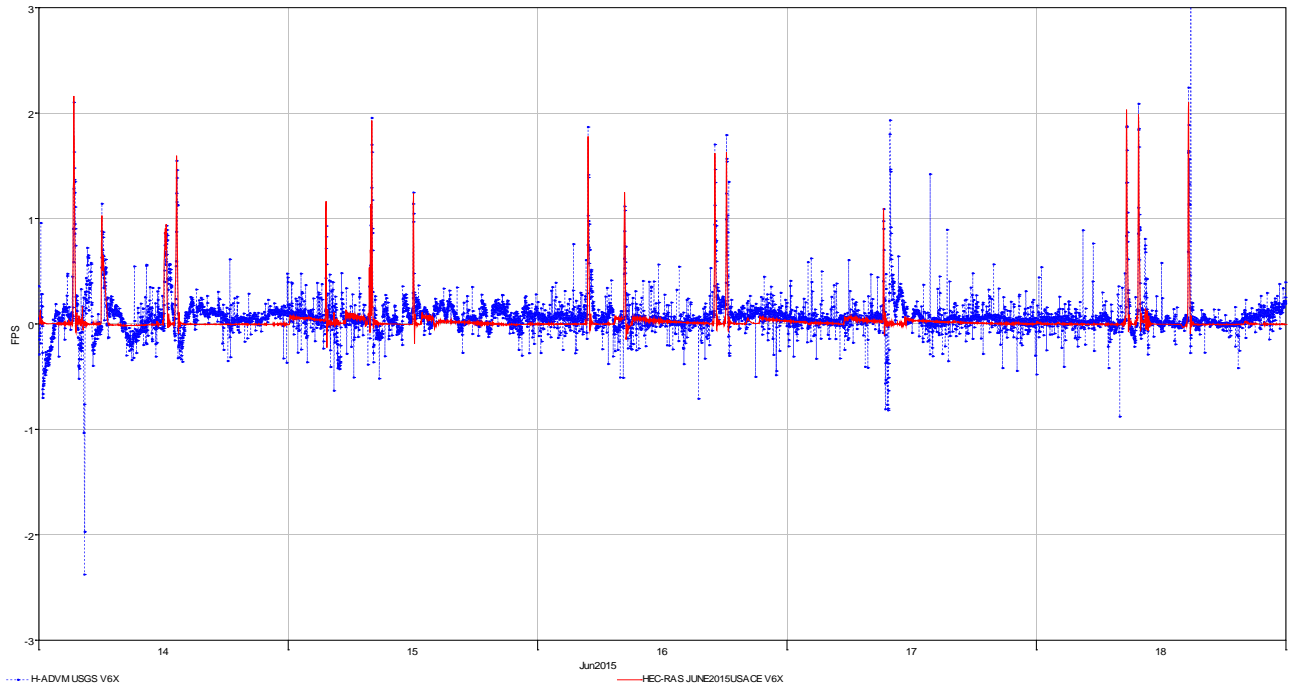


**Figure 13: Model results showing the comparison of channel velocities at Bin 6 (B6) between the HEC-RAS model results (red) and the observed ADVM data (blue) for the June 2015 run.**

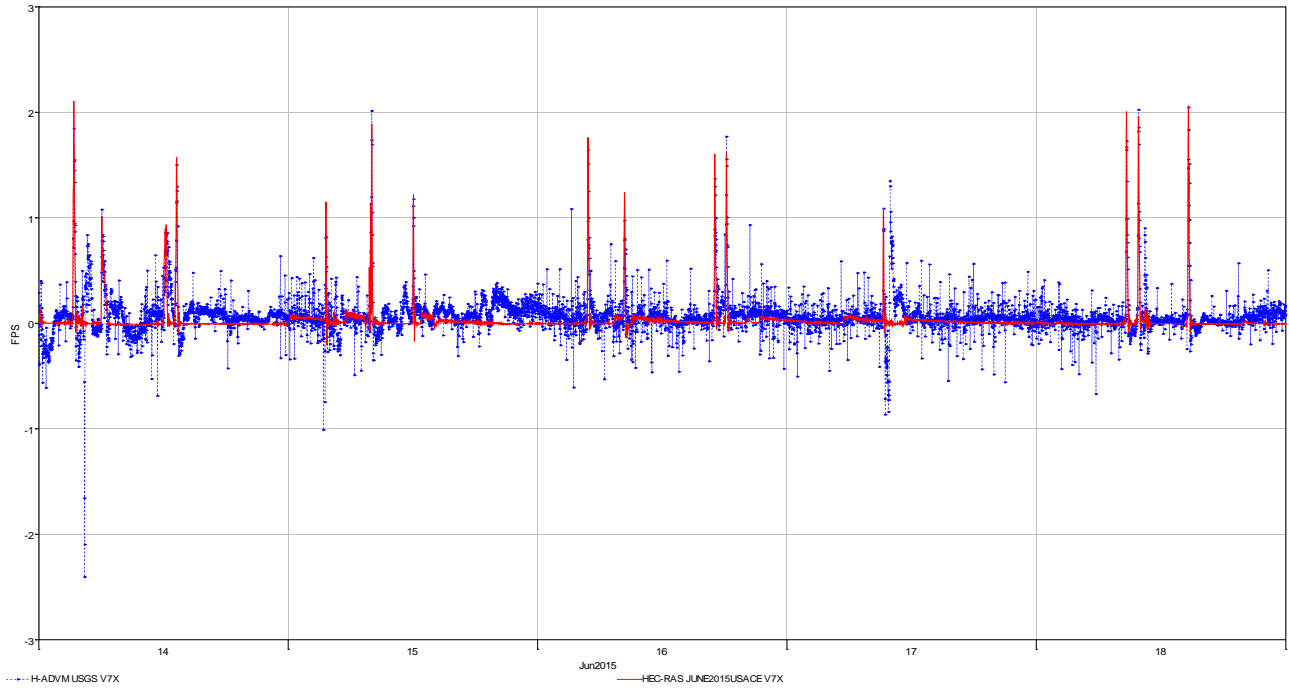


**Figure 14: Model results showing the comparison of channel velocities at Bin 7 (B7) between the HEC-RAS model results (red) and the observed ADVM data (blue) for the June 2015 run.**

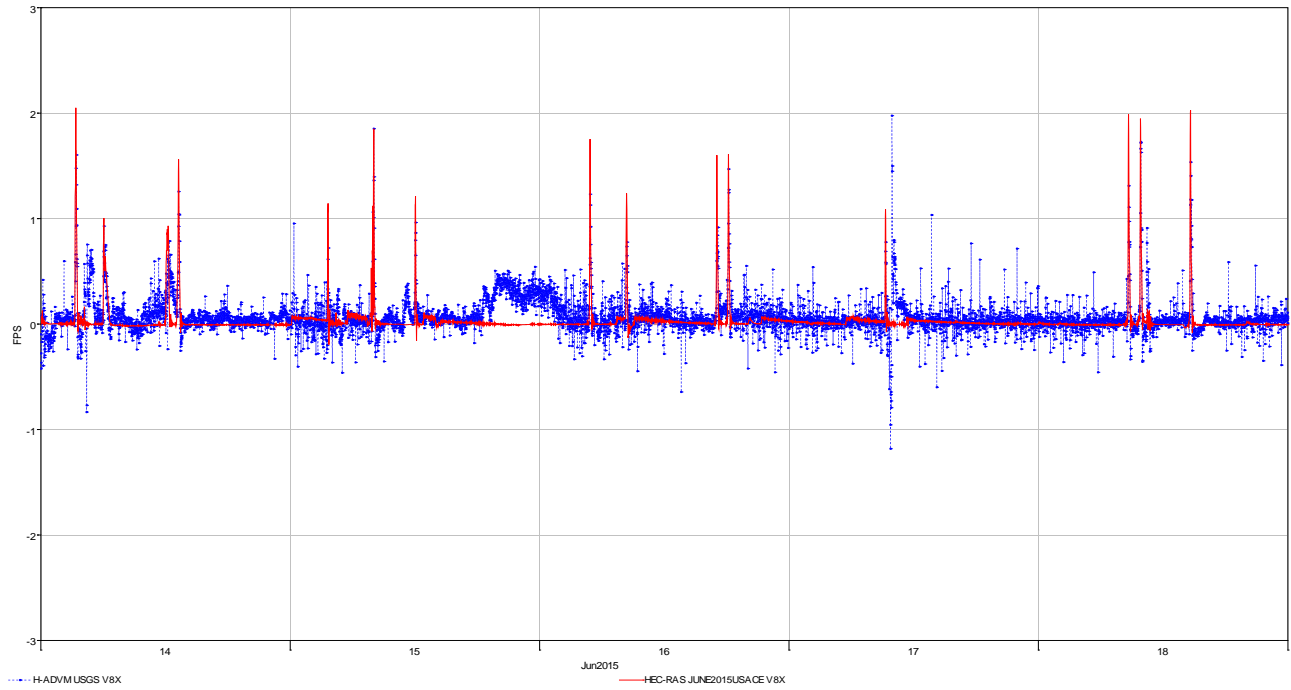


**Figure 15: Model results showing the comparison of channel velocities at Bin 8 (B8) between the HEC-RAS model results (red) and the observed ADVm data (blue) for the June 2015 run.**

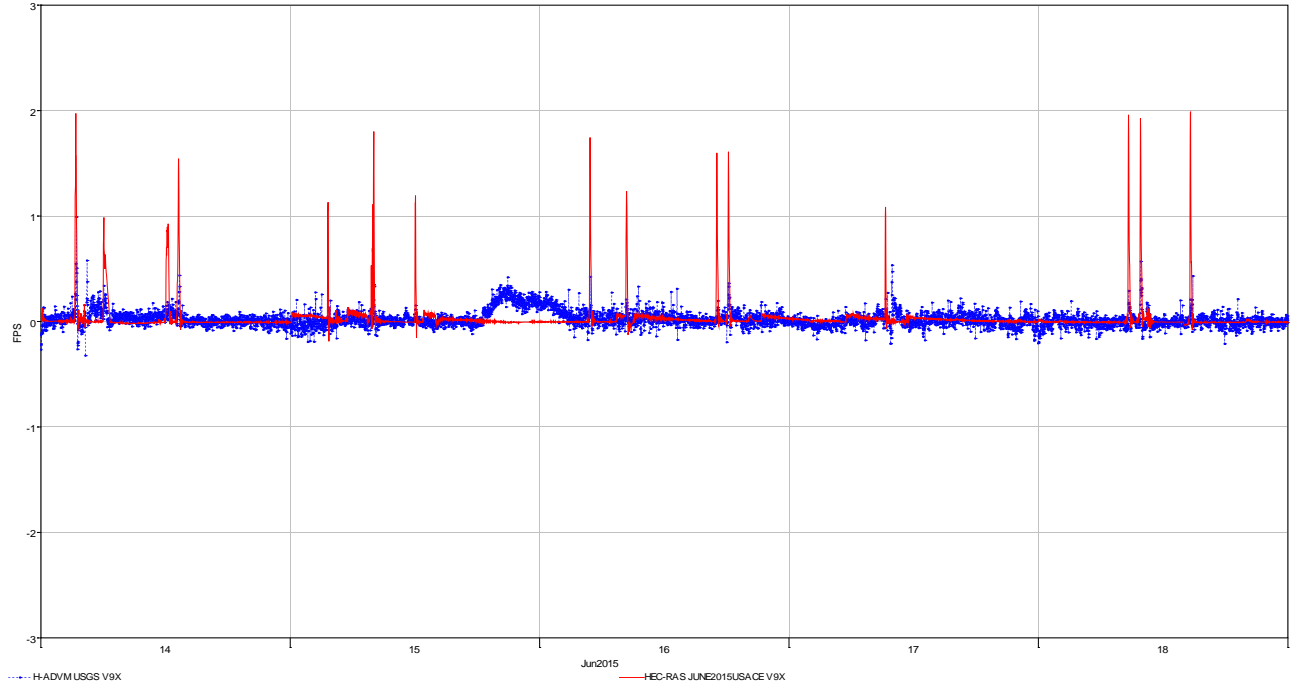


**Figure 16: Model results showing the comparison of channel velocities at Bin 9 (B9) between the HEC-RAS model results (red) and the observed ADVm data (blue) for the June 2015 run.**

### 3. Production Runs

In addition to the two continuous simulation periods, model simulations were performed to evaluate flow reversals for lock empties, head gate openings and head gate openings. The two different operation changes affect flow conditions differently. Average flow conditions were used in the channel. Future work could include an evaluation of a range of high and low flows.

#### 3.1 Lock Empty

When the lock chamber empties, the volume of the lock chamber between the headwater and tailwater elevation empties in approximately 15 minutes through two valves on the left and right bank downstream of the lock chamber. As previously described from the continuous simulation model runs, the peak and duration of discharge can be highly variable. A production simulation was performed to isolate the effects of a lock empty. A simplified lock empty flow time series was created based on measured peak discharges observed by USGS, the volume of water in the lock chamber, and the typical duration of a lock empty. Figure 17 shows the flow hydrograph from the simplified lock empty.

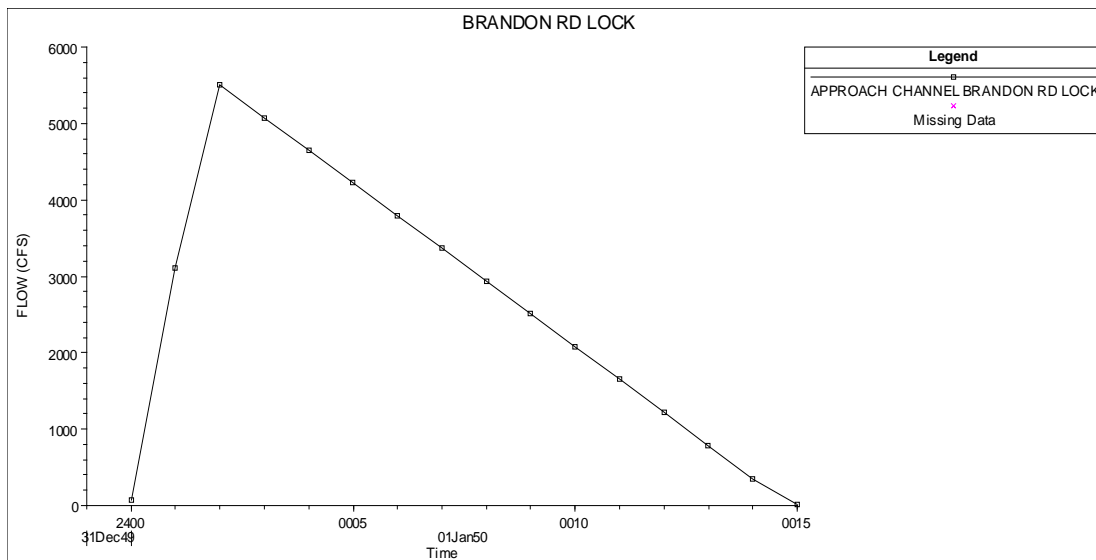


**Figure 17: Flow hydrograph for a simplified lock empty from the Brandon Road lock chamber. In the HEC-RAS model, the hydrograph is split evenly between the right and left empty valves.**

The lock empty process produces short duration, high flow conditions in the approach channel. The highest flow rate occurs several minutes after the lock empty is initiated when the head difference between the lock chamber and downstream approach channel is the greatest. As the water level in the lock chamber drops and the water level in the approach channel rises from the large inflow of water, the flow rate decreases. During a typical lock empty, this process takes approximately 15 minutes.

Figures 18 through 20 show the progression of water surfaces and velocities in and downstream of the approach channel. Figure 18 shows the water surface 3 minutes after the lock empty has been initiated. The blue shading and contours show the upper portion of the approach channel is approximately 1.5 foot higher than downstream end of the approach channel. Flow velocities are in a downstream direction across the entire channel cross-section (Figure 19). After the lock empty is complete, the simulation shows reverse flows in the approach channel.

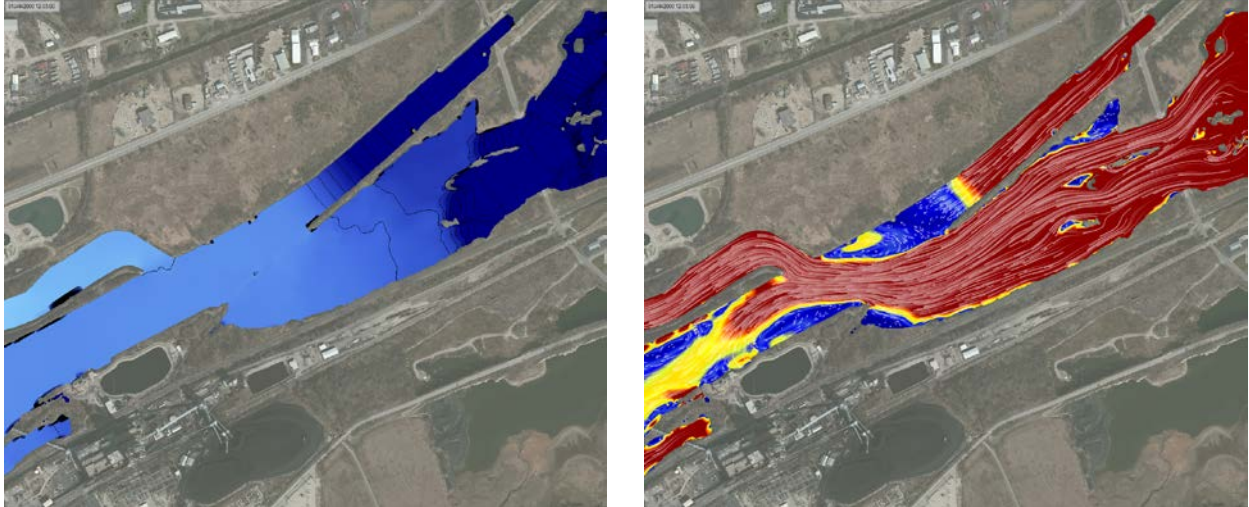


**Figure 18: Approximately 3 minutes after the lock empty is initiated, the upper portion of the approach channel is approximately 1.5 feet higher than the downstream end and flow velocities are in the downstream direction across the full channel cross-section.**

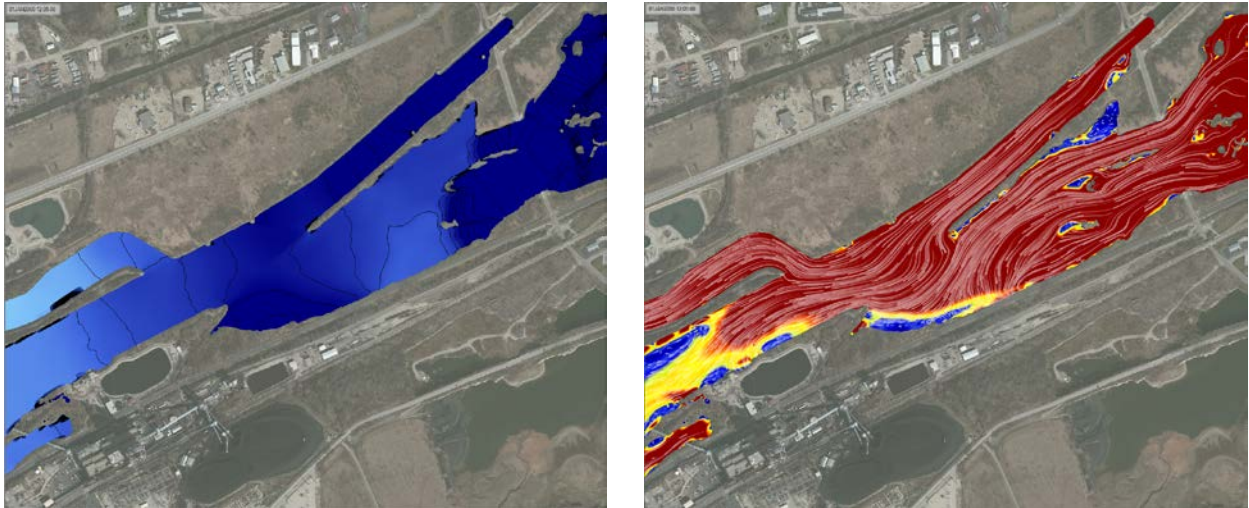


**Figure 19: Approximately 5 minutes after the lock empty is initiated, the channel downstream of the approach channel is elevated and the at the elevated velocities have moved downstream.**

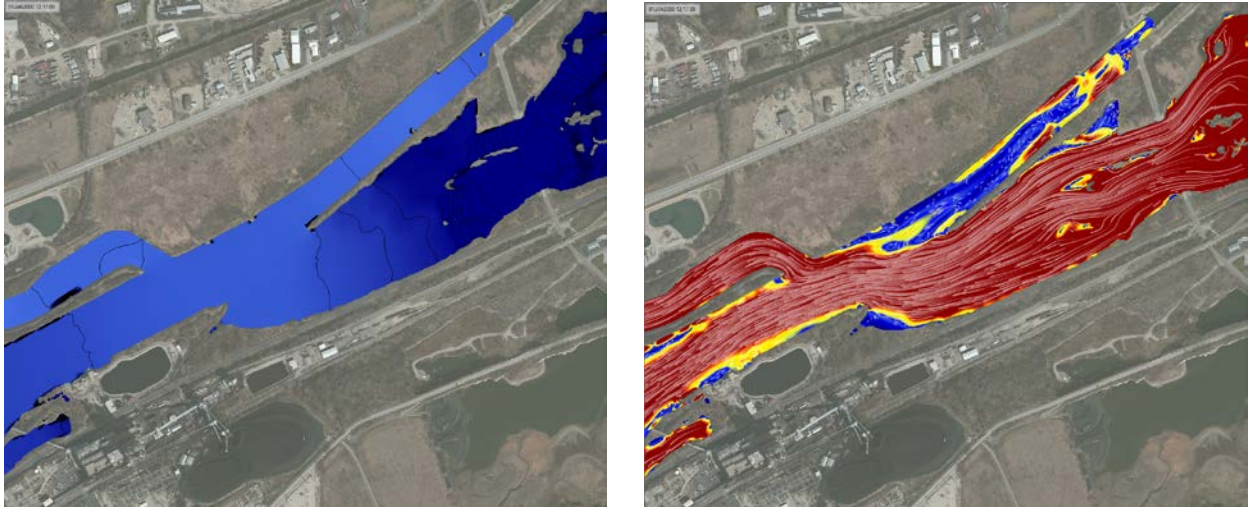


**Figure 20: Approximately 2 minutes after the lock empty complete, the channel downstream of the reverse flows in the approach channel appear.**

### 3.2 Head Gate Operations

During flood operations, a series of head gates are opened to release flood flows downstream to Dresden Pool. When this occurs, flow discharges increase quickly downstream of Brandon Road Road Dam. A production simulation was performed to isolate the effects of head gate operations. An average flow condition downstream of Brandon Road was increased by 12,400 cfs to simulate the opening of two head gates. The head gates cause an elevation of water surface downstream of the approach channel. This results in a flow and velocity reversals into the approach channel.

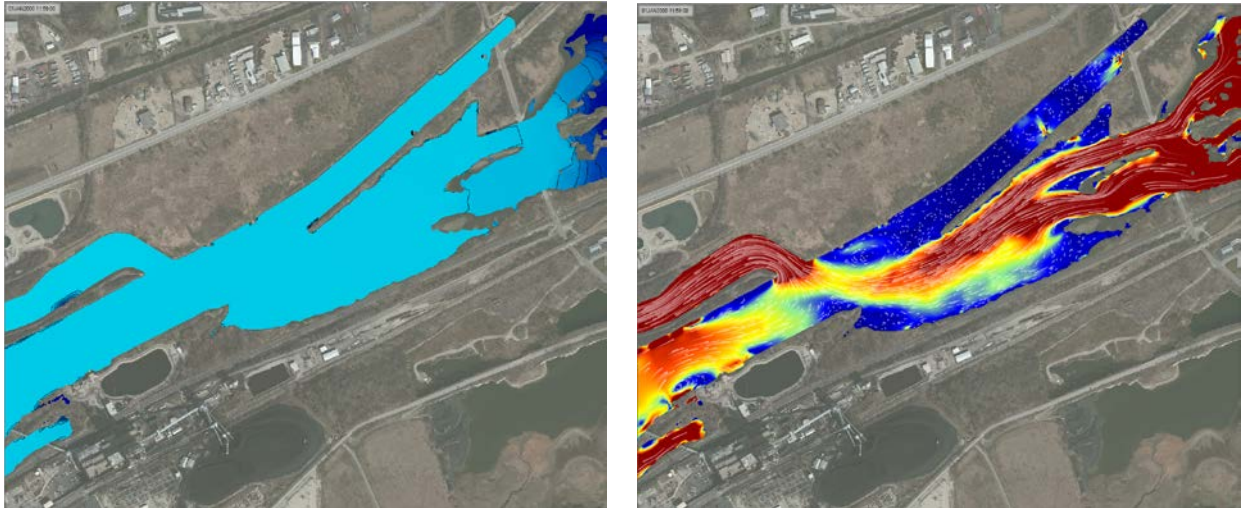


**Figure 21: Before the head gates are opened with average flow downstream of Brandon Road Dam.**

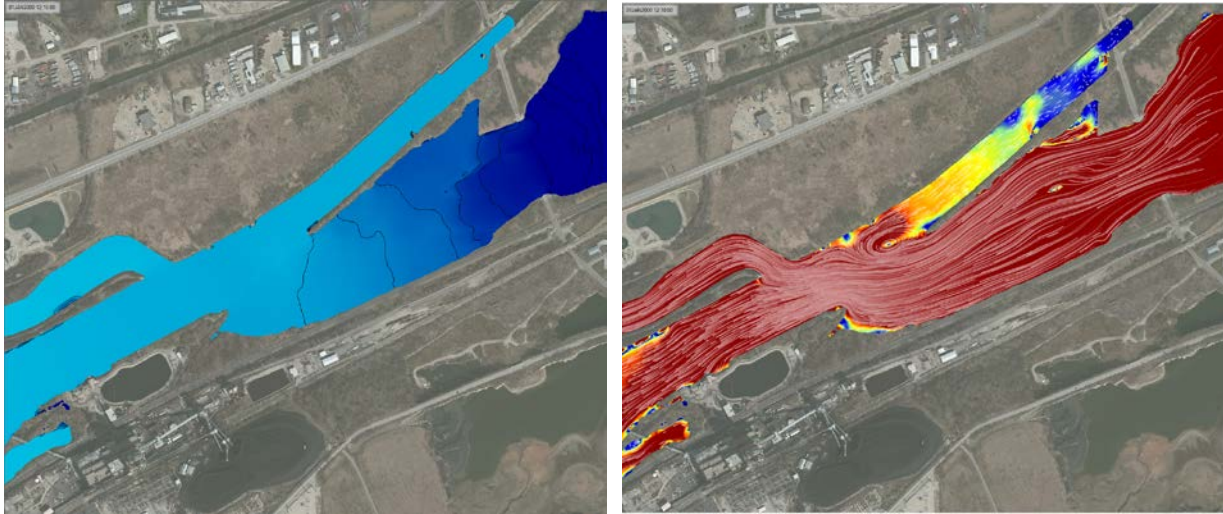


**Figure 22: Approximately 8 minutes after the head gates are opened, channel downstream of approach channel becomes elevated and reverse flow through approach channel is observed in the simulation.**

#### **4. Summary**

The one-dimensional, two-dimensional model shows reasonable agreement between the observed velocities in the approach channel during USGS's data collection period. The velocity data collected during this period and the modeling confirm that frequent flow reversals in the approach channel occur. The majority of these reversals occur during routine and daily lockages. The production runs also show that the operation of head gates, and the rapid increase in discharge associated with these gate operations, can also induce flow reversals in the approach channel.

The simulation runs performed to evaluate the reverse flows in the approach channel resulting from the lock empties and gate operating only were performed using average flow conditions in the channel. Future work with the model could include an evaluation of high and low flows to determine if the flow conditions in the channel significantly affect the magnitude and frequency of reversals. This future work could also evaluate how withdrawal flow rates from the power plants affects the reversal. Future work may also include an evaluation of alternatives to mitigate the impacts of the reversal through operation changes to the existing gate operating or proposed features.